Key Role for Matrix Metalloproteinases-19 and -28 in Maintenance of Intestinal Homeostasis

Dissertation

zur Erlangung des Doktorgrades

der Mathematisch-Naturwissenschaftlichen Fakultät

der Christian-Albrechts-Universität

zu Kiel

vorgelegt von

Rena Brauer

Kiel, Juni 2011

Referent: Prof. Dr. rer. nat. Dr. h. c. Thomas C. G. Bosch

Koreferent: Dr. Radislav Sedlacek

Tag der mündlichen Prüfung: 28.07.2011

Zum Druck genehmigt, Kiel, den 28.07.2011

In Memory

Irmgard Ida Emilie Brauer

Table of contents

List of abbrevations

Nucleotides

Base	Nucleotide code
Adenine	A
Cytosine	C
Guanine	G
Thymine	T
Uracil (only RNA)	U

Amino acids

Amino acid	3-letter code	1-letter code
Alanine	Ala	A
Arginine	Arg	R
Asparagine	Asn	N
Aspartic acid	Asp	D
Cysteine	Cys	C
Glutamic acid	Glu	E
Glutamine	Gln	Q
Glycine	Gly	G
Histidine	His	H
Isoleucine	Ile	I
Leucine	Leu	L
Lysine	Lys	K
Methionine	Met	M
Phenylalanine	Phe	F
Proline	Pro	P
Serine	Ser	S
Threonine	Thr	T
Tryptophan	Trp	W
Tyrosine	Tyr	Y
Valine	Val	V

Abbreviations continued

aa	amino acid
ADAM	a disintegrin and metalloproteinase
ADAMTS	a disintegrin and metalloproteinase with thrombospondin motifs
ALT	alanine aminotransferase
AST	aspartate aminotransferase
BCA	bicinchoninic acid
bp	base pair
BSA	bovine serum albumin
CEC	colon explant culture
CD	Crohn's disease
CD	cluster of differentiation
dbKO	double-deficient / double-knockout
DEPC	diethylpyrocarbonate
DC	dendritic cell
DNA	desoxyribonucleid acid
dNTPs	deoxyribonucleotides
DSS	dextran sulfate sodium
DTT	dithiothreitol
EDTA	ethylenediaminetetraacetic acid
ECM	extracellular matrix
EGF	epidermal growth factor
EMT	epithelial-mesenchymal transition
FACS	fluorescence-activated cell sorting
FCS	foetal calf serum
FGF	fibroblast growth factor
FKN	fractakine
g	gram
g	gravity
DTT	dithiothreitol
G-CSF	granulocyte colony-stimulating factor
GM-CSF	granulocyte marcophage colony-stimulating factor
GP	glycoprotein
IBD	inflammatory bowel disease
IEL	intraepithelial lymphocyte
IGFBP	insulin-like growth factor binding protein

IFN	interferon
IL	interleukin
ITF	intestinal trefoil factor
JAK	janus kinase
kDa	kilo Dalton
KC	keratinocyte chemoattractant
KO	knockout
l	liter
LPS	lipopolysaccaride
MCP-1	monocyte chemoattractant protein-1
mg / µg	milligram / microgram
ml / µl	milliliter /microliter
mM / µM	millimolar /micromolar
min	minute
MIP-1	macrophage inflammatory protein 1
MMP	matrix metalloproteinase
MT-MMP	membrane-type matrix metalloproteinase
NK	natural killer
NOD	nucleotide oligomerization domain
PAMP	pathogen-associated molecular pattern
PBS	phosphate-buffered saline
PCR	polymerase chain reaction
pH	power of hydrogen
PRR	pathogen recognition receptor
PVDF	polyvinylidene fluoride membrane
RANTES	regulated upon activation, normal T-cell expressed, and secreted
RECK	reversion-inducing-cysteine-rich protein with Kazal motifs
RFU	relative fluorescent units
RNA	ribonucleid acid
RT-PCR	reverse-transcriptase polymerase chain reaction
SCID	severe combined immunodeficiency
SDS	sodium dodecyl sulfate
sec	second
STAT	signal transducer and activation of transcription
Tab.	table
TACE	tumour necrosis factor alpha-converting enzyme

TAE	tris base/ acetic acid/ EDTA buffer
TBS	tris-buffered saline
TGF	tumour growth factor
TLR	toll-like receptor
TIMP	tissue inhibitor of metalloproteinase
TNBS	2,4,6-trinitrobenzenesulfonic acid
TNF	tumour necrosis factor
U	unit
UC	ulcerative colitis
VEGF	vascular endothelial growth factor
WT	wildtype
+/+	wildtype (homozygous)
+/-	heterozygous
-/-	knockout/deficient (homozygous)

List of figures

List of tables

1 Objectives

The human matrix metalloproteinases 19 and 28 (MMP-19 and -28) are abundantly expressed in epithelial tissues. However, their functions in this compartment and their functional overlap have not been elucidated so far. MMP-19 contributes to IGF-signaling, cell proliferation, and migration and is able to cleave several soluble proteins and components of extracellular matrix, including those found in the basement membrane. MMP-28 was shown to be important in wound healing.

Functional studies on MMP-19 and -28 were performed mainly *in vitro*, but their role *in vivo* is largely unknown. Mouse models are commonly used to establish functions of molecules in a living organism, which then enables us to draw conclusions to the human system. Mice with a functional deletion of a specific gene, so called knockout mice, are widely used to determine the *in vivo* role of the gene. Thus, the phenotype of such mice can characterize the function of the targeted molecule.

To study the function of both MMPs *in vivo*, mice with targeted disruption of the *Mmp19* and *Mmp28* genes were generated. Since little is known about the role of MMPs in inflammation, and as both MMP-19 and -28 show constitutive expression in the epithelium, the main goal of the work presented here was to reveal the impact of deletion of these MMPs in inflammatory reactions of the colon.

In order to delineate the role of MMP-19 and MMP-28 in the pathogenesis of induced colitis and, in a wider context, in the innate immunity of the intestine, the following aims were defined:

1. To establish the DSS-induced colitis model.
2. To elucidate MMP-19 and -28 functions in acute inflammation in the colon, so called acute colitis.
3. To analyze the influence of MMP-19 and -28 during the healing phase, so called recovery phase after an acute colonic inflammation.
4. To determine long-term effects of MMP-19 deficiency in chronic inflammation.

Analyzing the function of MMP-19 and MMP-28 in the colon using single and double-deficient mice can provide new insights into the pathophysiological role of these proteases in maintaining the epithelial barrier, especially in inflammatory reactions and immune responses. Furthermore, these studies can improve the understanding of MMP activity in healthy and inflamed colonic tissue and define a role of these proteolytic enzymes in inflammatory bowel disease (IBD).

2 Introduction

2.1 Intestine and epithelial barrier function

2.1.1 Intestine – a brief overview

The gut consists of the small and large intestine. The small intestine of vertebrates follows the stomach and is followed by the large intestine. It consists of three parts: the duodenum, the jejunum, and the ileum. The primary function of the small intestine is the digestion and absorption of nutrients and minerals found in food. The large intestine also comprises three parts: the caecum, the colon, and the rectum.

As the colon is central for the analyses in this work, this part of the large intestine will be described in more detail. In mammals, the colon consists of four sections: the ascending colon, the transverse colon, the descending colon, and the sigmoid colon. The colon is the last part of the digestive system; it extracts water and salt from solid wastes before they are eliminated from the body, and is the site, in which flora-aided (largely bacterial) fermentation of unabsorbed material occurs. Unlike the small intestine, the colon does not play a major role in absorption of foods and nutrients. However, the colon does absorb water, potassium and some fat soluble vitamins [1].

2.1.2 Architecture of the colonic wall

The large intestine of all mammals consists of several concentrically arranged layers, as the other organs of the digestive tract: lamina mucosa, lamina propria, lamina muscularis mucosa, lamina submucosa, lamina muscularis externa, subserosa, and serosa.

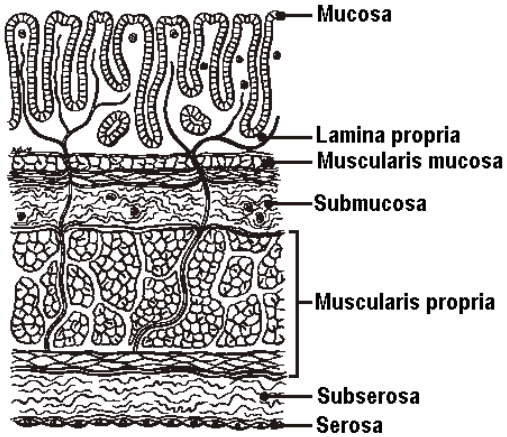

Figure 2-1: Schematic representation of the general structure and layers of the colon.
Taken from http://www.aboutcancer.com.

The mucosa lines the large intestinal lumen and lies at the critical interface between the external environment and the body's internal milieu. This is reflected in the mucosa being one of the most dynamic tissues in the body. The mucosa is comprised of an epithelium and a basement membrane, supporting connective tissue called the lamina propria, and a sheet of smooth musculature, the lamina muscularis. The luminal surface of the ceacum and colon wall is rich in microflora that is important for digesting complex carbohydrates and synthesizing products, such as vitamins and amino acids. Therefore, a barrier that avoids invasion by bacteria but is also permeable for water and ions, is essential. A simple epithelium lines the lumen and includes absorptive and secretory cells as well as varying numbers of goblet cells that produces mucin. The mucin coats the epithelium and is an integral and important part of the innate barrier against penetration of foreign substances. In addition, some lymphoid cells can be found in the epithelium, the intraepithelial leukocytes (IEL). It has been reported that IELs might be involved in the downregulation of the local immune response, preventing an over-reaction against luminal antigens crossing the epithelium. At the bottom of the crypts, a pool of undifferentiated cells (stem cell-like cells) persists in the so called proliferative area, which generates new cells that migrate to the epithelial layer. The turnover of the cells in the intestine is one of the fastest in the body. The basement membrane of the epithelium is supported by connective tissue elements, called lamina propria. In this layer, fibroblasts, endothelial cells, some smooth muscle cells, and a large number of immune cells (lymphocytes, plasma cells, macrophages, mast cells, eosinophils, and dendritic cells) are located. The numbers of immune cells vary with the state of inflammation in that area [2; 3]. The outer boundary of the mucosa is formed by a thin layer of smooth muscle cells, the lamina muscularis mucosa. This sheet only consists of two to six layers of cells [4]. The submucosa consists of connective tissue bordering the lamina muscularis mucosa and the outer two layers of smooth musculature (lamina muscularis externa). Cell types present in this area are mainly fibroblasts, some macrophages, mast cells, few eosinophils, and plasma cells. All cells are embedded in a matrix of loosely packed collagen bundles and some elastin fibres. There are also large arteries and veins present that branches to both the lamina mucosa and the lamina muscularis externa [5].

2.1.3 The epithelium – barrier function and interface to the gut lumen

Mucosal surfaces are lined by a simple epithelium. Epithelial cells establish and maintain a barrier between the external environment and the internal milieu. The mammalian intestine is covered by a single layer of epithelial cells that is renewed every 2–3 days. The function of the epithelium is enhanced by protective effects of products of goblet cells (mucins, trefoil peptides) in the intestine, which are secreted onto the mucosal surface. Functionally, the barrier results from tight junctions connecting the epithelial cells. Transmembrane proteins such as claudins play a crucial role in building and determining the function of tight junctions; claudins are regulated by several cytokines (e.g. TNF-α) and occludins, transmembrane proteins that can regulate the barrier. These proteins may

be a link between barrier function and inflammatory and immune response. Just as important as knowing how the epithelium is forming an effective barrier is the analysis of the epithelium playing an active role in the mucosal immune response. The epithelium mediates innate immune responses by expressing a large number of Toll-like receptors (TLRs) that serve as a pattern recognition receptors (PRRs) for microbial products such as LPS (binding to TLR-4), bacterial DNA (TLR-9) and viral replication intermediates (TLR-3) [6; 7]. These receptors enable epithelial cells to sample and monitor the intestinal flora and react on the luminal bacterial changes with an appropriate output of chemokines and cytokines. There are further PRRs expressed by the epithelium, including the NOD proteins, which serve as a signal transduction unit sensing contents of the lumen and co-ordinating a mucosal response to potential pathogens. Key cellular components mediating the mucosal immune response are antigen-presenting cells such as dendritic cells (DCs) and mucosal lymphocytes. DCs can be primed by antigens that permeated the epithelial barrier or been obtained by direct luminal sampling. They stimulate Th1 lymphocytes, which produce cytokines (mainly IL-2 and IFN-γ, also others) that results in the activation of macrophages. Active macrophages produce a broad spectrum of cytokines and other mediators, including IL-12, IL-18 and more IFN-γ, which further stimulates Th1 lymphocytes to create a feedback cycle. IL-1, IL-6, and TNF-α are also released by macrophages, which leads to the amplification of the inflammatory response by stimulating other, diverse cell types. Several chemokines are involved as well, for example MIF (macrophage inhibitory factor) that enhances the expression of TLR-4. The main signaling pathways involved in this activation of key immune and inflammatory cells are the NF-κB (nuclear factor-kappaB), the MAP (mitogen-activated protein) kinase and the PI3 (phosphotidyl inositol) kinase pathways [8; 9; 10].

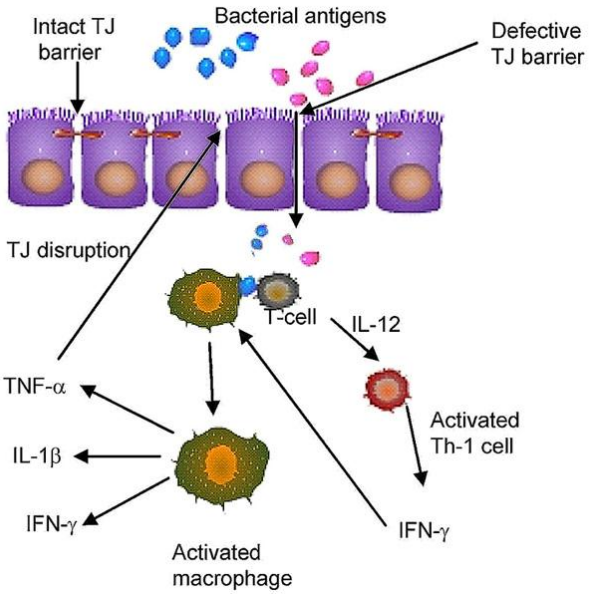

Figure 2-2: Barrier function of the intestinal epithelium.
In case of defective barrier bacterial contents can enter the tissue, activate macrophages and T cells, which then produce pro-inflammatory cytokines such as TNF-α. Taken from [11].

As the epithelium of the intestine is a very dynamic area with a very short turn-over in comparison to other tissues, repair and healing processes also occur fast under normal conditions. Such processes start with an initial phase called restitution [12; 13] in which the continuity of the surface epithelium is re-established. This is done by extension and migration of the epithelial cells from the edge of the wound (mucosal ulceration), cell proliferation, the production of extracellular matrix components, and finally remodelling to rebuild the normal intestinal architecture. Restitution provides a rapid mechanism for covering a defect in the barrier and does not involve proliferation of epithelial cells [12; 14]. It results in an area that, while protected, is not physiologically functional. Healing requires that the epithelial cells on the margins of the defect proliferate, differentiate, and migrate into the damaged area to restore the normal cellular architecture and function. These events are regulated by cytokines, growth factors (EGF, TGF-α) and trefoil factors [15; 16]. Remodelling is also dependent on the balance between the production of extracellular matrix (ECM) components, matrix metalloproteinases (MMPs) and their inhibitors, the tissue inhibitors of metalloproteinases (TIMPs)[17].

To know about the function of the epithelium is important to understand the susceptibility to IBD, as there are several mouse mutant lines deficient in the expression of epithelial-specific proteins (e.g. keratin-8, intestinal trefoil factor (ITF)) that spontaneously develop colitis [18]. A better knowledge of mucosal physiology would provide important insights into the pathology of IBD, which is still incompletely understood. Also, the impact of MMPs on the development, onset, and recovery of the disease remains elusive.

2.2 Inflammatory Bowel Disease (IBD)

Inflammatory bowel diseases (IBDs) are chronic inflammatory disorders of the gastrointestinal tract. In the Western World about 1 in 1000 people is affected by this relapsing and remitting disease, which is still incurable. Genetic, psychosomatic, and environmental factors such as gut flora and nutrition are known to be involved in the onset as well as progression of the disease. The onset of IBD typically occurs in the second and third decades of life and a majority of affected individuals progress to relapsing and chronic disease. Family aggregation has long been recognized. The inheritable component seems stronger in Crohn's disease than in ulcerative colitis [19; 20].

The two major types of IBD are Crohn's disease (CD) and ulcerative colitis (UC). There are also other forms of IBD that are less prevalent, e.g. collagenous colitis or lymphocytic colitis [21; 22; 23]. The main difference between Crohn's disease and ulcerative colitis is the site of inflammation: UC is restricted to the large intestine whereas CD can occur in the small and/or the large intestine (Figure 2-3).

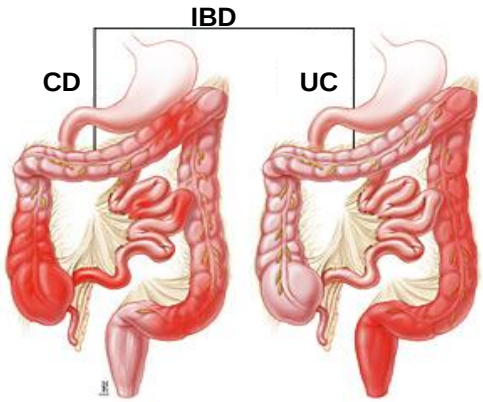

Figure 2-3: Schematic representation of the affected areas of patients suffering from IBD.
Both CD and UC are characterized by mucosal ulceration, which is continuous and restricted to the colon in UC but patchy and possibly spread through the whole intestinal tract in CD. Taken from http://www.hopkinsmedicine.org.

Histologically, ulcerative colitis is restricted to the mucosa, while Crohn's disease is affecting the whole bowel wall. Key features of UC include diffuse mucosal inflammation extending proximally from the rectum to different intensities. Together with severe inflammation and the associated production of a complex mixture of inflammatory mediators, extensive superficial mucosal ulceration develops [19]. Histopathological features include the accumulation of neutrophils within the lamina propria and the crypts, where they form micro-abscesses (Figure 2-4). Depletion of goblet cell mucin is also common. In contrast, CD is rather characterized by the aggregation of macrophages that frequently form granulomas (Figure 2-4). Although any site of the gastrointestinal tract may be affected, involvement of the terminal ileum is most common [19; 23].

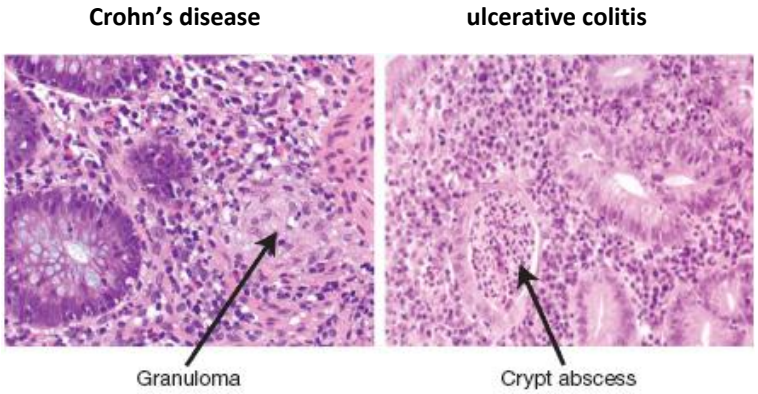

Figure 2-4: Histological features of IBD: CD versus UC.
Crohn's disease-biopsy from a terminal ileum with active disease. The picture shows a granuloma composed of compact macrophages, giant cells, and epithelioid cells. The nodule is surrounded by marked infiltration of lymphoid cells, plasma cells and other inflammatory cells. Ulcerative colitis-colonic mucosal biopsy was taken from a patient with active disease as well. The crypt abscess is composed of transmigrated neutrophils and the surrounding epithelium exhibits features of acute mucosal injury. Adapted from [23].

The main clinical features of IBD are diarrhoea, abdominal pain, blood loss, loss of peristaltic function, and bowel obstructions. Both diseases are associated with several extra-intestinal manifestations such as liver problems, arthritis, skin manifestations and eye problems [24; 25]. In general, people suffering from IBD have a higher risk of developing colon cancer, especially those with UC [26].

Concerning the cytokine secretion by activated lymphocytes, a typical and strong T helper type 1 (Th1) cytokine profile (increased secretion of tumor necrosis factor (TNF)-α, interleukin (IL)-2, interferon (IFN)-γ, IL-12, IL-18) was described in individuals suffering from CD, in contrast to much weaker support for a T helper type 2 (Th2) pathogenesis (increased secretion of IL-4, IL-5, IL-10) in UC patients [27; 28; 29; 30; 31; 32]. While Th1 cytokines are not raised in UC, there is only little evidence for increased Th2 cytokine levels. However, the presence of autoantibodies, such as the anti-neutrophil cytoplasmatic antibody, is suggestive of a Th2 pathogenesis in UC [33]. A massive overexpression of matrix-degrading enzymes was also found in fibroblasts in UC. These cells are ultimately responsible for ulceration and fistula formation [34; 35].

2.2.1 Factors leading to IBD

Genetic and environmental factors act together to cause inflammation in IBD. In susceptible individuals, the luminal microflora can provide antigens and adjuvants that stimulate either pathogenic or protective immune responses. Environmental triggers are necessary to initiate or reactivate the disease (Figure 2-5).

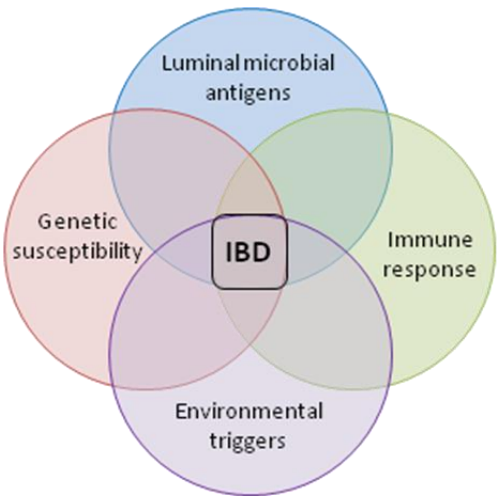

Figure 2-5: Interaction of various factors influencing IBD.
The main factors contributing to the development of IBD are a genetic susceptibility and an impaired immune response; both are influenced by the luminal bacteria. Several environmental triggers are necessary to initiate the disease. Adapted from [36].

Concerning environmental factors, it has to be stated that both UC and CD are predominantly associated with industrialized temperate regions and are rare in tropical countries with poor sanitation and a low level of overcrowding. The highest incidence rates and prevalence of UC and CD have been reported from northern Europe, the UK, and North America. Low incidence areas can be found in southern Europe, Asia, and most developing countries [37]. Interestingly, migration to developed countries leads to an increased risk of coming down with IBD [38; 39; 40], further supporting the hypothesis that genetic factors are not solely responsible for the disease. Various environmental factors have been proposed to contribute to the enhanced risk of IBD in industrialized countries; including nutrition, infections [41; 42], smoking status [43; 44; 45; 46; 47], and the level of stress experienced [48; 49; 50].

Ulcerative colitis and Crohn's disease are polygenic diseases (Figure 2-6). Genetic predisposition was further substantiated by the discovery of susceptible regions on 12 chromosomes so far. Susceptible loci for UC were found on chromosome 12, for CD on chromosome 5, 14, and 16, and on chromosome 1, 6, and 19 for both UC and CD [21; 51; 52]. Alterations in genes of the immune system such as NOD2, IL23R and ATG16L1 are specifically associated with CD in white populations but are not observed in patients suffering from UC [53; 54; 55].

Concerning NOD2, three major polymorphisms in or around the external leucine-rich repeat within the recognition region of the nucleotide-binding oligomerization domain molecule 2 (NOD2) on chromosome 16 were detected [54; 56]. Nod molecules (NOD1 and NOD2) together with Toll-like receptors (TLR1 to 9) belong to the pattern recognition receptor family, which are expressed by gut epithelial cells, monocytes, and particular dendritic cells (DCs) in the intraepithelial and subepithelial layers. These cells are specialized for sampling microbial and other luminal antigens [57; 58] already within the gut by sending long dendrites into the lumen.

Therefore, a genetically determined disturbance in recognizing the conserved pathogen associated molecular patterns (PAMPs) of these microbial antigens and/or subsequent signaling may result in decreased activation of nuclear factor κB (NF- κB), which is a pivotal transcriptional factor controlling proinflammatory cytokines. A consequence of mutations in NOD2 may therefore be a decreased ability to kill pathogenic gut bacteria [59; 60]. In addition, there is a possible role for TLR4 polymorphisms in IBD suggested by the observation that mice with a missense mutation of the *Tlr4* gene have a high incidence of spontaneous colitis [61; 62]. Altogether, mutations in PAMP signaling seem to be generally associated with IBD, and diminished PAMP signaling itself may be a contributing factor to the development of the disease [63]. Interestingly, NOD2 has not been found to be associated with CD in Japan [64], highlighting the complex nature of this disease.

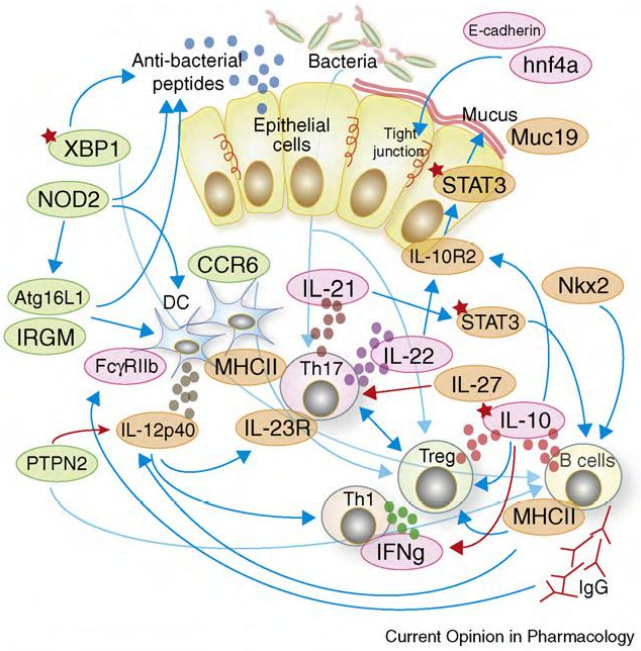

Figure 2-6: IBD immune network.
Genes specific for both CD and UC (orange ellipses), for CD (green ellipses) and for UC (pink ellipses) have been identified. Previous and current data from animal models indicate that IBD-associated genes are positively (blue lines) or negatively (red lines) linked together, making a complicated network. For example, both NOD2 and autophagy, which are primarily involved in epithelial defense against commensal microbiota, are controlling IL-23/Th17 axis through antigen presentation. The IL-23/Th17 axis can directly activate epithelial defense through IL-22 and also represent a key determinant of differentiation of effector versus regulatory immune responses. Regulatory immunity can modify the IL-23/Th17 axis and also influence epithelial defense. Taken from [65].

It is also known that the gut microbial flora plays an important role in the induction of IBD. Multiple bacterial strains as well as special bacterial products (e.g. flagellin, LPS) are able to induce proinflammatory cytokines like TNF-α and interleukin-8 (IL-8) in macrophages and epithelial cells in the gut [66]. In general, it was shown that experimental colitis cannot develop when mice are kept in a germ-free environment [67; 68]. This suggests that the normal intestinal microflora is required to initiate or maintain the inflammatory process of IBD. A dysregulation of the gut flora could be one of the causes of IBD. There is also some indication that IBD could be considered an autoimmune disease as antigens (bacteria) are present in the body from birth onwards and, to some degree, have always access to the internal milieu. Thus, in case the immune system fails to differentiate between self and foreign antigens, an autoimmune reaction against the normal intestinal flora might be the consequence [69; 70].

2.2.2 Animal models of IBD

Several animal models have been developed to mimic IBD. In an ideal model, the key characteristics like morphological alterations, inflammation, symptoms, pathophysiology, and course of disease are similar to human IBD. Treatments applied should exhibit the same effects. The genetic background of the animal should be well defined and the immune system well characterized. Environmental factors, especially nutrition and enteric flora, should be controllable, and the induction of colitis should be stable, reproducible, and predictable.

Mice are relatively easy and cheap to maintain compared to other mammals, have a short reproduction cycle, and allow genetic manipulation, including the cell type specific deletion of genes. The mouse genome is 95% identical to that of humans. Inbred strains provide a stable and characterized genetic background. Furthermore, mice, if bred in animal facilities equipped with individually ventilated cages (IVC), environmental factors and microflora can be controlled (reviewed in [71]).

Commonly used animal models for IBD include gene knock-out, chemically induced, and adoptive transfer models (Figure 2-7). The IL-2 knock-out [72] and IL-10 knock-out [73] mouse models are examples for gene knock-out models of IBD; in both models colitis is most probably due to an increased Th1 immune response accompanied by a lack of regulatory T-cells. Inducible colitis models include the induction by 2,4,6-trinitrobenzene sulfonic acid (TNBS) enema or dextran sulfate sodium (DSS) [74; 75; 76; 77; 78; 79; 80]. TNBS and DSS are thought to induce colitis by damaging the mucosal barrier [77; 78; 81; 82]. Frequently applied adoptive transfer models use the transfer of CD4+ T-cells expressing high levels of CD45RB (CD45Rbhigh) [83] or the marker for naive T-cells CD62L [84] into mice with severe combined immunodeficiency (SCID).

A shared characteristic of the described models (Figure 2-7) is the combined impact of genetic factors, intestinal flora and other environmental triggers on the severity of the inflammation [85; 86; 87; 88]

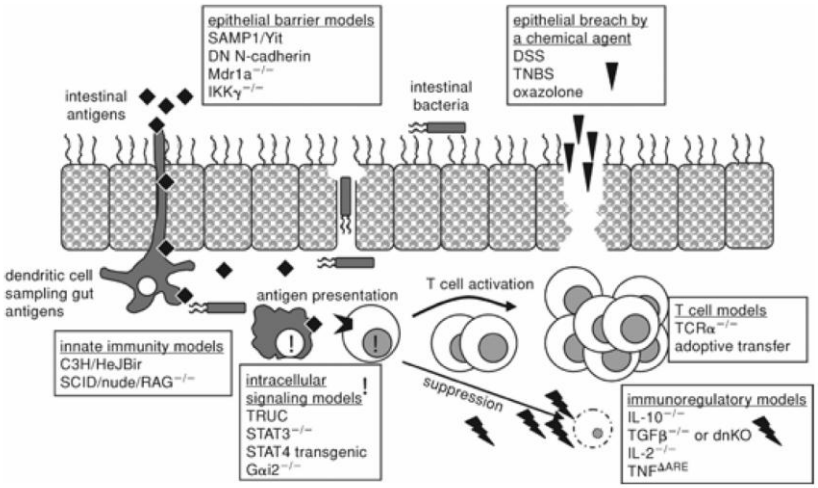

Figure 2-7: Overview of Mouse Models of Inflammatory Bowel Disease.
Several mouse models for IBD are known, including various gene-deficient mice as well as chemical models, and T cell transfer models, which allow studying different aspects of the disease. Taken from [89].

2.2.2.1 Induction of colitis by dextran sulfate sodium (DSS)

Dextran sulfate sodium (DSS) is a heparin-like polysaccharide containing up to three sulfate groups per glucose molecule (Figure 2-8). Induction of colitis in rodents by application of DSS in the drinking water is a widely used and well characterized model of colitis in mice, first described by Okayasu *et al.* 1990 [80]. Morphological changes are similar to human ulcerative colitis [80]. Additionally, anti-colitis drugs applied in human ulcerative colitis such as sulfasalazine, olsalazine and mesalazine have a therapeutic effect in DSS colitis [90; 91]. The inflammation is restricted to the large intestine [80; 92]. Erosion and inflammation of the mucosa are both most frequent and severe in the distal part of the colon [74; 80; 92]. Its severity is dependent on the concentration of DSS [93], but also on the molecular weight [75]. Concentrations described in the literature range between 1% and 7%. The most commonly used molecular weight is 40,000 Da.

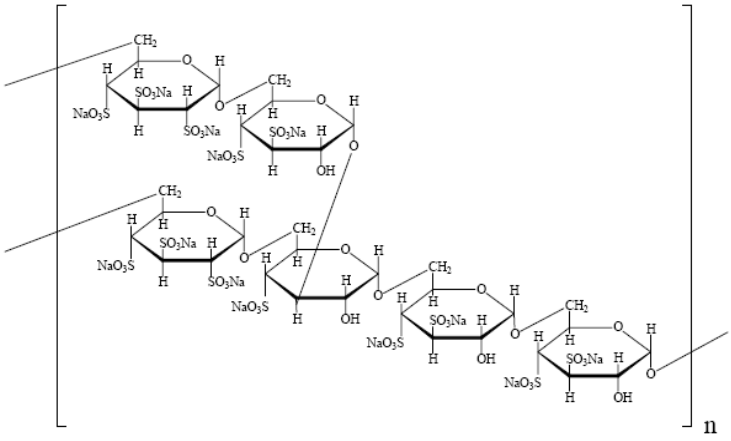

Figure 2-8: Chemical structure of dextran sulphate sodium (DSS).
The picture was taken from www.sigmaaldrich.com/fluka/product.

The exact mechanism of colitis induction by DSS remains unknown. A direct toxic effect on the epithelium could lead to the inflammation [94]. In the acute phase (from day 3 to 7), prior to the appearance of inflammatory processes, an increased permeability of the intestinal mucosa has been shown [81]. Due to the damage of the epithelial barrier, toxic products of luminal bacteria such as endotoxin or peptidoglycans might permeate into the mucosa causing damage to the epithelial cells of basal crypts and thereby inducing an inflammatory reaction. As DSS is taken up by macrophages, inhibition of phagocytic capacity is another possible mechanism rendering the intestinal epithelium more susceptible to bacterial infection [74].

The role of lymphocytes in the induction and maintenance of the disease is a matter of debate and published results have so far been contradictory. Acute DSS-induced colitis occurs in SCID-mice, lacking B- and T-lymphocytes [95; 96], though in Rag-1 knock-out mice, lacking lymphocytes in general, severity of DSS-induced colitis is decreased dramatically [97]. While acute DSS-induced colitis is characterized by proinflammatory cytokines *e.g.* IL-1 and TNF-α accompanied by the Th1 immune response through the expression of IL-12 and IFN-γ [93], chronic DSS-induced colitis shows a mixed Th1/Th2 cytokine profile [98].

Another controversy in the DSS model is the effect of enteric bacteria: On one hand, it was shown that DSS treatment of germfree IQI/Jic mice leads to an even more severe colitis compared to SPF mice [99]. On the other hand, it was reported that the molecular weights of DSS in the feces were the same as those of the DSS in the drinking water [75], suggesting that the chemical cannot be degraded by gut bacteria in the intestinal lumen . Antibiotic treatment improves acute DSS colitis but has no effect on established chronic colitis [100].

Several studies using mouse models to analyze Toll like receptor (TLR) signaling have suggested a role of this pathway in DSS-induced colitis. While MyD88 knock-out mice showed severe colitis after DSS treatment that is refractory to antibiotic treatment [101],

colitis in TLR9 knock-out mice was reduced compared to wildtype mice [102], indicating that disturbance of multiple TLR-pathways is detrimental for the homeostasis of the intestinal epithelium, while CpG-motifs of the bacterial flora might trigger DSS-induced colitis. Recently, probiotic bacteria, such as *Proprionibacterium freudenreichii, Bifidobacterium infantis* and *Bifidobacterium adolescentis* have been reported to be able to attenuate DSS colitis [103; 104; 105]. Mähler *et al.* described the influence of inbred background on the extent and severity of colitis after exposure to DSS: significant differences for all parameters scored have been found for all strains. Susceptibility to caecum lesions decreased from C3H/HeBir, C3H/HeJ, C57BL/6J to 129S2/SvPas. Concerning lesion formation in the colon, C3H/HeBir, C3H/HeJ, C57BL/6J and 129S2/SvPas mouse strains were highly susceptible whereas, DBA/2J was less susceptible to DSS [86; 102]. Melgar *et al.* found that five days of treatment with 3% for C57BL/6 and 5% for BALB/c strains revealed similar symptoms in the acute phase. However, disease resolved in BALB/c mice but became chronic in C57BL/6, indicating that BALB/c are more resistant to DSS than C57BL/6 mice [106].

2.3 Matrix metalloproteinases (MMPs)

MMPs, also known as matrixins, build a large family of highly homologous zinc-dependent endopeptidases, which are widely distributed in all kingdoms of life [107]. They belong to the superfamily of metzincin proteases, together with a disintegrin and metalloproteinases [108] [108] and ADAM proteases with thrombospondin motifs (ADAMTSs) [109]. MMPs play important roles in many physiological processes such as embryonic development, wound healing, and tissue repair. However, they also show unwanted activities in a variety of disorders, including cancer, arthritis, and cardiovascular diseases [110; 111; 112; 113; 114]. Although they are best known for their capacity to degrade extracellular matrix (ECM) components, they have become increasingly recognised for their functions in processing of cell surface receptors, chemokines and signaling molecules [115].

2.3.1 Classification and substrate specificities

The 24 MMPs that have been identified in humans to date can be classified in two main groups based on their structural characteristics: secreted-type and membrane-anchored or membrane-type (MT)-MMPs (Figure 2-9). Domain organisation and substrate specificity are criteria for further division [116]. The molecular structure shared by most MMPs consists of four functional domains: a signal peptide that targets them for secretion, a propeptide of around 10 kDa containing the conserved cysteine switch motif PRCGXPD, a catalytic domain of around 20 kDa featuring the conserved zinc-binding motif HEXXHXXGXXH, and a C-terminal hemopexin-like domain of around 30 kDa that mediates substrate and inhibitor interactions. A linker peptide of variable length, also called the ‘hinge region’, separates the catalytic domain from the hemopexin-like one. Divergence from this basic core design reflects the evolution of MMPs into distinct subgroups. The secreted-type MMPs can be further divided into collagenases, stromelysins, gelatinases, matrilysins, and other MMPs, according to differences in structure as well as substrate specificity (Figure 2-9). MMP-1, MMP-8 and MMP-13 are designated as collagenases and have the ability to cleave collagens I, II and III at a specific site three-fourths of the distance from the N-terminus [17; 107]. In addition, they are also able to proteolytically process other ECM proteins as well as certain cytokines such as IL-8 [117] and TNF [118]. Stromelysins, which share their structural design with the collagenases, degrade a variety of ECM components but are not able to cleave native collagen. Other substrates of the stromelysins include stromal-cell derived factor-1, E-cadherin, and pro-interleukin-1 beta [119]. The gelatinases comprise two members, MMP-2 (gelatinase-A) and MMP-9 (gelatinase-B). They feature three fibronectin type II repeats located inside the catalytic domain which facilitate binding and digestion of denatured collagens (gelatines). Collagen

types I, IV, V, VII, X, IX, elastin, fibronectin, aggrecan, vitronectin, and laminin are among the substrates for gelatinases as well as various non-ECM molecules like pro-TNF, TGF-β, pro-IL-1β, pro-IL-8, and monocyte chemoattractant protein (MCP)-3 [118; 119; 120; 121]. MMPs with the simplest domain arrangement of all are the matrilysins (MMP-7 and MMP-26) as they lack the hinge region and the hemopexin domain. Whereas both family members share the ability to degrade ECM proteins like type IV collagen, laminin, and entactin, they also exhibit differential activities: MMP-7 mediates the ectodomain shedding of several cell surface molecules like Fas ligand [122], E-cadherin [123], and syndecan-1 [124], and MMP-26 has been shown to activate proMMP-9 (see 1.2 Regulation of MMP activity). In comparison, only little is known about other secreted-type MMPs which diverge too much in sequence and substrate specificity to be classified in one of the previous subgroups. MMP-11 shows weak proteolytic activity against a number of ECM components such as collagen type VI, gelatine, and laminin but it also digests α1-proteinase inhibitor and insulin-like growth factor binding protein-1 (IGFBP-1). MMP-12 or metalloelastase is a very potent enzyme for degradation of the fibrous ECM protein elastin [17; 107; 116].

The group of MT-MMPs includes type I and type II transmembrane MT-MMPs as well as GPI-anchored MT-MMPs (Figure 2-9). The type I transmembrane proteases comprise MT1-MMP (MMP-14), MT2-MMP (MMP-15), MT3-MMP (MMP-16) and MT5-MMP (MMP-24). They are characterized by a long hydrophobic sequence followed by a short cytoplasmic tail that is involved in numerous cellular events, such as activation of MERK/ERK and src-tyrosine pathways. Besides their capacity to cleave a variety of substrates including ECM components, they are the major physiological activators of proMMP-2. MT4-MMP (MMP-17) and MT6-MMP (MMP-25) belong to the GPI anchored MT-MMPs. In contrast to the low enzymatic activity of MT4-MMP against ECM proteins, MT6-MMP potently processes gelatin, collagen IV, fibronectin, fibrin, and proteoglycans. The two members of the type II transmembrane MT-MMPs, MMP-23A and MMP-23B, have identical amino acid sequence, but are encoded by distinct genes. They are unique among the matrixin family as they lack the signal peptide, the cysteine-switch motif and the hemopexin domain. Instead, they contain cysteine array and immunoglobulin domains in their shortened cytoplasmic tail. So far, no substrate for the MMP-23 enzymes has been identified [17; 107; 116].

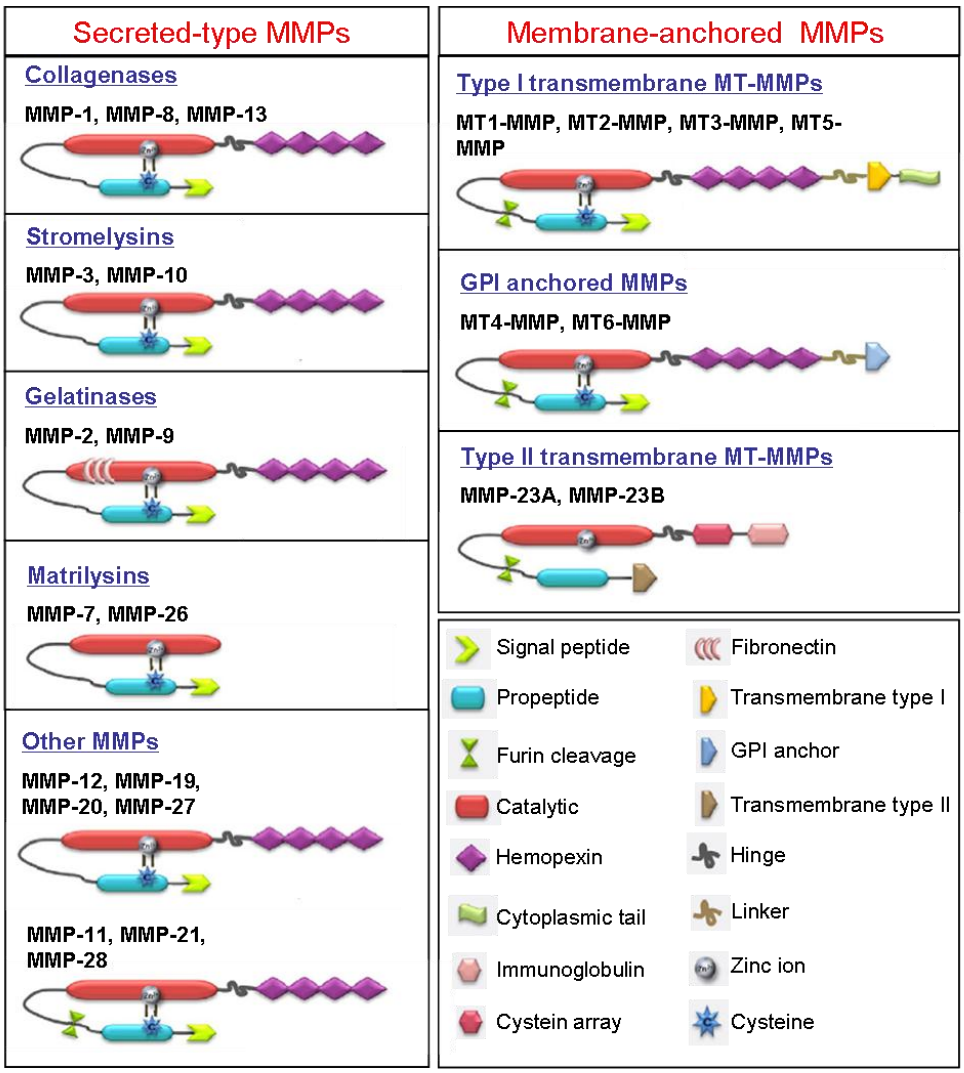

Figure 2-9: Classification of MMPs based on structural characteristics.
Adapted from [107].

2.3.2 Regulation of MMP activity

MMP activity is regulated at three main levels: gene transcription, posttranslational activation of zymogens, and interaction of MMPs with inhibitors [110; 113]. Additional mechanisms that fine-tune MMP activity include mRNA stability, cell-surface recruitment, and autolysis [113] (Figure 2-10).

2.3.2.1 Transcriptional regulation

Transcription is considered as key regulatory step for most MMPs (excluding MMP-2) [107; 110; 113]. Whereas under normal physiology, the majority of MMPs is expressed at low or non-detectable levels, their gene transcription can be induced in a highly cell and tissue specific manner by a variety of signals. These include pro-inflammatory cytokines such as TNF-α, IL-1, and IFNs, growth factors such as EGF, KGF, and VEGF, and ECM

proteins or cell-cell interaction [113] (Figure 2-10). The main signaling pathways involved are the p38 mitogen activated protein kinase (MAPK, ERK1/2) pathways, the NF-κB, and the JAK-STAT pathways [107; 113]. MMP-1 transcription, for example, is induced in dermal fibroblasts in response to IL-1 via MAPK signaling. This pathway activates members of the Jun and Fos families of oncoproteins, which bind to the AP-1 transcription-factor binding site. The AP1-site is thought to be the major mediator of MMP gene regulation and is present in most MMP promoters. The polyomavirus enhancer-A binding protein-3 (PEA3) site, which binds oncoproteins of the ETS family, is another important transcription-factor binding site shared by many MMPs. It is thought to act cooperatively with the AP-1 site to promote MMP production in cancer cells. Transcription of MMP-1, -3, -9, -13 and -14 can be induced by TNF-α through NF-κB signaling, and the effect of interferons on MMP expression are mediated by STAT sites [107; 113; 125]. Constitutive expression, as observed for MMP-2, MT1-MMP, and MMP-28, is associated with the lack of a TATA box and the presence of the GC cis-element, which binds the ubiquitous Sp1 family of transcription factors [125].

MMP transcription can also be influenced by genetic variation in the promoter region of MMP genes, which affects affinities for transcription factors or creates or abolishes transcription factor binding sites. Such functional polymorphisms have been demonstrated in various MMP genes, for example MMP-2, MMP-3, MMP-9, and MMP-12, and are often associated with disease susceptibility [125].

2.3.2.2 Activation of zymogens

MMPs are initially synthesized as inactive zymogens (proMMPs) with a pro-peptide domain that must be removed to activate the enzyme (Figure 2-10) [17; 116]. In its inactive conformation, the cysteine in the propeptide (the ‘cysteine switch’) ligates the catalytic zinc to maintain latency of the proMMP. For activation, the prodomain of MMPs is removed in an autocatalytical manner or by other proteases, and the cysteine is replaced by a water molecule to allow enzyme catalysis to proceed. Dependent on the type of MMP, this process takes place either in the pericellular space, intracellularly or at the cell surface. Most MMPs are secreted as proMMPs and activated by other active MMPs or serine-proteases. For example, MMP-1, MMP-2, and MMP-26 are able to activate proMMP-9, and MMP-7 activates proMMP-1, proMMP-2, and proMMP-9. Plasmin is thought to be a major contributor to initiate extracellular proMMP activation via the cysteine switch. Some MMPs (MMP-11, MMP-28, and the MT-MMPs) can also be activated intracellularly. These proteases contain a conserved RXRXKR furin-like enzyme recognition motif between their pro- and catalytic domains and, thus, can be activated by furin, a serin protease, within the Golgi network [17]. MMP-2 is activated at the cell surface through a unique multistep pathway that involves MT1-MMP and the tissue inhibitor of metalloproteinases 2 (TIMP-2): The C-terminal domain of TIMP-2 facilitates non-inhibitory binding to the proMMP-2 C-terminal domain via electrostatic interactions to allow an adjacent free, active MT1-MMP to process proMMP-2 into an active enzyme.

More recently, it has also been suggested that proMMP-2 can be activated by coagulation factors such as protein C, thrombin, and factor Xa via an MT-MMP independent route [17; 110; 113].

2.3.2.3 Interaction with inhibitors

MMP activities are blocked by two major types of endogenous inhibitors: general inhibitors, such as α2-macroglobulin that are present in the plasma and tissue fluids, and by more specific inhibitors, such as TIMPs (Figure 2-10) [17; 126]. α2-macroglobulin is a glycoprotein, consisting of four identical subunits of 180 kDa. It inhibits most proteases by entrapping the proteinase within the macroglobulin, followed by clearance of the complex through receptor-mediated endocytosis (by Low density lipoprotein receptor-related protein 1, LRP-1 (CD91)). Four human TIMPs (TIMP-1, -2-, -3- ,-4) have been identified; they are anchored in the ECM or secreted extracellularly. TIMPs consist of 184 - 194 amino acids. The N-terminal region binds to the MMPs' catalytic domain and inhibits MMP activity, whereas the C-terminal region interacts with the hemopexin domain of proMMP-2 and proMMP-9 to stabilize the proenzyme inhibitor complex. TIMPs inhibit all MMPs tested so far, although TIMP-1 is a poor inhibitor for most type I MT-MMPs [17]. TIMP-3 has been shown to potently block MMP-2 and MMP-9 as well as the majority of ADAMs. TIMP-2 is unique in that it also functions as activator of MMP-2 by specific interaction with MT1-MMP and proMMP-2 at the cell surface (see above, Activation of zymogens) [17; 127].

Several other proteins have been described to inhibit MMPs: RECK, a GPI-anchored glycoprotein that suppresses angiogenesis, inhibits MMP-2, MMP-9, and MMP-14 [128]. Other molecules that can block MMP activity include TFPI2, a serine protease inhibitor, and PCPE, a C-terminal proteinase enhancer [17; 127].

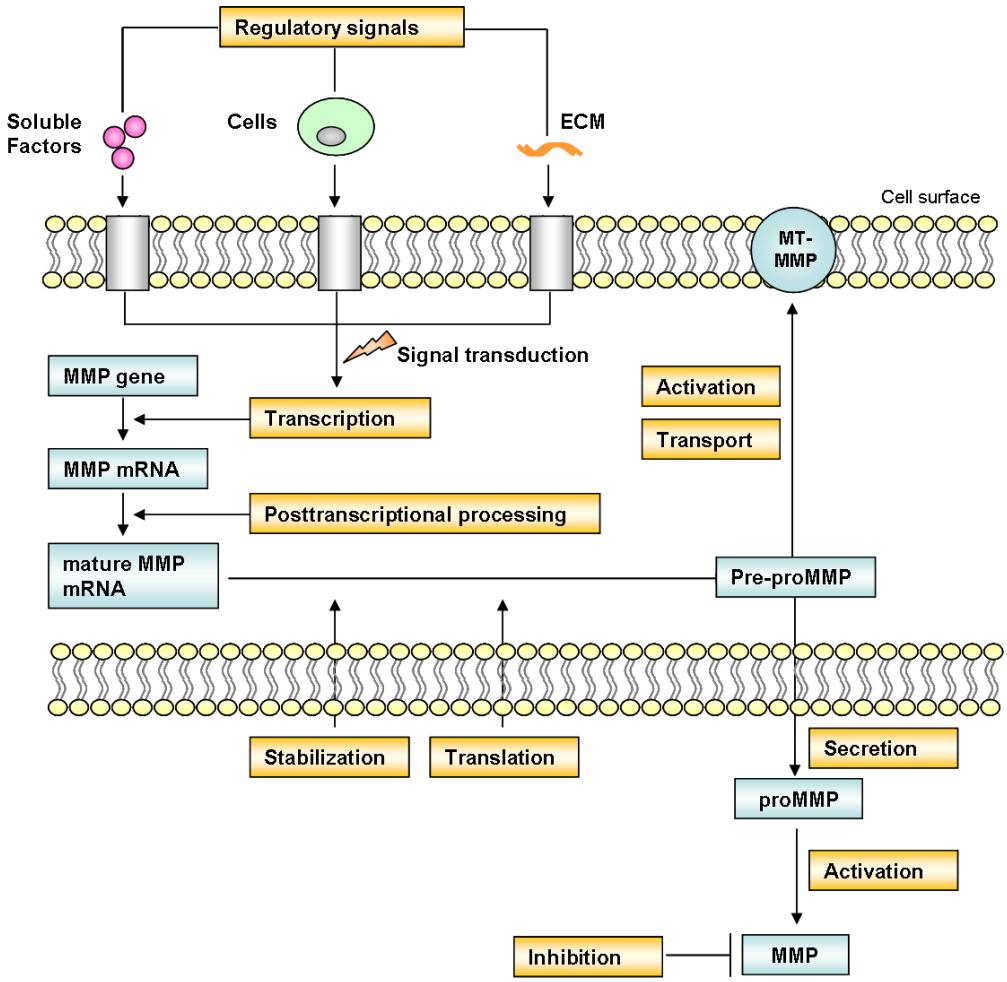

Figure 2-10: Levels of regulation of MMP expression and activity.
Diverse regulatory signals, such as soluble factors, extracellular matrix (ECM)-cell interactions or cell-cell contacts interact with specific receptors at the cell surface and initiate a cascade of events that lead to the generation of functional matrix metalloproteinases (MMPs), which are localized to the cell surface (MT-MMPs) or secreted to the extracellular space (proMMPs). ProMMPs are activated in an autocatalytical fashion or by other activated MMPs. MMP activity can be inhibited by diverse endogenous inhibitors. Adapted from [113].

2.3.3 MMP functions in health and disease

MMPs play a primary role in many aspects of normal physiology, including embryonic development, cell migration, wound healing, and tissue resorption. At the same time, MMP deregulation is implicated in diverse human pathologies, like cardiovascular diseases, rheumatoid arthritis, neurological disorders, cancer, and other [107; 110; 113].

Early characterisation of MMP knockout mouse models has provided insight into the role of some of the proteases: MMP-14 deficiency, for example, caused multiple abnormalities in the remodelling of skeletal and connective tissues, as well as impaired angiogenesis. Mice lacking MMP-20 had defects in tooth development and Mmp3-null mice showed altered mammary gland morphogenesis. However, the vast majority of MMP single-knockout mice displayed no major physiological alterations, pointing towards

mechanisms of enzymatic compensation and redundancy. Transgenic mouse models overexpressing different members of the MMP family validated the contribution of the proteases to tumour progression, since high levels of MMPs often correlate with poor clinical outcome in cancer patients [107].

Several activities of the proteases can be linked to tumour growth: first, MMPs can support vascularisation by mobilising proangiogenic factors, such as basic fibroblast growth factor (bFGF), vascular endothelial growth factor (VEGF) or transforming growth factor-β (TGF-β) [115]; they can also process cell-adhesion molecules, thereby promoting cancer metastasis. MMP-7 has been shown to cleave the proapoptotic FAS ligand, allowing tumour cells to become resistant to apoptosis signals [113; 115]. Nevertheless, early clinical studies involving synthetic MMP inhibitors (MMPIs) have not shown the desired efficacy. In fact, MMPIs even promoted cancer progression in some cases by enhancing tumour vascularisation or expression of MMPs, such as MMP-9 in human fibrosarcoma cells. With hindsight, these results are not surprising as MMP function has turned out to be far more complex than previously thought. MMP-8, -12, and -19, for example, have been shown to act as tumour suppressors [129], and the sheddase activities of some MMPs has been linked to angiogenesis inhibition rather than promotion. MMP-2, -7, -9, and -12, for instance, can process plasminogen to release the potent angiogenesis inhibitor angiostatin [115]. Furthermore, MMPs have recently been demonstrated to be able to activate or degrade chemokines and cytokines [115]. In summary, MMPs exhibit functions that exceed their well-accepted role in extracellular matrix remodelling. Future therapeutic strategies for intervention with MMP activity need to consider their emerging roles as regulators of inflammation and cell signaling.

2.3.4 MMPs in healthy and diseased colon

2.3.4.1 MMP and TIMP protein expression in healthy colon

Under normal conditions, MMPs are present at low levels, usually in the inactive form, and are responsible for normal tissue homeostasis. MMP-2 expression was observed in subepithelial and pericryptal fibroblast/myofibroblasts, in lamina propria mononuclear cells (macrophages and lymphocytes), and in vascular endothelial cells. Also some expression was seen in the laminar muscularis mucosa. In contrast, only a few cells in the lamina propria were found to express MMP-3 and MMP-9. Neither MMP-1 nor MMP-7 was expressed in normal colon. MMP-10 expression was detected at low levels in colonic epithelial cells. Expression of their inhibitors TIMP-2 and -3 were observed in the epithelium of the colon as well as in few lamina propria mononuclear cells [130]. In addition, also MMP-19, -26, and -28 expression was shown in normal intestine [131].

Normal colonic epithelial cells express transcripts for MMP-1, -3, -7, -10, and -12. Weak expression for MMP-2, -8, and -9 could be found, whereas MMP-11, -13, and -14 were not detected at RNA level [132]. The inconsistence in detecting MMPs in healthy colon

tissue can be explained by using different methods for detection – immunostaining [130] versus mRNA analysis [132]. MMPs released by intestinal epithelium may be involved in the pathogenesis of IBD by promoting local mucosal damage.

2.3.4.2 MMP and TIMP expression in intestinal epithelial cell lines

MMP expression has been detected so far in several cell types of the intestinal mucosa, like myofibroblasts, smooth muscle cells, activated T cells, and macrophages. However, only little is known about expression pattern, regulation, and function of these proteinases in the epithelium of the gut. Spontaneous expression of MMP-1, -3, -7,-10, -11, and -13 was detected in several intestinal epithelial cell lines (HT-29, DLD-1), whereas other MMPs were undetectable [132]. After stimulation with TNF-α, levels of MMP-3, -10, and -13 were increased. MMP-12 mRNA, which was not expressed in unstimulated cells, could be induced by TNF-α treatment. By contrast, MMP-2, -8, -9, -14 mRNA remained undetectable even after cytokine exposure. TIMP mRNA levels remained unchanged as well.

2.3.4.3 MMPs and TIMPs in IBD

The expression and functional activity of several MMPs are increased in epithelial cells from patients with active IBD. Ulceration is a main feature of IBD. High levels of both MMP-1 and MMP-3 were detected in the granulation tissue around ulcers in specimens of IBD patients. Fibroblasts in these ulcers expressed MMP-13 and TIMP-3 [133]. The epithelium at the edge of the ulcers expressed MMP-7, which appeared to be important for re-epithlization after injury [134]. Myofibroblasts in the mucosa expressed high levels of MMP-1, -3 and -9 in IBD [135], whereas MMP-2 and -10 expression was increased in the epithelium [133; 136]. MMP-12 and MMP-14 were overexpressed in macrophages and myofibroblasts in the lamina propria of the inflamed gut.

Similar to healthy colon, abundant MMP-2 expression was found in fistulae of Crohn's disease samples. Differences could be seen between acute inflammation with granulation tissue and chronic inflammation characterized by fibrosis. In case of acute inflammation MMP-2 was detected in large mononuclear macrophage-like cells, and in endothelial cells, whereas during chronic inflammation the proteinase was localized in fibroblasts and large mononuclear macrophage-like cells. High levels of MMP-3 expression were detected in both types of inflammation and in the same cell types that expressed MMP-2. MMP-9 protein was abundant in leukocytes, in granulocytes, and in giant cells in acute specimens, whereas only few granulocytes stained positive for the protease in the chronic state. MMP-1, -7, and -10 expression was virtually not detectable [130].

Up-regulation of MMP activity in inflammation can induce a breakdown of the ECM, provided that levels between active MMP and their inhibitors are deregulated. This is believed to happen in patients suffering from IBD: an overproduction of MMPs in the

intestine and the failure to control their activity by TIMPs is probably the main cause of ulceration, tissue inflammation, and fistulae formation in CD and UC [137; 138; 139; 140].

Expression of MMPs and TIMPs is also deregulated in other diseases of the intestine, like enterocolitis (upregulation of MMP-3) [141], collagenase colitis (upregulation of TIMP-1, downregulation of MMP-1, -13) [142; 143] and colorectal cancer where MMPs are involved in metastasis (upregulation of MMP-1, -2, -3, -7, -9, -13, 14) [144]. In contrast to other MMPs, overexpression of MMP-12 is associated with increased survival in colon cancer [144].

2.3.4.4 MMPs and the intestinal immune system

Many MMPs such as MMP-1 and MMP-7 play an important role in tissue homeostasis and the repair of different epithelial tissues [134]. However, there is increasing evidence that in addition to their direct effects on extracellular matrix, MMPs are also involved in immune responses, for example the recruitment of inflammatory cells to the intestine. Another possible mechanism of MMP action is the modulation of biologically active mediators (chemokines and cytokines) such as TNF-α and interleukins. The following section describes MMP functions in cell recruitment, chemokine and cytokine release, and antimicrobial peptide activation.

The presence of MMPs is necessary for lymphocyte transmigration through the basement membrane [145; 146; 147; 148]. The role of MMP-9 in migration of neutrophils across the basement membrane is not well understood but TIMP-1, the preferential MMP-9 inhibitor, was found to inhibit neutrophil migration. In several animal models of colitis, MMP inhibitors have been shown to reduce neutrophil accumulation in the intestinal wall [149; 150]. It was also reported that neutrophil infiltration is reduced in MMP-3- or MMP-12-deficient mice [151; 152]. MMP-3 was also shown to control the mobilization of T cells in the lamina propria [153].

MMPs can modulate biologically active mediators such as TGF-β, TNF-α, and interleukins (IL-1 and IL-6). They have the ability to shed the proinflammatory cytokines from the surface of macrophages, which are known to upregulate MMP production in macrophages and parenchymal cells. Cleavage of TGF-β by MMP-3, -9, and -14 was reported in cell and tissue culture models, the activation *in vivo* has to be shown [154; 155]. The main activator for IL-1β is caspase-1 (ICE) but at least three MMPs can cleave and activate the precursor as well: MMP-2, -3, and -9. Here MMPs show a dual role as they either activate (MMP-3, -9) or degrade (MMP-3) the cytokine [156]. Similarly, ADAM17 (TACE) is the main sheddase of TNF-α [157; 158] but also several MMPs (MMP-1, -2, -3, -9, -17) can process proTNF-α to its active form. It seems that ADAM17 is mainly responsible for the inducible shedding where high levels of TNF-α are needed and MMPs like MMP-7 and MMP-12 constitutively shed proTNF-α from macrophages which is required for normal tissue repair [118; 158; 159; 160]. Macrophages play an important role in tissue damage and their numbers are strongly increased in the mucosa of IBD

patients; thus, macrophages are a potentially important source of MMPs at the inflammatory site.

MMPs can also directly modulate chemokine activity and establish chemokine gradients. Several members of the monocyte-chemotactic protein (MCP) group of CC-chemokines can be activated or inactivated by cleavage through MMPs. For example MMP-2 cleaves CCL7 and the truncated chemokine than acts as an antagonist. Similarly, MMP-1, -3, -13, and -14 cleave CCL2, CCL8, and CCL13 to produce receptor antagonists [121]. Also several CXC-chemokines are processed by MMPs (CXCL11, CXCL5, CXCL6). In all cases, the cleavage leads to a loss of chemotactic activity [161]. In contrast the cleavage of CXCL8 (IL-8, the mouse homolog is KC) by MMP-9 leads to a significant increase of its chemotactic activity [162; 163].

Host recognition of bacteria is an important factor in IBD; it is thought that patients have a deregulated immune response to endogenous gut flora. MMP-7, as one of the few MMPs steadily expressed in healthy mucosal tissue, has been shown to activate antimicrobial peptides (AMPs) like α-defensins that are produced by Paneth cells and are bactericidal. Coexpression of MMP-7 and defensins was shown in these cells of the small intestine in mice. Also in this context MMP-3 plays an important role as it activates the proforms of MMP-7 and -9 [164; 165; 166].

2.3.4.5 MMPs and animal models of IBD

Over the last several years mouse models of IBD have been developed to identify the role of MMPs in the disease. Higher mRNA levels of MMP-3, -7, -9, -12, and TIMP-1 in colonic tissues of mice treated with DSS to induce colitis were reported [149]. During the development of DSS-induced colitis, the expression of MMPs is up-regulated, accompanied by increased production of pro-inflammatory cytokines.

Several MMP-deficient mice were used in different models of colitis to reveal the role of MMPs in IBD. It turned out that, for example, MMP-10 is protective in DSS-induced colitis. MMP-12-deficient mice were less susceptible to TNBS-induced colitis than WT animals [167] and the lack of MMP-7 protects mice against acute injury in a DSS colitis model [168], which shows the negative effect of these proteinases in colitis .

MMP-9, according to the expression level, is the main MMP involved in TNBS-induced colitis, whereas levels of MMP-2 remain unchanged [169; 170]. Epithelial derived MMP-9 plays a crucial role in DSS-induced colitis as it is important for tissue damage and in *Salmonella typhimurium*-induced enterocolitis [170; 171]. Interestingly it was found that neutrophil MMP-9 is neither needed for migration nor for induction of tissue damage. MMP-9 deletion leads to reduced inflammation and severity of colitis [171]. In contrast to MMP-9-deficiency, deletion of MMP-2 exacerbates colitis; these mice are highly susceptible to DSS- and *Salmonella typhimurium*-induced colitis [172]. Using a double-deficient mouse for MMP-2 and -9, it turned out that MMP-9-mediated tissue injury overrides the protective effect of MMP-2 during colitis [173].

In contrast to MMP-9, mucosa-derived MMP-2 may be a critical host factor that is involved in the regulation of the host response to luminal pathogens or toxins, an important aspect of healing and tissue resolution. A critical balance between the two gelatinases determines the outcome of inflammatory response during acute colitis.

In general, it seems that the inducible MMPs such as MMP-9 and -12 mediate tissue damage and other negative effects in colitis whereas the constitutively expressed MMPs, like MMP-2 and -10 are more protective in the disease.

Recently, several MMP inhibitors were tested in mouse models of IBD which all resulted in reduced tissue injury and inflammation in the treated mice (Table 2-1).

Table 2-1: MMP inhibitors tested in animal models of colitis.
Adapted from [149; 150; 169; 170; 174]

Inhibitor	Chemical class	MMP inhibition	Dose (mg/kg)	Model	Outcome
1,10-Phenanthroline	Phenanthroline	Broad spectrum	20	DSS, TNBS	effective
Marimastat	Hydroxamate	Broad spectrum	40	TNBS	effective
Batimastat	Hydroxamate	Broad spectrum	5-20	TNBS	effective
CGS-27023	Hydroxamate	Collagenase, gelatinase, stromelysin	20	DSS, TNBS	effective
ONO4817	Hydroxamate	Broad spectrum except for MMP-1 and -7	30	DSS	effective

2.3.5 Matrix metalloproteinases-19 and -28

2.3.5.1 Matrix metalloproteinase-19 (MMP-19)

The human matrix metalloproteinase 19 was first cloned from a cDNA library, generated from the synovium of a rheumatoid arthritis patient by Sedlacek et al. [175]. It was discovered as an autoantigen in rheumatoid arthritis. Thereafter it was also named RASI (rheumatoid arthritis sign of inflammation) which indicates the origin of the enzyme [176]. Independently and in parallel, MMP-19 was cloned by two other groups from cDNA of the liver and mammary gland [177; 178].

The human MMP-19 gene is located on chromosome 12 mapping to the 14q region [179], while several other MMP genes are found on chromosome 11. Whereas most other MMPs are encoded by 10 exons, human and murine MMP-19 are encoded by 9 exons. Therein, exons 1-3 determine the prodomain, exons 4 and 5 mainly encode for the catalytic domain, and the hemopexin-like domain is distributed over 4 exons [180; 181].

The human proenzyme consists of 508 amino acids and has a molecular weight of 57.4 kDa. Detailed characterization of the sequence and comparison to all other known MMPs showed that MMP-19 had the least similarity to all other family members [182]. It does not belong to any of the described subgroups like collagenases, gelatinases, stromelysins, or membrane-type MMPs. Lately, another novel MMP, MMP-28 (epilysin) was discovered that is the closest homologue to MMP-19 [183; 184]. The identity of the catalytic domain is 46%. Further analysis revealed more similarities to MT1-MMP and the group of stromelysins (especially stromelysin-3) and thus it was also termed stromelysin-4 (Gordon Research Conference, 2001).

MMP-19 is, like most other members of the MMP family, secreted as a zymogene and displays the typical structural features characterizing this enzyme family. The proteinase consists of a signal peptide, a propeptide domain, a catalytical domain, a hinge region, and a hemopexin-like domain. The active part of MMP-19 matches the ones of other matrix metalloproteinases but the hemopexin-like domain shows less than 25% identity to other MMPs. Despite of the typical domain structure of the family of matrix metalloproteinases MMP-19 also exhibits specific features. At first, there is a characteristic threonine-rich region at the C-terminal part consisting of 27 amino acids. This hydrophobic region has no known function so far and does not show any sequence homology to other members of the MMP family. Differences are also found in the auto-inhibitory part of the sequence within the propeptide domain where the consensus sequence is PRCGLED in contrast to the generally found PRCXXPD. This unique feature enables the enzyme to be autocatalytic active [185]. Mutation studies where the carboxy-terminal proline was replaced by glutamic acid on other MMPs showed the same effect of self-activation of the proenzyme [186; 187]. Within the hinge region, a unique oligoglutamic acid stretch followed by a proline-rich sequence (NH2-EEEEETELPTVPPVPTEPSPM) is located; the function is unknown so far. The catalytic

domain of MMP-19 contains an additional cysteine that is also present in MMP-28 and MMPs from chicken (CMMP) and xenopus (XMMP) [184; 188]. hMMP-19 contains two putative N-glycosylation sites and mMMP-19 has four [176; 180; 181].

It was reported that the hemopexin-like domain is responsible for the association of MMP-19 to the cell surface [189]. The mechanism of the interaction with the cell surface is unclear.

MMP-19: expression pattern, regulation, and proteolytic activity

MMP-19 expression differs from the other MMPs as it is expressed in normal, healthy tissue, suggesting a role in tissue homeostasis. Its mRNA is highly expressed in various tissues except of brain [178; 179]. Protein expression is more restricted to several cell types like vascular smooth muscle cells, myoepithelial cells, basal keratinocytes, epithelial cells of different tissues (mammary gland [190], colon [131], intestine, lung, ovary, spleen [191]), and microglia that express the enzyme constitutively. Other cells (also epithelial cells and endothelial cells) show differential regulation of MMP-19. In healthy blood specimens, PBMC (peripheral blood mononuclear cells) that are positive for the surface marker CD14 produce MMP-19 as well i.e. macrophages [189]. This specific expression pattern suggests a specific role for MMP-19 in the epithelium and the basal membrane as well as macrophages.

Role in wound healing

The role of MMP-19 in the wound healing process is still poorly understood and controversial. Despite its association with cell proliferation, Suomela *et al* have demonstrated that MMP-19 is not expressed in healing wounds of the skin [192]. By contrast, a study by Hieta *et al* suggests that the protease is expressed during later phases of wound repair by skin-resident and infiltrating cells including fibroblasts and endothelial cells. The same authors have also shown that macrophages located in the wound bed produce MMP-19 protein [193], a finding that is in line with other reports demonstrating expression of the enzyme in blood mononuclear cells and myeloid cells [175; 189]. Thus, the role of MMP-19 in tissue repair might be associated with macrophage function. This cell population is believed to be essential in wound healing due to its capacity to remove cellular debris and to release a large number of growth factors. It seems plausible that MMP-19 could be involved in the release of membrane-associated cytokines and growth factors from the macrophages or could facilitate their migration in the wound bed [194]. However, further studies are needed to verify these hypotheses.

Expression in cancer

During tumor growth, MMP-19 acts as a negative regulator of angiogenesis and invasion [195] and induction of fibrosarcomas is reduced in MMP-19-deficient mice [177]. MMP-

19 shows differential expression in squamous cell carcinoma (SCC),it is up-regulated during melanoma progression [196] but down-regulated in colon cancer [131]. High expression was detected in human lung cancer and astroglial tumors where it promotes invasion of glioma cells [197]. The loss of MMP-19 is associated with malignant progression in chronic wounds [198] and it can act as a tumor suppressor and shows anti-angiogenic activities in nasopharyngeal carcinoma [199].

Regulation

Analysis of the promoter region of MMP-19 revealed that several transcription factors like AP-1, AP-2, Ets, NF-κB, Myc, and E12/E47 can bind to the promoter sequence. Also regulatory elements as RARE (retinoic acid response element) and TIE (TGF-β inhibitory element) are present in this region [181]. Potent inhibitors of MMP-19 activity are TIMP-2, -3, and -4, whereas TIMP-1 is less capable of inhibiting this proteinase [185].

Proteolytic activity and substrates

Known substrates of MMP-19 are mainly members of the extracellular matrix (ECM) like collagen type IV, laminin5 γ2 chain, tenascin-C, and nidogen. Also fibrinogen, fibrin, COMP (cartilage oligomeric protein), aggrecan, and brevican are processed by MMP-19 [185; 197; 200; 201; 202]. The analysis of substrate specificity was done mainly in *in vitro* experiments by using the recombinant catalytical domain [185]. Also non-matrix proteins like IGFBP-3 (insulin-like growth factor binding protein-3) and a variant of VEGF (vascular endothelial growth factor) are cleaved by MMP-19 [203; 204]. MMP-19 is also able to cleave MMP-9 but this does not lead to enzyme activation [185].

Because of its unique features including expression pattern, autocatalytic activity, and the ability to cleave several important ECM proteins, MMP-19-deficient mice were generated.

2.3.5.2 Generation of MMP-19-deficient mice

The murine *Mmp19* gene was first amplified from liver cDNA and from a mouse myoblast cell line [180]. The gene is located on chromosome 10 and shows 79% similarity to its human ortholog. The homology for the catalytic domain is 84%, while the hemopexin-like domain with only 65% is less identical to human MMP-19 (Figure 2-11). All characteristics of the human MMP-19 are also displayed in the murine one. mMMP-19 protein consists of 527 amino acids and has a molecular weight of 59.1 kDa. In comparison to the human protein the murine one lacks one glutamic acid residue in the oligoglutamic acid stretch [180; 205].

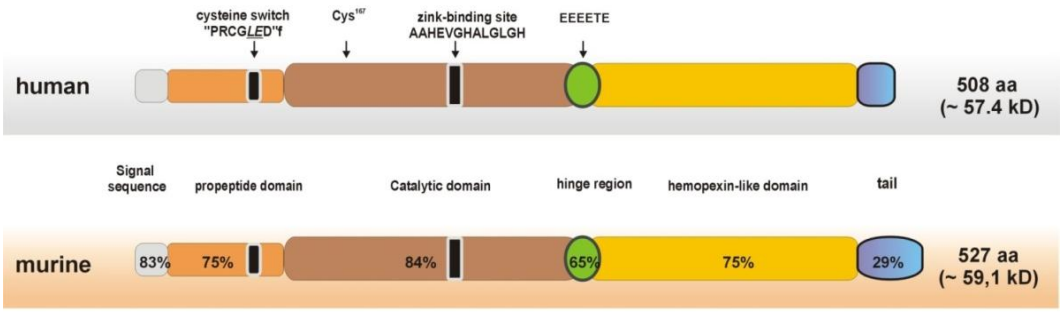

Figure 2-11: Human and murine orthologues of MMP-19.
The schematic picture of human and murine MMP-19 is showing the homology of the two enzymes (by courtesy of Dr. Radislav Sedlacek)

MMP-19-deficient mice were generated by targeted disruption of the *Mmp19* gene, as shown in figure 2-12 [206]. To design a targeting construct, a part of exon 3 and whole exon 4 encoding for the catalytic domain were replaced by a neomycin resistance cassette orientated in the opposite direction to the endogenous *Mmp19* gene. For construction of the 5'-arm homology of the targeting construct, a 2.8 kb fragment spanning a region including exon 2 and most of exon 3 was amplified from genomic DNA using PCR. The 3'-arm homology was created the same way; it is spanning a region of 2.8 kb including exon 5 and part of exon 8. The complete construct, called pPNT/mmp19del, was injected into mouse embryonic stem cells derived from 129 strain. The neomycin-resistant colonies were screened for homologous recombination by Southern blotting [207]. Two selected clones (G5 and F6) were introduced into blastocysts via microinjection and chimeras were generated [208]. Mice were analysed by PCR and animals positive for the disrupted MMP-19 allele were backcrossed to C57BL/6NCrl mice. Resulting MMP-19-deficient mice develop without obvious alteration in morphology, weight, size, and fecundity compared to wild-type mice, which is consistent with the work of Pendas et al., who generated MMP-19-deficient mice by replacing the *Mmp19* promoter region and exons 1 and 2 [177]. Breeding of mice heterozygous for the targeted gene for MMP-19 produces the expected Mendelian ratio of knockout animals of 25%. Thus, MMP-19 does not seem to be essential for blastocyst implantation or embryonic development. No apparent changes in the histology of brain, bones, heart, kidney, liver, lung, reproductive organs, pancreas, skin, and spleen of MMP-19-deficient mice were seen at 1, 3, 6, and 12 months.

Previous studies showed that MMP-19 is steadily expressed in the normal healthy epithelia, macrophages, and smooth muscle cells; it may play a role in wound healing, cell proliferation, migration, and vascularisation. The impact of this metalloproteinase in acute as well as chronic inflammatory diseases is not known so far.

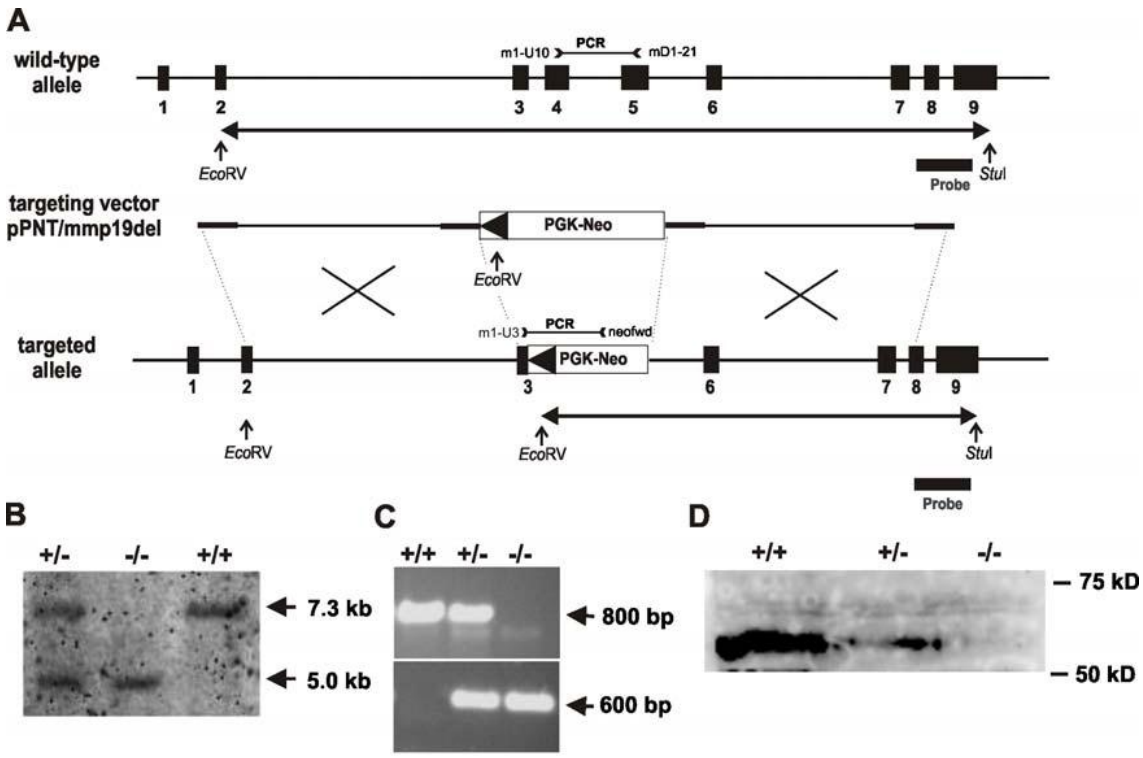

Figure 2-12: Generation of MMP-19-deficient (MMP-19 -/-) mice.
(A) Schematic representation of the murine *Mmp19* gene and its exon/intron-organization as previously described by Mueller et al.; pPNT targeting vector construct, and the resulting deleted active site locus of the mouse mmp19 gene are depicted. The targeting construct was generated by replacement of 1088 bp region of *Mmp19* gene spanning the end of exon 3 and the whole exon 4 encoding the catalytic domain by the neomycin resistance cassette. (B) For screening of MMP-19-deficient mice Southern blot analyses were performed. Probing led to identification of either a 7.3 kb band (wild-type allele, +/+) or a 5 kb band for the targeted allele (-/-). In heterozygous mice (+/-) both alleles are present. (C) Genotyping of targeted alleles using PCR. Wild-type alleles are detected by an 800 bp band, while PCR for the MMP-19-deficient allele results in a 600 bp product. (D) Primary keratinocytes isolated from wild-type, heterozygous, and homozygous MMP-19-deficient mice were analyzed for MMP-19 expression by western blotting using anti-MMP-19 antibodies purified against a peptide derived from the hinge region of murine MMP-19, that is detected in size of 59 kDa. [206]

2.3.5.3 Matrix metalloproteinase 28 (MMP-28)

Epilysin (MMP-28) is the latest member of the mammalian matrix metalloproteinase (MMP) family of extracellular proteases. It was cloned from human keratinocyte and testis cDNA libraries [183; 209]. The cDNA contains an open reading frame of 1560 nucleotides coding for a 520 aa protein. The human *Mmp28* gene is located on chromosome 17 (17q11.2) [209], which is a locus that differ from all other known *Mmp* genes. *Mmp28* gene consists of only eight exons instead of ten, which is typical for Mmp genes [183]. This unique gene organisation can just be found in one other MMP, MMP-11 (Stomelysin-3). It seems that these two MMPs are the most similar ones but concerning overall gene organization *Mmp28* resembles most closely *Mmp19* [181].

MMP-28 contains a prodomain, a zinc-binding catalytic domain, and a hemopexin-like domain. In contrast to most other MMPs (except of MMP-11 and the membrane-bound MT-MMPs) it also contains a furin activation sequence and can be activated during its secretion. The furin site is conserved and functional as well in the MMP-28 homologues in mouse and *Xenopus leavis* (XMMP-28) [210]. The catalytic domain is typical for soluble MMPs although the sequence of the Zn-binding site (HEIGHTLGLTH) is unique as no other MMP contains threonine within this sequence.

The identity between human and mouse epilysin is 85% of the overall amino acid sequence and 97% in the catalytic domain [211], which suggests a well-conserved function of this proteinase. These findings are supported by the high identity to XMMP-28, as 56% of the overall amino acids and 65% in the catalytic domain are identical to the human sequence [212]. The epilysin homologue in *Xenopus laevis* (XMMP-28) is expressed in neural tissues, where it cleaves the neural cell adhesion molecule.

Comparison of the amino acid sequence of MMP-28 with other MMPs showed that it is most closely related to MMP-19. This resembles the results from the gene analysis.

MMP-28: expression pattern, regulation, and proteolytic activity

Epilysin differs from most other MMPs as it is expressed in normal, healthy tissue, suggesting a role in tissue homeostasis. Its mRNA is highly expressed in testis, at lower levels in lung, heart, gastrointestinal tract (small intestine, colon), brain, and in wounded epidermis [211] in humans. The expression pattern in mice is slightly different; the highest expression is found in lung but mRNA could be also detected in placenta, heart, uterus, and the gastrointestinal tract. A peak of epilysin expression can be found during the embryonal development at day E14 in developing neural system. The expression pattern in rats resembles the one in mice. This pattern of expression is different from most other members of the MMP family, as most MMP are expressed only under special conditions, like injury, inflammation, or several diseases [213]. The MMP-28 expression pattern suggests that epilysin plays an important role in normal tissue homeostasis and turnover.

Regarding tissue and cell culture, MMP-28 is expressed in epithelial cells (from skin, placenta, and lung) and bone marrow derived macrophages [183]. mRNA could be also detected in unstimulated and PMA and ionomycin stimulated T lymphocytes. Cytokines like TNF-α were proposed to induce the expression of MMP-28 *in vitro* [214].

Role of MMP-28 in wound healing

As MMP-28 was found to be expressed in keratinocytes and in intact human skin, several wound healing experiments were done to analyze a putative role of epilysin. In *ex vivo* models, MMP-28 was detected in non-migrating keratinocytes at a distance from the wound edge as well as in migrating ones at the wound edge [183; 214] (Figure 2-13).

These observations may indicate a role of MMP-28 in epithelial cell proliferation or rebuilding of the newly formed basement membrane during wound repair.

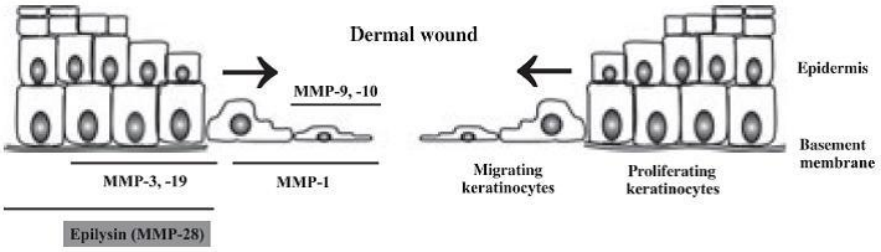

Figure 2-13: MMPs in wound healing.
MMPs are expressed in different areas of the epithelium during dermal wound healing. Taken from [209].

Expression in cancer

MMP-28 expression is up-regulated in various different types of cancer (e.g. invasive ductal cell carcinoma [215], squamous cell carcinoma (grade I) [214], but also several cases of down-regulation of this enzyme are reported (e.g. basal and squamous cell carcinoma (grades II and III) [214], colon carcinoma (epithelium) [131]. The role and expression of MMP-28 seems to be dependent on the type and stage of cancer. In cell culture, MMP-28 mRNA has been detected in colon adenocarcinoma cells, ovarian carcinoma cells, pancreatic adenocarcinoma cells and breast carcinoma cells.

Regulation

Like all other MMPs, MMP-28 is tightly regulated on the transcriptional level because of overlapping biological functions and substrate specificity. Promoter analysis of epilysin revealed a sequence known as GT-box, a homologue to the consensus binding site for the Sp-family of transcription. It is highly conserved in human and mouse promoters indicating an important role in regulation of gene expression. The transcription factors Sp1 (inducer of transcription) and Sp3 (inducer or repressor of transcription) bind to the GT-box. A mutation in the GT-box resulted in significantly reduced transcriptional activity especially in keratinocytes [210].

Histone deacetylation inhibitors (HDAC) can induce MMP-28 transcription as well as few other *Mmp* genes. In general, most *Mmp* genes are repressed by these inhibitors [216]. The actual target of the HDAC inhibitors seems to be Sp1 as it is regulated by acetylation itself [217].

Another mechanism of MMP-28 regulation is the compartmentalization of the cell. Experiments showed that MMP-28 is attached to the cell membrane; the responsible structural part of the enzyme is the hemopexin domain. This mechanism of pericellular localization seems to be an epithelial-cell specific structure as it does not occur in other

cell types. Cells which went through EMT showed no longer cell surface expression of epilysin that suggests that during EMT there is a downregulation of the receptor binding epilysin to the cell surface. MT1-MMP induction during EMT may cause the destabilization or degradation of the surface receptor and with this a loss of bound MMP-28 [218].

Proteolytic activity

Recombinant MMP-28 was used to determine substrates of this new proteinase; the first one verified was casein [183]. The proteolytic activity could be inhibited by EDTA and batimastat, a selective MMP inhibitor. In vitro XMMP-28 and recombinant human MMP-28 degraded the neural cell adhesion molecule (NCAM).

The functions of epilysin still are largely unknown. As several MMPs function in immunity, it was hypothesized that also MMP-28 may have a regulatory role in the tissue response to environmental challenge. To test this, MMP-28 KO mice were generated in the laboratory of William C. Parks, Washington University (St. Louis, MO, USA).

2.3.5.4 Generation of MMP-28-deficient mice

The murine *Mmp28* gene was cloned from the SV129 genome (gene ID 118453). For construction of the homologous extensions of the targeting construct, a 4.8 kb *Eco*RI-*Xba*I fragment containing the 3' terminus of intron 1, exons 2 and 3, and ~ 4 kb of intron 3 and a 2.1 kb *Xho*I-*Eco*RI fragment containing the 3' untranslated end of exon 8 and downstream sequence (Fig. x*A*). Two cassettes were inserted into the target gene; a pgk-neomycin resistance cassette was inserted between the two arms and a diphtheria toxin (dta) cassette was fused to the 3' end. Linearization of targeting construct was done with *Xho*I (the *Xho*I site at the 5' end of the short arm was deleted by ligating to the *Sal*I site in the neomycin cassette). Transfection of 129X1/SvJ (RW4) embryonic stem (ES) cells was done by the Murine Embryonic Stem Cell Core of the Siteman Cancer Center at Washington University (St. Louis, MO). For screening of ES cell clones, genomic DNA was isolated and digested with *Bam*HI. Southern blotting of the digests was done using a 694-bp probe to the 3' terminal end of intron 1, upstream of the targeting construct (Fig. x*A*). Positive ES cells were injected into C57BL/6 blastocysts by the Mouse Models Core at Washington University. Genotyping of mouse tail DNA was done by PCR and positive results were confirmed by Southern hybridization (Fig. 1*B*). For PCR, we used two forward primers, one specific to the WT locus (5'GTGAAGATGTCCCATGCCCACAGT3') and the other to the target construct (5'GAGGAAATTGCATCGCATTGTCTGAG3'), and a common reverse primer (5'CACATTCCCTCCTGCTCTGCATCC3') to generate a 259 bp product from the WT *Mmp28* gene and a 324 bp product from the mutated gene (Figure 2-14). Male chimeric mice were bred to female C57BL/6 mice to generate germline heterozygotes, which were then bred to yield homozygous nulls. MMP-28 KO mice were then backcrossed for more than 10 generations with C57BL/6 mice from Taconic. Wild-type and MMP-28 KO mice

(C57BL/6NTac background) were housed as described in 'Material and Methods', section 3.1.1. Age-matched mice of both genotypes were used for all studies. Similar to many other MMP knock out mice, also MMP-28 KO mice revealed no overt phenotype.

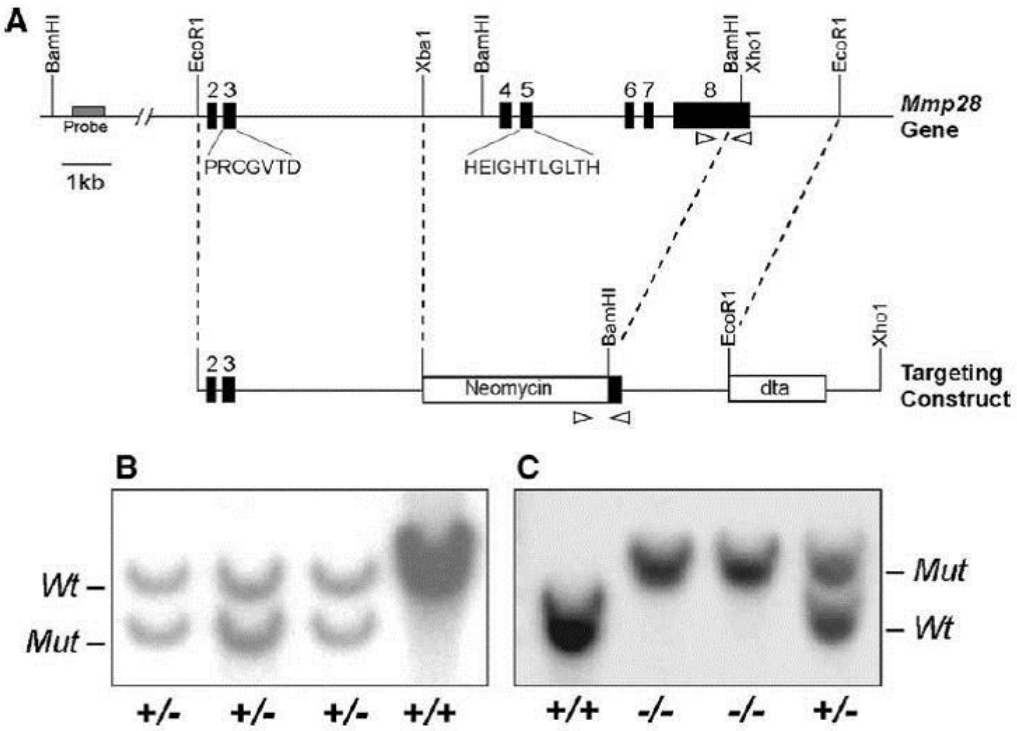

Figure 2-14: Generation of MMP-28-deficient (MMP-28 -/-) mice.
(A) The targeting construct was designed to replace most of the exons, including exon 5, which codes for the catalytic domain. After recombination, exons 4 –7 and the full coding portion of the exon 8 are removed, and the epilysin transcript only contains exons 1–3. (B) ES cell clones were screened by Southern hybridization; WT epilysin gene gives a 9 kb band while targeted gene gives a 7.5 kb band. (C) F1 offspring of chimeric mice were screened by Southern and PCR analysis. For the PCR assay, the recombined locus produces a larger DNA fragment (324 bp) than that from the WT gene (259 bp). Three primers were used, the position and orientation of which are indicated by arrowheads: a WT forward primer, a neomycin cassette forward primer, and a common reverse primer [219].

3 Material and methods

3.1 Mice and *in vivo* models

3.1.1 Animal housing

Housing of mice and *in vivo* experiments were performed after approval by the Animal Care Committee of the Institute of Molecular Genetics, Prague, Czech Republic in compliance with national and institutional guidelines. Mice were housed in open cages with 12h/12h light/dark cycle under standard conditions and were provided with autoclaved food (Rod18-A10, LASvendi, Soest, Germany) and acidified drinking water ad libitum.

Health monitoring was performed on a quarterly basis according to the recommendations of the Federation of European Laboratory Animal Science Associations (FELASA). Additionally, *Helicobacter* species were tested every three months. Test results showed an infection with *Helicobacter* during the time of the breeding and the experiments for this study. Mice with targeted disruption of the *Mmp*19 gene were generated as described above (introduction). For colony maintenance, MMP-19 -/- mice were backcrossed to C57BL/6NCrl background (Charles Rivers Laboratories, Sulzfeld, Germany). All assays were performed with MMP-19 -/- mice that have been backcrossed at least to the F20 generation. Studies focussing on the role of MMP-19 were performed using the MMP-19 F6 line as the second line, G5, did not show any different characteristic in previous experiments.

MMP-28-deficient mice were kindly provided by William C. Parks (University of Washington, Seattle, USA). The generation of MMP-28 -/- mice was published previously by Manicone et al. [219]. Experiments to study the role of MMP-28 were carried out with MMP-28-deficient mice backcrossed more than 10 times to C57BL/6NCrl background. In order to obtain aged-matched MMP-deficient mice for the experiments, backcrossed mice heterozygous for MMP-19 or MMP-28 were crossed. After genotyping of the newborn mice, those with homozygous deletion of the MMP locus were crossed further.

To generate mice lacking MMP-19 and -28 homozygous mice of both strains were crossed which resulted in double heterozygous animals in the F1 generation, which were then further breed to obtain double-deficient animals, named MMP-19/-28 dbKO.

3.1.2 Genotyping of mice

3.1.2.1 Isolation of genomic DNA from mouse tail

For MMP genotyping, genomic DNA was isolated according to a protocol described by Hogen et al [220]. A short part of the tail (0.3-0.4 cm) was cut from 3-weeks old animals; the tail biopsy was then cut into smaller pieces and incubated in 1 ml lysis buffer (200 mM NaCl, 100 mM Tris, 5 mM EDTA, 0.2% SDS, pH 8.0) with proteinase K (7.2 mU) and placed in a water bath at 55°C overnight. 1 ml phenol: chloroform (1:1) was added to the digested tissue and mixed for 15 s and centrifuged (900 x *g*, 2 min) to separate the phases. The upper phase was transferred to a new tube and mixed with 1 ml chloroform, and centrifuged again (900 x *g*, 2 min). The aqueous supernatant was transferred into new tube and mixed with 1 ml 100 % ethanol and 100 μl sodium acetate (3 M, pH 6.0). For precipitation of DNA the solution was mixed carefully. Following another centrifugation step the pellet was washed with 75% ethanol. After discarding ethanol, the pellet was dried at room temperature and dissolved in 100 μl dH_2O overnight at 4 °C. Quality of the DNA was measured at 260 and 280 nm. The genomic DNA samples were stored at 4 °C until they were used for PCR.

3.1.2.2 PCR of genomic DNA

Mice were genotyped by PCR according to the original method [220; 221; 222]. After isolation of genomic DNA two separate PCR set-ups for detecting the targeted and the wildtype allele of MMP-19 were performed. Components for the reactions such as PCR buffers, dNTPs, MgCl2, and Taq-polymerase were purchased from Fermentas (St. Leon-Rot, Germany). The forward primer for the wildtype allele was designed on exon 4 (m1-U10, 5'-CCGCATCTTCAATGTGCCC-3'), the reverse one on exon 5 (mD1-21, 5'-GATCGCCAGGTTCACTCC-3'). These primers amplified a fragment of 800 bp. For the targeted allele a forward primer on exon 3 (m1-U3, 5'-AGATGGATGACGCCACAAG-3') and a reverse one based on the sequence of the PGK-Neo cassette (neofwd, 5'-CTTCTATCGCCTTCTTGACG-3') were used, the reaction resulted in a product of 600 bp. Control setups with DNA from MMP-19 -/-, MMP-19 +/-, and WT mice as well as without DNA template were run additionally. One reaction consisted of 1.5 mM $MgCl_2$, 2 mM dNTPs, 0.5 μM of each primer, 1.25U Taq-polymerase, and 50 - 100 ng genomic DNA in PCR buffer (10 mM Tris, 50 mM KCl, 0.8% Nonidet P40, pH 8.8). The PCR program is described in table 3-1. Steps 2 to 4 were repeated 30 times.

Table 3-1: PCR conditions for genotyping of MMP-19 knockout mice.

Step	Temperature	Time
1 - initial denaturation	95°C	2 min
2 - denaturation	95°C	30 sec
3 - annealing	60°C	30 sec
4 - extension	72°C	2 min
5 - final extension	72°C	5 min

Detection of the MMP-28 wild-type or mutated allele was performed in one reaction. The following primers were used: The wild-type allele was amplified with a forward (Epi WT, 5'-GTGAAGATGTCCCATGCCCACAGT-3') and a reverse primer (MMP28 rev common, 5'-AGGGCCCTCTTTCATCTTCCTGATG-3'). The mutated MMP-28 allele was detected by a forward primer (MMP28 KO For, 5'-GCTGACCGCTTCCTCGTGCTTTAC-3') and the same reverse primer (MMP28 rev common). The set up is the same as for genotyping of MMP-19 allele. The PCR program is described in table 3-2. Steps 2 to 4 were repeated 30 times. The size of the PCR fragment for the WT allele was 535 bp, and the one for the disrupted allele of MMP-28 834 bp.

Table 3-2: PCR conditions for genotyping of MMP-28 knockout mice.

Step	Temperature	Time
1 - initial denaturation	95°C	2 min
2 - denaturation	95°C	30 sec
3 - annealing	66°C	30 sec
4 - extension	72°C	1 min
5 - final extension	72°C	5 min

3.1.2.3 Agarose gel electrophoresis

PCR products were analyzed by agarose gel electrophoresis. PCR products were mixed with 10 x loading buffer (40% glycerol, 0.1% (w/v) bromephenole blue, 0.1% (w/v) xylene cyanole, 40 mM Tris, pH 8.0) and loaded into slots of agarose gels (1% in TAE buffer) that were run with 9 V/cm2 in TAE buffer (10 mM Tris, 20 mM Acetic acid, 1 mM EDTA; pH = 8.0). A DNA standard (Fermentas) was used to compare the size of amplified DNA. PCR fragments were visualized by ethidium bromide (Roth, Karlsruhe, Germany) staining (final concentration in the gel: 0.5 µg/ml) and UV trans-illumination at λ=312 nm (BioRad, München, Germany).

3.1.3 Animal model of DSS-induced colitis

3.1.3.1 Induction of DSS-colitis and determination of the disease activity index score

Acute colitis was induced by administration of 2% dextran sulfate sodium (DSS) (TdB Consultancy, Uppsala, Sweden) in the drinking water for 6 days. To study the recovery phase of colitis the disease was induced by 2% DSS in the drinking water for 5 days followed by 10 days of regular, non-acidified, UV irradiated and filtrated drinking water. For maintaining chronic colitis this procedure was repeated twice. Groups of four to eight mice were used to monitor the disease activity index (DAI) [223], which consists of three parameters: loss of body weight, intensity of bleeding and stool consistency. Faecal blood loss was determined using the hemoccult test (Beckman Coulter, Krefeld, Germany). All parameters were recorded daily. DAI and histology were performed as previously described by Siegmund et al. [224] and Grivennikov et al. [225].

The murine colitis phenotypes were measured by the disease activity index score, which is the sum of body weight, diarrhea, and bleeding scores determined daily during the treatment, as previously described [224; 226]

All scores were relative to the scores on day 0, which were set as 0. For body weight, no weight loss was scored as 0. The scoring system was following: loss of 1% – 5% weight, 1; loss of 5% – 10% weight,2; loss of 10% – 20%,3; 20% and higher body weight loss, 4. For stool consistency, 0 was scored for well-formed stool pellets, 1 was scored for loose stool pellets, 2 was scored for pasty and semi-formed stools that did not adhere to the anus (mild diarrhea), 3 was scored for slimy stool (moderate diarrhea) and 4 was scored for severe watery diarrhea that adhered to the anus and contained blood. For bleeding, which was analyzed by the Hemoccult faecal occult blood test (Beckman Coulter), 0 was assigned for no blood, 2 was assigned for positive Hemoccult test, and 4 was assigned for gross bleeding. The determination of the DAI is summarized in table 3-3.

Table 3-3: DAI assessment.

Body weight loss	
0	No loss
1	1–5% loss of body weight
2	5–10% loss of body weight
3	10–20% loss of body weight
4	>20% loss of body weight

Stool consistency	
0	Normal feces
1	Loose stool
2	Watery diarrhea
3	Slimy diarrhea
4	Severe watery diarrhea with blood

Bleeding	
0	No blood
2	Positive Hemoccult test
4	Visible bleeding

3.2 Tissue analysis

3.2.1 RNA analysis

3.2.1.1 RNA extraction from colon tissue samples

Total RNA was extracted from 10 mg colon tissue samples using the TissueLyserII (Qiagen, USA) in combination with the RNeasy Mini kit (Qiagen, USA). In brief, tissue samples stored in RNALater (Ambion, USA) at -20°C were placed in 2 ml RNAse-free plastic tubes containing 600 µl RLT lysis buffer and stainless steel beads (Qiagen), followed by disruption through high-speed shaking (2 x 1.5 min at 20 Hz) at room temperature. Total RNA was then isolated using the RNAeasy Mini kit according to the manufacturer's instructions.

3.2.1.2 cDNA synthesis

First Strand cDNA Synthesis kit (Fermentas, Canada) was used to prepare cDNA from isolated RNA. Per one sample, 500 ng of RNA was mixed with 1 µl of oligo $(dT)_{18}$ primer and diluted by DEPC- treated water to a final volume of 10 µl. The mixture was incubated at 70 °C for 10 min, centrifuged and cooled on ice for 2 min. The mixture of 4 µl of 5x Reaction buffer, 2 µl of 10 mM dNTP mix, 1 µl of RiboLock RNase Inhibitor (20 U/µl) was added to each sample. Afterwards, 2 µl of M-MuLV Reverse Transcriptase (20 U/µl) was added and the mixture incubated at 37 °C for 60 min. The reaction was terminated by incubation at 70 °C for 5 minutes, and the cDNA was stored at -20 °C.

3.2.1.3 Semi-quantitative real-time PCR

To determine MMP-19 and MMP-28 transcript levels in colon of wild-type or mutant mice, semi-quantitative real-time PCR was performed. Expression of murine GAPDH (mGAPDH_RT_F: 5'-AACTTTGGCATTGTGGAAGG-3' and mGAPDH_RT_R: 5'-GTCTTCTGGGTGGCAGTGAT-3', PCR fragment size 65 bp) served as endogenous control. The exon-spanning primers used for MMPs were able to distinguish between transcripts of WT and deficient mice as they were designed in the modified exons of the genes and could not bind to cDNA from MMP-deficient animals. The forward primer for murine MMP-19 binds in exon 4 (mMMP19_RT_F3: 5'-ATCTTCAATGTGCCCTCCAC-3') whereas the reverse primer binds in exon 5 (mMMP19_RT_R3: 5'-CCACGCTGCTCCAGTACTTA-3'). The resulting product had a size of 82 bp. The primers for detecting murine MMP-28 bind DNA in exon 4 and 5, generating a product of 101 bp (mMMP28_RT_F3: 5'-CCTGTACGGAAAGCCTCTGG-3' and mMMP28_RT_R3: 5'-GTCTGCTCTGGGAGTTGTGG-3'). The PCR set-up was the same as for the genotyping

(3.2.1) but instead of genomic DNA 2 µl of cDNA were used in the reaction. The PCR program is described in Table 3-4. Steps 2 to 4 were repeated 35 times. The products were analyzed by gel electrophoresis using a 1.5% agarose gel.

Table 3-4: PCR conditions of the RT-PCR.

Step	Temperature	Time
1 - initial denaturation	95°C	2 min
2 - denaturation	95°C	15 sec
3 - annealing	60°C	20 sec
4 - extension	72°C	30 min
5 - final extension	72°C	3 min

3.2.2 Colon organ culture

Colons were excised, flushed with PBS containing 2% Penicillin/Streptavidin, and opened along the longitudinal axis. Thereafter, from the distal colon 3 x 8 mm (24 mm^2) biopsies were excised and incubated for 24 h in a 12-well plate containing 1 ml fresh RPMI 1640 lacking FCS but supplemented with 2% penicillin and streptomycin at 37°C and 5% CO_2. Culture supernatants were harvested and kept at -20°C until assessed for cytokines/chemokines by ELISA or Bio-Plex suspension array system (Bio-Rad Laboratories Inc., CA, US).

Supernatants were analyzed for KC and MCP-1 levels by ELISA (R&D Systems, Germany) according to the manufacturer's protocols. Optical densities were measured at 450 nm using ELISA plate reader (Tecan Reader Infinite M200) and were evaluated using a standard curve. Other cytokines and chemokines were determined by Bio-Plex bead array (see 3.2.3.2).

3.2.3 Cytokine analysis

The concentrations of 23 cytokines (IL-1α, IL-1β, IL-2, IL-3, IL-4, IL-5, IL-6, IL-9, IL-10, IL-12 (p40), IL-12 (p70), IL-13, IL-17A, eotaxin, G-CSF, GM-CSF, IFN-γ, KC, MCP-1, MIP-1α, MIP-1β, RANTES, TNF-α) were analyzed in plasma and CEC supernatants using Bio-Plex Pro Mouse Cytokine 23-Plex Assay with a Bio-Plex instrument based on Luminex xMAP technology (Bio-Rad). The procedure was carried out according to manufacturer's instructions with high sensitivity range standard settings. The conditions of the assay were standardized and optimized, prior to the analysis, to ensure optimal reproducibility. The plasma samples were centrifuged for 10 min at 13300 x *g* before the assay and diluted 1:3 in an appropriate sample matrix. Pooled plasma sample was used to control

for inter-assay variation. The results were automatically calculated with Bio-PlexManager Software version 4.3 with five-parameter logistic equations.
Cytokine levels of KC, MCP-1 additionally were measured in colon explant culture (CEC) supernatants using the ELISA Duo-Set kit according to the manufacturer's instructions (R&D Systems).

3.2.4 Myeloperoxidase activity measurement

Myeloperoxidase (MPO) activity, which is widely used to quantify neutrophil accumulation in tissues, was assessed using the *O*-dianisidine method [227]. Tissue samples were harvested and immediately frozen in liquid nitrogen. MPO activity was measured in colon tissue taken from the distal colon. After freezing in liquid nitrogen, equal aliquots of tissue samples (30 µl buffer/mg colon tissue) were homogenized in MPO buffer (50 mM potassium phosphate buffer (KPO_4), pH 6.0, containing 0.5% hexadecyltrimethylammonium bromide buffer ($C_{19}H_{42}BrN$) (0.1 g/20 ml KPO_4)), incubated at 60°C for 2 h and centrifuged at 10,000 rpm for 5 min. 10 µl of the supernatant were mixed with 50 µl peroxidase substrate. After 20 min 50 µl of H_2SO_4 were added to stop the reaction and the absorbance was measured at 450 nm on an ELISA plate reader (Tecan Reader Infinite M200) and evaluated using a standard curve.

3.2.5 Histochemistry techniques

3.2.5.1 Tissue processing

The isolated colon was divided into three parts, proximal (containing the ceacum), middle, and distal part, and fixed in 4% neutral buffered formaldehyde (10% formalin) in 1 x PBS for 24 h. Fixed tissue was rinsed under running tap water for at least 30 min. Tissues were dehydrated in an ascending ethanol and xylol series in a 16h protocol using a Tissu-Tek® Vacuum Infiltration Processor (Sakura, USA). Samples were embedded in paraffin (Tissue-Tek® TEC™ 5 Embedding Console System, Sakura, USA) and sectioned to 4 µm using a microtome (Leica RM2165). Mouse spleens were treated the same way.

3.2.5.2 Hematoxylin-eosin staining

Sections were deparaffinized by washing three times with xylene for 5 min. Descending alcohol set (2 x 100%, 1 x 95% , 1 x 70% ethanol, 10 min each) was used for rehydration. The sections were rinsed in distilled water twice for 5 min, stained by hematoxylin (50 ml of 5% $KAl(SO_4)_2$ x 12 H_2O), 1 ml of 10% hematoxylin (Sigma-Aldrich, Czech Republic) in 96% ethanol, 1 ml of 2% H_5IO_6, and 10 drops of 35% HCl) for 1 min and differentiated by running tap water for 3 min. Sections were washed once in distilled water and

counterstained by Eosin-Y for 20s and rinsed in tap water for 1 min. Dehydration was performed by ascending alcohol set (1 min in 70%, 80%, and 100% ethanol) and the sections were incubated with xylene for 3 min. Slides were allowed to dry and PERTEX Mounting Media (CellPath) was used as a mounting reagent. For histological evaluation of the tissue damage, areas of inflammatory lesions were microscopically evaluated and quantified, essentially by the method of Cooper et al. [92].

3.2.5.3 Trichrome staining

After deparaffinization and dehydration, slides were stained with Mallory Trichrome kit (DIAPATH, Italy) according to the manufacture's protocol. In brief, slides were washed with distilled water three times and incubated for 3 min with reagent A (fuchsine acid), washed again and incubated with reagent B (phosphomolybdate) for another 3 min. Reagent B was allowed to run of the slide and immediately after reagent C (Mallory solution: methylen blue, Orange G, oxalic acid) was added and slides were incubated for 5 min. Slides were washed with distilled water and differentiated in 96% ethanol for 1 min followed by dehydration and mounting.

3.2.5.4 Immunohistochemistry (IHC)

Slides were stained for proliferation marker Ki-67 (DAKO, Denmark), macrophage marker F4/80, as well as for collagen I and IV (all AbD Serotec, UK). Antibodies were summarized in table 3-5. For the Ki-67 and the collagen I antibody the pre-treatment for epitope retrieval was done by boiling the slides in 10 mM Citrate buffer, pH 6.0 at 96 °C for 20 min. For the F4/80 and the collagen IV antibodies the epitope retrieval was done by incubation with 0.01% Proteinase K (20 mg/ml) (Biolabs, Germany) in 20 mM Tris-HCl buffer (pH 7.4) for 5 min at RT. Afterwards, slides were washed in 1 x PBS three times for 5 min and blocked for endogenous peroxidase with 3% H_2O_2 in 1 x PBS for 10 min. A second blocking step with 3% low-fat milk powder, 2% BSA, and 0.1% NaN_3 in 1 x PBS was carried out for 1h at RT to reduce unspecific binding. Subsequent incubation with the primary antibody, which was diluted in 1 x PBS containing 10% FCS and 0.1% NaN_3 , was done for 1h at RT (F4/80) or overnight at 4°C (Ki-67, collagen I and IV). The secondary antibody was diluted 200 times in 1 x PBS + 10% FCS without NaN_3 and slides were incubated for 1.5h at RT. As these antibodies were biotinylated, streptavidin-HRP (BD Pharmingen, USA) was added to the slides and incubated for 30 min at RT. The visualization of positive cells by the chromogen DAB (3,3- diaminobenzidin) (DAKO, Denmark) was performed according to the manufacturer's protocol for 5 to 10 min. The staining procedure was completed by a counterstaining with hematoxylin (30 sec) to visualize the nuclei of the cells.

Table 3-5: Primary antibodies used for immunohistochemistry.

primary antibodies	distributor	dilution
monoclonal rat anti-mouse F4/80 (clone Cl:A3-1, # MCA497GA)	AbD Serotec, UK	1 : 2000
polyclonal rabbit anti-mouse Collagen I (# 2150-1410)	AbD Serotec, UK	1 : 1000
polyclonal rabbit anti-mouse Collagen IV (# 2150-1470)	AbD Serotec, UK	1 : 1000
monoclonal rat anti-mouse Ki-67 (clone TEC-3, # M7249)	DAKO, Denmark	1 : 50

Table 3-6: Secondary antibodies used for immunohistochemistry.

secondary antibodies	distributor	dilution
biotinylated polyclonal rabbit anti-rat IgG (# E0468)	DAKO, Denmark	1 : 200
biotinylated polyclonal goat anti-rabbit IgG	Vector Laboratories, UK	1 : 300

3.3 Cell analysis

3.3.1 Migration assay

RAW 264.7 cells were cultured under standard cell culture conditions in RPMI-1640 media (Media facility, Institute of Molecular Genetics, Prague, Czech Republic) supplemented with 10% FCS (PAA, Austria) and 1% penicillin/streptomycin (PAA, Austria) at 37°C with 5% CO_2. CIM-plate16 with the xCELLigence RTCA DP Instrument (Roche) were used to monitor migration of macrophages in real-time using label free conditions. The CIM-plate16 is a 16-well modified Boyden chamber composed of an upper chamber and a lower chamber. The upper chamber is sealed at its bottom by a microporous polyethylene terephthalate membrane. These micropores permit the physical translocation of cells from the upper part to the bottom side of the membrane. The lower side of the membrane (side facing the lower chamber) contains interdigitated gold microelectrode sensors which will come in contact with migrated cells and generate an impedance signal. The lower chambers contain 16 wells, which each of them serves as reservoir for a chemoattractant solution on the bottom side of the wells. For optimal RAW 264.7 cell migration, it was determined that extracellular matrix proteins are necessary. The membrane therefore was coated with 10 µg/cm^2 of collagen type IV. After CIM-plate16 assembly, 100 µl of cell suspension (30 000 cells per well) were added to each well of upper chamber. The CIM-plate16 was placed in the RTCA DP Instrument equilibrated in a CO_2 incubator and migration of RAW 264.7 cells was continuously monitored. The combination of chemoattractants (colon explant culture supernatants, RPMI media including various cytokines/chemokines) provides a signal, which induces the directional migration of RAW 264.7 cells through the micropores of the CIM-plate16. Migrating cells were detected by the electronic sensing and data are expressed as slopes of cell index values.

3.3.2 Isolation and analysis of murine cells

To further analyze the impact of MMP-deficiency, different cell types were isolated from wild-type, MMP-19-, MMP-28-deficient, and MMP-19/28-double-deficient mice. Experiments were carried out with peripheral blood mononuclear cells (PBMCs) and splenocytes. Blood collection was performed by retro-orbital bleeding of anaesthetized mice. Blood was collected in heparin coated tubes (Microvette® CB 300, Sarstedt, Nümbrecht, Germany) to avoid clotting.

Cells were washed in PBS and centrifuged for 5 min at 300 x *g*. To remove erythrocytes, cells were treated with sterile filtrated 1 x ammonium chloride lysis buffer (150 mM NH_4Cl, 10 mM Na_2CO_3, 1 mM EDTA, pH 7.4) for 5 min on ice. After centrifugation (5 min at

300 x *g*) and washing with PBS, cells were resuspended in PBS containing 1% BSA and 0.1% NaN_3, counted using the Neubauer counting chamber, and used for FACS analysis.

Spleens were isolated from C57BL/6NCrl mice and passed through a nylon mash into a 50 ml tube containing 5 ml 1 x PBS supplemented with 1% penicillin/streptomycin. The cell suspension was centrifuged at 300 x *g* for 5min at room temperature. The cell pellet was resupended in red cell lysis buffer, incubated for 5 min on ice and centrifuged again at 300 x g for 5 min. The supernatant was discarded, cells were washed with 1 ml PBS and resuspended in FACS solution (PBS, 1% BSA, 0.1% NaN_3), and counted using Neubauer counting chamber.

3.3.3 Flow cytometry

Analysis by flow cytometry was performed using cells isolated from blood and spleen. Once the cells were resuspended in FACS solution (PBS, 1% BSA, 0.1% NaN_3) following steps were performed on ice. For each analysis 300 000 cells were taken and centrifugation steps were run with 300 x *g* for 5 min at 4°C. For detection of surface molecules only antibodies directly conjugated with fluorochromes were used. Staining with antibodies was performed in 100 μl FACS solution for 30 min on ice in the dark. Antibodies used for flow cytometry are listed in following table (Tab. 3-7). Before incubation with fluorochrome-conjugated antibodies cells were pre-treated with rat anti-mouse CD16/CD32 antibodies to block Fc-receptors to reduce unspecific binding. Additionally, in each experiment unstained cells were prepared to generate the settings of the FACS (LSRII, BD, CA, USA) before starting the measurement. Also, all antibodies were used in single stainings for compensation.
Single-cell suspensions were washed with FACS buffer (PBS, 1% BSA, 0.1% NaN_3) and incubated with combinations of the following antibodies:

Antibody cocktail	
Mix 1 (T cells)	CD3 ε, CD4, CD8, CD69
Mix 2 (T and B cells)	CD4, CD25, B220
Mix 3 (NKT cells)	CD45, CD3 ε, NK1.1
Mix 4 (macrophages)	CD45, CD11b, F4/80
Mix 5 (granulocytes)	CD45, CD69, Ly6G/C

Cells were analyzed on an FACS LSRII (BD Immunocytometry Systems, CA, USA), and analysis was performed using FlowJo software (Tree Star, OR, USA).

Table 3-7: Antibodies used for flow cytometry.

Molecule	Host and Species Specificity	Fluorochrome	Distributor
CD3ε	monoclonal hamster anti-mouse	FITC	EXBIO
CD4	monoclonal rat anti-mouse	APC	EXBIO
CD8	monoclonal rat anti-mouse	Alexa700	EXBIO
CD11b	monoclonal rat anti-mouse	FITC	BD Biosciences
CD25	monoclonal rat anti-mouse	FITC	BD Biosciences
CD45 (pan)	monoclonal rat anti-mouse	Alexa647	gift of Dr. Waldman
CD69	monoclonal rat anti-mouse	PE	BioLegend
Ly6 G/C	monoclonal rat anti-mouse	FITC	BD Biosciences
F4/80	monoclonal rat anti-mouse	PE	BioLegend
NK1.1	monoclonal mouse anti-mouse	PE	BD Biosciences
B220/CD45R	monoclonal rat anti-mouse	PE	BD Biosciences
CD16/CD32	monoclonal rat anti-mouse	--	BioLegend

3.4 Protein analysis

3.4.1 Expression and purification of human MMP-19 GST-fusion protein (GST-MMP19)

MMP-19 was produced as a fusion protein with glutathione-S-transferase [228] in the BLR (DE3) strain of *E. coli* (Novagen, Germany) using the expression vector pGEX-2T. The recombinant protein starts N-terminally with the GST fused in frame to Phe, the first amino acid of the propeptide domain, and ends with Arg, the first amino acid of the 36 amino acid-long C-terminal tail. The expression of MMP-19 was induced by 0.6 mM IPTG. MMP-19 was produced as a fusion protein of glutathion-S-transferase [228] and MMP-19 as described [203; 229]. Purification was done according to Rohman and Harrison-Lavoie [230] with slight modifications. In brief, the pelleted bacteria were resuspended in 20 ml buffer A (sonication buffer, 100 mM triethanolamine-HCl (TEA-HCl), 150 mM NaCl, 1% Triton X-100, pH 7.4) and disrupted in the presence of Complete™ proteinase inhibitor (Roche, Mannheim, Germany) by sonification. The sonicate was pelleted and the supernatant transfered into 4 ml of buffer B (100 mM TEA-HCl, 200 mM $MgCl_2$, 500 mM KCl, 100 mM ATP, pH 7.4) and incubated for 30 min at room temperature. This step was followed by an incubation for 45 min with 0.5 ml 50% slurry of Glutathione Sepharose 4B (GE Healthcare, UK). The sepharose mixture was washed three times with 10 ml buffer C (100 mM TEA-HCl, 150 mM NaCl, 20 mM $MgCl_2$, 50 mM KCl, 1% Triton, 10 mM ATP, protease inhibitors, pH 7.4). In the last washing step buffer D was used (100 mM TEA-HCl, 150 mM NaCl, 20 mM $MgCl_2$, 50 mM KCl, 5 mM ATP, pH 7.4). For elution of the bound fusion protein we used 50 mM Tris-HCl with 10 mM reduced glutathione, pH 8.0 which was prepared freshly prior use. 5 elutions were performed and analyzed by SDS-PAGE. The fractions were pooled and dialysed over night at 4°C against 2 l TNC buffer (50 mM Tris-HCl, 150 mM NaCl, 5 mM $MgCl_2$, 5 mM $CaCl_2$, pH 7.4) using a Slide-a-lyser cassette (PIERCE, USA) to get rid of the reduced glutathione. The concentration was determined using BCA kit (PIERCE, USA).

3.4.2 Determination of GST-MMP-19 activity

To test whether the purified MMP-19 protein was active, a cleavage assay using a quenched fluorescence substrate (MMP-2 Substrate, fluorogenic, Calbiochem) was performed for 1h at 37°C. Cleavage of the fluorogenic substrate resulted in increasing fluorescence. Different concentrations of GST-MMP-19 WT (1.5 - 6 µg/well) were used in order to evaluate the protein dependency of the activity. A sample without GST-MMP-19 served as control to exclude self degradation of the fluorogenic substrate during the assay. To verify the specific effect of recombinant GST-MMP-19 the inhibitor MMP-9/MMP-13

Inhibitor II (10 µM, N-Hydroxy-1-(4-methoxyphenyl)sulfonyl-4-benzyloxycarbonyl-piperazine-2-carboxamide, Calbiochem) was used to block its activity. All assays were carried out in TNC buffer (50 mM Tris-HCl, 150 mM NaCl, 5 mM $MgCl_2$, 5 mM $CaCl_2$, pH 7.4) containing 10 µM $ZnCl_2$.

3.4.3 Fractalkine cleavage assay

The processing of 1 µg human fractalkine (R&D Systems, USA) was done in TNC buffer (50 mM Tris-HCl, 150 mM NaCl, 5 mM $MgCl_2$, 5 mM $CaCl_2$, pH 7.4) containing 10 µM $ZnCl_2$ with 4 µg GST-MMP-19 at 37°C for 35h. To determine the specificity of the cleavage, the inactive MMP-19 mutant (E213A) was used instead of the active protein as well as a set-up without any enzyme to observe self-processing of fractalkine.

3.4.4 Protein isolation from tissue biopsies

Colon biopsies were snap-frozen in liquid nitrogen and stored at -80°C. Colon from DSS-treated WT and MMP-19-deficient mice were excised, crushed in liquid nitrogen and lysed for 45 min on ice in modified RIPA buffer (50 mM Tris HCl, 150 mM NaCl, 0,1% SDS, 0.5% DOC (sodium deoxycholate), 1% Triton X-100, pH 7.5) containing 1 mM EDTA, and proteinase inhibitors (Complete EDTA-free, Roche, Germany).

3.4.5 BCA protein assay

BCA Protein Assay kit (PIERCE, IL, USA) was used to determine the protein concentration in tissue lysates. The protein samples were 10 times diluted in dH_2O, standards and working reagent were prepared according to the manufacturer´s protocol. To the 25 µl of the sample or standard, 100 µl of working reagent was added. The mixture was incubated at 37 °C for 30 minutes and absorbance of standards or samples was measured at 562 nm by a Tecan Reader Infinite M200 (Tecan group, Switzerland). The concentration of samples was calculated from the standard curve.

3.4.6 TCA protein precipitation

Supernatants (RIPA media without FCS) of colon explant cultures had to be concentrated before analysis by immunoblotting. Concentration was done by TCA (Trichloroacetic acid) protein precipitation. In brief, to one volume protein 1/100 volume of 2% DOC (sodium deoxycholate) were added and the mixture were kept on ice for 15 min. Afterwards 1/10 volume of 100% TCA were added and kept on ice for 1 h. The precipitated proteins were

collected by centrifugation at 10000 x *g* for 10 min at 4°C. The resulting pellet was washed in ice-cold acetone to get rid of residual TCA. The protein pellet was resuspended directly in reducing Laemmli sample buffer. In case the protein mixture changed to yellow, indicating remains of TCA a few microlitres of 1 M Tris, pH 8.8 were added until the colour changed back to blue.

3.4.7 Preparation of protein samples for SDS-PAGE

Lysates or mixture of recombinant proteins were mixed with reducing loading dye (250 mM Tris, 40% glycerol, 20% *β*-mercaptoethanol, 8% SDS, 0.05% bromophenol blue). Samples were mixed by vortexing and incubated at 95 °C for 5 minutes. In case of the colon lysates, 30 µg of protein and 10 µl of concentrated CEC supernatants were loaded on a polyacrylamide gel. For the analysis of the fractalkine cleavage assay 15 µl of the digest were loaded.

3.4.8 Immunoblotting (Western blotting)

Proteins were separated on 12.5% SDS gels, followed by electrophoretic transfer (transfer buffer: 3.03 g Tris, 14.27 g Glycine, 20% methanol) onto a PVDF membrane, pore size (0.45 µm) (Macherey-Nagel, Germany). Membranes were blocked with 5% non-fat milk in TBST buffer containing 20 mM Tris-HCl, 500 mM NaCl, and 0.1% Tween-20, pH 7.5 (5% TBSTM buffer) for an hour at room temperature. For detection, polyclonal goat anti-fractalkine antibody (Santa Cruz, CA, USA) or anti-fractalkine serum (gift of Dr. Andreas Ludwig, Aachen, Germany) were diluted in 2% TBSTM buffer and incubated on the membrane overnight. After three washing steps, the bound antibody was detected using peroxidase-conjugated rabbit anti-goat antibody (Jackson Immuno Research, West Grove, PA) and the ECL plus Western Blotting Detection System (GE Healthcare, UK). Signals were recorded with a Luminescent Image Analyzer (LAS-3000, Fujifilm Life Science, USA).

Table 3-8: Primary antibodies used for immunoblotting.

primary antibodies	distributer	dilution
polyclonal goat anti-fractalkine antibody (C-20) (sc-7225)	Santa Cruz, USA	1 : 500
fractalkine anti-serum (polyclonal rabbit)	Dr. Andreas Ludwig, Germany	1 : 2000

Table 3-9: Secondary antibodies used for immunoblotting.

secondary antibodies	distributer	dilution
peroxidase-conjugated rabbit anti-goat antibody	Jackson Immuno Research, USA	1 : 20 000
peroxidase-conjugated goat anti-rabbit antibody	PIERCE, Germany	1 : 10 000

3.4.9 Zymography

For the detection of gelatinase activity (e.g. MMP-2 (gelatinase A) and MMP-9 (gelatinase B)) an 8% SDS-PAGE containing 1 mg/ml gelatine was prepared. Colon homogenates of healthy and DSS-treated WT and MMP-19-deficient mice were used in this analysis. The gel was prepared as follows:

After finishing the protein separation, gels were washed two times for 20 min in 2.5% Triton X-100 to remove the SDS. Afterwards they were incubated for 24h in TNC buffer (50 mM Tris-HCl, pH 7.5, 5 mM $CaCl_2$, 10 µM $ZnCl_2$, 0.05% Triton X-100) at 37°C. The parts of gelatinase activity were displayed by staining with 0.5% Coomassie Blue R-250 (Sigma, Germany) and appeared in white on a blue background.

3.5 Barrier function

3.5.1 FITC dextran administration

Intestinal permeability was assessed by administration of non-metabolizable macromolecule FITC-dextran 4 (MW: 4000 Dalton) (TdB Consultency, Uppsala, Sweden). FITC-dextran was administered by gavage (0.6 g/kg body weight) 4 h before sacrifice. Food and water were removed 4 h before administration. Whole blood and plasma were obtained by retro-orbital bleeding of anaesthetized mice. Blood was collected in heparin coated tubes (Microvette® CB 300, Sarstedt, Nümbrecht, Germany) to avoid clotting. Dilutions of FITC-dextran 4 in PBS were used as a standard curve and absorption of 100 µl serum or standard was measured in a fluorometer at 488 nm.

3.6 Statistical analysis

All parametric data are presented as means ± standard deviation [155]. Statistical analyses were performed with GraphPad Prism. Data from two groups were analyzed for significance using a student's unpaired t-test. More groups were compared using one-way ANOVA (Kruskal-Wallis and Dunns Post test). Differences were considered significant at $p < 0.05$ and marked with *. ** designates $p < 0.005$ and *** $p < 0.001$.

4 Results

4.1 Constitutive expression of MMP-19 and MMP-28 in mouse colon

Unlike human MMP-19 and MMP-28, which have been shown to be expressed in normal intestine [131], expression of the murine orthologs in the colon is less well characterized. To address this point, colonic tissue samples of wildtype (n = 3), MMP-19-, and MMP-28-deficient mice (both n = 3) were analysed for basal expression of MMP-19 and MMP-28 by semi-quantitative PCR. GAPDH mRNA expression served as endogenous control (Figure 4-1A and C). The expected PCR fragment had a size of 65 bp. As shown in Figure 4-1, MMP-19 and MMP-28 were constitutively expressed at similar levels in colonic tissue of wildtype mice. The absence of MMP-19 or MMP-28 transcript in the tissue of the respective knockout mice was in agreement with the genotyping data confirming the disruption of the MMP genes. MMP-19 expression levels in the colon of MMP-28 -/- mice as well as MMP-28 expression levels in the colon of MMP-19 -/- mice were comparable to those observed in the wildtype animals (Figure 4-1B and D). The size of the PCR products was 82 bp for MMP-19 and 101 bp for MMP-28.

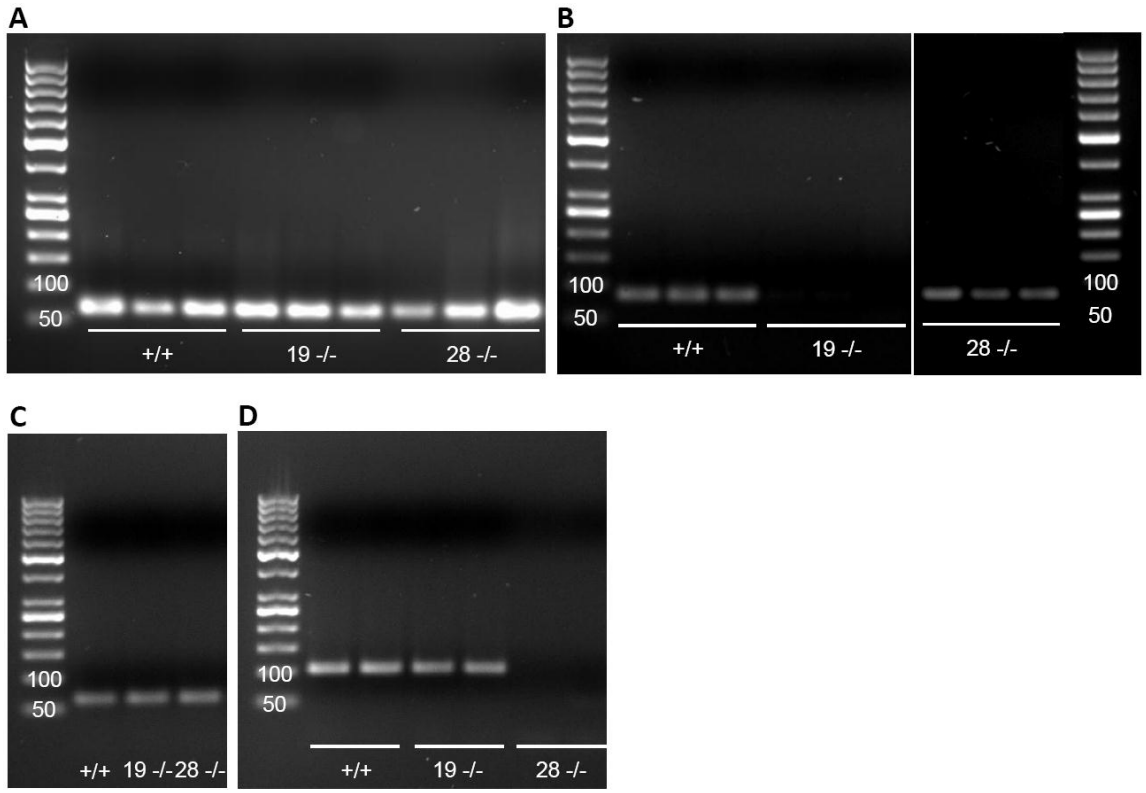

Figure 4-1: mRNA expression of MMP-19 and MMP-28 in mouse colon.
mRNA for both MMPs was detected in murine colonic tissue by semi-quantitative RT-PCR. Transcripts could not be detected in tissues from MMP-deficient mice. +/+: wildtype; 19-/-: MMP-19 -/-; 28 -/-: MMP-28 -/-.

4.2 Acute colitis

To investigate the impact of MMP-19 and MMP-28 deficiency on colitis development, acute colitis was induced in WT (n = 10), MMP-19 -/- (n = 11), MMP-28 -/- (n = 7) as well as MMP-19/-28 double-deficient (n = 12) mice by administration of 2% DSS in the drinking water for six days. Only males was used for all experiments as a significant gender bias in susceptibility to DSS-induced colitis were reported. Female mice seemed to be more susceptible to the treatment [168]. The use of females was also avoided from the beginning of the study because of the probable influence of hormonal changes during long-term experiments (e.g. chronic colitis). Untreated mice, wildtype, and single MMP-deficient mice (n = 5) were used as control. The mice were sacrificed after they had received normal drinking water for another two days (Figure 4-2). Body weight, disease activity index (DAI) [223], and survival rates were monitored daily. Besides, changes in colon length, spleen size and weight were recorded, and histological analysis of colon and spleen tissue was performed.

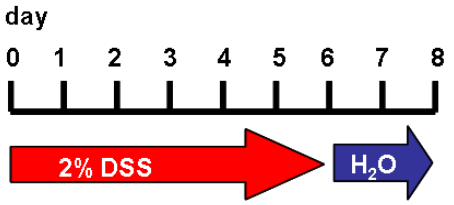

Figure 4-2: Induction of acute colitis, course of experiment.
Mice were treated with 2% DSS for 6 days and then received 2 days normal drinking water.

4.2.1 MMP-19- but not MMP-28-deficient mice show increased susceptibility to colitis

In contrast to the DSS-treated MMP-28 -/- mice, which only started to lose weight from day 5 and had not lost more body weight than the treated wildtype animals after day 8, the MMP-19-deficient mice lost weight starting at day 3 and, at the end of the experiment, showed a significantly higher weight loss than the wildtype mice (25 ± 5% versus 12 ± 3%, $p < 0.005$) (Figure 4-3A). The untreated control animals did not lose any weight. The prominent weight loss of the MMP-19 -/- mice was reflected in a higher disease activity index [223] score compared to the MMP-28 -/- mice (DAI on day 7: 4.0 ± 0.58 (MMP-19 -/-) versus 2.3 ± 0.56 (MMP-28 -/-) versus 2.0 ± 0.3 (WT), $p < 0.05$) (Figure 4-3B). The more severe colitis in the MMP-19 -/- mice also resulted in the death of about 15% of the animals. In contrast, all MMP-28-deficient mice survived (Figure 4-3C).

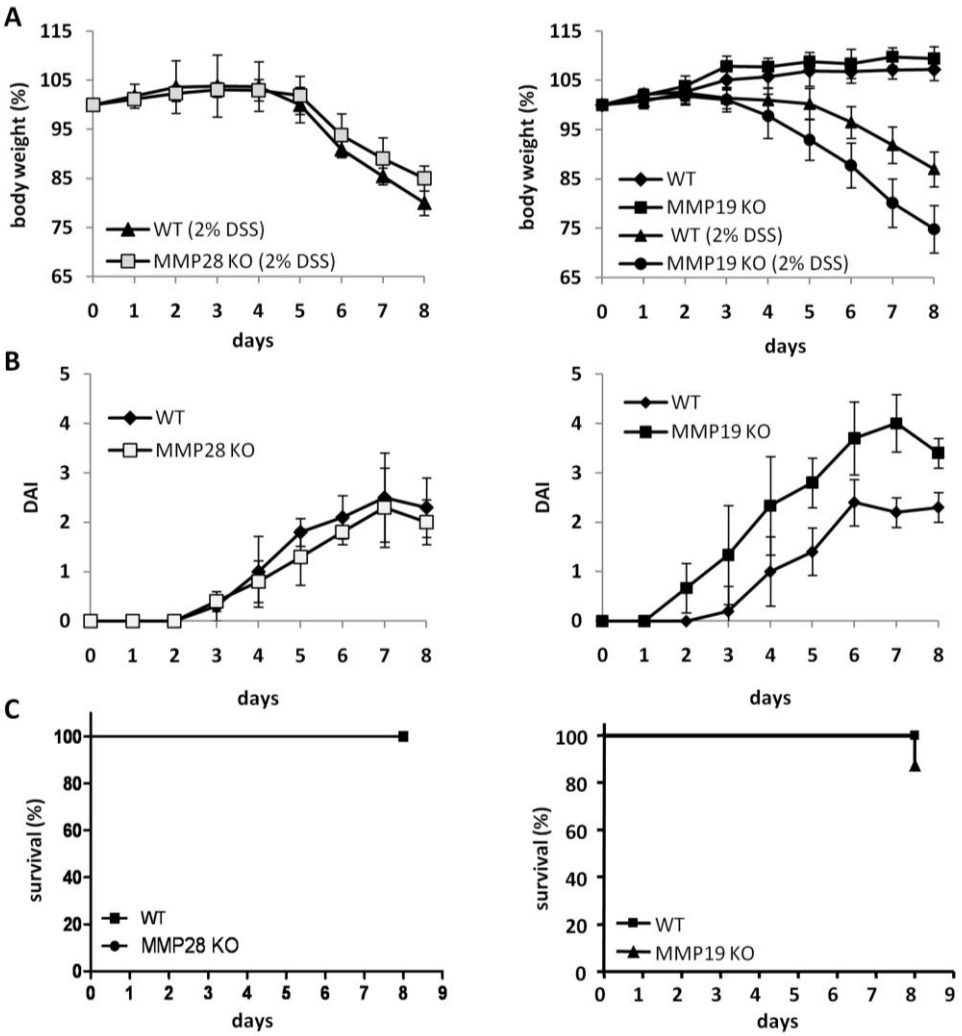

Figure 4-3: MMP-19 -/- but not MMP-28 -/- mice are more susceptible to colitis than WT mice. (A) Body weight development of DSS-treated WT (n = 10), MMP-28 -/- (n = 7, left panel) and MMP-19 -/- (n = 9, right panel) mice over the course of acute colitis (8 days). The body weight of untreated animals was recorded as control (right panel). (B) Development of disease activity index [223] of DSS-treated MMP-28 -/- (left panel) and MMP-19 -/- (right panel) mice. Data points for body weight and DAI are expressed as the mean value of all surviving animals within one group ± SD. (C) Survival curves (Kaplan-Meier) for MMP-28 -/- (left panel) and MMP-19 -/- (right panel).

Analyzing the colon of the mice on day 8, all DSS-treated animals displayed a shortened colon compared to the untreated control group (average: 6.8 ± 0.53 cm, set as 100%). However, whereas the colon length of the treated MMP-28 -/- mice (4.82 ± 0.43 cm, i.e. 70.9% of untreated colon length) was not significantly different from the one of the treated wildtype animals (4.65 ± 0.37 cm, i.e. 68.4%), the colon length of the MMP-19 -/- mice was reduced to 3.8 ± 0.27 cm, i.e. 55.9% , $p < 0.01$) (Figure 4-4A and C).

Size and weight of the spleen were increased in the DSS-treated WT mice compared to the untreated control (Figure 4-4B). This was not observed for the spleens of the MMP-28- or MMP-19-deficient mice. Accordingly, the spleen weight of the MMP-19 -/- mice was similar to the one measured for the control animals and significantly reduced compared to the spleen weight of the WT mice (Figure 4-4B and C). MMP-28 -/- mice had

a similar body weight than MMP-19 -/- and untreated mice but also in this experiment there was a tendency for an increased spleen in WT animals.
Taken together, most of these data demonstrate an increased susceptibility of MMP-19-deficient mice to DSS-induced colitis.

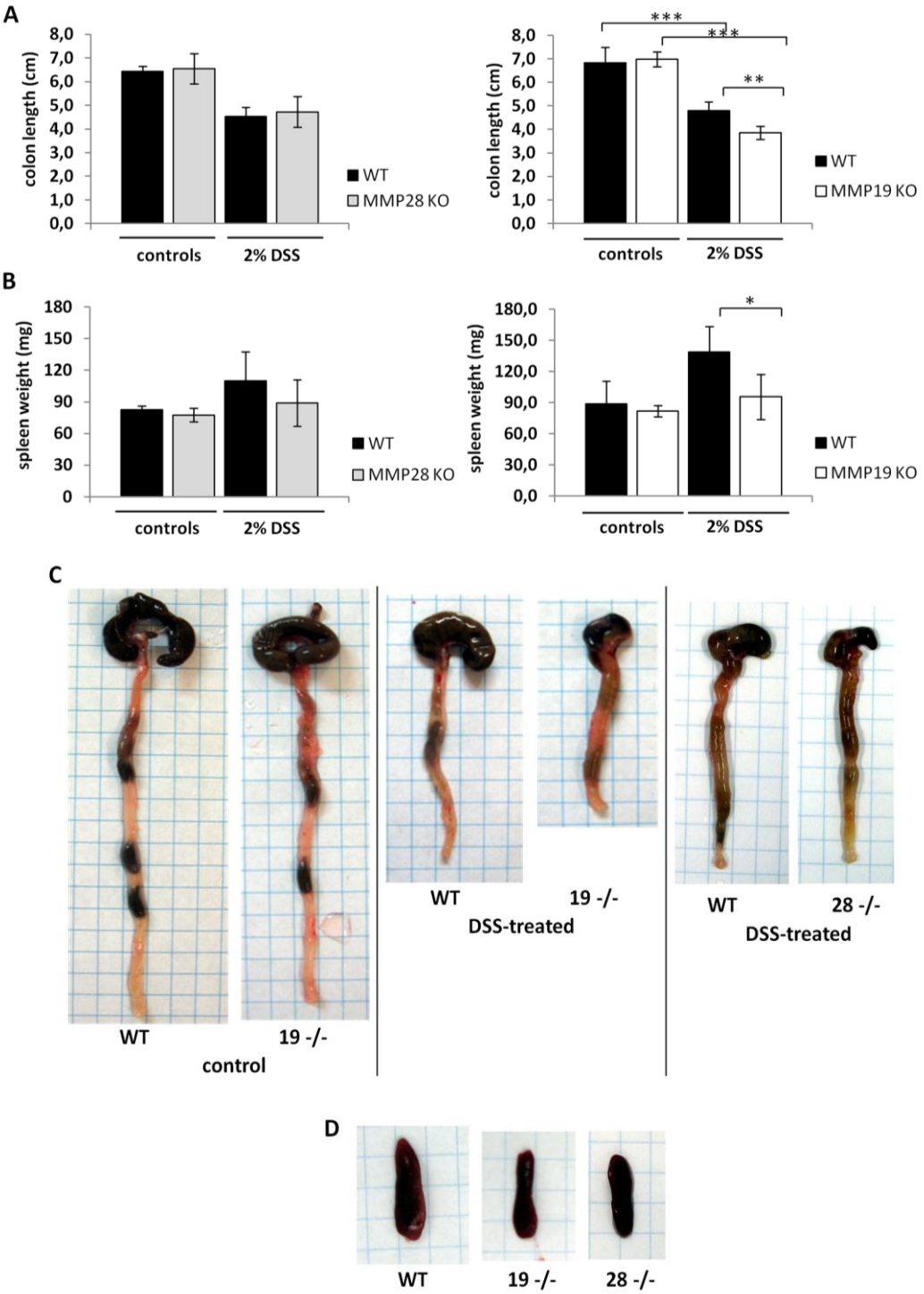

Figure 4-4: Colon length and spleen weight of MMP-19- and MMP-28-deficient mice with acute colitis.

(A) Colon length of DSS-treated MMP-28 -/- (left panel) and DSS-treated MMP-19 -/- (right panel) compared with the treated wildtype and the untreated controls. Whereas no significant differences were observed in the colon length between treated WT and MMP-28 knockout mice, the colon length of the MMP-19 -/- mice was significantly reduced compared to the wildtype (-12.5%, $p < 0.01$). (B) Spleen weight of DSS-treated MMP-28 -/- (left panel) and DSS-treated MMP-19 -/- (right panel) compared with the treated wildtype and the untreated controls. The spleen weight of the MMP-19 -/- (right panel) but not the MMP-28 -/- (left panel) mice was significantly reduced compared to the wildtype. Data for (A) and (B) are expressed as means ± SD. (C,D) Representative pictures showing colon length (C) and spleen size (D) of treated WT, MMP-19 -/-, and MMP-28 -/- mice.

4.2.2 Acute colitis is most severe in MMP-19/-28 double-deficient mice

Functional redundancy and compensation mechanisms due to overlapping substrate specificity are common among the MMP family members. To assess if MMP-19 and MMP-28 could compensate for each other in the single-deficient mouse models, the acute colitis experiment was repeated with MMP-19/-28 double knockout mice. Wildtype and MMP-19 -/- mice served as controls.

The most striking result was a dramatic reduction in survival of the MMP-19/-28 double-deficient mice compared to the control animals (survival rate on day 8: WT, 100%; MMP-19-/-, 85%; MMP-19/-28 -/-, 25%) (Figure 4-5C). Those MMP-19/-28 dbKO mice that survived lost also more weight and showed a higher DAI score than the MMP-19 single-deficient or wildtype mice (Figure 4-5A and 4-5B).

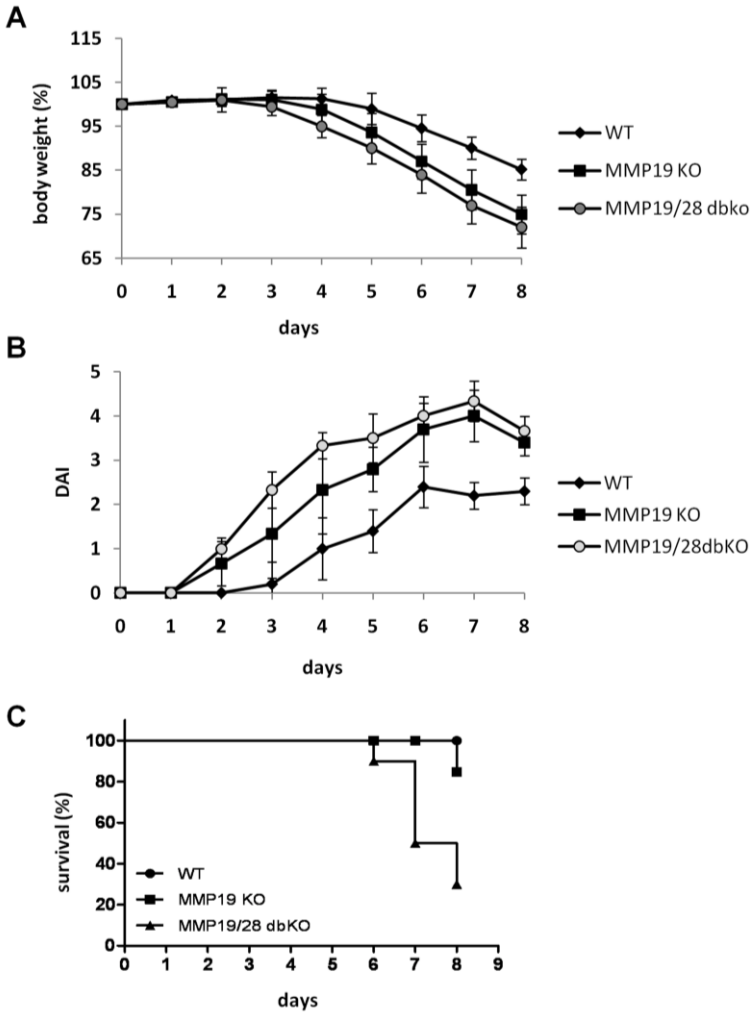

Figure 4-5: Acute colitis is considerably exacerbated in MMP-19/-28 double-deficient mice.
Body weight changes (A), disease activity index [223] (B) and survival (C) of DSS-treated WT (n = 10), MMP-19 -/- (n = 9) and MMP-19/-28 dbKO (n = 3) were recorded daily and monitored over 8 days. Data points for body weight and DAI are expressed as mean values of all animals within one group ± SD.

In addition, the colon length was significantly reduced compared to wildtype animals (4.11 ± 0.29 cm, i.e. 60.4%) but similar to the length of MMP-19 -/- colons. The spleen, however, did not display any major changes in size and weight (Figure 4-6).
Together, these findings demonstrate that the phenotype of the MMP-19/-28 double knockout mice is more severe than the one observed for the MMP-19 -/- single-deficient mice. Considering that the MMP-28 -/- animals did not show a phenotype, this indicates the capacity of MMP-19 to at least partially compensate MMP-28 function but not vice versa.

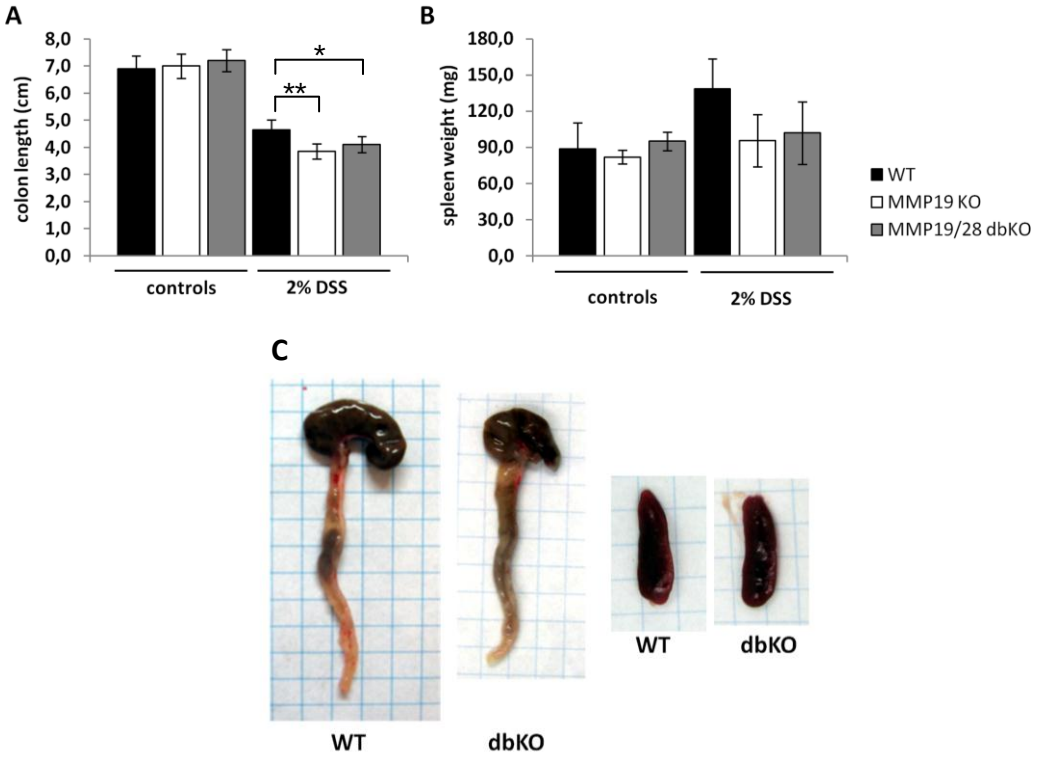

Figure 4-6: Colon length and spleen weight of MMP-19/-28 double-deficient mice with colitis.
(A) Colon length of DSS-treated MMP-19/-28 double-deficient, MMP-19 -/- , wildtype (WT) and untreated control mice. The MMP-19/-28 dbKO (-7.9%) and the MMP-19 single-deficient mice (-12.5%) showed a significantly reduced colon length compared to the wildtype animals. (B) Spleen weight. No significant differences were detected between the groups. (C) Representative pictures showing the shortened colon and the unchanged size of spleen of the MMP-19/-28 dbKO mice.

To evaluate if the onset or progression of colitis was different between the strains, a time course experiment was performed (Figure 4-7). Acute colitis was induced as described, and every second day three mice per strain were sacrificed in order to analyze the development of the shortening of the colon, the size of the spleen as well as histological parameters. Up to day 2, no shortening of the colon was detected in any of the strains, and differences to the healthy control mice were not significant. The first signs of disease were observed at day 4, with a reduced colon length of the MMP-19 -/- mice compared to the WT and MMP-28 animals. However, the differences were not significant at this point. By contrast, in case of the double-deficient mice, the colon was shortened to an average

of 5 cm, which was highly significant ($p < 0.005$). Analyzing the colon length two days later (day 6), a statistically significant difference was seen in MMP-19 single- as well as MMP-19/-28 double-deficient mice compared to the wildtype group ($p < 0.05$). This difference was still observed at day 8 ($p < 0.05$).

The weight of the spleen did not change significantly throughout the experiment but at day 8, spleens of wildtype mice were markedly bigger than those of MMP-19 -/- animals (see also 4.2.1). However, no significant difference was detected among the mutant strains, MMP-19 -/-, MMP-28 -/-, and MMP-19/-28 double-deficient mice.

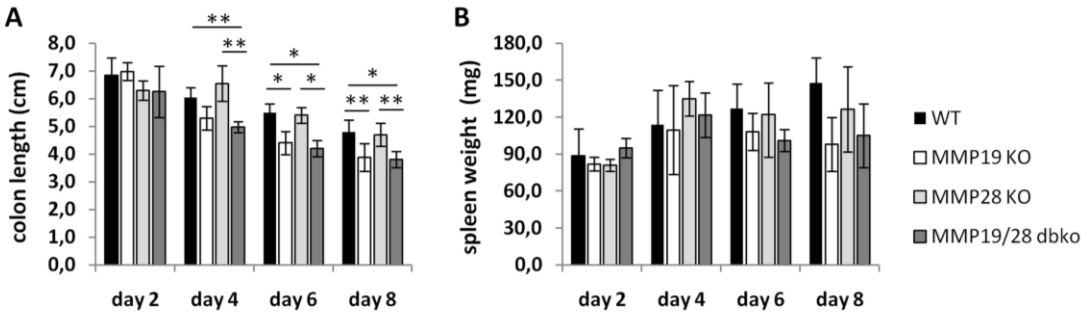

Figure 4-7: Monitoring colon length and spleen weight during the course of colitis.
Acute colitis was induced in WT (n = 12), MMP-19 -/- (n = 12), MMP-28 -/- (n = 12), and MMP-19/-28 dbKO mice (n = 12). Every other day until the end of the experiment (day 8), 3 mice per group were sacrificed, and colons and spleens were analyzed for changes in size and weight. (A) A continuous reduction in colon length was observed in all groups, with no significant differences between MMP-28-deficient and wildtype mice. In contrast, the colon length of the MMP-19-deficient and the MMP-19/-28 double-deficient mice were markedly reduced compared to the wildtype animals throughout the experiment. (B) The spleen weight of wildtype mice increased steadily during the course of the experiment, whereas the one of the other groups increased only until day 4 and afterwards remained largely unchanged or even decreased. *, $p < 0.05$; **, $p < 0.005$.

4.2.3 MMP-19 single- and MMP-19/-28 double-deficient mice developed anemic spleens

The spleen consists of two major parts, the red pulp and the white pulp. Whereas the white pulp is responsible for the immune response, the red pulp filters the blood for pathogens and dying cells and serves as a reservoir for monocytes [231]. Under normal conditions the red pulp is always filled with blood in order to clean it. Analysis of mouse spleens after acute DSS-treatment revealed signs of severe anemia (loss of red blood cells) in case of the MMP-19-deficient and MMP-19/-28 double-deficient animals. This phenotype is due to the excessive blood loss caused by the acute colitis and damaged epithelia, which leads to internal bleeding into the colon and is detectable during the course of colitis. At day 8 all strains had anemic spleens; however, the double-deficient mice were most affected as all surviving mice depicted this phenotype.

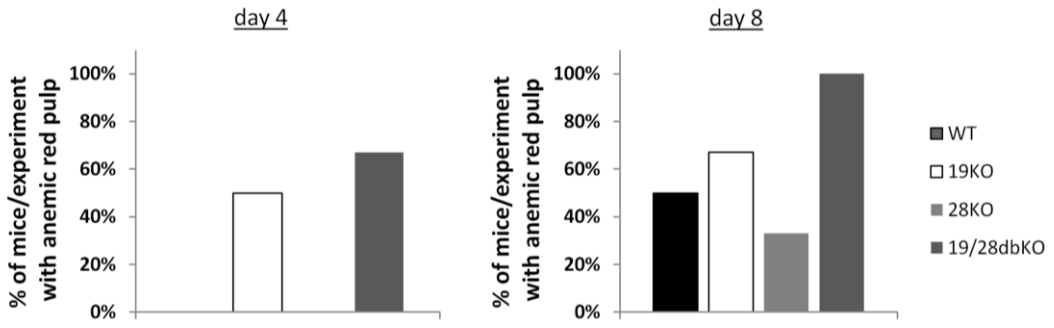

Figure 4-8: Development of anemic spleens during the course of acute colitis.
Spleens were found to be anemic already at day 4 in more than half of the experimental cohort of MMP-19 -/- and MMP-19/-28 double-deficient mice. At day 8 also the other strains showed a decreased number of red blood cells in the spleens. All double-deficient mice were showing this phenotype. Two independent experiments were performed.

4.2.4 Extensive colon inflammation and damage in MMP-deficient mice with acute colitis

For histological analysis, the mouse colon was divided into three parts – proximal, middle, and distal. All parts were analyzed throughout the study. Only results of the distal part of the colon are shown as this area was reported to be the most affected one in DSS-induced colitis [98; 232], which is in line with the obtained results. Three mice per group and experiment were randomly picked and the tissue sections evaluated in a blind analysis by a pathologist. Colon sections stained with hematoxylin/eosin were analyzed for parameters related to tissue destruction and inflammation (Figure 4-11).

All untreated mice did not show any signs of disease, even if analyzed in detail (Figure 4-9).

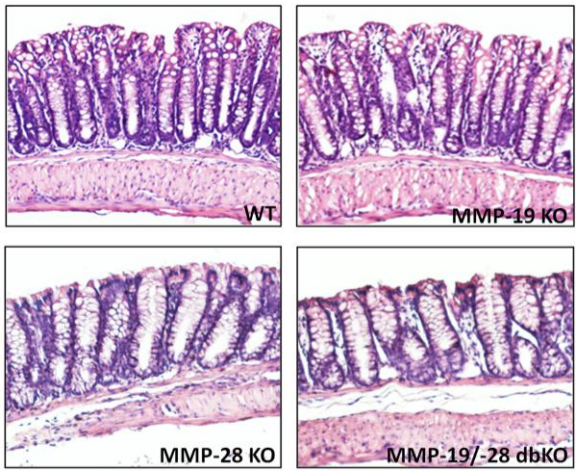

Figure 4-9: Representative pictures of colons of untreated (healthy) mice.
Hematoxylin/eosin staining of WT, MMP-28 -/-, MMP-19 -/-, and MMP-19/-28 dbKO mice, magnification x 100.

All DSS-treated mice showed clear signs of colon inflammation and damage. Thus, about 50% of the colon mucosa of WT mice displayed inflamed lesions and oedema (Figure 4-10 and 4-11A and 4-11B), and about 40% of the tissue was affected by crypt damage (Figure 4-11G). An oedema is an abnormal accumulation of fluid in the tissue due to increased blood vessel wall permeability e.g. during inflammation. It is one of the first signs of inflammation caused by a strong acute inflammatory response. The spatial extent of crypt damage needs to be seen in conjunction with the depth of damage. A damage score of 1 means the whole crypt is destroyed and not recognizable anymore.
A considerable neutrophil influx was another symptom of increased inflammation (Figure 4-11B). However, the most severe colon damage was observed for the MMP-19-deficient mice. The area showing inflamed lesions covered about 80% of the tissue, which was significantly more than seen in all other groups (Figure 4-11A). Ulceration intensity and depth as well as crypt damage and depth were also significantly increased compared to the WT and the MMP-28 -/- mice (Figure 4-11C, D, G and H). Ulceration describes the loss of the epithelium in the colon during DSS-treatment. In case of 100% ulceration intensity the whole epithelium is absent. The depth score also describes how deep the ulceration affects the mucosa. Remarkably, the MMP-28-deficient mice displayed generally less severe colon inflammation and destruction than the WT animals. For instance, the extent of inflamed lesions and the intensity of ulceration were markedly reduced, although no significance was achieved. The MMP-19/-28 double-deficient mice showed a trend towards more severe colon damage than observed in the MMP single- deficient animals. However, the differences were not significant, which probably resulted from the fact that only surviving mice were analyzed. Furthermore, especially the MMP-19-deficient mice showed a high percentage of hyperregenerative tissue (Figure 4-11F). Regeneration means normal restoration/repair of the epithelium, which is a positive effect. In contrast, the term hyperregeneration means that large numbers of immature epithelial cells are present at the site of restoration, the repair mechanisms are not controlled properly, which can lead to tumor development.

Taken together these findings further support the increased susceptibility of the MMP-19-deficient mice to DSS-induced colitis and suggest that they are also more prone to develop colon cancer.

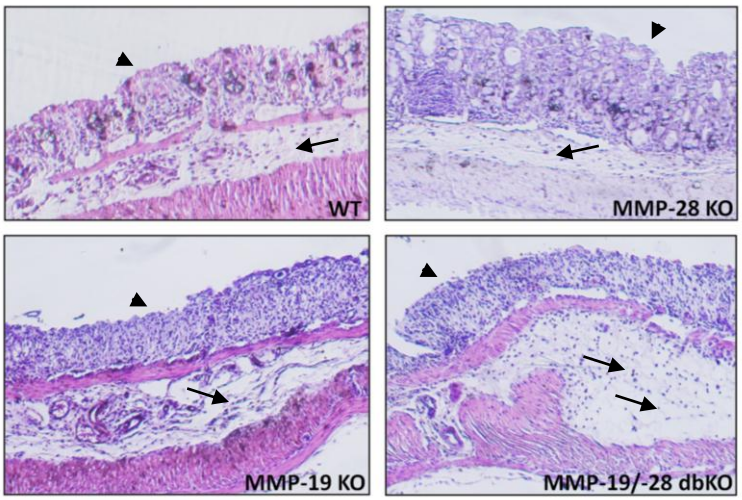

Figure 4-10: Representative pictures of proximal colon after acute colitis of WT, MMP-28 -/-, MMP-19 -/-, and MMP-19/-28 double-deficient mice.
Extensive oedema formation could be observed in MMP-19 -/- and MMP double-deficient mice (arrows), compared to milder influx of liquids in WT and MMP-28 -/- animals. Arrowheads are pointing to the epithelium of the mucosa, which is still present in WT and MMP-28 -/- mice but nearly completely absent in MMP-19 -/- and MMP double-deficient mice. Hematoxylin/eosin staining, magnification x 40.

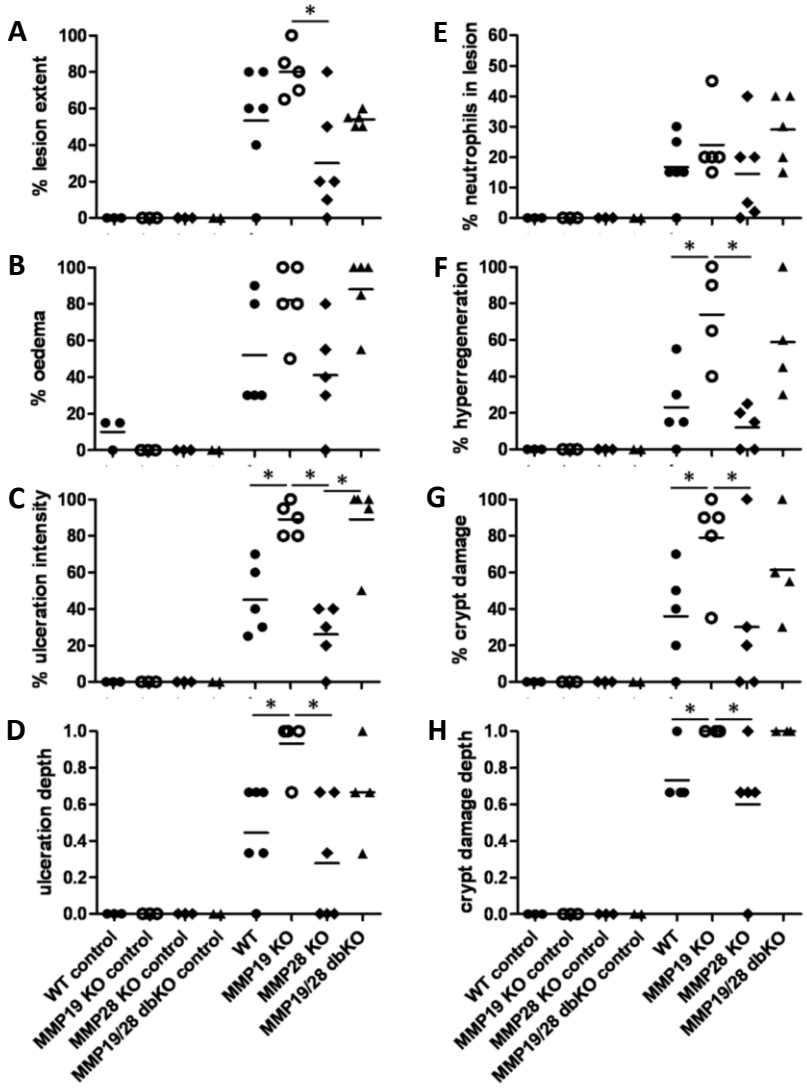

Figure 4-11: Histological analysis of colon tissue of MMP-deficient mice with colitis.
Colon tissue sections of DSS-treated WT, MMP-19 -/-, MMP-28 -/-, and MMP-19/-28 double-deficient mice were stained with hematoxylin/eosin and analyzed for parameters related to inflammation and tissue destruction. Untreated mice of each group served as controls. All DSS-treated animals showed clear signs of colon inflammation and tissue damage. The most severe symptoms, however, were observed for the MMP-19-deficient mice, which displayed a significantly higher percentage of inflamed lesions (A), ulceration (C) and crypt damage (G) as well as hyperregenerative tissue (F) than WT and MMP-28 -/- mice. The MMP-19/-28 double-deficient mice showed a trend towards more severe colon inflammation and damage compared with the WT animals but no significant differences were seen (data are shown as dot plot with means. *, $p < 0.05$).

4.2.5 Decreased and delayed neutrophil influx and higher inflammation scores in MMP-19-deficient mice

Analysis of hematoxylin/eosin stained distal parts of the colon over the course of acute colitis revealed that the percentage of inflamed colonic tissue in MMP-19 -/- mice is higher during the whole treatment (Figure 4-11A), whereas oedema formation is similar in both lines at the beginning and only significantly increased at day 8 in the MMP-19-

deficient mice (Figure 4-11B). The amount of neutrophils in the inflamed tissue rose to 90% of all cells in WT mice on day 2 of the treatment, during the progression of the disease the numbers of neutrophils decreased to 20% of all cells at day 8. At this time point of the colitis, WT and MMP-19-deficient mice showed the same numbers of neutrophils in the inflamed colon tissue, whereas at the beginning neutrophils were not accumulating at the sites of inflammation in MMP-19 -/- mice (Figure 4-12C). An ulcer is a sore in the lining of the colon epithelium, accompanied by disintegration of tissue. Ulcers could result in a complete loss of the epithelium and often affect the underlying layers of the colon wall as well. The disrupted bleeding tissue causes inflammation in the colon, causing diarrhea. It was a few days before ulceration developed in the DSS-treated mice but it was earlier seen in the MMP-19 -/- mice and around 90% of the tissue was affected in these animals compared to only 20% in WT mice (Figure 4-11D).

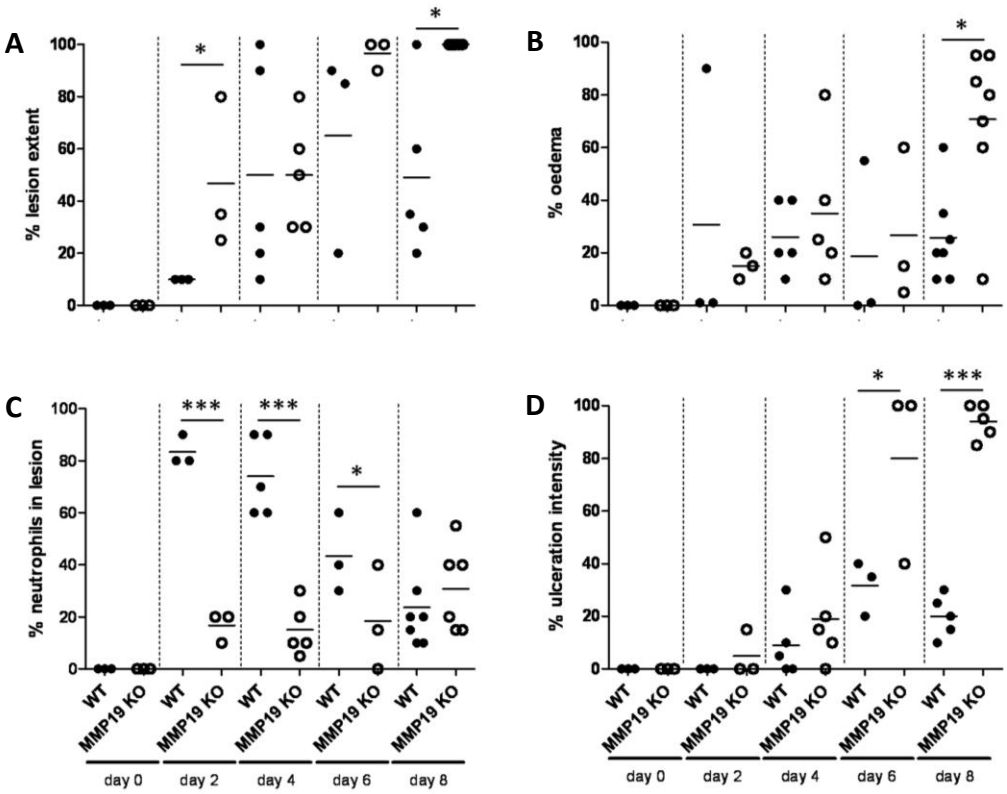

Figure 4-12: Higher inflammatory lesion extent and low numbers of neutrophils in lesions over the course of acute colitis in MMP-19-deficient mice.
The percentage of inflamed colonic tissue (A) in MMP-19 -/- mice is higher during the whole treatment, whereas oedema formation (B) is similar in both lines at the beginning and only significantly increased at day 8 in the MMP-19-deficient mice. Neutrophils are not accumulating in the tissue of MMP-19 -/- mice, numbers stayed at low levels during the course of colitis (C). In contrast, the amount of tissue affected by ulceration of the mucosa rose to 90% until the end of the experiment (D).

In addition to the evaluation of the amount of neutrophils in the tissue, MPO (Myleoperoxidase) activity was measured in WT and MMP-19 -/- mice at day 8 of the experiment. MPO is an enzyme produced mainly in neutrophils [233; 234] but also other inflammatory cells like macrophages. MPO is secreted by activated neutrophils and

macrophages during inflammation and after phagocytosis of bacteria. The higher the amount of this enzyme the more neutrophil granulocytes are present in the analyzed tissue, which indicates higher inflammation. An increase of MPO levels was detected in MMP-19-deficient mice, whereas WT mice showed only low activity (Figure 4-13). Thus, these results supported the histological findings where a slight tendency of higher numbers of neutrophils was observed (Figure 4-12C) and indicated more severe inflammation in MMP-19-deficient animals than in wildtype mice at day 8. The elevated numbers of neutrophils in the knockout tissue fit with the increased activity of gelatinases in the tissue as neutrophils are one source of these enzymes (see section 2.4.).

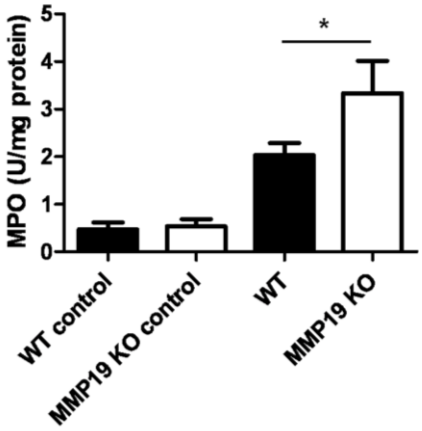

Figure 4-13: Increased MPO levels in MMP-19-deficeient mice.
MPO levels in the colon of MMP-19-deficient mice (n = 3) were increased compared to WT animals (n = 3). Data are shown as means ± SD. * $p < 0.05$.

4.2.6 Higher amount of active gelatinases in colon tissue of MMP-19-deficient mice after administration of 2% DSS

To analyze the regulation of other MMPs in WT and MMP-19 -/- mice under normal and disease conditions a method called zymography was applied. Zymography is an electrophoretic technique to detect gelatinolytic activity. It is based on SDS-PAGE that includes a substrate, in this case gelatine, copolymerized with the polyacrylamide gel. Areas of gelatinolytic activity appear as clear bands against a darkly stained background. Gelatine is the most commonly used substrate, and is useful for demonstrating the activity of gelatine-degrading proteases, such as MMP-2 and MMP-9 (gelatinases A and B). Pro-forms of MMP-2 and MMP-9 could be detected in colon lysates of untreated mice. Also a faint signal for the active enzymes was visible (Figure 4-14A). Analysis of the band intensities revealed that around 20% of MMP-2 and less than 10% of MMP-9 were present in their active form (Figure 4-14C). Analyzing DSS-treated mice suffering from acute colitis, no changes were observed for levels of active MMP-2 in WT animals, whereas the MMP-19 -/- mice showed a fourfold higher amount of active gelatinase A. Concerning MMP-9, there was a slight increase in the active form of the enzyme, which

was not significant. In MMP-19-deficient mice in contrast, the amount of active MMP-9 was elevated five times (Figure 4-14B and C).

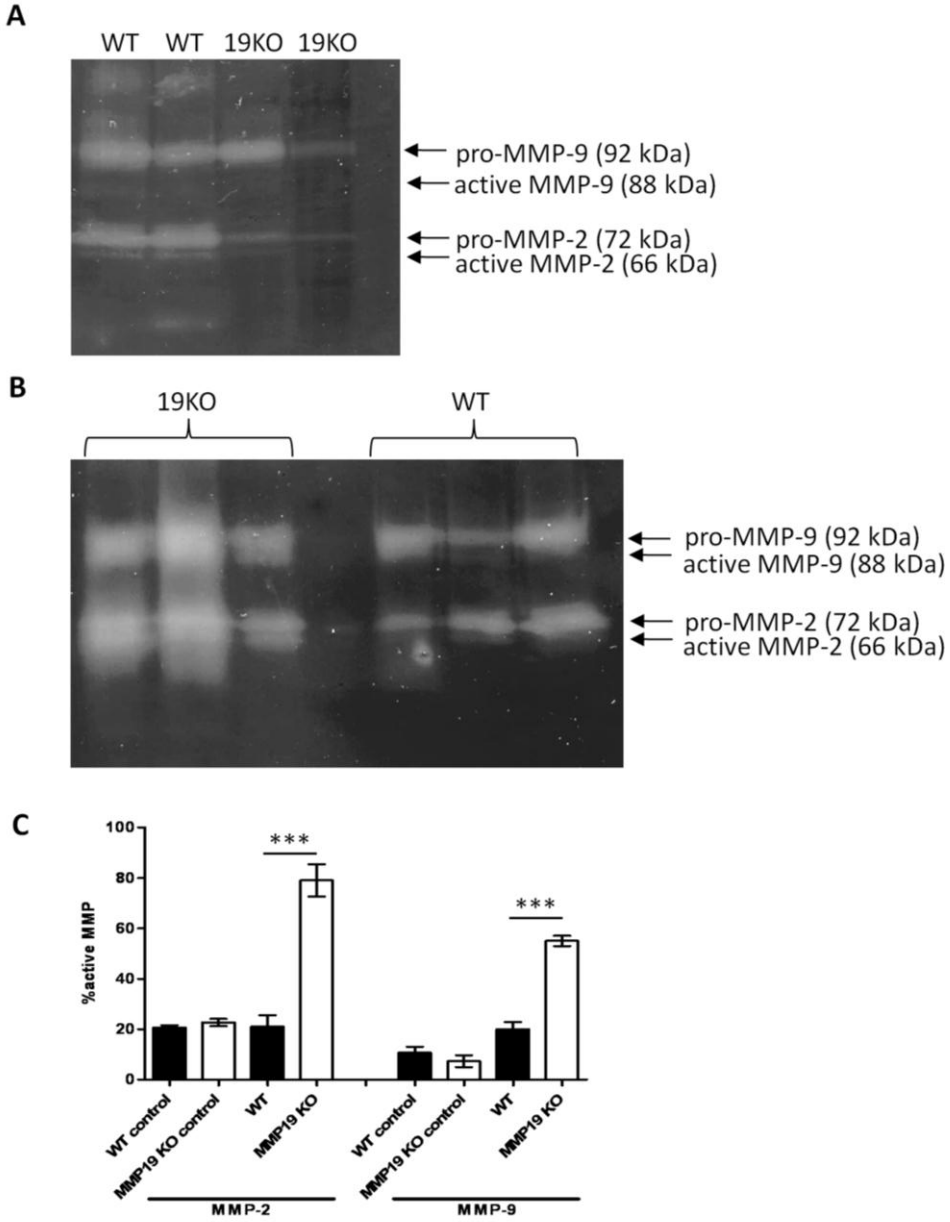

Figure 4-14: Zymography of colon lysates of healthy and diseased WT and MMP-19 -/- mice.
(A) Zymogram of colon lysates of healthy WT and MMP-19 -/- mice (n = 2). (B) Zymogram of colon lysates of WT and MMP-19 -/- mice treated with DSS (n = 3). (C) Evaluation of percentage of active MMP-2 and MMP-9 in the colon lysates of WT and MMP-19 -/- mice by Aida Image Analyzer software. Data are shown as means ± SD, *** $p < 0.001$.

4.2.7 MMP-19-deficient mice had increased permeability of the mucosa

A coordinated regenerative response is required to maintain the intestinal barrier function. Impaired barrier integrity leads to fast and severe progression of intestinal diseases. Membrane integrity was measured in the experiment by permeability of FITC-dextran [235]. FITC-dextran was administered by oral gavage four hours before sacrifice

and plasma was analyzed for the presence of FITC. In untreated animals, only low levels of FITC were detected and no difference could be found between WT and KO mice. Upon DSS administration, the intestinal barrier became permeable for FITC-dextran in both lines although to higher extent in MMP-19-deficient mice (Figure 4-15). This demonstrated the highly destroyed barrier in the MMP-19-deficient animals.

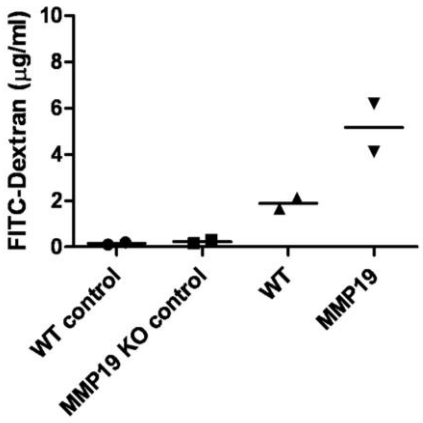

Figure 4-15: Permeability in colon of WT and MMP-19 -/- mice.
Acute colitis was induced as described. Plasma FITC-dextran concentrations in WT (n = 2) and MMP-19-deficient (n = 2) mice 4h after administration. No significance was detected as only two mice per group were used but there is a strong trend towards an increased permeability in the MMP-19-deficient mice.

4.2.8 Reduced proliferation and no significant change in amount of macrophages in MMP-deficient mice with acute colitis

Proliferation in the colon tissue was analyzed by immunohistochemistry using an antibody against murine Ki-67, which is a nuclear antigen expressed by all proliferating cells. Only dark brown stained nuclei were counted as positive.
Renewal of the colonic epithelial cells starts from the basal part of the crypts, from where dividing cells migrate towards the apical side. In the intestine, a constant cell turnover is needed to replace cells damaged through contact with luminal contents. Under normal conditions, cells migrate at a constant speed to the non-dividing segments of the crypts. In untreated mice a normal proliferative pattern was observed (Figure 4-16A).
In contrast, the proliferation was diminished in the DSS-treated animals (Figure 4-16B and C). A significant difference was detected among WT, MMP-19-deficient, and MMP-19/-28 double-deficient mice; in WT animals 25% of Ki-67 positive cells were present, whereas in the MMP-deficient mice only 10% of the epithelial cells were proliferating. This strong reduction of proliferating cell in acute colitis is due to the destructive effect of DSS to the epithelial cells, especially the basal ones.

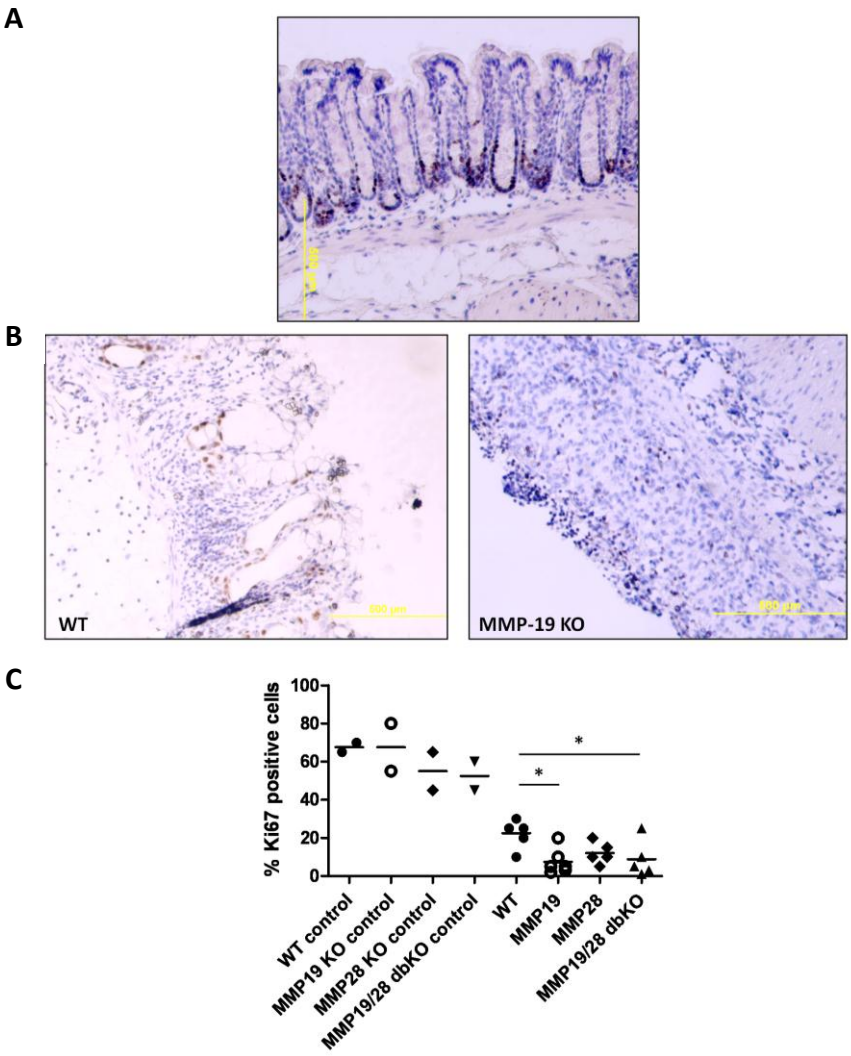

Figure 4-16: Decreased proliferation of epithelial cells in colon of WT, MMP-19 -/-, MMP-28 -/- and MMP-19/-28 dbKO mice.
The proliferation pattern in healthy colon mucosa was the same for all strains, a representative picture is shown (A and C). Strongly diminished numbers of proliferating epithelial cells were observed in all DSS-treated mice (C) although MMP-19 -/- and MMP-19/-28 double-deficient mice showed significantly less cells positive for the proliferation marker Ki-67 in the mucosa (B and C). Data are shown as individual data points with means, n = 2 for untreated mice; n = 5 for DSS-treated mice. *, $p < 0.05$.

Macrophages function in both innate as well as adaptive immunity of vertebrate animals and are the most important mediators in wound healing. They phagocytose (engulf and then digest) cellular debris and pathogens, either as stationary or as mobile cells, and in addition stimulate lymphocytes and other immune cells to respond to pathogens by releasing various cytokines. Another important function of macrophages is phagocytosis of ageing and apoptotic neutrophils, which are the predominant cells at the early stages of inflammation. Under normal conditions, only few macrophages are present in the colon mucosa (10%) (Figure 4-17B). Acute inflammation leads to activation and migration of macrophages to the site of tissue damage to initiate the healing process. At day 8 of acute DSS-induced colitis, inflammation was already well established in the colon.

Macrophages were detected with an antibody against F4/80, a transmembrane glycoprotein specific for these cell type. High numbers of macrophages were found in the mucosa of all analyzed mouse strains, although with no significant differences. Still, F4/80 positive cells were reduced by trend in the MMP-19/-28 double-deficient mice (Figure 4-17A and B), an observation that fits well with the severe phenotype as the healing process in those mice appears to be impaired.

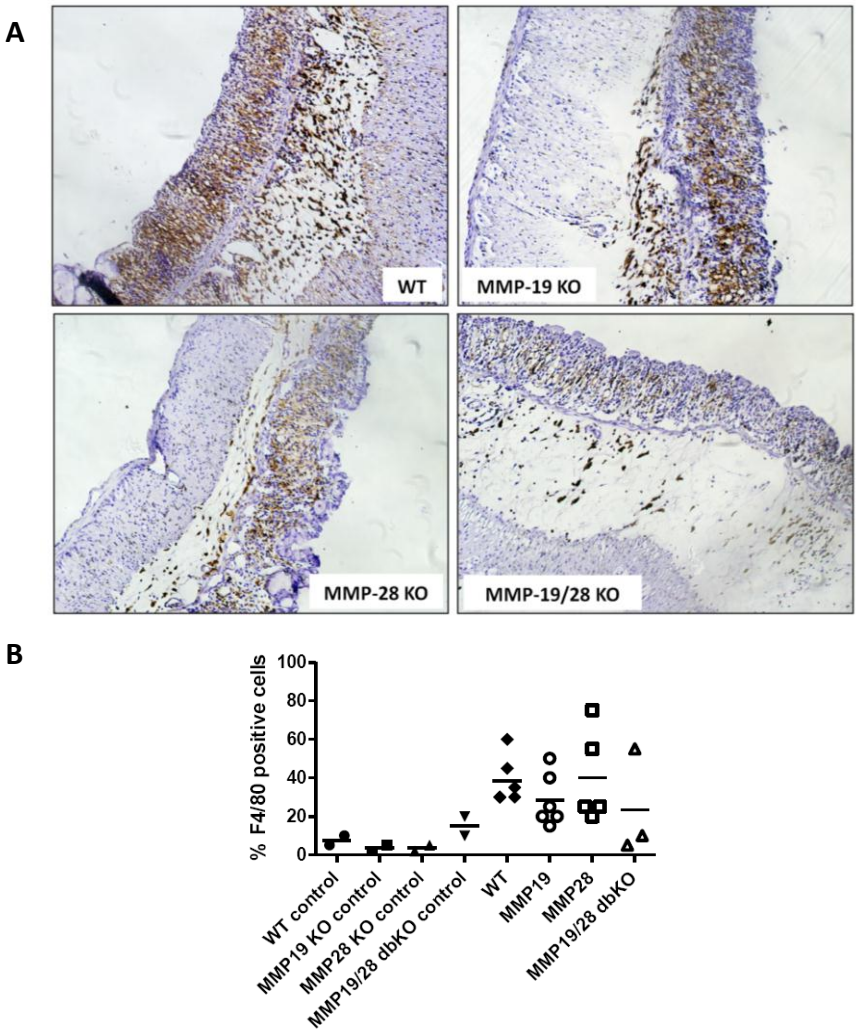

Figure 4-17: Similar numbers of macrophages present in colon of WT, MMP-19 -/-, MMP-28 -/- and MMP-19/-28 dbKO mice in acute colitis.
The amount of macrophages in the inflamed colon tissue was not significantly different in the analyzed mice (B), representative pictures are shown (A). Brown cells were positive for the macrophage marker F4/80. Data are shown as individual data points with means, n = 2 for untreated mice; DSS-treated mice: n = 5, WT; n = 6, MMP-19 -/-; n = 5, MMP-28 -/-; n = 3, MMP-19/-28 dbKO. *, $p < 0.05$.

4.2.9 Levels of cytokines and chemokines remained unchanged in plasma of MMP-19-deficient mice

Only a few samples could be analyzed by BioPlex assay, as the number of tests available was limited. Plasma and supernatant of colon explant cultures were randomly picked (but both from the same mouse). In case of the untreated control animals, two samples were analyzed, for the treated ones three to six. Selected cytokines/chemokines out of a panel of 23 are shown in this study.

To reveal the severity of acute colitis and the systemic impact of the inflammation in mice, levels of various inflammatory cytokines and chemokines in mouse plasma were assessed. Overall, there was no significant difference in the cytokine/chemokine levels. Acute phase cytokines like IL-1α and IL-6 were elevated in comparison to control although not changed between the DSS-treated mice of different genotype. Levels of TNF-α and IFN-γ did not change significantly (Figure 4-18A) and the same was true for the chemokine concentrations, no significant differences were detected between the treated groups (Figure 4-18B). Interestingly, very high levels of G-CSF (granulocyte colony-stimulating factor) were observed in plasma samples from all mouse strains. This chemokine stimulates the bone marrow to produce granulocytes that are released into the blood stream in order to migrate to sites of inflammation. All together, as no pro-inflammatory cytokine exhibited an increase in the plasma, the mice suffering from acute colitis did not exhibit any systemic inflammatory response.

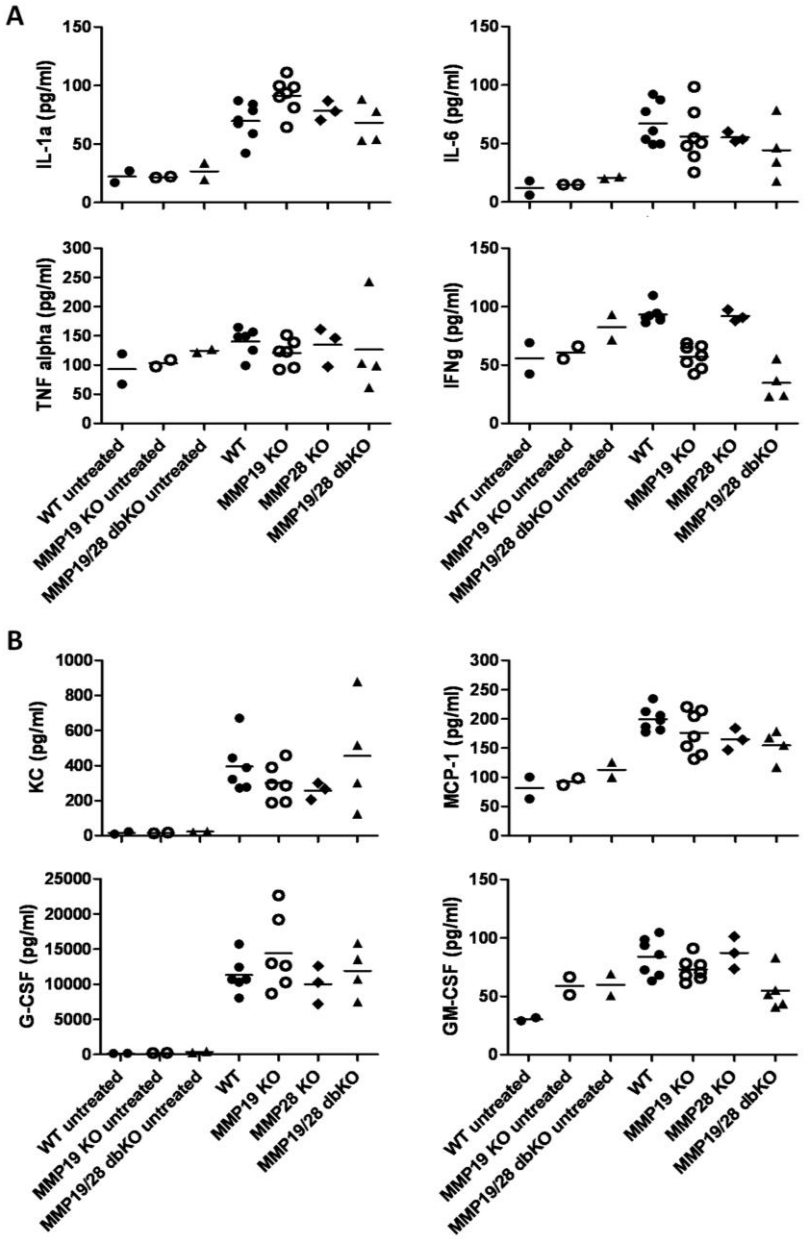

Figure 4-18: No significant differences in levels of cytokines and chemokines in plasma of mice with acute colitis.

In general, concentrations of pro-inflammatory cytokines (A) and chemokines (B) in murine plasma were elevated compared to untreated samples but no differences were detected between the treated groups. Data are shown as individual data points with means, n = 2 for untreated groups; DSS-treated mice: n = 7, WT; n = 7, MMP-19 -/-; n = 3, MMP-28 -/-; n = 4, MMP-19/-28 dbKO. No significant differences were detected.

4.2.10 Pro-inflammatory cytokines are highly elevated in mice with acute colitis

All chemokines assessed in the supernatants of colon explant cultures (CEC) were enhanced in DSS-treated mice compared to control animals (Figure 4-19). In general, Th1 cytokines like TNF-α and IFN-γ were increased in MMP-19 single- and MMP-19/-28 double-deficient mice and showed higher values than wildtype mice. MMP-19 -/- mice exhibited also remarkably high values of the pro-inflammatory cytokine IL-6 secreted from colon tissue, which points to a high local acute phase response in the mice. IL-6 can be secreted by macrophages in response to specific microbial molecules, referred to as pathogen associated molecular patterns (PAMPs). The high IL-6 concentrations correlated with the destroyed epithelium and likely invasion of bacteria into the tissue. IL-1 was significantly increased in supernatants of MMP-19/-28 double-deficient mice, only a tendency to higher concentrations was observed in case of MMP-19 -/- mice. Anti-inflammatory Th2 cytokines analyzed were IL-4 and IL-10, which were found to be significantly increased in colonic tissue of MMP-19 single- and MMP-19/-28 double-deficient animals pointing to an attempt of the immune system to suppress the inflammation. Th2 cytokines stimulate the humoral immune system; they induce B cell proliferation, and increase neutralizing antibody production.

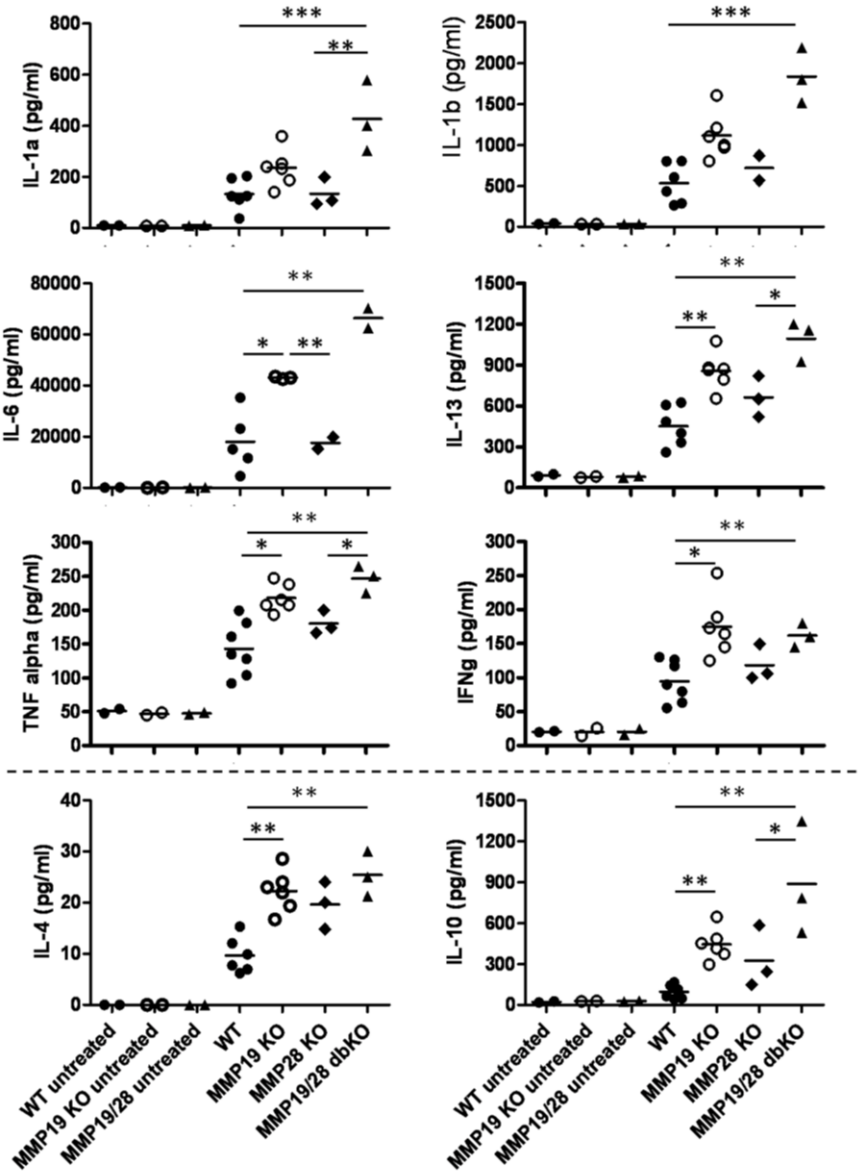

Figure 4-19: Highly elevated cytokine levels in colon tissue of MMP-19 single- and MMP-19/-28 double-deficient mice.

Pro- and anti-inflammatory cytokines were analyzed by BioPlex assay in supernatants of CEC. Increased levels of all depicted cytokines were found especially in the double-deficient animals. Data are expressed as dot plot with means, n = 2 for control mice, n = 3 for MMP-28 single- and MMP-19/-28 double-deficient animals, and n = 7 for MMP-19-deficient and WT mice (* $p < 0.05$, ** $p < 0.005$, *** $p < 0.001$).

4.2.11 Extremely high increase in chemokines release from colon tissue of MMP-19/-28 double-deficient mice

To be able to complete the picture obtained from the histological analysis, amounts of chemoattractants released from mouse colon tissue in *ex vivo* colon explant culture model were analyzed. Levels of chemokines in all lines were elevated in comparison to

unchallenged control mice. Comparing the DSS-treated mice, it was obvious that WT and MMP-28 -/- mice produced the same amounts of chemokines, which were significantly lower than those of MMP-19 -/- and the double-deficient animals (Figure 4-20). Interestingly, extremely high values were found for G-CSF, KC, and MCP-1. These three proteins play an important role in the attraction of neutrophils and macrophages to sites of inflammation. KC (keratinocyte chemoattractant protein that replaces the activity of human IL-8) and MCP-1 (monocyte chemoattractant protein) act on activated neutrophils as well as macrophages. RANTES, which was elevated as well, plays an active role in recruiting leukocytes into inflammatory sites and induces proliferation and activation of Natural Killer (NK) cell subsets.

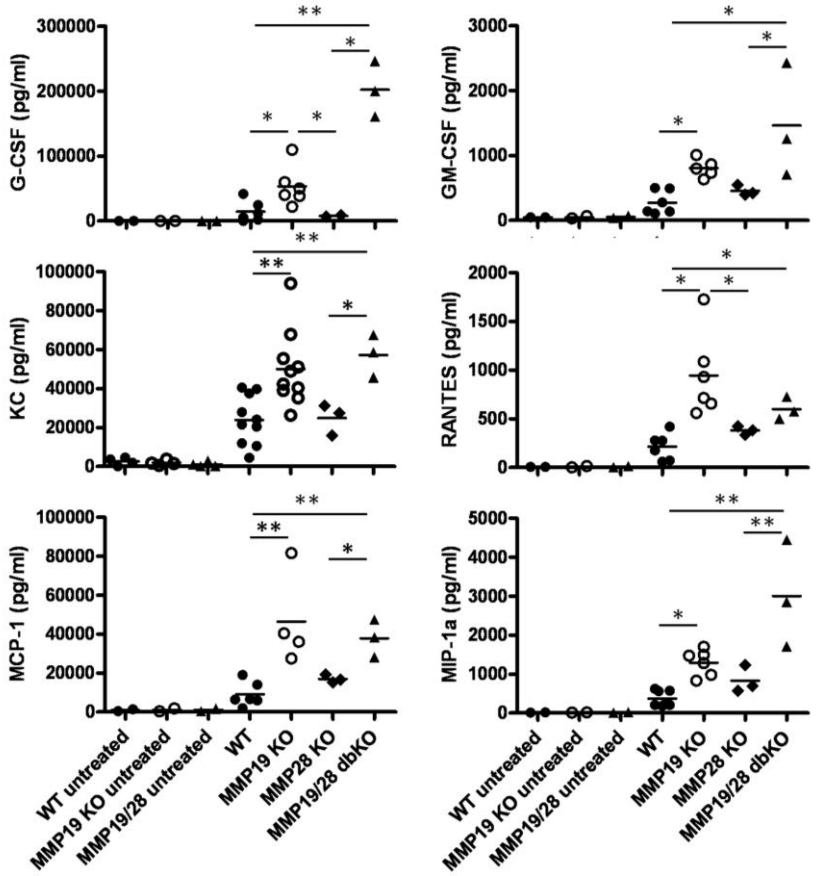

Figure 4-20: Increased chemokine levels released from colon tissue of MMP-19 single- and MMP-19/-28 double-deficient mice.

Chemokines responsible for the attraction of inflammatory cells, especially neutrophils and macrophages, depicted enhanced levels in CEC supernatants of MMP-19 -/- and double-deficient mice. Data are expressed as dot plot with means, n = 2 for control mice, n = 3 for MMP-28 single- and MMP-19/-28 double-deficient animals, and n = 6 for MMP-19-deficient and WT mice (* $p < 0.05$, ** $p < 0.005$, *** $p < 0.001$). Concentrations of KC and MCP-1 were analyzed by ELISA, whereas all other values were obtained from the multiplex analysis (BioPlex).

4.2.12 Enhanced production of chemokines released from MMP-19 -/- colon tissue promotes higher migratory level of RAW cells

Migration of cells is essential for inflammatory processes, since granulocytes, macrophages, and other blood cells have to cross the basement membrane of the vascular endothelium to act at the site of affected tissues. Collagen type IV is the main component of the basement membrane that has to be disrupted upon transmigration. Migration through connective tissues containing high amounts of collagen type I requires activity of collagen type I-cleaving enzymes. Cells often migrate in response to, and towards, specific external signals, a process called chemotaxis. Chemoattractants are inorganic or organic substances possessing chemotaxis-inducer effect in motile cells. The chemoattractant moiety of a ligand is often target cell specific and concentration dependent. Most frequently investigated chemoattractants are chemokines. As remarkable high levels of several chemoattractants were observed in explants of colonic tissue of MMP-19-deficient and MMP-19/-28 double-deficient mice, the functionality of these chemokines was addressed. RAW 264.7 cells, a mouse leukaemic monocyte macrophage cell line, were used in a migration assay towards supernatants of colon explant cultures derived from WT and MMP-19 -/- tissues to study if some chemokines were not active due to absence of MMP-19 processing. Cells migrated three times faster towards the supernatant of MMP-19 -/- colon tissue (Figure 4-21), which resembled the higher concentrations of various chemokines in these samples. Probably non-active chemokines in this mixture did not impair the migratory efficiency of a monocytic cell line.

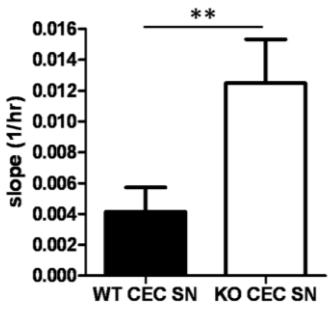

Figure 4-21: Mouse macrophages migrate faster towards colon explant culture supernatants of DSS-treated MMP-19 -/- mice.
Migration of RAW264.7 cells exhibited three fold higher level through a layer of collagen type IV towards supernatants of colon explants cultures from DSS-treated MMP-19-deficient mice, which contained significantly higher levels of cytokines and chemokines than the samples obtained from WT mice. (n = 4; **, $p < 0.005$)

4.2.13 Increase in granulocytes but reduced T cell numbers in peripheral blood of MMP-19-deficient mice with acute colitis

To investigate if MMP-19-deficiency had an impact on cell populations present in blood or spleen, leukocytes from peripheral blood and spleen of wildtype and MMP-19 -/- mice were isolated and analyzed by flow cytometry. CD3, CD4, and CD8 were used as cell-surface markers for T cells, representing the adaptive arm of the immune system, whereas Ly6G/C (for granulocytes) and F4/80 (for monocytes/macrophages) were the markers chosen to identify innate immune cells. The NK marker NK1.1 was used in combination with CD3 to detect unconventional NKT cells, which have the capacity to elicit both adaptive and innate immune responses.

Analyzing the peripheral blood, a highly significant decrease in CD4+ and CD8+ T cell numbers was observed for the MMP-19-deficient mice compared to the WT and untreated animals (CD4+ T cells: MMP-19 -/-, 14.3 ± 2.3% versus WT, 24.1 ± 2.2 versus untreated control group, 22.5 ± 2.9% of CD3+ cells; $p < 0.001$). In contrast, NK1.1+ NKT cells were significantly increased in both groups of DSS-treated mice, although not as pronounced in the MMP-19 knockout mice as in the WT animals (Figure 4-22A). The decrease in conventional CD3+ T cell numbers was accompanied by a marked increase in CD45+/CD11b+/Ly6G/C+ granulocytes in the peripheral blood of the MMP-19-deficient mice. This increase was about 2-fold compared to the DSS-treated wildtype group and highly significant (MMP-19 -/-, 31.4 ± 4.4 versus WT, 16.4 ± 6.2, $p < 0.001$). Compared to the untreated control animals, the blood of the WT also contained a significantly higher proportion of this cell population (Figure 4-22C). The increase of granulocytes in mouse blood nicely goes together with the elevated levels of G-CSF in plasma. Remarkably, the F4/80+ monocyte population in the blood of the MMP-19-deficient mice remained largely unchanged compared to the healthy controls and was significantly diminished compared to the DSS-treated WT mice (WT, 8.8 ± 2.4 versus MMP-19 -/-, 3.8 ± 0.7, $p < 0.005$) (Figure 4-22C).

In the spleen, CD4+ T cell numbers of the MMP-19 -/- mice were similar to those observed in the control group, although significantly higher than those of the DSS-treated WT mice. In contrast, the CD8+ T cell population was increased about 50% compared to the WT and the control animals (untreated control, 11 ± 0.2% versus WT, 10.4 ± 1.7% versus MMP-19 -/-, 16 ± 0.9%; $p < 0.005$) (Figure 4-22B).

Despite a trend towards increased numbers of granulocytes (Ly6G/C+ cells) in spleen of MMP-19-deficient mice, no significant differences were seen between the three groups (Figure 4-22D). The macrophage population (F4/80+ cells) was only increased in spleens of treated WT but normal in MMP-19 -/- mice (Figure 4-22D).

Taken together, these data indicate an abnormally strong innate immune response of the MMP-19-deficient mice to DSS-induced colitis, which negatively affects components of the adaptive immune system.

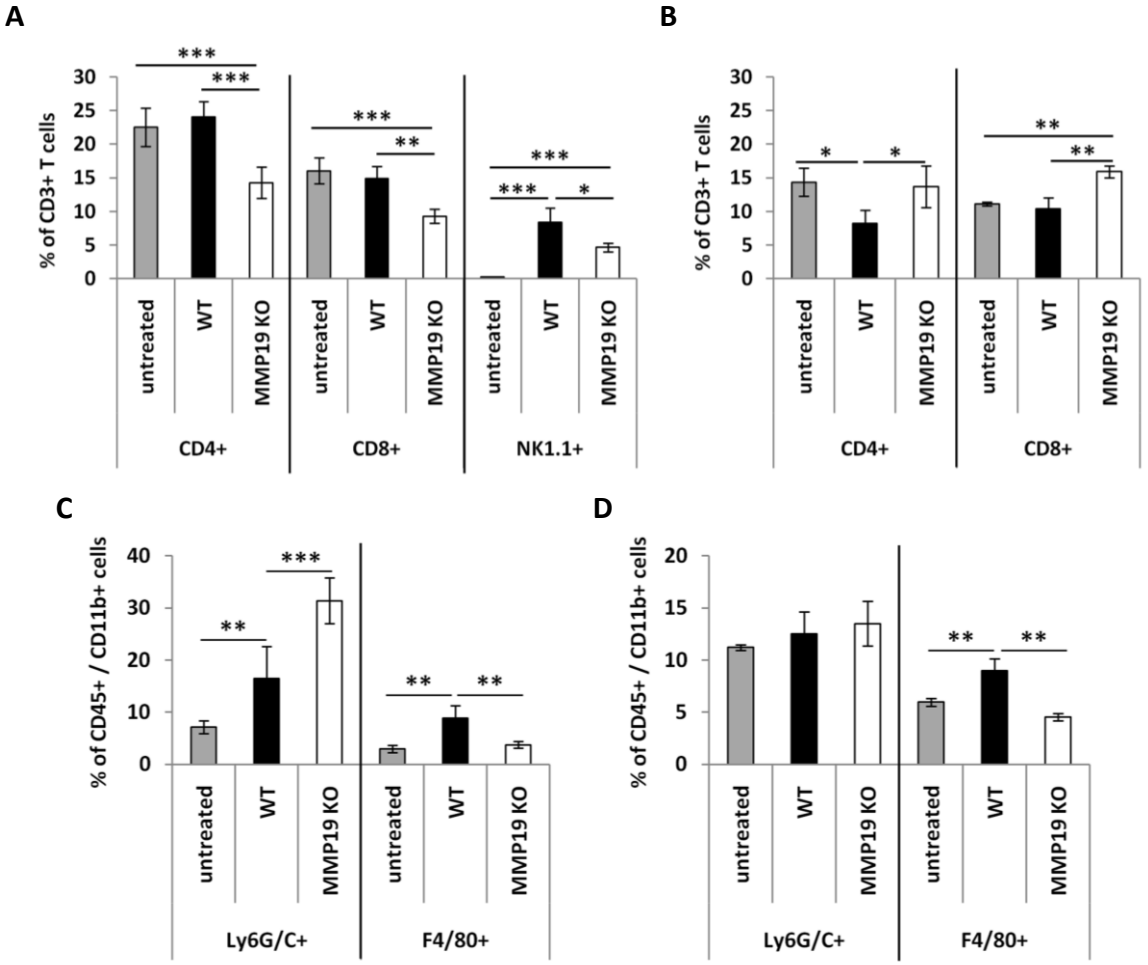

Figure 4-22: Adaptive and innate immune cell populations in blood and spleen of wildtype and MMP-19-deficient mice with acute colitis.

Leukocytes were isolated from peripheral blood and spleen from wildtype and MMP-19 -/- mice and analyzed by flow cytometry. A significant decrease in T cell numbers in the blood of MMP-19 -/- mice was matched by a significant increase in granulocytes compared to the WT. In contrast, the monocyte population was reduced (A and D). CD8+ T cells were increased in the spleen of MMP-19 -/- mice, whereas granulocyte numbers remained unchanged and macrophages were reduced compared to the WT (B and D). * $p < 0.05$; ** $p < 0.005$, *** $p < 0.001$.

4.3 Recovery phase

In this experiment, the acute colitis was induced by administration of 2% DSS for 5 days and this period was followed by an extended recovery phase of 10 days (Figure 4-23). The objective of this experiment was to analyze the significance of the MMPs studied in the wound healing process in colitis.

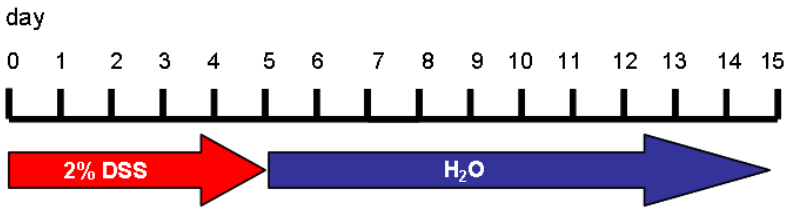

Figure 4-23: Induction of acute colitis followed by a recovery phase.
Five days of DSS administration led to acute colitis, during a ten day water period the mice could recover from the acute disease.

4.3.1 Reduced survival and incomplete recovery of MMP-19-deficient mice

In contrast to the wildtype and MMP-28 -/- mice, which behaved similarly during the experiment, the MMP-19-deficient mice showed a more severe colitis from which they never fully recovered. Survival of the MMP-19 -/- mice was significantly reduced compared to the WT animals, with mice starting to die from day 9. Opposed to the WT mice, which all survived the experiment, 40% of the MMP-19-deficient animals did not survive (Figure 4-24C). For the remaining mice, maximum body weight loss was observed at day 8 for WT (94.4 ± 3.2%), at day 9 for MMP-28 -/- (86 ± 5%), and at day 8 for MMP-19 -/- mice (83.0 ± 3.1%). Whereas the wildtype and MMP-28 -/- mice regained their body weight relatively fast and still showed an increasing trend at day 14 (Figure 4-24A, left panel), the recovery of the MMP-19 -/- mice was less pronounced and their body weight ceased to increase towards the end of the experiment (92.7 ± 5% versus 103.5 ± 3% in the WT mice) (Figure 4-24A, right panel). They also showed a higher DAI score than the WT mice with a peak value of 3.6 at day 7 (Figure 4-24B). In contrast, WT and MMP-28 -/- mice did not differ significantly in DAI and survival rate (Figure 4-24B and C). The survival rates of WT and MMP-28 -/- mice, however, was relatively poor compared to the survival rates observed for both groups in other experiments. Here, a possible explanation could be the slightly lower mean body weight of the mice at the beginning of the experiment.
Consistent with disease development, WT and MMP-28 -/- mice did not display any significant differences in colon length or spleen weight (Figure 4-25A and B, left panel). In contrast, MMP-19 -/- mice showed a shortened colon and an increase in spleen weight, which was reflected in a markedly enlarged spleen (Figure 4-25A and B, right panel).

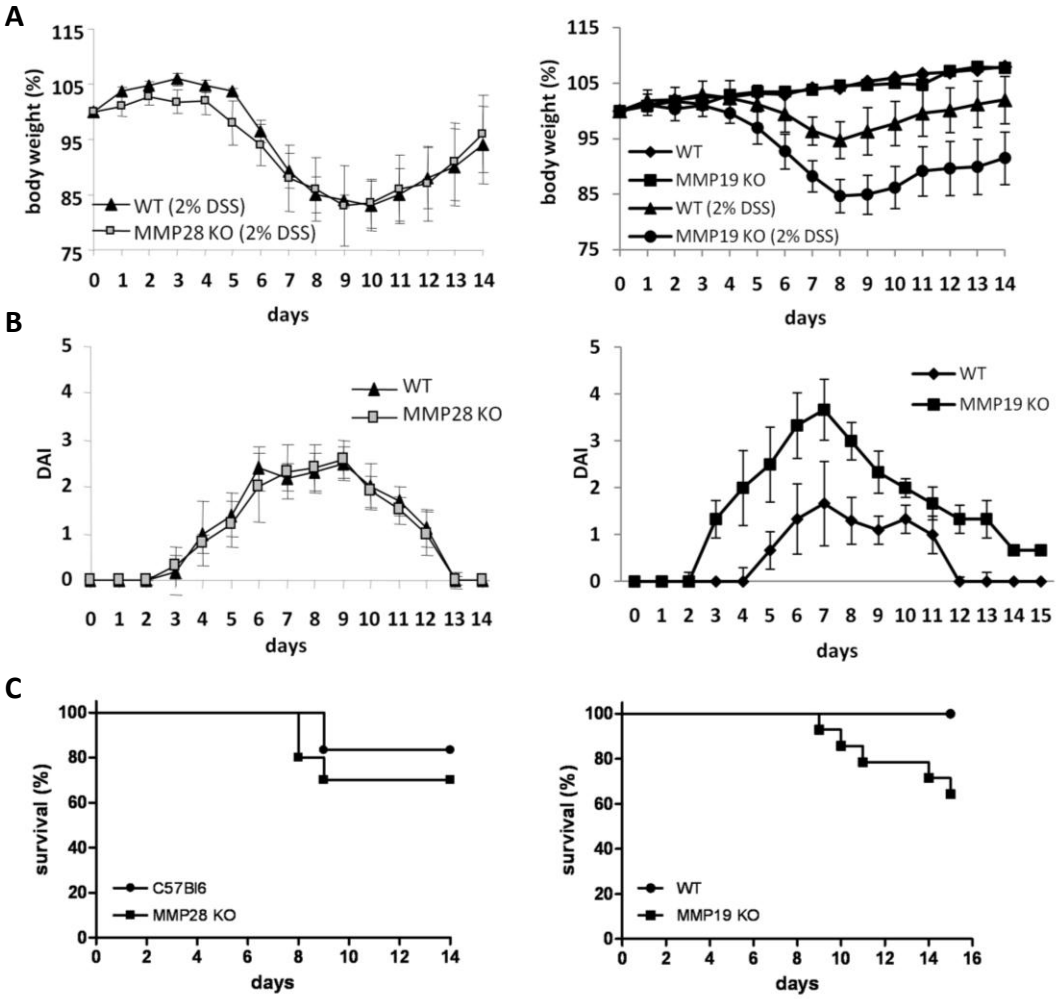

Figure 4-24: MMP-19-deficient mice show impaired recovery from colitis.
(A) Weight development during recovery from acute colitis. Whereas the body weight of MMP-28 -/- and WT mice developed in a similar way (left panel), the MMP-19 -/- mice lost more weight than the WT animals and never regained their original weight. (B) DAI score. In contrast to the MMP-28 -/- mice (left panel), the DAI score of the MMP-19-deficient mice was consistently higher than the one of the WT mice. (C) Survival curves (Kaplan-Meier). MMP-19 -/- but not MMP-28 -/- mice showed a significantly reduced survival compared to the WT mice. Data are expressed as mean ± SD (left panel: n = 6, DSS-treated WT group; n = 6, DSS-treated MMP-28 -/- group; right panel: n = 14, DSS-treated WT group; n = 14, DSS-treated MMP-19 -/- group).

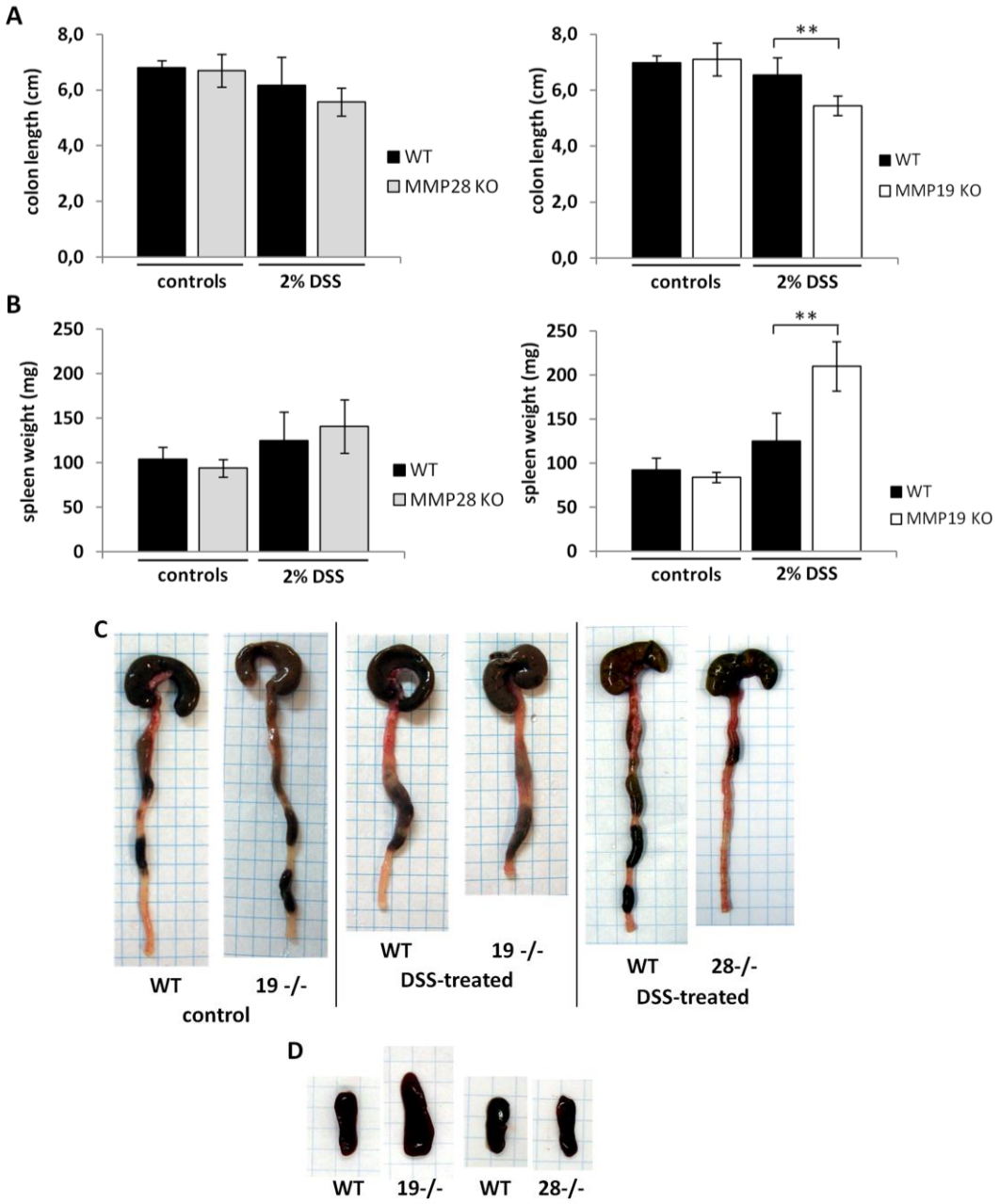

Figure 4-25: Colon length and spleen weight of MMP-19- and MMP-28-deficient mice after recovery from acute colitis.

(A) Colon length. Whereas no significant differences were observed in the colon length between treated WT and MMP-28 -/- mice (left panel), the colon length of the MMP-19 -/- mice was significantly reduced compared to the wildtype (-19.1%, $p < 0.005$)(right panel). (B) Spleen weight. The spleen weight in the MMP-19 -/- mice (right panel) but not in the MMP-28 -/- mice (left panel) was significantly enhanced compared to the wildtype (+76.7%, $p < 0.005$). (C, D) Representative pictures of colon (C) and spleen (D). Data are expressed as mean ± SD (left panel: n = 6, DSS-treated WT mice; n = 6, DSS-treated MMP-28 -/- mice; right panel: n = 14, DSS-treated WT mice; n = 14, DSS-treated MMP-19 -/- mice). **, $p < 0.005$.

4.3.2 MMP-19 -/- mice showed impaired recovery from colon tissue destruction depicted in increased inflammatory lesion extent and depth of tissue damage

After the recovery phase, histological analysis of the distal part of the colon tissue was performed to assess potential differences in the wound-healing capacity of the MMP-19- and MMP-28-deficient mice. Colon sections stained with hematoxylin/eosin were analysed for various parameters related to tissue destruction and inflammation as described before (4.2 Acute colitis) (Figures 4-26 and 4-27).

The most significant differences were seen between the colons of the wildtype and the MMP-19-deficient mice: Whereas the wildtype had recovered and did not show any signs of inflammation, about 40% of the MMP-19 -/- colonic tissue were still inflamed (Figure 4-27A). In contrast, the extent of remaining lesions in the colon of MMP-28-deficient mice was clearly reduced. The persistent inflammation in the MMP-19 -/- mice was also reflected in a considerable influx of neutrophils into the lesional colon tissue, which was significantly higher than the one observed for the MMP-28 -/- mice (MMP-19 -/-, 15% versus MMP-28 -/-, 3%, $p < 0.05$) (Figure 4-27E). Further major differences between the MMP-19- and the MMP-28-deficient group were related to the extent of tissue destruction: The depth of ulceration (Figure 4-27D) as well as the percentage of crypt damage (Figure 4-24G) and crypt damage depth (Figure 4-27H) were significantly greater in the MMP-19-deficient mice. However, the percentage of oedema and hyperregenerative tissue was similar in both groups (Figure 4-27B and C).

Taken together, these data clearly show that MMP-19-deficient mice exhibit lower capability to recover from the colon damage and inflammation inflicted by DSS-induced colitis than the wildtype and MMP-28-deficient mice.

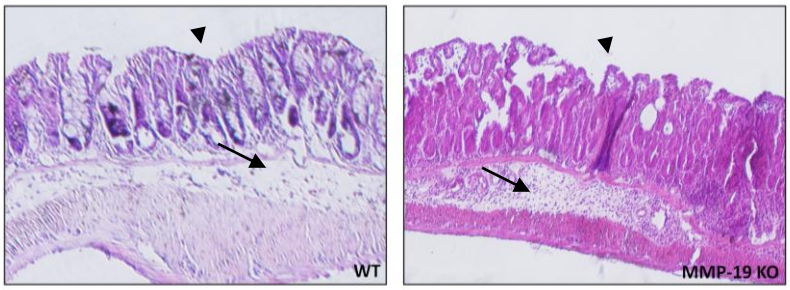

Figure 4-26: Representative pictures of colon sections of WT and MMP-19-deficient mice after ten days of recovery. Arrows are pointig to oedema, which in case of the MMP-19 -/- was filled with inflammatory cells. Arrowheads show the rebuilt mucosal architecture (crypts and epithelium were present) in the WT mice, whereas in the MMP-19 -/- the tissue was still destroyed. Hematoxylin/eosin staining, magnification x 40.

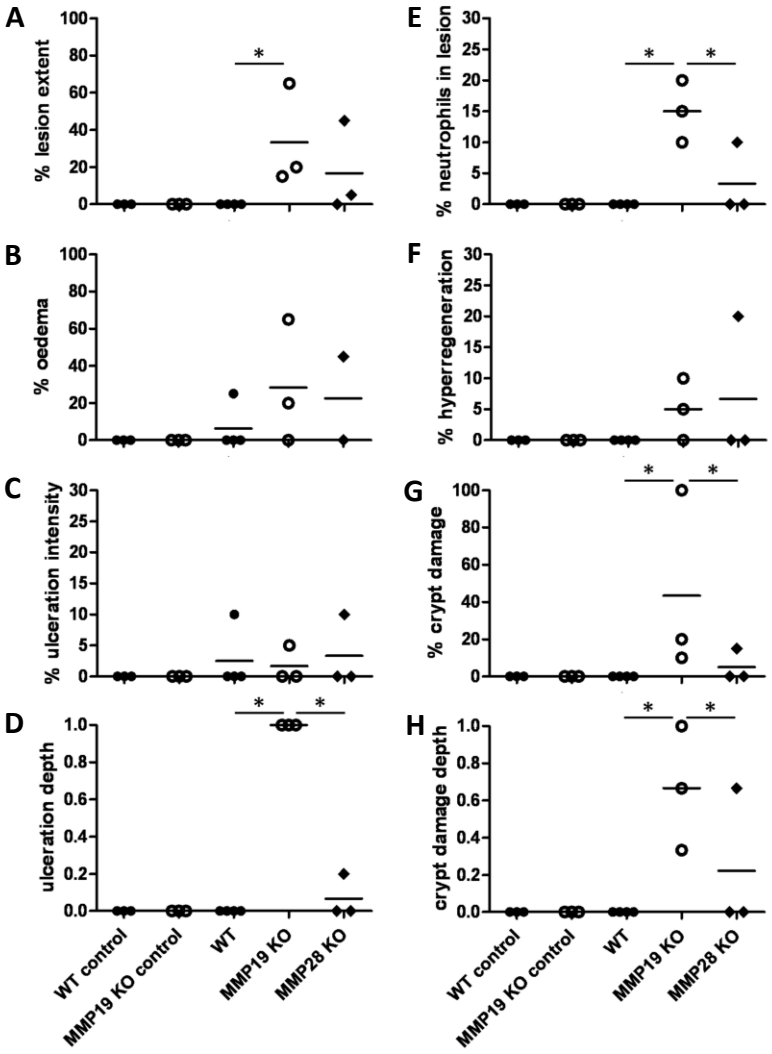

Figure 4-27: Histological analysis of colon tissue after recovery from colitis.
Sections of colon tissue of DSS-treated WT, MMP-19- and MMP-28-deficient mice were stained with hematoxylin/eosin and analyzed for parameters related to inflammation and tissue destruction. Compared to the MMP-28 -/- mice, the extent of inflamed lesions (A), the neutrophil influx (B), ulceration depth (D), percentage of crypt damage (G), and crypt damage depth (H) were significantly increased in the colon of the MMP-19 -/- mice ($p < 0.01$). Although the colon of the MMP-28-deficient mice showed some remaining signs of destruction, it had mostly recovered from the colitis, similarly to the colon of the DSS-treated wildtype mice which was indistinguishable from the untreated control animals. Data are expressed as means ± SD (n = 3 for all groups).

4.3.3 Decreased proliferation of colon epithelial cells in MMP-19- and MMP-28-deficient mice

The strongly reduced proliferation of epithelial cells in the acute phase of colitis was totally restored in the WT mice. In contrast, numbers of epithelial cells positive for the proliferation marker Ki-67 in the mucosa of MMP-19-deficient were decreased dramatically – only some hyperproliferative areas were found (Figure 4-28A and B). Interestingly, also the MMP-28-deficient mice showed impaired proliferation activity when compared to WT animals (Figure 4-28B).

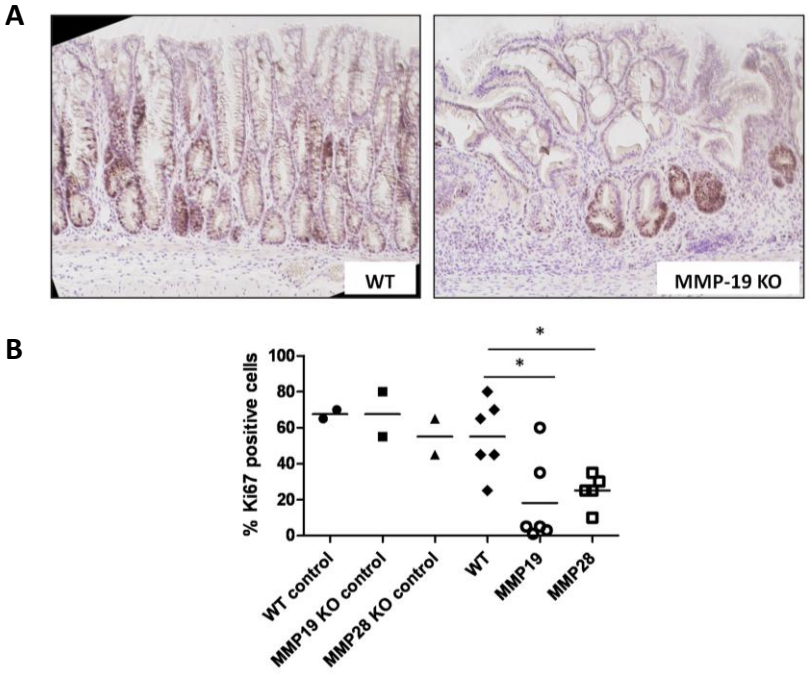

Figure 4-28: Proliferation of colon epithelial cells is decreased in MMP-deficient mice.
The amount of proliferating cells was decreased more than 40% in MMP-deficient mice compared to WT animals (B). Representative pictures are shown for WT and MMP-19 -/- mice (A). n = 2, MMP-19 -/-, and MMP-28 -/- mice in control group; n = 6, WT and MMP-19 -/- mice and n = 5, MMP-28 -/- mice in DSS-treated group. *, $p < 0.05$.

The number of macrophages (F4/80 positive cells) seen in the colon increased by more than 20% in all analyzed mouse strains in comparison to the acute phase of the colitis. There was no significant difference between the WT, MMP-19-, and MMP-28-deficient mice (Figure 4-29). High amounts of macrophages in the tissue indicate the healing process.

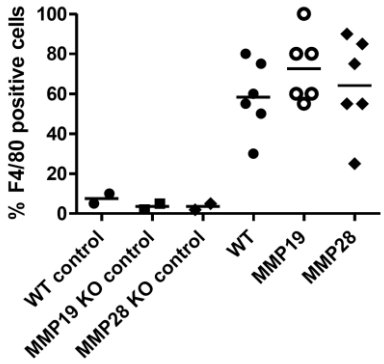

Figure 4-29: Similar numbers of macrophages incolon tissue of mice recovering from colitis. The numbers of F4/80 positive cells increased compared to the acute phase of colitis, however, the amount of macrophages did not differ among WT, MMP-19 -/-, and MMP-28 -/- mice. n = 2 for untreated mice; n = 6 DSS-treated mice.

4.3.4 Increased cytokine and chemokine concentrations in plasma of MMP-19-deficient mice point to a systemic inflammatory response

To compare the development of the recovery and healing process in the inflammatory response among DSS-treated wildtype, MMP-28 -/-, and MMP-19 -/- mice, plasma cytokine and chemokine concentrations were analyzed at day 14, i.e. at the end of the defined recovery phase. In contrast to the non-significant results in plasma of acute inflamed mice, now the immune response became a more systemic one as elevated levels of pro-inflammatory cytokines were detected in plasma of recovered mice. Whereas the cytokine levels in plasma of the treated WT and MMP-28-deficient mice were not significantly different from those measured in the untreated control group, the IL-1α and IL-6 concentrations in the plasma of the treated MMP-19 -/- animals were markedly increased. Levels of IL-6 were shown to be at least ten times higher than in plasma of WT mice. Such high levels of IL-6 could denote an acute phase response in recovering MMP-19-deficient animals. Analysis of the liver enzymes ALT (alanine aminotransferase) and AST (aspartate aminotransferase) revealed no enhanced systemic response similar to acute colitis (see section 4.3.6, Figure 4-33). However**,** TNF-α and IFN-γ levels remained largely unchanged (Figure 4-30A). Furthermore, the levels of the chemokines MCP-1, G-CSF, and KC were also significantly higher in plasma of MMP-19 -/- mice than in WT animals (Figure 4-30B). High levels of these chemokines in the blood marked as well a starting systemic response to the injury in the gut. Strikingly increased levels of G-CSF (Granulocyte colony-stimulating factor) pointed to the beginning of a systemic response as this chemokine stimulates the bone marrow to produce granulocytes. Corresponding to the high values in MMP-19-deficient mice inflammation was more pronounced in these animals. No difference was found in levels of GM-CSF.

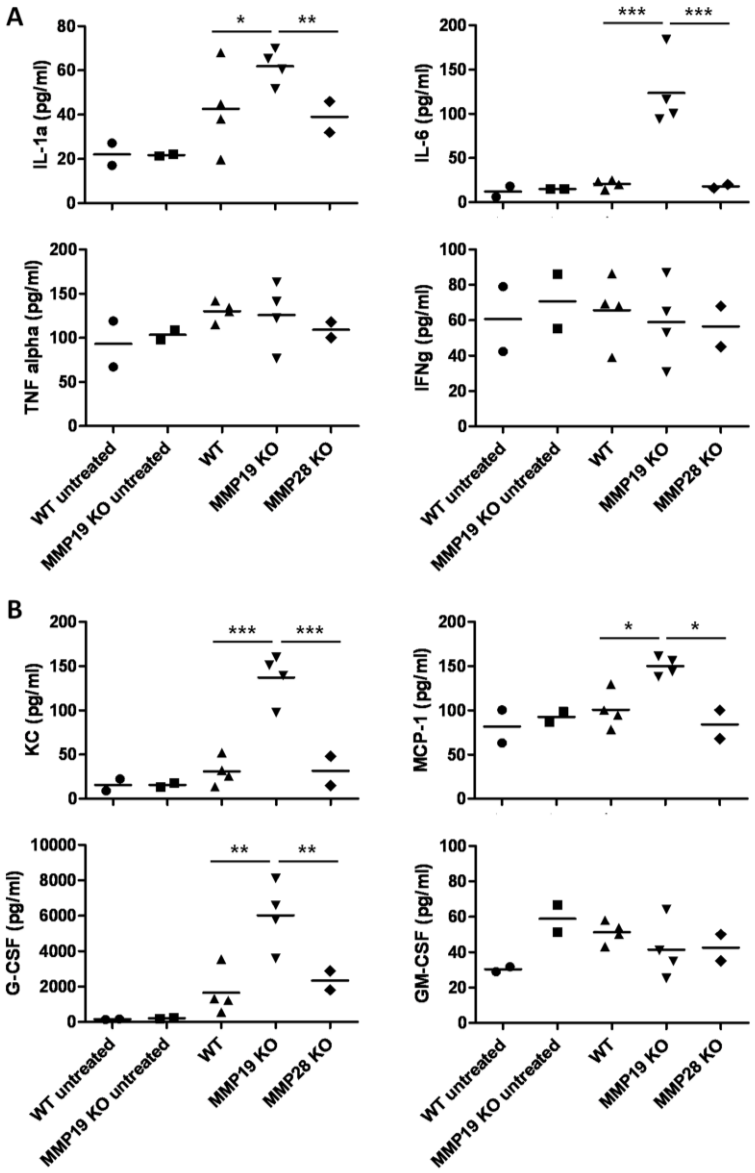

Figure 4-30: Cytokines and chemokines in plasma of healthy mice and MMP single-deficient mice during recovery phase following acute colitis.
Cytokine (A) and chemokine (B) levels in plasma prepared on day 14 were determined by BioPlex bead assay. Data are represented as individual data points and mean of duplicate measurements (n = 2, WT and MMP-19 -/- mice in control group; n = 4, WT and MMP-19 -/- mice and n = 2, MMP-28 -/- mice in DSS-treated group). *, $p < 0.05$; **, $p < 0.005$; ***, $p < 0.001$.

4.3.5 Enhanced release of cytokines and chemokines from colon tissue of MMP-19-deficient mice

Whereas the levels of cytokines were going back to normal values in case of wildtype mice, MMP-19-deficient mice still depict increased concentrations in the supernatant of colon explant cultures (Figure 4-31). IL-1 levels are even higher after recovery then they were in acute colitis. Concentrations of IL-10 in MMP-19 -/- mice were found to be increased twice compared to acute colitis (see section 4.2.10, Figure 4-19), which pointed to a strong anti-inflammatory reaction in these animals. In WT mice IL-10 concentrations

are normal. Levels of TNF-α and IFN-γ did not change much in comparison to the acute inflammation; they are just slightly decreased but still significantly enhanced in the MMP-19-deficient mice.

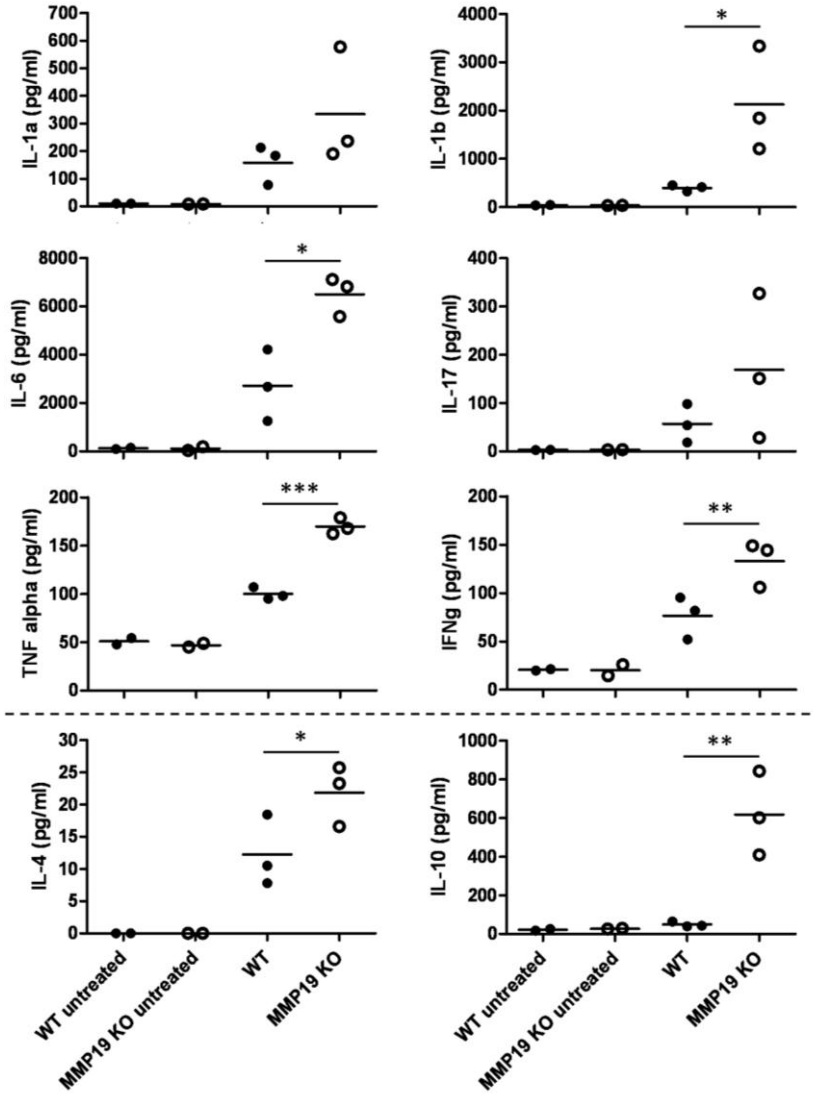

Figure 4-31: Cytokines in supernatants of colon explant cultures were significantly increased in MMP-19 -/- mice.

CEC supernatants analyzed by BioPlex bead assay showed high levels of pro-inflammatory cytokines IL-1 β and IL-6 in MMP-19-deficient animals whereas the WT mice showed much lower levels of these cytokines. TNF-α and IFN-γ are still released in high amounts that were similar to the acute colitis although in general the cytokine levels are lower than in the acute experiment. Also anti-inflammatory cytokines like IL-4 and IL-10 were highly elevated in MMP-19-deficient mice. (n = 2, WT and MMP-19-/- mice in control group; n = 3, WT and MMP-19-/- mice in DSS-treated group; *, $p < 0.05$; **, $p < 0.005$; ***, $p < 0.001$).

Concentrations of various chemokines released from the healing tissue were lower when compared to the acute phase of colitis (Figure 4-32). The extremely high levels of G-CSF and MCP-1 were reduced to moderate ones but still the MMP-19-deficient mice showed increased values when compared to WT mice. Levels for KC and RANTES did not change much during the recovery phase and were increased in knockout animals all the time.

Interestingly, the amount of produced MIP-1α (macrophage inflammatory protein 1) was doubled in the MMP-19 -/- mice, whereas it was only slightly increased in WT mice. MIP-1 is crucial for immune responses towards infection and inflammation, it is a major factor produced by macrophages after they are stimulated with bacterial endotoxins and activate human granulocytes which can lead to acute neutrophilic inflammation. MIP-1 also induces the synthesis and release of other pro-inflammatory cytokines such as IL-1, IL-6, and TNF-α from fibroblasts and macrophages.

The recovery resulted in a decreased inflammatory response and a starting healing process in the WT mice, whereas MMP-19-deficient mice still suffered from pronounced inflammation. As they showed high levels of both pro- and anti-inflammatory cytokines, there are both stages present – acute inflammation and healing.

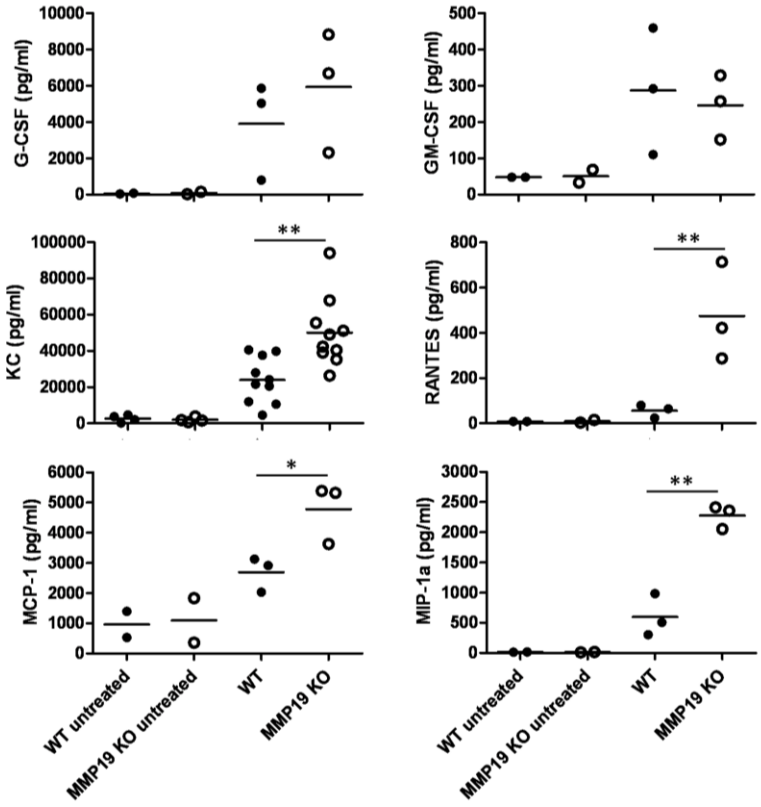

Figure 4-32: Chemokines in supernatants of CECs of healthy and MMP-19-deficient mice during recovery phase following acute colitis.

The levels of several chemokines (KC, MCP-1, MIP-1, and RANTES) were significantly higher in the supernatants of MMP-19 -/- mice than in those of the WT animals. Concentrations of G-CSF and GM-CSF are lower than in the acute colitis but not significantly different between the analysed groups. A twofold increase in MIP-1 was observed in the knockout animals, which did not occur in WT mice (n = 2, WT and MMP-19 -/- mice in control group; n = 3, WT and MMP-19 -/- mice in DSS-treated group; levels for KC were analyzed by ELISA, n = 4, WT and MMP-19 -/- mice in control group; n = 10, WT and MMP-19 -/- mice in DSS-treated group * $p < 0.05$, ** $p < 0.005$).

4.3.6 No significant changes in ALT and AST plasma concentrations of wildtype and MMP-19-deficient mice: the systemic response does not involve liver

Alanine aminotransferase (ALT) and aspartate aminotransferase (AST) are crucial enzymes in the amino acid metabolism. They are found in various organs but are most abundant in the hepatocytes found in the liver. Leakage of the enzymes, particularly ALT, into the blood stream is an important marker for liver damage or abnormal liver function [236; 237]. However, both enzymes can also be dysregulated in a variety of disorders and diseases that are not directly associated with liver dysfunction. Since imbalanced ALT and AST levels often indicate systemic inflammation [236; 237] levels of both enzymes were measured in the plasma of wildtype and MMP-19-deficient mice during acute colitis and after the recovery phase.

The normal range of ALT and AST plasma levels, as described for healthy C57Bl/6 mice are 24 ± 10 U/ml for ALT and 47 ± 13 U/ml for AST (Charles River Laboratories). As shown in Figure 4-33, both ALT and AST plasma levels of WT and MMP-19 -/- mice remained within the normal range during acute colitis and after the recovery phase, despite a clear increase of the transferases in MMP-19 -/- mice in acute colitis .

These results suggest that DSS-induced acute colitis did not lead to systemic inflammation, neither in the WT nor in the MMP-19-deficient mice but there was a tendency to develop a more systemic immune response in MMP-19-deficient animals.

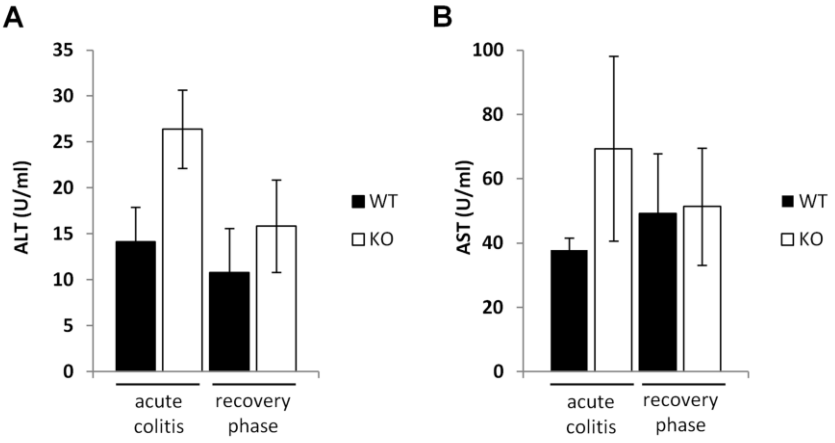

Figure 4-33: ALT and AST levels in mouse plasma remain within the normal range.
ALT (alanine aminotransferase) (A) and AST (aspartate aminotransferase) (B) levels in plasma of WT and MMP-19 -/- mice during acute colitis and after the recovery phase.

4.3.7 MMP-19/-28 double-deficient mice do not recover from acute colitis

In order to be able to analyze the recovery of the MMP-19/-28 double-deficient mice from acute colitis, the experimental conditions had to be modified, as initial studies showed that the mice did not survive the treatment applied for the single-deficient animals (Figure 4-34).

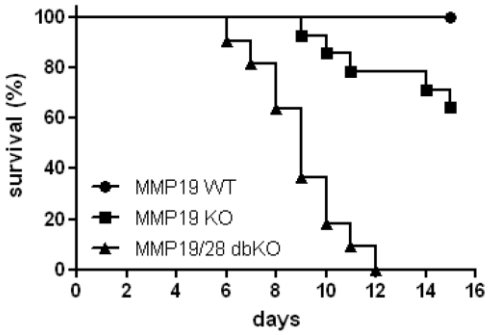

Figure 4-34: 100% mortality of MMP-19/-28 double-deficient mice during recovery from acute colitis.
The Kaplan-Meier survival curve clearly depicts the fast progress in mortality of the double-deficient mice. After 9 days 50% of mice and after 12 days all mice were dead (n = 12; WT and MMP-19 -/-: n = 14, MMP-19/-28 dbKO: n = 12).

Thus, a much milder treatment was chosen to analyze double-deficient mice in the recovery phase from acute colitis. The five days lasting supply of DSS in the drinking water that was established for the previous experiment was shortened to just three days of treatment (Figure 4-35), which basically showed no effect in WT animals.

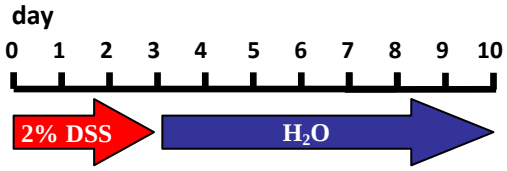

Figure 4-35: Modified recovery experiment for the treatment of MMP-19/-28 double-deficient mice.
The shorter treatment with 2% DSS was used to decrease the mortality of double-deficient mice during the recovery.

Despite the relatively mild treatment, the MMP-19/-28 double-deficient mice developed colitis rapidly and showed a steep increase in the DAI score that peaked at day 6 (Figure 4-36B). In contrast to the wildtype mice, which all survived the experiment, the MMP-19/-28 dbKO started to die from day 6 and displayed a very poor overall survival rate of just 50 % (Figure 4-36C). The remaining mice lost about 12% of their body weight until day 8, and afterwards, recovered only moderately and never regained their original weight (Figure 4-36A). These results were highly significant and in strong contrast to the

data obtained for the WT animals, which showed only very mild symptoms of disease throughout the experiment.

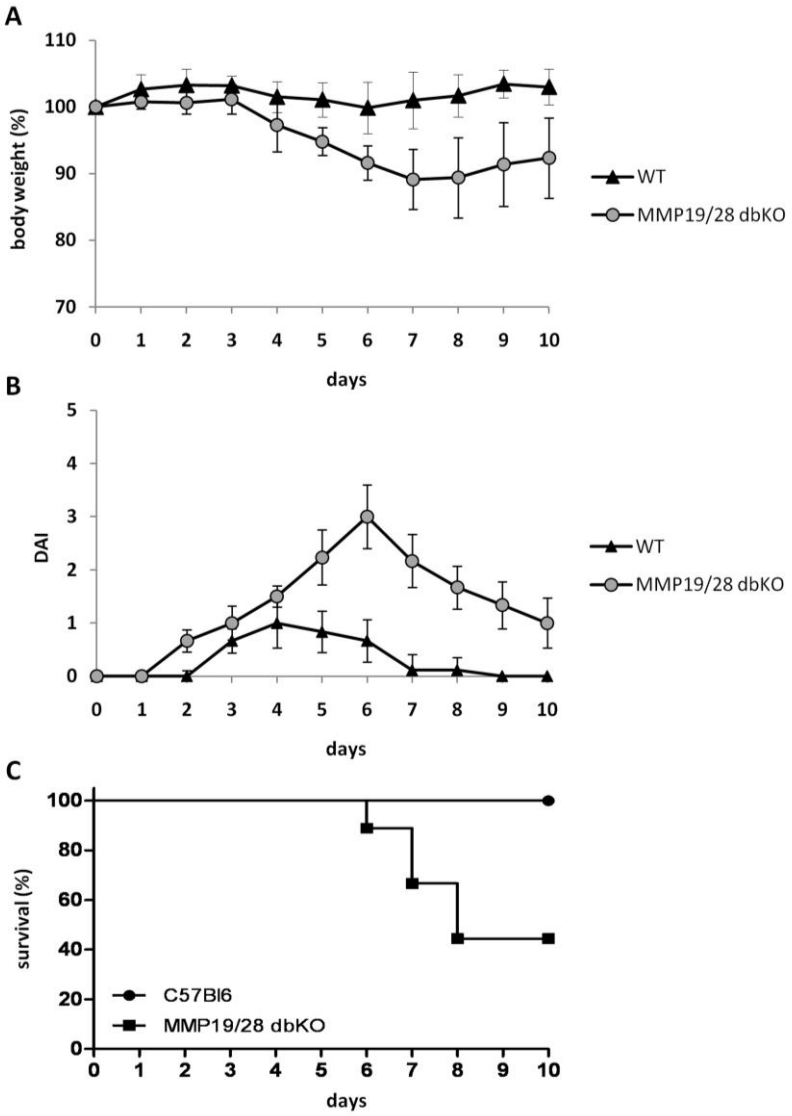

Figure 4-36: Body weight changes, disease activity index [223], and survival curves of MMP-19/-28 double-deficient and WT mice after recovering from colitis.
(A) Weight development after recovery from acute colitis. MMP-19/-28 double-deficient mice lost significantly more weight than the WT animals, which did not lose any weight (maximum weight loss at day 8: 10 ± 3%, $p \leq 0.005$). The double-deficient animals never regained their original weight (day 10: 10 ± 7%, $p \leq 0.005$). (B) MMP-19/-28 double-deficient mice showed a higher DAI than WT even at the end of the experiment. (C) Survival curves (Kaplan-Meier) showed that only 50% of the double-deficient animals survived the milder treatment and managed to recover. Data are expressed as mean ± SD (n = 6, DSS-treated WT mice; n = 10, DSS-treated MMP-19/-28 dbKO mice).

Whereas the colon of treated WT mice (7.0 ± 0.5 cm) did not display any significant changes to untreated mice, the colon of MMP-19/-28 double-deficient animals (4.7 ± 0.4 cm) was one third shorter than in WT mice (Figure 4-37A and C). Comparing the size and

weight of the spleen, no enlargement was observed in WT animals but double-deficient mice showed an increase in weight about 45% (Figure 4-37B and C). Splenomegaly is usually associated with increased workload (such as in anemias), which suggests that it is a response to hyperfunction.

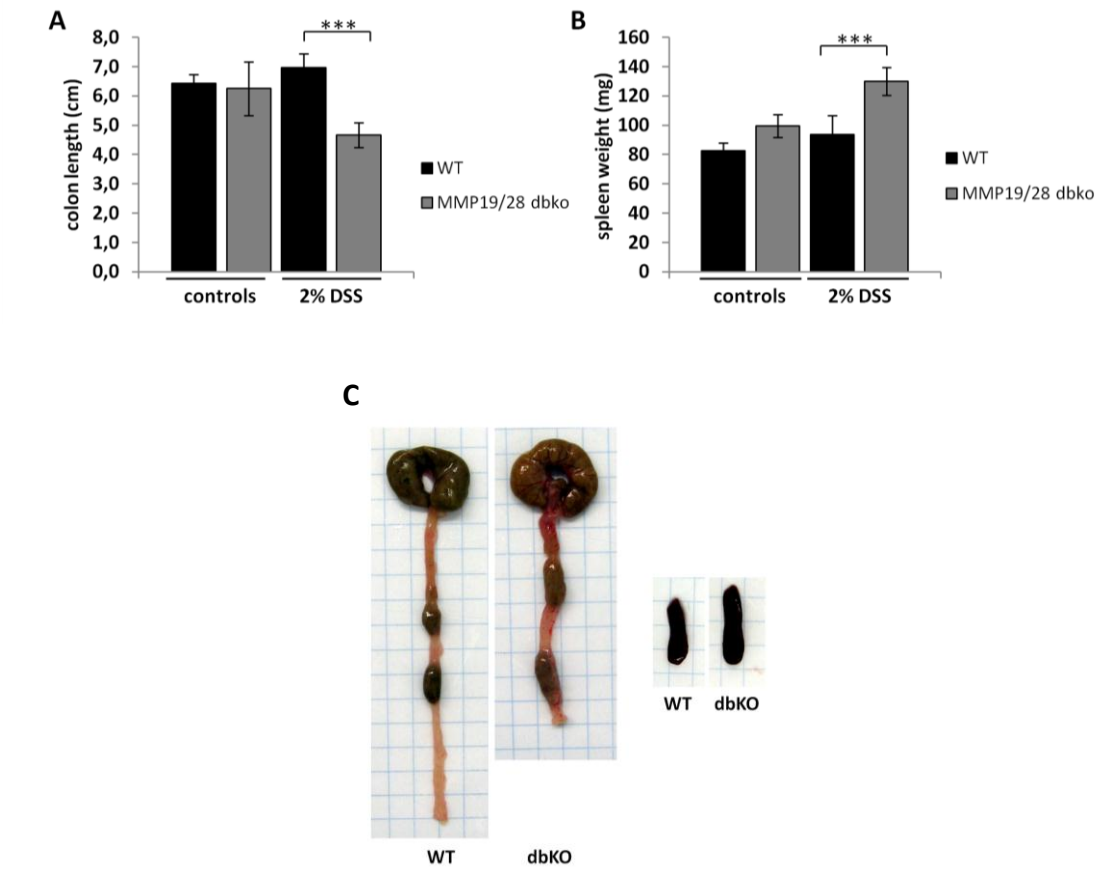

Figure 4-37: Colon length and spleen weight of WT and MMP-19/-28 double-deficient mice. The parameters were measured in untreated, healthy mice as well as in mice which are recovering from colitis (day 10) (A and B) and representative pictures are shown (C). Data are expressed as mean ± SD (n = 4, control mice; n = 6, DSS-treated WT mice; n = 5, DSS-treated MMP-19/-28 dbKO mice). *** $p < 0.001$

4.3.8 Hyaline arteries are present in the spleen of all MMP-19/-28 double-deficient mice

As the spleen from MMP-19/-28 dbKO mice exhibited a significantly higher weight, spleen tissue after the recovery was isolated, sectioned and stained with hematoxylin/eosin to reveal the reason of the spleen enlargement. Strikingly, arteries from the double-deficient mice showed deposition of hyaline material in 100 % of tissue sections. In wildtype mice only about 30 % of mice showed hyaline material in the inner wall of the blood vessels (Figure 4-38). Thickening of the walls of arterioles by the deposition of homogeneous pink hyaline material is called hyaline arteriolosclerosis and leads to hardening of the vessel

wall [238]. This process is due to the accumulation of extracellular matrix components. This phenotype might be responsible for the enlargement of the spleen as cells do not have proper access to the blood stream. Two experiments were performed showing similar results.

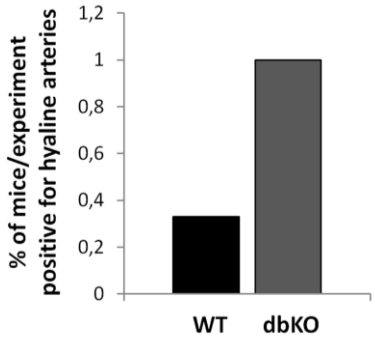

Figure 4-38: Hyaline arteries in the spleen of MMP-19/-28 double-deficient mice recovering from colitis.
Percentage of mice in an experiment (two in total) showing hyaline arteries in the spleen. 100% of spleen sections stained with hematoxylin/eosin showed deposition of hyaline material in the blood vessel; only 36% of WT mice depict this phenotype.

4.3.9 MMP-19/-28 double-deficient mice showed severe signs of colitis at cellular level in the colon wall

At the end of the recovery experiment, histological analysis of the distal part of the colon tissue was performed. Colon sections stained with hematoxylin/eosin of WT (n = 3) and MMP-19/-28 double-deficient mice (n = 3) were analyzed for the same parameters as described before (see 4.2 Acute colitis) (Figure 4-39 and 4-40). Colon tissue of untreated mice was analyzed as well and served as control. In addition, the colon tissue was also assessed for symptoms of acute and chronic inflammation as well as for inflammation depth.

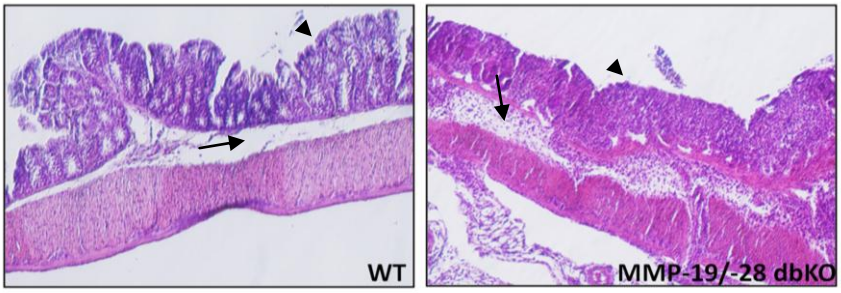

Figure 4-39: Representative pictures of WT and MMP-19/-28 double-deficient mice recovering from acute colitis.
Colon tissue sections of DSS-treated WT and MMP-19/-28 dbKO mice were stained with hematoxylin/eosin, arrows mark oedema in the tissue (only present in the MMP-19/-28 double-deficient mice), and arrowheads are pointing to the epithelium. Hematoxylin/eosin staining, magnification x 40.

Whereas the DSS-treated WT mice showed hardly any signs of colon inflammation or tissue destruction, the colons of the MMP-19/-28 double-deficient mice were highly inflamed and damaged (Figure 4-39 and 4-40). All parameters measured were significantly increased compared to the WT group (Figure 4-40, $p < 0.05$).

Colon tissue of this experiment was accessed for differences in acute versus chronic inflammation (Figure 4-41). Simplified, acute inflammation is described by a majority of neutrophils present in the tissue, oedema formation, and severe tissue alterations may be present as well as necrosis. During chronic inflammation predominantly lymphocytes and plasma cells are accumulated in the tissue and usually fibrosis is present. The colon tissue of treated wildtype mice appeared essentially healthy, whereas about 50% of the colon in MMP-19/-28 dbKO tissue was chronically inflamed and about 20% showed signs of acute inflammation. Inflammation depth was also very pronounced in these animals, and differences to the other groups were significant (Figure 4-41).

These results illustrate that the healing process of the colonic tissue in MMP-19/-28 double-deficient mice suffering from acute colitis is severely impaired and the inflammatory response dramatically exacerbated.

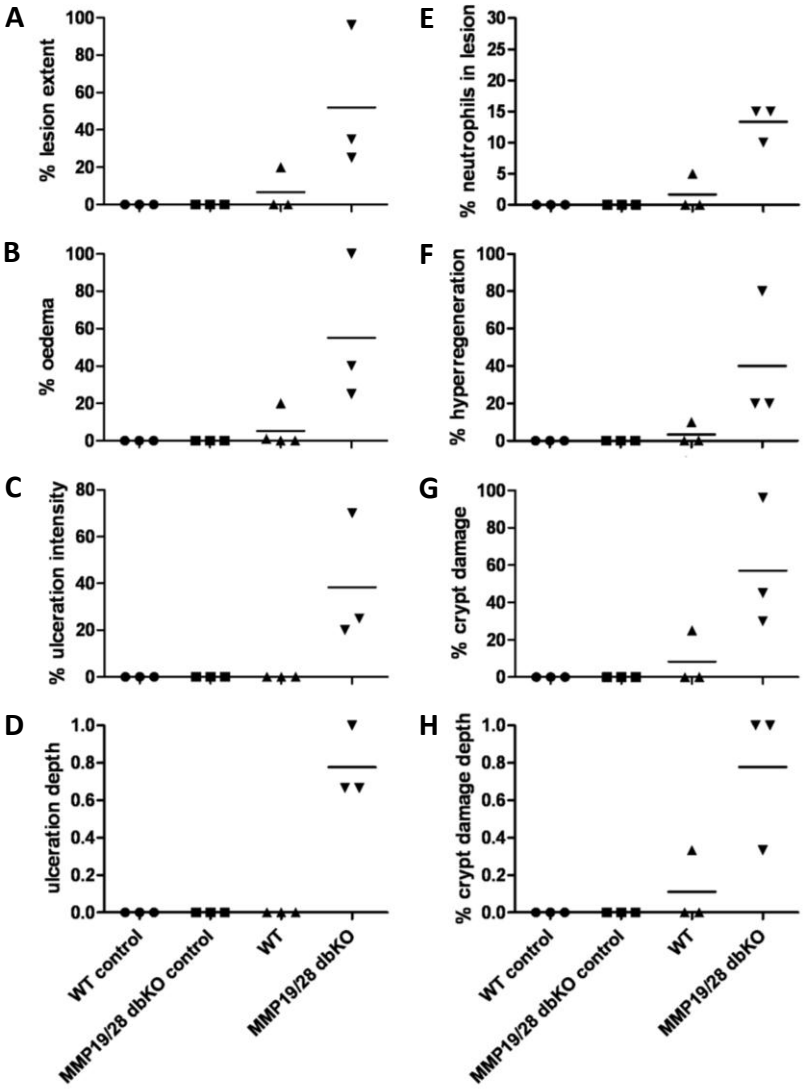

Figure 4-40: Histological analysis of colon tissue of MMP-19/-28 double-deficient mice recovering from acute colitis.

Colon tissue sections of DSS-treated WT (n = 3) and MMP-19/-28 dbKO mice (n = 3) were stained with hematoxylin/eosin and analyzed for parameters related to inflammation and tissue destruction. Compared to the WT mice, the values of all parameters measured were significantly higher in the MMP-19/-28 dbKO group. DSS-treated wildtype mice did not show major differences to the untreated control animals. Data are shown as dot plot with means. The difference between the treated WT and MMP-19/-28 dbKO mice was significant in all panels (*, $p < 0.05$).

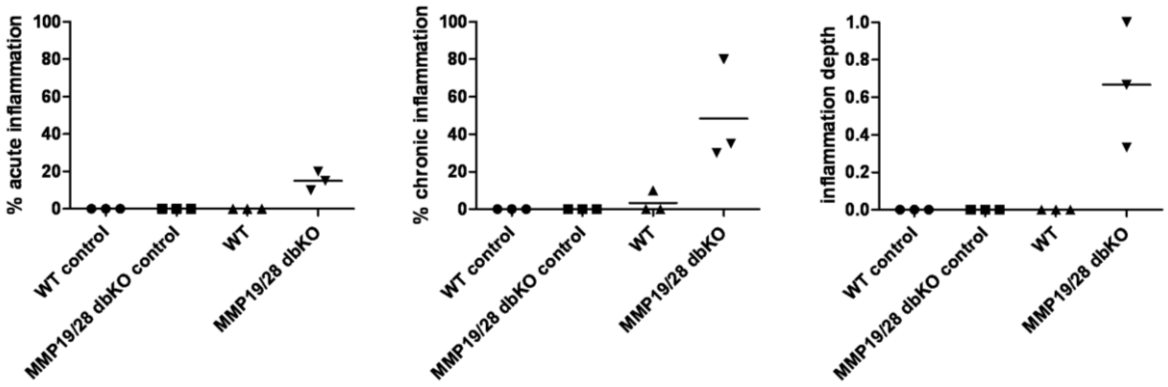

Figure 4-41: Extent of acute and chronic inflammation in colonic tissue of DSS-treated MMP-19/-28 mice.
MMP-19/-28 dbKO mice showed a higher percentage of acute and chronic inflamed tissue. WT animals appeared healthy. The depth of inflammation was significantly increased in deficient versus wildtype mice. Data are shown as mean. Differences between DSS-treated WT and dbKO mice are highly significant, $p < 0.005$.

4.3.10 Reduced epithelial cell proliferation and macrophage accumulation in colon tissue of MMP-19/-28 double-deficient mice

The number of proliferating cells was dramatically decreased in the colonic tissue of animals with acute colitis (see section 4.2.8, Figure 4-16). Proliferation was normal in the WT mice that recovered from colitis but still decreased in MMP-19-deficient mice. In the modified recovery experiment for the double-deficient mice, significantly lower numbers of Ki-67 positive epithelial cells were seen compared to the WT, so proliferation was reduced (Figure 4-42A and B).

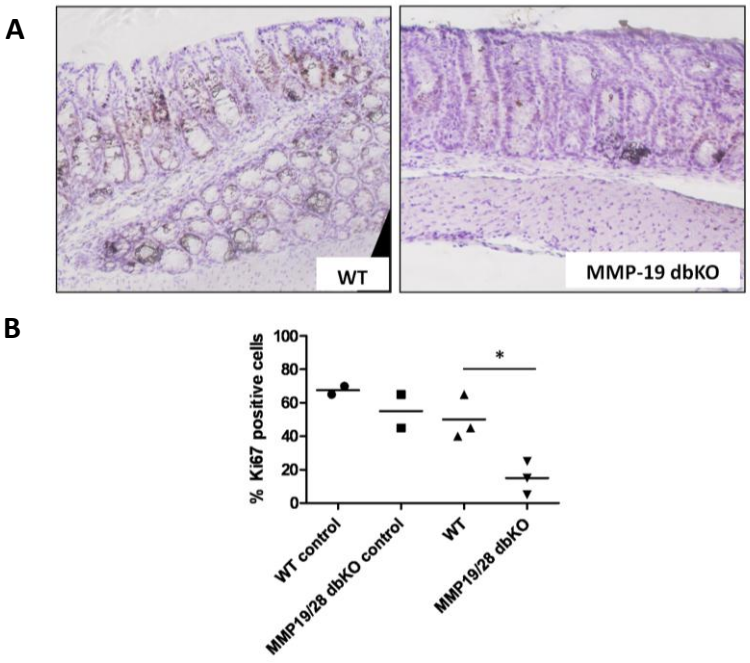

Figure 4-42: Epithelial cell proliferation was decreased in MMP-19/-28 dbKO mice.
Whereas WT mice showed nearly normal amount of proliferating cells in the intestine, the number of Ki-67 positive cells in double-deficient mice was decreased 75% compared to wildtype colons (B). Representative pictures of DSS-treated animals are shown (A). n = 2, WT and MMP-19/-28 double-deficient mice in control group; n = 3, WT and MMP-19/-28 double-deficient mice in DSS-treated group, * $p < 0.05$.

Macrophages are required for initiation of the healing process by phagocytosis of bacteria and cell debris. They also release numerous cytokines (e.g. growth factors like EGF, TGF, and FGF as well as interleukins) to attract fibroblast to the site of repair. After a short DSS-treatment and seven days to recover, WT mice hardly showed any signs of colitis. Macrophages were still present in the colon tissue to support the healing process. In the tissue of treated MMP-19/-28 double-deficient mice no significant increase in the amount of macrophages was seen (Figure 4-43A and B).

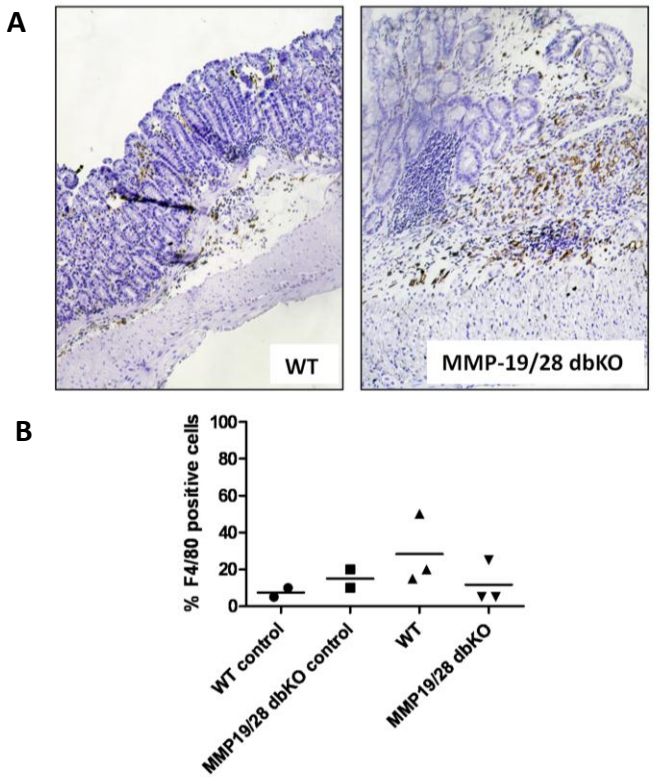

Figure 4-43: Reduced macrophage accumulation in colon tissue of MMP-19/-28 dbKO mice. Macrophages were present in slightly higher amounts in WT mice, numbers in double-deficient mice did not differ significantly from untreated mice (B). Representative pictures of DSS-treated animals are shown (A). n = 2, WT and MMP-19/-28 double-deficient mice in control group; n = 3, WT and MMP-19/-28 double-deficient mice in DSS-treated group.

4.3.11 MMP-19/-28 double-deficient mice recovering from colitis had highly elevated levels of cytokines and chemokines in plasma

Plasma levels of a variety of cytokines and chemokines were determined by BioPlex bead analysis. The MMP-19/-28 double-deficient mice showed enhanced levels of several pro-inflammatory cytokines in plasma. For instance, the IL-1α and IL-6 concentrations increased more than twofold compared to those measured for the wildtype animals (Figure 4-44A). These differences were highly significant ($p < 0.005$), and not observed for other cytokines. Strikingly, TNF-α levels were slightly decreased compared to the WT, and IFN-γ levels remained unchanged. In line with the results of the colon histology, the DSS-treated WT mice had recovered from colitis and showed similar cytokine levels than the untreated control groups.

The concentrations of several additional chemokines were also significantly elevated in the plasma of the MMP-19/-28 dbKO mice, most notably KC and G-CSF, which in the DSS-treated wildtype and the untreated control animals remained at very low levels. In contrast, no significant differences were detected in the amounts of MCP-1 and GM-CSF (Figure 4-44B), which means only chemoattractants for neutrophils are upregulated in the double-deficient mice.

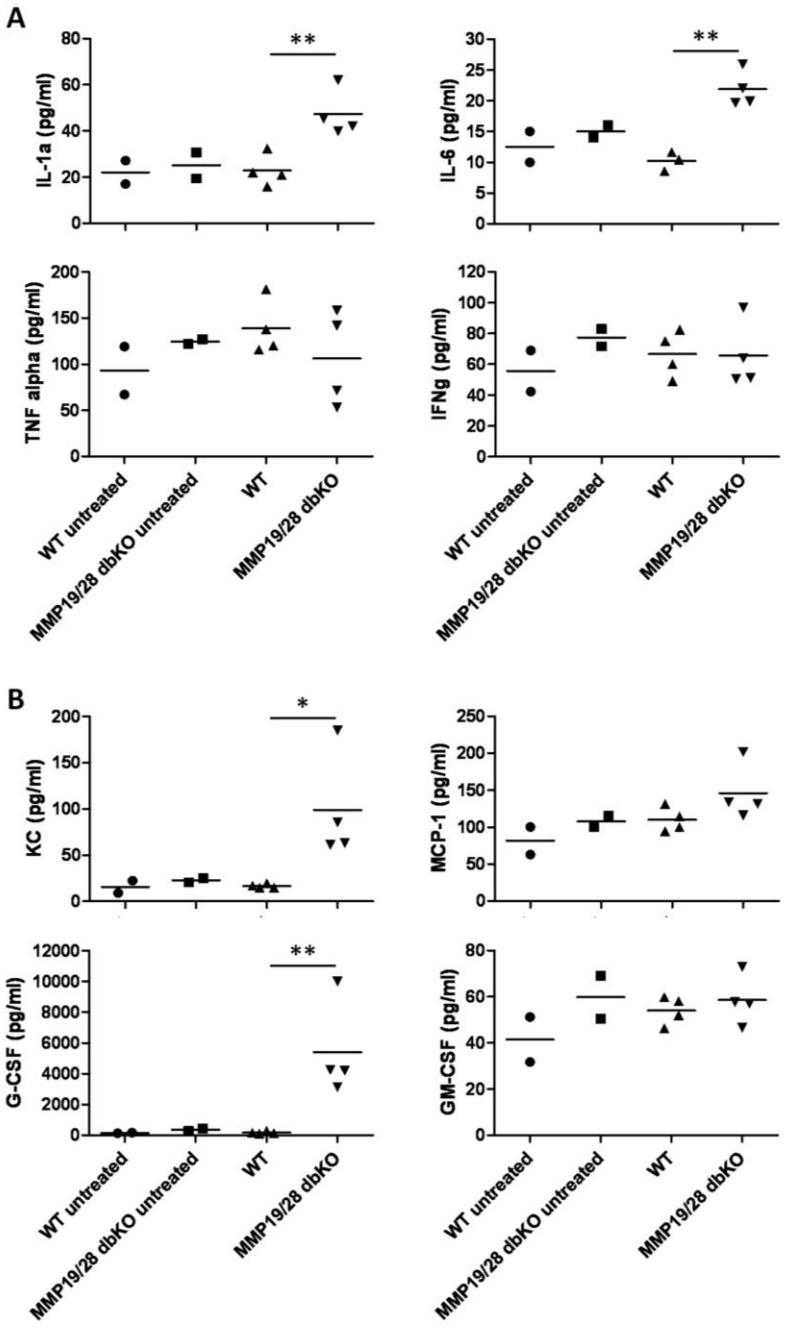

Figure 4-44: Cytokines and chemokine levels in plasma of healthy and MMP-19/-28 double-deficient mice recovering from acute colitis.

Cytokines analyzed by BioPlex bead assay showed high levels of pro-inflammatory cytokines such as IL-1β and IL-6 in MMP-19/-28 double-deficient animals whereas cytokines of the WT mice remained at normal levels. There were no significant differences in TNF-α and IFN-γ levels, including the control mice (A). Levels of the chemokines KC and G-CSF were significantly higher in the plasma of MMP-19/-28 dbKO mice compared to the WT animals. For MCP-1, a non-significant increase was observed, whereas GM-CSF levels did not change (B). (n = 2, WT and MMP-19/-28 double-deficient mice in control group; n = 4, WT and MMP-19/-28 double-deficient mice in DSS-treated group) * $p < 0.05$, ** $p < 0.005$.

4.3.12 Highly enhanced release of cytokines and chemokines from colon tissue correlates with DAI in MMP-19/-28 double-deficient mice

Colon explant cultures (CEC) from DSS-treated wildtype, MMP-19/-28 dbKO and untreated control mice were prepared after the recovery phase. The supernatants were analyzed after 24h culture for cytokine and chemokine concentrations by BioPlex bead assay.

Whereas no significant differences were detected in DSS-treated WT and the untreated control groups, the levels of pro- and anti-inflammatory cytokines as well as several chemokines were highly elevated in the supernatants of the MMP-19/-28 double-deficient mice. The upregulated pro-inflammatory cytokines included IL-1, IL-6, TNF-α, IFN-γ and the Th17 cytokine IL-17. IL-4 and IL-10 were among the upregulated anti-inflammatory cytokines (Figure 4-45).

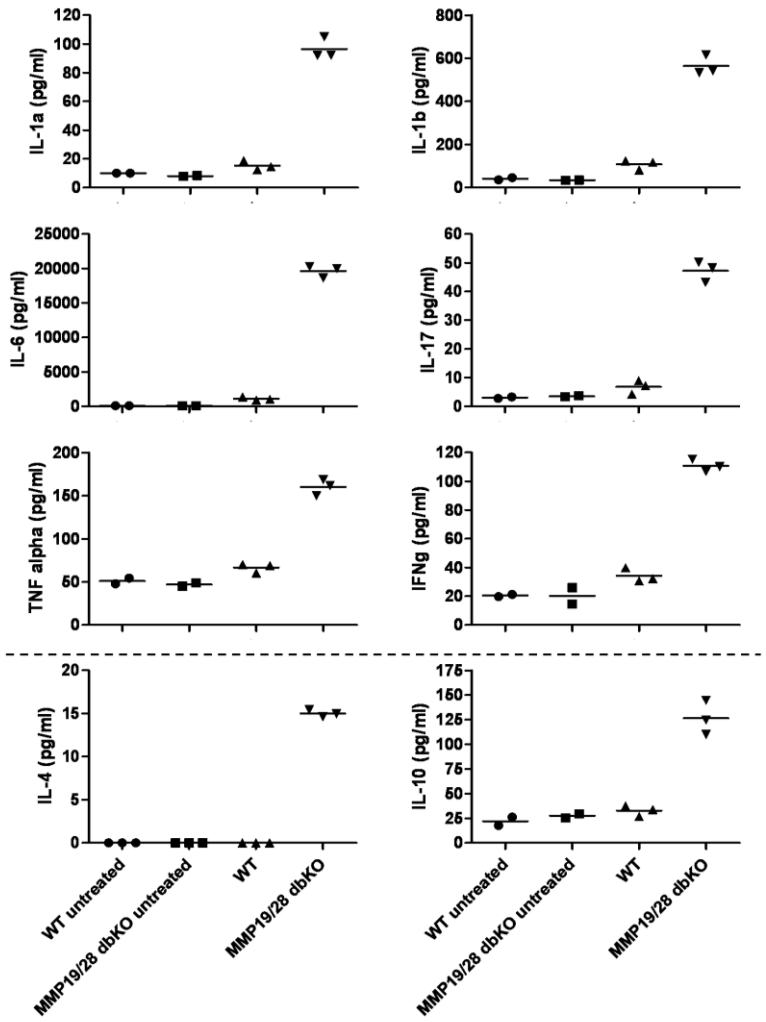

Figure 4-45: Cytokines in supernatants of colon explant cultures from healthy and recovering tissues.

Cytokines analyzed by BioPlex bead assay showed high levels of pro-inflammatory cytokines IL-1 (α and β), IL-6, and IL-17 in MMP double-deficient animals whereas the WT mice showed no elevation of these cytokines. Anti-inflammatory cytokines such as IL-4 and IL-10 were highly elevated in MMP-19/-28 dbKO mice (A), n = 2, WT and MMP-19/-28 double-deficient mice in control group; n = 3, WT and MMP-19/-28 double-deficient mice in DSS-treated group. All differences were highly significant (*** $p < 0.001$ for all cytokines).

All chemokines measured showed also highly elevated levels in the MMP-19/-28 dbKO mice. They included G-CSF, GM-CSF, KC, RANTES, MCP-1, and MIP-1a. In contrast, concentrations in the CECs of the DSS-treated WT mice were only moderately upregulated or remained unchanged compared to the WT group (Figure 4-46).

These data are in agreement with the observed severity of disease in the MMP-19/-28 dbKO mice and the histological analysis of the colon. The increased levels of pro-inflammatory cytokines and chemokines indicate ongoing inflammation and illustrate the impaired healing process seen in the MMP double-deficient mice. On the other hand, the presence of anti-inflammatory cytokines suggests the initiation of disease resolving mechanisms, too.

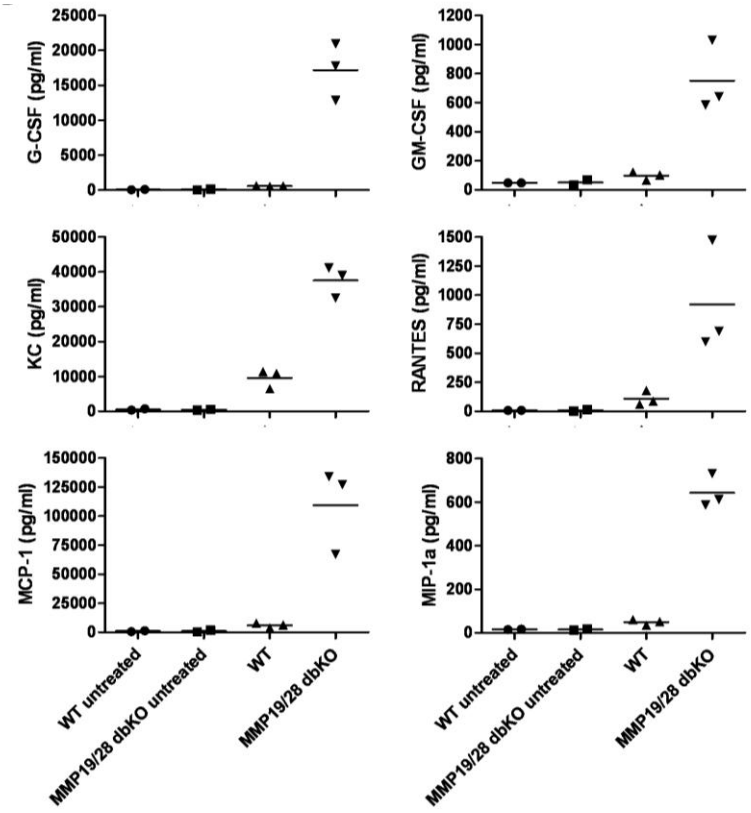

Figure 4-46: Chemokines in supernatants of colon explant cultures from healthy and recovering tissues.

The levels of several chemokines (KC, MCP-1, MIP-1, G-CSF, and GM-CSF) were significantly higher in the supernatants of MMP-19/-28 double-deficient mice than in those of the WT (B), n = 2, WT and MMP-19/-28 double-deficient mice in control group; n = 3, WT and MMP-19/-28 double-deficient mice in DSS-treated group. All differences were highly significant (***, $p < 0.001$ for all cytokines).

4.4 Chronic colitis

4.4.1 Reduced body weight, increased DAI and reduced survival of MMP-19-deficient mice

Chronic colitis was induced by two cycles of 2% DSS (Figure 4-47). In this experiment, only MMP-19-deficient and wildtype mice were analyzed.

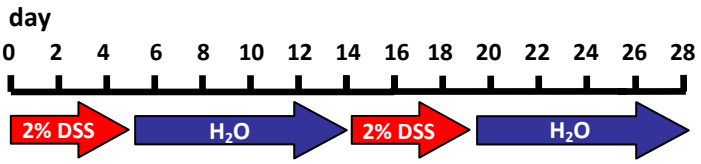

Figure 4-47: Induction of chronic colitis, course of experiment.
To induce acute colitis mice were treated by two cycles of DSS-induced colitis followed by a recovery phase.

A group of 12 MMP-19 -/- mice and 14 wildtype animals was used in this experiment. The control group of untreated mice consisted of five mice of each strain. Disease severity was monitored daily by weight progression, hemoccult test, and stool consistency. During the course of the experiment the MMP-19-deficient mice lost significantly more weight than the WT animals, a trend, which was already obvious at the beginning of the first cycle (Figure 4-48). The maximum weight loss was observed at day 8 (22 ± 3% in MMP-19 -/- mice versus 5 ± 1.5% in WT mice, $p \leq 0.005$). After establishing chronic colitis, the MMP-19-deficient mice never regained their original weight and showed a profound weight loss after day 28, the endpoint of the experiment (-10 ± 5%). In contrast, the WT animals returned to their original weight at day 18 and then further increased the weight until the end of the experiment (day 28; +9 ± 2%). The weight difference between the MMP-19 -/- and the WT mice at the endpoint of the experiment was highly significant ($p \leq 0.005$) (Figure 4-48A). The DAI considers body weight loss, stool consistency, and amount of blood in stool. MMP-19 -/- mice showed a much higher DAI during all phases of colitis (Figure 4-48B). The Kaplan-Meier-survival curves demonstrate that nearly all WT mice survived the chronic treatment whereas the survival rate of MMP19 -/- mice was only 50% (Figure 4-48C).

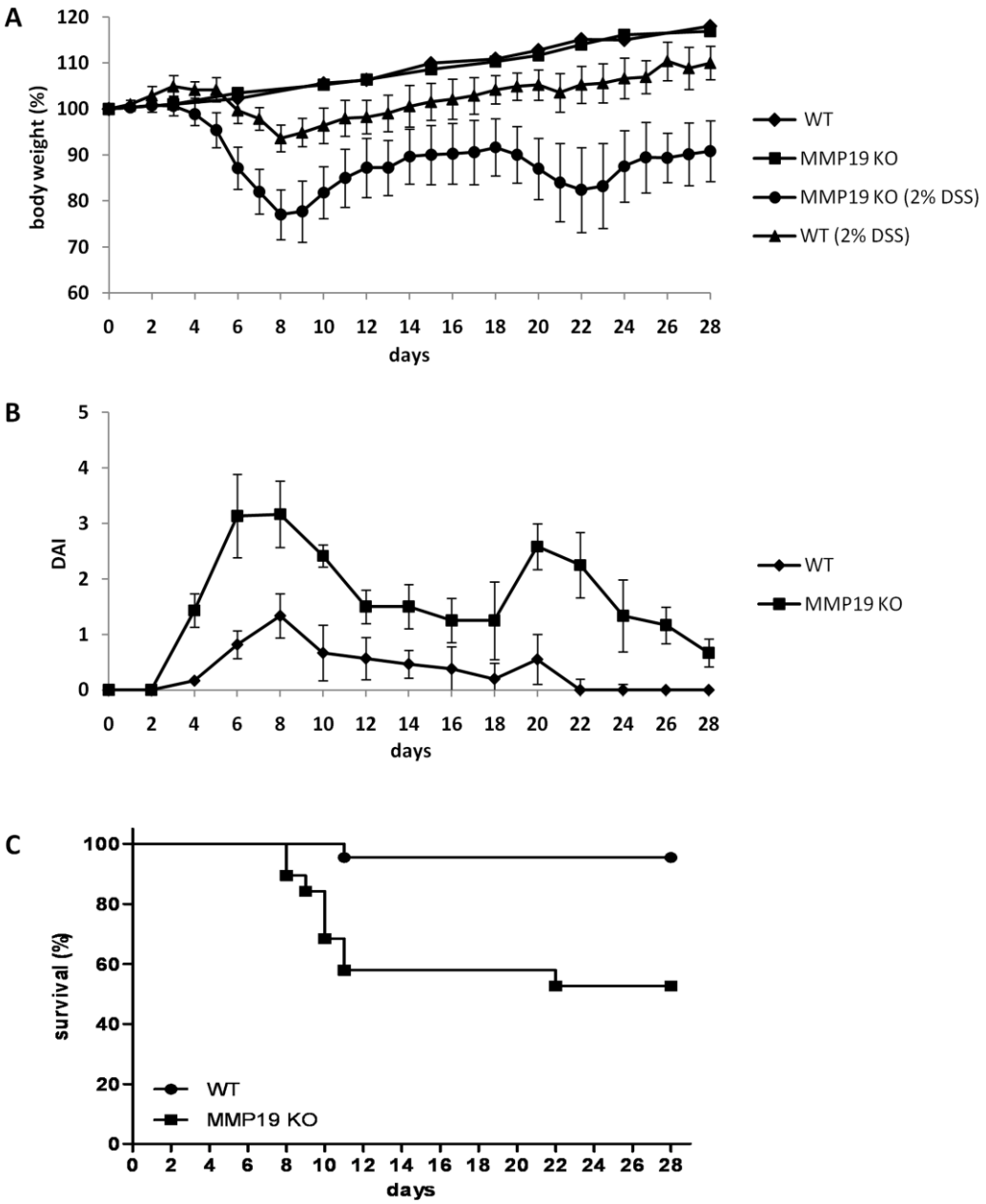

Figure 4-48: Body weight changes, disease activity index and survival curves of MMP-19 -/- and WT mice suffering from chronic colitis.

(A) Weight development after applying two cycles of 2% DSS followed by normal drinking water. MMP-19-deficient mice lost significantly more weight than the WT animals. Whereas the MMP-19-deficient mice never regained their original weight, the WT animals recovered and from day 18 even increased their weight (day 28: MMP-19 -/-; -10% ± 5% versus WT; +9% ± 2%, $p \leq 0.005$). (B) MMP-19 -/- mice showed a higher DAI during all phases of colitis. (C) Survival curves (Kaplan-Meier) showed nearly all WT mice survived the chronic treatment but the survival rate of MMP-19 -/- mice was only 50%. Data are expressed as mean ± SD (n = 5, control mice; n = 14, DSS-treated WT group; n = 6, DSS-treated MMP-19 -/- group).

4.4.2 Reduced colon length and splenomegaly in MMP-19-deficient mice

At the endpoint of the chronic colitis experiment (day 28), colons and spleens of DSS-treated wildtype (n = 14) and MMP-19-deficient (n = 6) mice were removed and analyzed for their size and weight (spleen only), and compared to the control group of untreated animals (n = 5 for WT and KO). Whereas the mean colon length of the DSS-treated wildtype mice was largely unchanged compared to the one measured in the control group, the treated MMP-19 -/- mice showed a significantly reduced colon length (WT, 6.64 ± 0.35 cm versus MMP-19 -/-, 5.4 ± 0.2 cm, $p < 0.001$) (Figure 4-49A and C). Even greater differences were observed in the spleen: The mean spleen weight of the DSS-treated MMP-19 -/- mice increased by more than 150% compared to the one of the treated wildtype mice ($p < 0.001$). This increase in weight was reflected in splenomegaly, i.e. a profound enlargement of the spleen (Figure 4-49C). The spleen weight of the treated wildtype mice was only marginally larger than that of the control mice (non-significant, $p > 0.5$).

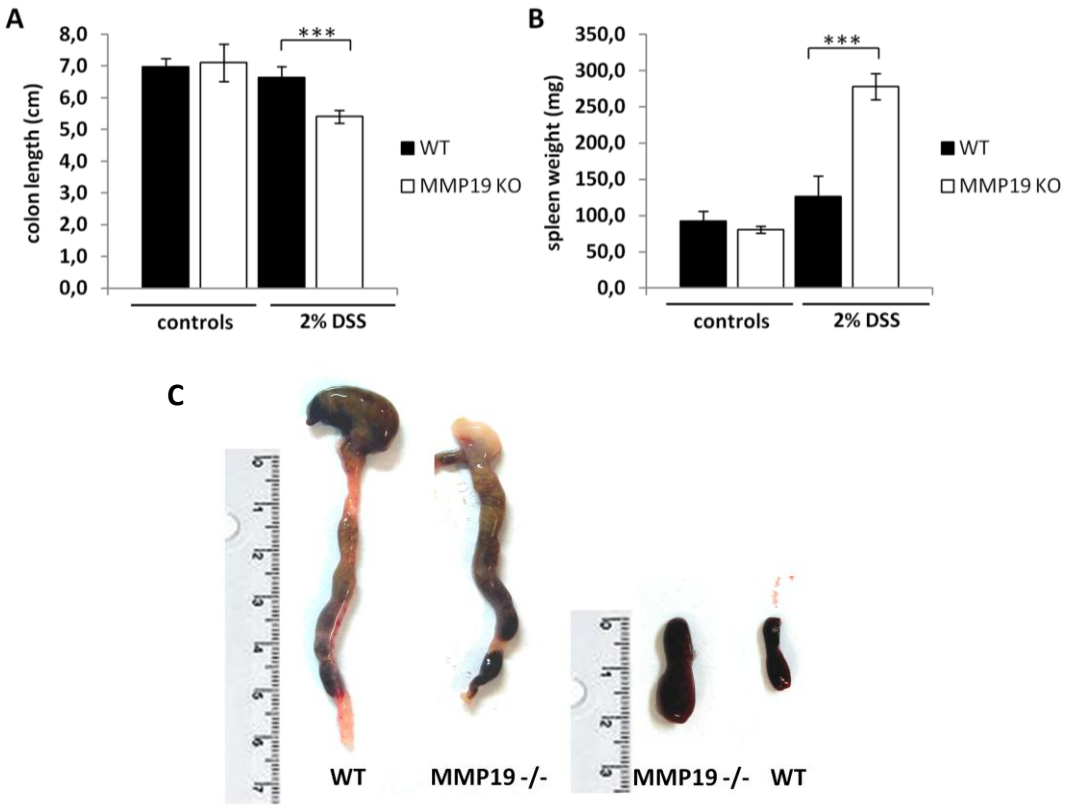

Figure 4-49: Colon length and spleen weight of WT and MMP-19 -/- mice.
Colon length (A) and spleen weight (B) of untreated as well as DSS-treated WT and MMP-19 -/- mice was determined on day 28. The colon of MMP-19 -/- mice was significantly shorter than the WT one (-18.24%) and the spleen weight was more than doubled. Data are expressed as mean ± SD (n = 5, control mice; n = 14, DSS-treated WT group; n = 6, DSS-treated MMP-19 -/- group). *** $p < 0.001$. (C) Representative pictures of colon (left panel) and spleen (right panel) from DSS-treated WT and MMP-19 -/- mice are shown.

4.4.3 Increase in hyaline arteries and proliferation in spleen of MMP-19-deficient mice

To investigate if the splenomegaly seen in MMP-19-deficient mice was accompanied by structural alterations of the spleen, spleen tissue sections of DSS-treated wildtype and MMP-19 -/- mice were stained with hematoxylin/eosin and evaluated. Strikingly, arteries in MMP-19-deficient mice showed remarkable depositions of hyaline material. Whereas 100 % of tissue sections from the MMP-19 -/- mice stained positive for hyaline material at the inner wall of the blood vessels, only 25% of wildtype mice exhibited such pathology (Figure 4-50A). Two experiments were performed giving similar results.

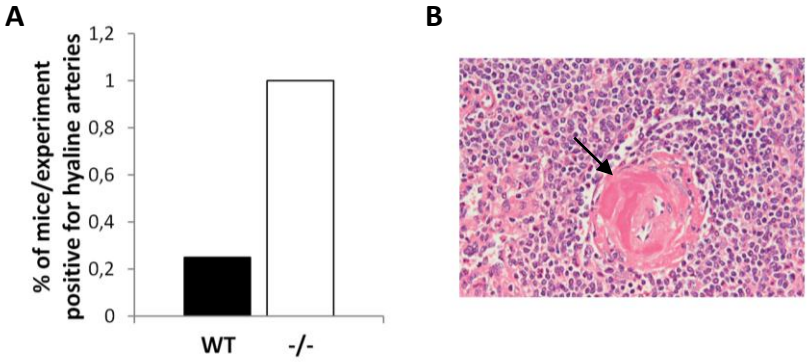

Figure 4-50: Hyaline arteries are more frequent in MMP-19-deficient mice.
Percentage of mice per experiment (two in total) that were showing hyaline arteries in the spleen (A). Hematoxylin/eosin staining of spleen section showed deposition of hyaline material in the blood vessel (hematoxylin/eosin staining, magnification x 200) (B).

To investigate further the pathology of the spleen in chronic colitis, immunohistochemistry was used. The amount of proliferating cells in the spleen, especially in the red pulp, was analyzed by staining with Ki-67 antibody, which is a cellular marker for proliferation. It is strictly associated with cell proliferation. During interphase, the Ki-67 antigen can be exclusively detected within the cell nucleus, whereas in mitosis most of the protein is relocated to the surface of the chromosomes. Ki-67 protein is present during all active phases of the cell cycle (G_1, S, G_2, and mitosis), but is absent from resting cells (G_0) [239; 240]. Only mitotic cells with a dark brown nucleus were counted as positive for proliferation. In the spleens of WT and MMP-19-deficient mice increased proliferative activity was observed compared to healthy mice (Figure 4-51A and B). In agreement with the splenomegaly, 20% more proliferating cells were found in the MMP-19 -/- animals.

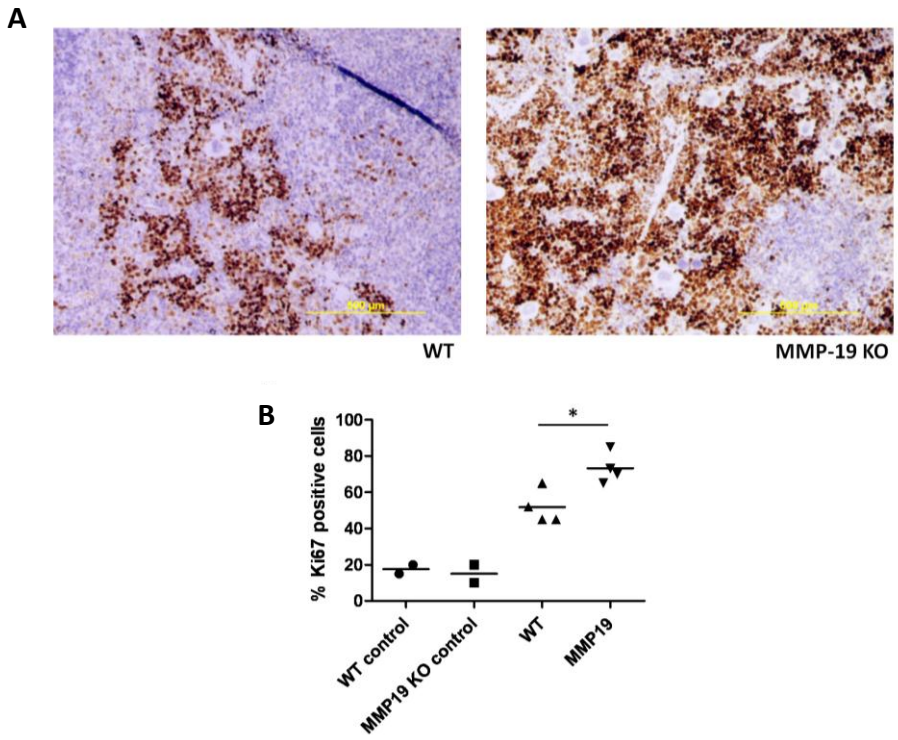

Figure 4-51: Increased proliferative activity in MMP-19-deficient mice.
Representative pictures of WT and MMP-19 -/- spleens stained for the proliferation marker Ki-67 (original magnification x 40) (A)**.** Percentage of Ki-67 positive cells in the red pulp of the spleen. MMP-19 -/- mice showed elevated numbers of proliferating cells (B). Untreated mice, n = 2; DSS-treated mice, n = 4, * $p < 0.05$.

4.4.4 MMP-19-deficient mice with chronic colitis show severe colon damage and inflammation

At the end of the chronic colitis experiment, histological analysis of the distal part of the colon tissue was performed. Colon sections of WT (n = 4) and MMP-19-deficient mice (n = 4) stained with hematoxylin/eosin were analyzed for the same parameters as described before (see 4.2 Acute colitis) (Figure 4-52). Arrows are pointing to oedema in the mucosa, which is stronger in MMP-19 -/- mice. Differences in crypt damage are marked with arrowheads.

Whereas the DSS-treated WT mice showed only minor signs of colon inflammation or tissue destruction, e.g. inflamed lesions covered about 10% of the colon (Figure 4-53A) or certain extent of crypt damage (Figure 4-53G), the colons of the MMP-19-deficient mice were highly inflamed and damaged. All parameters measured were significantly increased compared to the WT group. The most significant differences ($p < 0.01$) were observed for neutrophil influx (Figure 4-53E) and percentage of hyperregenerative tissue (Figure 4-53F). These findings depicted a persistent inflammation in the MMP-19 -/- mice and an attempt of re-epithelialization to remodel the normal mucosal architecture.

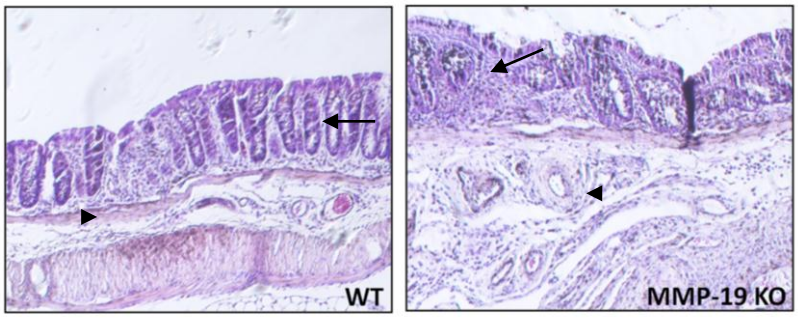

Figure 4-52: Representative pictures of WT and MMP-19-deficient mice with chronic colitis. Hematoxylin/eosin staining, arrowheads are pointing to oedema in the tissue; arrows are marking crypt damage (hematoxylin/eosin staining, magnification x 40).

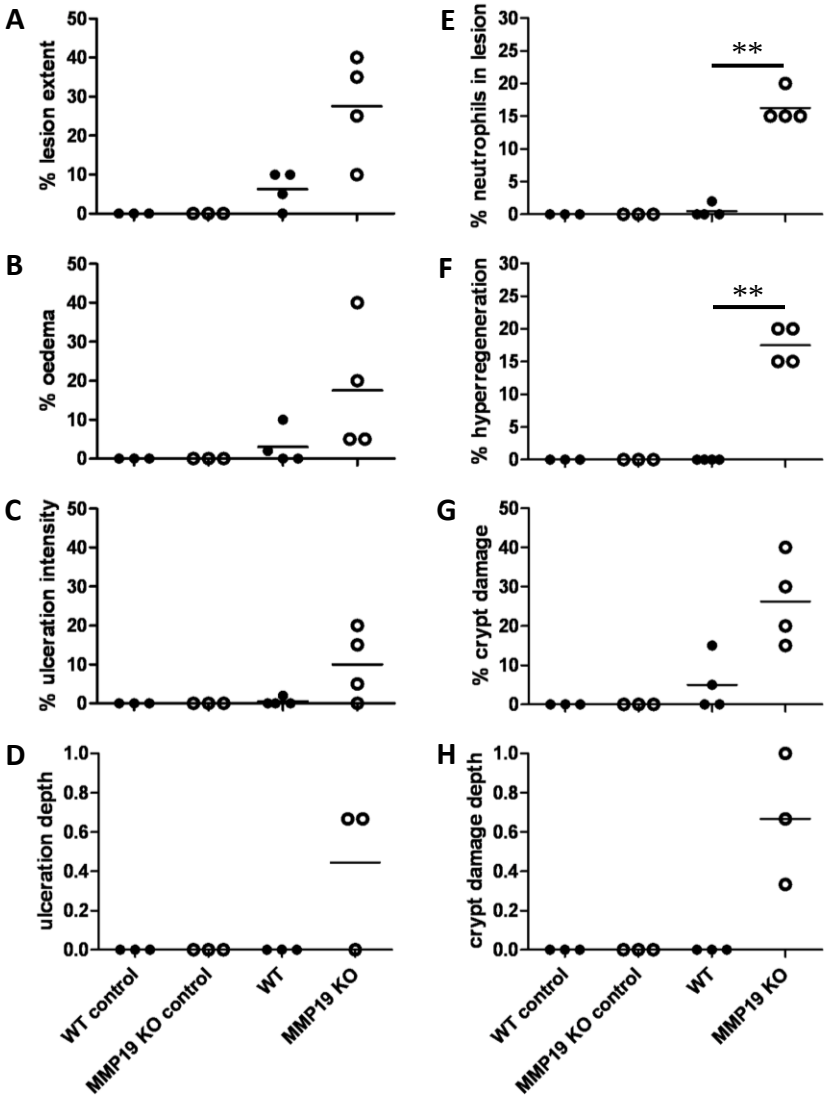

Figure 4-53: Histological analysis of colon tissue of MMP-19-/- mice with chronic colitis.
Colon tissue sections of DSS-treated WT and MMP-19-deficient mice were stained with hematoxylin/eosin and analyzed for parameters related to inflammation and tissue destruction. Compared to the WT mice, the extent of inflamed lesions (A), the percentage of oedema (B), ulceration intensity (C), ulceration depth (D), percentage of crypt damage (G), and crypt damage depth (H) were all significantly increased in the colon of the MMP-19 -/- mice ($p < 0.05$). An even higher significance was observed for neutrophil influx and percentage of hyperregeneration

($p < 0.005$). In contrast to the MMP-19 -/- group, the WT group had recovered from the colitis and did not show any major colon inflammation or damage. Data are shown as dot plot with means, all panels showed a significance of *, $p < 0.05$ except of those two which are marked ** for $p < 0.005$.

The colonic tissue was further analyzed for areas showing acute (neutrophils, oedema, severe tissue damage) or chronic (plasma cells, fibrosis) inflammation and for depth of inflammation. In the MMP-19 -/- mice, over 40% of the colon was chronically inflamed and about 20% of the area showed signs of acute inflammation (Figure 4-54, left and middle panel). This was highly significant as compared to the DSS-treated WT group, which appeared similar to the untreated control groups. The inflammation depth was also very pronounced and significantly greater than the one observed for the controls (Figure 4-54, right panel).

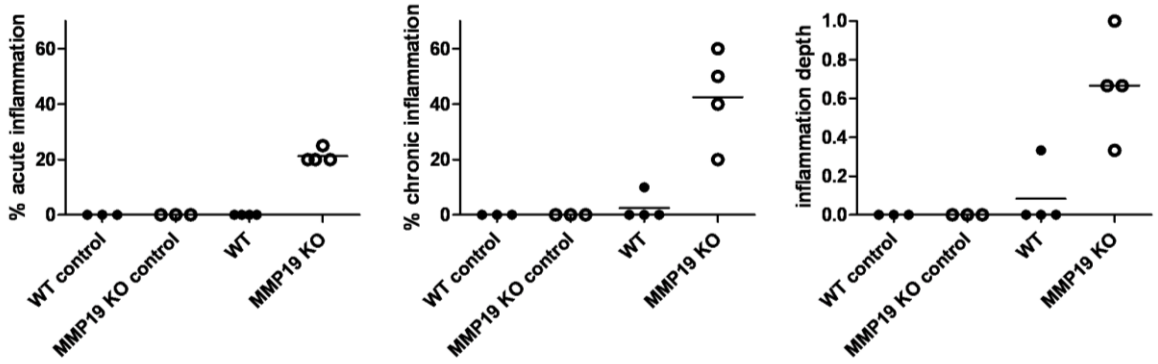

Figure 4-54: Amount of acute and chronic inflammation in colonic tissue of DSS-treated mice and controls.
MMP-19 -/- mice depicted higher percentage of acute and chronic inflamed tissue. WT animals appear healthy. Also the depth of the inflammation was significantly increased in deficient towards wildtype mice. Data are shown as dot plot with means, all panels showed a significance of *, $p < 0.05$. Untreated mice, n = 3; DSS-treated mice, n = 4.

4.4.5 MMP-19-deficient mice show signs of fibrosis

To investigate if MMP-19 deficiency and the exacerbated progress in chronic colitis promoted the development of fibrosis, collagen deposition in the colon wall of treated wildtype and MMP-19 -/- mice was analysed using trichrome staining. In contrast to the colon wall of the WT animals, which had recovered and showed a similar architecture to the one observed in untreated mice, the colon wall of the MMP-19 -/- animals exhibited clear signs of damage and, moreover, the mucosa of the colon displayed an extensive increase in collagen disposition (Figure 4-55).

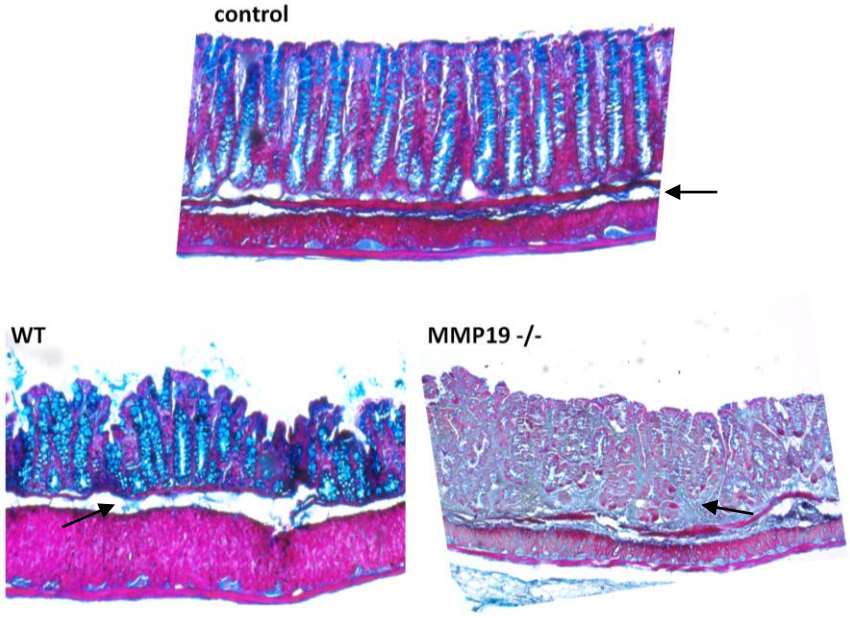

Figure 4-55: Trichrome staining of mouse colon.
Trichrome staining of the middle part of the colon (day 28) was performed to visualize collagen deposition (blue staining, also the mucus in the goblet cells was stained in blue) in the colon wall. Upper panel: section of untreated mouse, lower panels: sections of DSS-treated WT and MMP-19 -/- animals. Collagen deposition is indicated by arrows. Representative pictures of two independent experiments are shown, magnification x 40.

In addition staining for the expression of collagen type I, which is the most abundant collagen present in healing tissue and fibrosis, was performed. Fibrosis is developing due to injury or long-term inflammation. The tissues harden and the permeability decreases, which in case of the colonic mucosa is a disadvantage as it impedes the function of the colon. Consistent with the results of the trichrome staining, collagen type I was more abundant in the colon of the MMP-19-deficient mice (Figure 4-56).

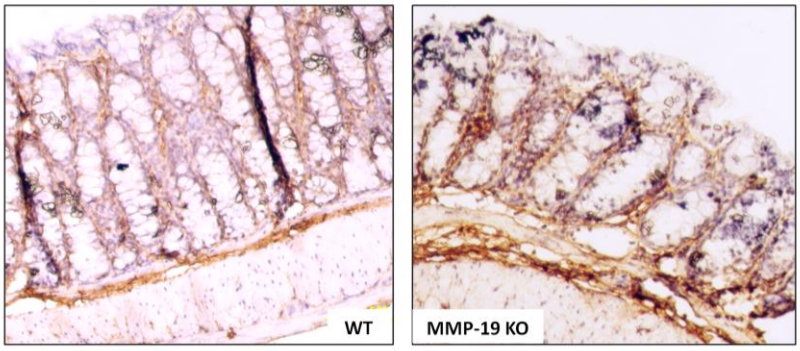

Figure 4-56: Enhanced collagen type I expression in colon tissue of MMP-19-deficient animals. Collage type I (brown colour) colocalized with the trichrome staining. Collagen type I is the most abundant component in fibrotic tissue. Representative pictures of collagen type I immunostaining (magnification x 100) from WT and MMP-19 -/- mice are shown.

4.4.6 Elevated levels of IL-1α and IL-6 but not TNF-α or IFN-γ in plasma of MMP-19-deficient mice during the chronic phase

To compare the inflammatory response between DSS-treated wildtype and MMP-19 -/- mice, plasma cytokine and chemokine concentrations at day 28 were determined by BioPlex bead assay. Whereas the cytokine levels in plasma of the treated WT mice were not significantly different from those measured in the untreated control group, the IL-1α and IL-6 concentrations in plasma of the treated MMP-19-deficient animals were highly elevated (about 3-fold and 5-fold, respectively). However**,** TNF-α and IFN-γ levels remained largely unchanged (Figure 4-57A). Furthermore, the levels of several chemokines (MCP-1, G-CSF, and GM-CSF) were significantly higher in plasma of MMP-19 -/- mice than in WT ones (Figure 4-57B). No difference was found in levels of the chemokine KC. Concentrations of G-CSF in plasma of MMP-19 -/- mice were still as high as during the recovery phase, whereas the other chemokine levels decreased slightly

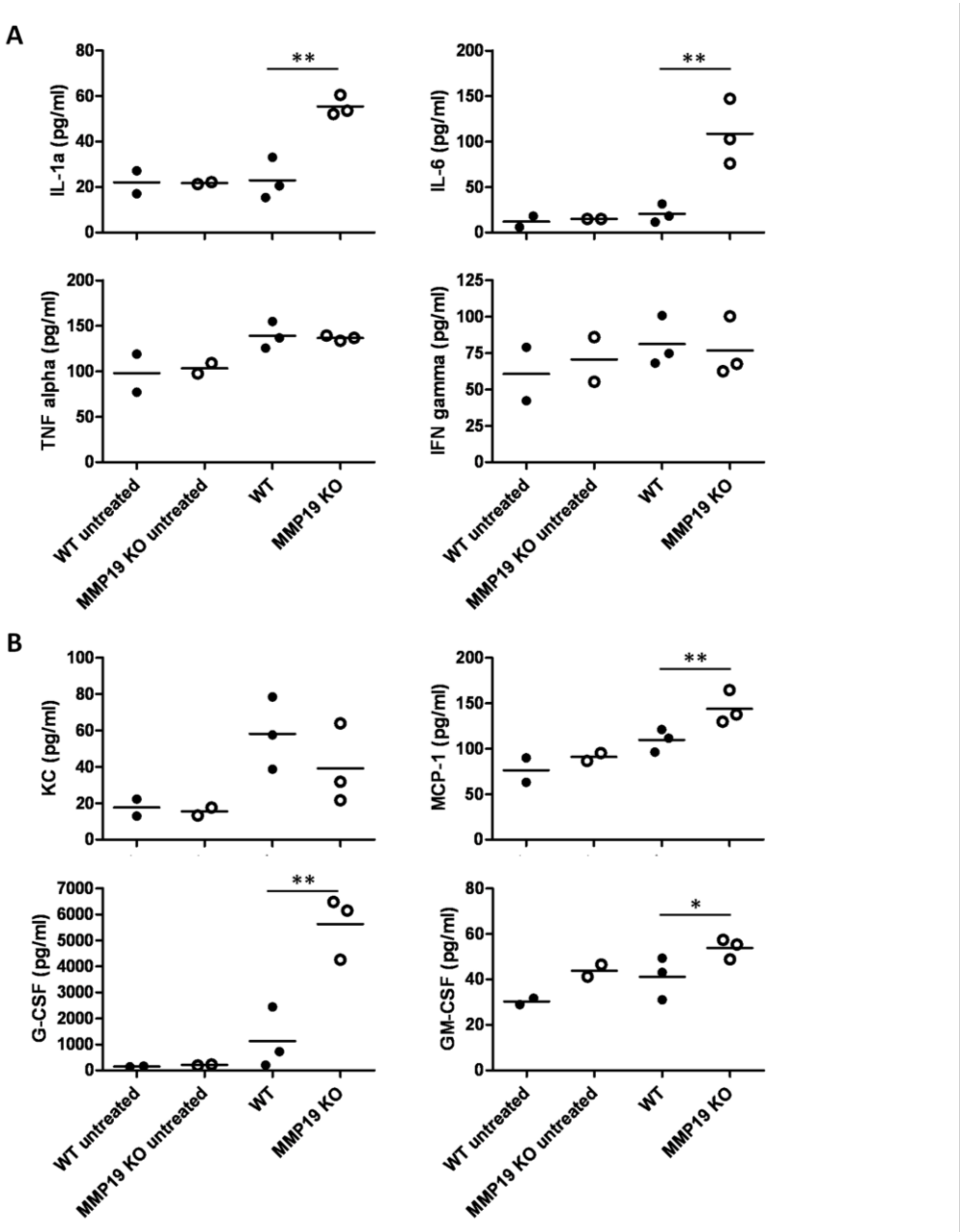

Figure 4-57: Cytokines and chemokines in plasma of healthy mice and mice suffering from chronic colitis.

Cytokine (A) and chemokine (B) levels in plasma prepared on day 28 were determined by BioPlex bead assay. Data are represented as individual data points and mean of duplicate measurements (n = 2, WT and MMP-19 -/- mice in control group; n = 3, WT and MMP-19 -/- mice in DSS-treated group) * $p < 0.05$, ** $p < 0.005$.

4.4.7 Elevated levels of pro- as well as anti-inflammatory cytokines in CEC supernatants of MMP-19-deficient mice

In addition to elevated levels of cytokines in plasma, MMP-19-deficient mice depicted even higher values of pro- and anti-inflammatory cytokines in the supernatants of colon explant cultures (Figure 4-58). The levels of pro-inflammatory cytokines in WT animals were around normal values, they were just slightly elevated. Cytokines analyzed showed

clearly high levels of pro-inflammatory cytokines like IL-1 (α and β), IL-6, and IL-17 in MMP-19-deficent animals, the values for the MMP-19 -/- mice were in all cases more than two times higher than the WT ones. Especially levels of IL-17 that acts as a potent mediator in delayed-type reactions by increasing chemokine production to recruit monocytes and neutrophils to the site of inflammation were six times higher when compared to WT mice. All together, pro-inflammatory as well as anti-inflammatory cytokines are increased in the colonic tissue of MMP-19-deficient animals. Levels of IL-4 and IL-10 are at least two times higher in the knockout mice. These cytokines are important in chronic inflammations and the healing process as they are major deactivators of activated, cytokine-producing monocytes and macrophages.

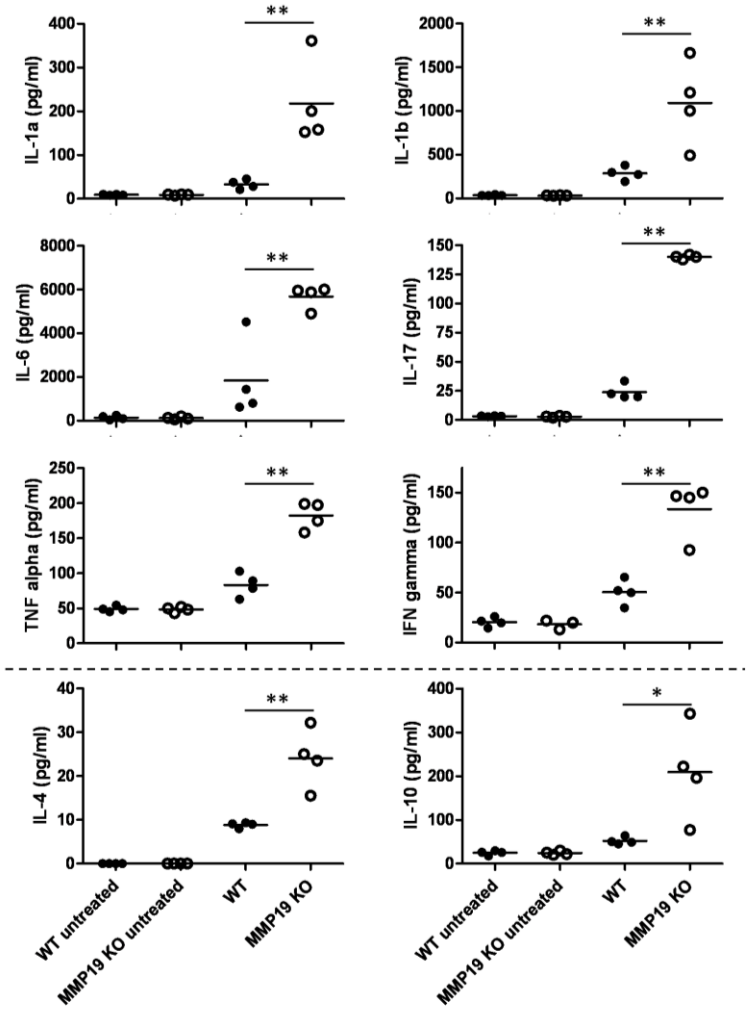

Figure 4-58: Cytokines in supernatants of colon explant cultures from healthy and colitic tissues. Cytokines analyzed by BioPlex bead assay showed elevated levels of pro-inflammatory cytokines such as IL-1 (α and β), IL-6, and IL-17 in MMP-19-deficent animals whereas the WT mice just showed slightly increased levels. Also anti-inflammatory cytokines like IL-4 and IL-10 were more elevated in MMP-19 -/- mice (A). n = 4, WT and MMP-19 -/- mice in control group; n = 4, WT and MMP-19 -/- mice in DSS-treated group), * $p < 0.05$, ** $p < 0.005$.

4.4.8 Increased levels of chemokines in CEC supernatants of MMP-19-deficient mice

The levels of chemokines in the CEC supernatants from wildtype mice returned in general to normal values or were slightly elevated. In contrast, the supernatants from MMP-19 -/- colons contained still extremely high levels of chemoattractants (Figure 4-59). Nevertheless, the levels of chemokines were lower than those in acute colitis. Peculiarly high amounts of MCP-1, and G-CSF were produced by MMP-19 -/- mice. G-CSF is produced by macrophages and then stimulates the bone marrow to release new granulocytes into the blood to fight inflammation; MCP-1 attracts macrophages. In case of MCP-1 there was only a tendency seen of more elevated levels in MMP-19-deficient than in WT mice. Levels of RANTES were three times higher in knockout animals than in WT. The synthesis of RANTES is induced by TNF-α and IL-1α, it is produced by circulating T-cells and plays an active role in recruiting leukocytes into inflammatory sites. In general, all addressed chemokines depicted similar levels as in the recovery experiment for MMP-19 -/- mice. Concentrations of chemoattractants in WT animals decreased in comparison to the recovery experiment, leading to less acute inflammation in the colon tissue.

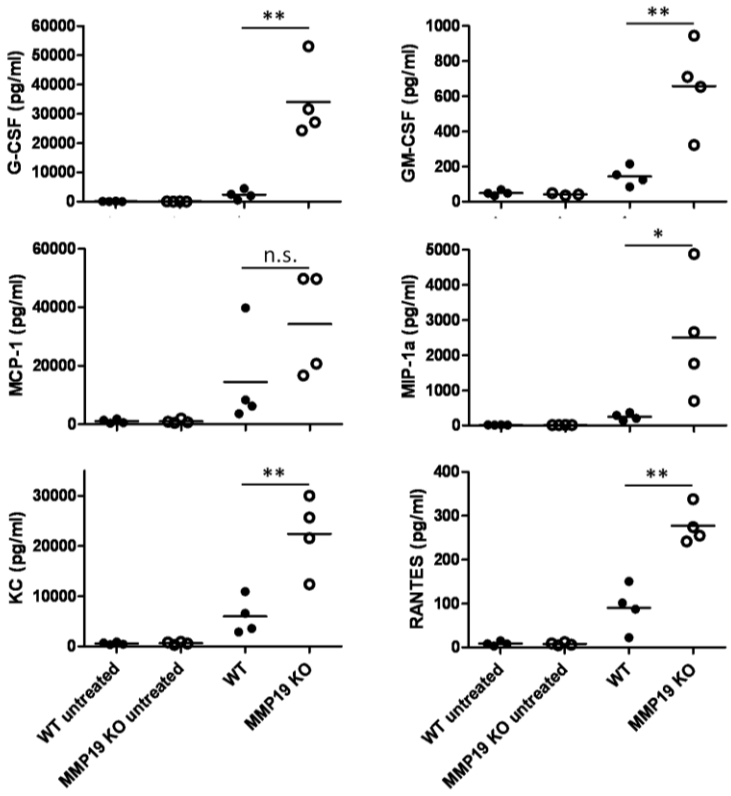

Figure 4-59: Chemokines in supernatants of colon explant cultures from healthy and diseased tissues.

The levels of several chemokines (KC, MCP-1, MIP-1, G-CSF, and GM-CSF) were significantly higher in the supernatants of MMP-19 -/- mice than in WT ones. The values in the deficient animals were still extremely high. (n = 4, WT and MMP-19 -/- mice in control group; n = 4, WT and MMP-19 -/- mice in DSS-treated group) n.s. non significant, * $p < 0.05$, ** $p < 0.005$.

4.5 Fractalkine – a novel substrate of MMP-19

Fractalkine (FKN, CX3CL1) is a unique chemokine combining adhesive and chemotactic properties. Its membrane-bound form promotes leukocyte adhesion, whereas its soluble form, generated by proteolytic ectodomain shedding, functions as a chemoattractant for cells expressing the receptor CX3CR1. The FKN-CX3CR1 system has been shown to play a major role in many inflammatory diseases such as atherosclerosis and rheumatoid arthritis [241; 242], and more recently, has also been implicated in IBD pathogenesis. At least two studies have reported an increase in circulating CX3CR1+ T cells in patients with IBD [243; 244], and it has also been demonstrated that CX3CR1+ cells are more abundant in IBD mucosa [244] and that FKN mRNA is upregulated in inflamed colonic tissues [243]. Moreover, a study by Kostadinova et. al has suggested a role for the CX3CL1-CX3CR1 axis in a DSS mouse model of colitis through regulation of iNOS [245].
Since MMPs have emerged as major regulators of chemokine release, it seemed interesting to ask whether MMP-19 might have a role in leukocyte recruitment in IBD through processing of FKN.

4.5.1 Purification of human recombinant MMP-19

The MMP-19 fusion protein was generated and purified by using an N-terminal GST-tag. The expected size of the purified fusion protein was 85 kDa as detected by Coomassie staining and immunoblotting using an anti-MMP-19 antibody against the hinge domain of the protein (Figure 4-60A and B, arrowhead). The strong protein band of approximately 40 kDa appearing in the Coomassie stained SDS-PAGE is a peptide composed of the N-terminal GST-tag and the propeptide domain of MMP-19, which is generated during purification due to autocatalytic activity of MMP-19 (Figure 4-60A).

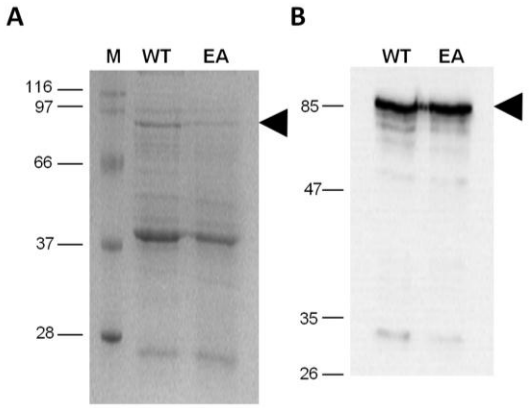

Figure 4-60: Purified recombinant MMP-19.
(A) SDS-PAGE of purified GST-MMP-19 WT and Inactive mutant (EA). The full-length protein has a size of 85 kDa. (B) Immunoblot of recombinant MMP-19 proteins resulted as well in a signal at 85 kDa. Taken from [246].

To test whether the purified wildtype protein was active a cleavage assay using a quenched fluorescence substrate (fluorogenic MMP-2 substrate, Calbiochem) was performed. In case of the active protein the quencher was released and an increase in fluorescence (RFU = relative fluorescent units) was detected. The activity was protein dependent and could be inhibited with an MMP inhibitor (MMP-9/MMP-13 inhibitor II, Calbiochem) (Figure 4-61).

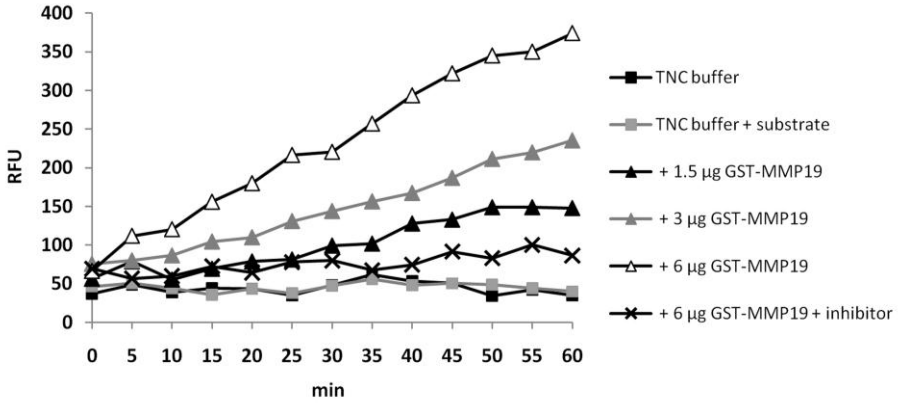

Figure 4-61: Determination of activity of recombinant MMP-19 WT protein.
The buffer controls showed no increase in fluorescence (boxes), whereas the sample containing the recombinant MMP-19 depicted increasing RFUs. The activity was dependant on protein amount (triangles) and could be inhibited by a MMP inhibitor (x).

4.5.2 MMP-19 degrades recombinant fractalkine

To address the question if FKN can be processed by MMP-19, recombinant human FKN was incubated together with proteolytic active MMP-19 (GST-MMP-19 WT), or with an inactive mutant variant (GST-MMP-19 EA) at 37°C for 35h. The digests were then analyzed by immunoblotting. As shown in Figure 4-62A, FKN incubation with GST-MMP-19 WT resulted in the almost complete processing of the 90 kDa full-length form of the protein and the generation of at least three cleavage products of around 70, 20 and 15 kDa. In contrast, the inactive MMP-19 EA mutant was not able to process the chemokine. These findings suggest that FKN is a substrate of MMP-19 that can be cleaved by the protease at multiple sites.

4.5.3 Reduced release of soluble fractalkine from colon of MMP-19-deficient mice

To get further insight into the *in vivo* relevance of FKN-processing by MMP-19, colon tissue lysates as well as colon explant cultures were prepared and analyzed by immunoblotting, using antibodies against the N- or C-terminus of FKN. N-terminal detection revealed a fragment of about 40 kDa in colon tissue lysates of MMP-19 -/- mice which was virtually absent in lysates from WT animals (Figure 4-62B, upper panel). In

contrast, using antibodies against the C-terminus, a smaller fragment of about 25 kDa was detected in the WT lysates; this fragment was also present, although in lower amounts, in the MMP-19 -/- samples (Figure 4-62B, lower panel). Analyzing the concentrated supernatant of colon explant cultures (CECs), a soluble FKN variant of about 23 kDa was detected in all samples. However, considerably less protein was detected in the supernatants of the MMP-19 -/- mice (Figure 4-62C).

Together, these results not only demonstrate that mouse colon constitutively expresses FKN at protein level, but moreover suggest that FKN expressed in colon is cleaved by MMP-19 to generate a soluble variant that likely has chemotactic activities.

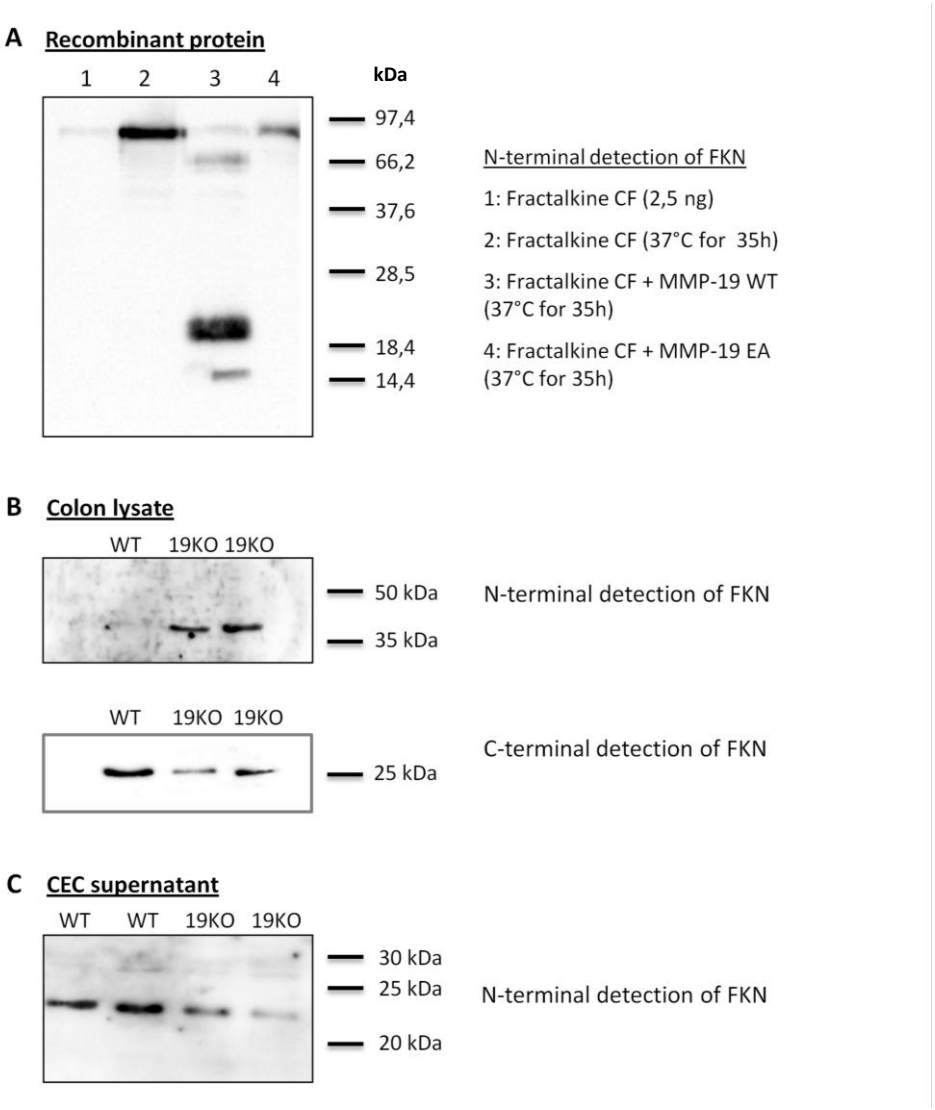

Figure 4-62: *In-vitro* and *ex-vivo* processing of fractalkine (FKN) by MMP-19.
(A) Western blot showing degradation of recombinant human FKN (carrier-free, CF) by an active form of MMP-19 (GST-MMP-19 WT). FKN protein was detected using an anti-FKN rabbit antibody serum raised against the N-terminal chemokine domain. Lane 1, 2.5 ng FKN; lane 2, 100 ng FKN in TCN buffer; lane 3, 100 ng FKN in TCN buffer plus GST-MMP-19 WT; lane 4, 100 ng FKN in TCN buffer plus an inactive mutant of MMP-19 (MMP-19 EA). The digest containing the active GST-MMP-19 WT protease (lane 3) but not the controls showed degradation of full-length FKN giving rise to at least 3 fragments of about 70, 20 and 15 kDa. (B) Immunoblotblot showing fractalkine expression in colon of healthy WT and MMP-19 -/- (19KO) mice. 30 µg of lysate/sample was loaded onto the gel. FKN protein was detected using antibodies against the extracellular N-terminus (upper panel) or the intracellular C-terminus (lower panel) of the molecule. Using N-terminal detection, a fragment of about 40 kDa was detected in the lysates of the MMP-19-deficient mice but not in those of the WT mice. In contrast, using the antibody against the C-terminus, a fragment of about 25 kDa was detected in all lysates, although the signal was stronger for those of the WT mice. (C) Immunoblot showing N-terminal detection of FKN in concentrated supernatants of colon explant cultures (CEC). A clear signal for a soluble FKN variant of about 23 kDa is detected in the CEC supernatant of WT mice. Although present, the signal is much less prominent in case of the MMP-19 -/- mice.

5 Discussion

The etiology and the cascade of events leading to intestinal inflammation like IBD still remain unclear. Deregulation of MMP expression and activity has been associated with IBD and is thought to be a major factor in the development of colon inflammation and cancer, as administration of broad-spectrum metalloproteinase inhibitors reduced inflammation and disease severity in mouse models of colon injury [149; 150]. MMPs are thought to play a certain causative role in disease pathogenesis of IBD (Figure 5-1) [169; 247]. Several MMPs such as MMP-2 and -9 are associated with tissue destruction and remodelling in the disease. The destructive effect of MMPs in the gut has been shown in several *in vivo* studies [168; 172; 248]. An exception is MMP-2, for which a protective influence was shown. Additionally, a function for many MMPs in immunity was reported [249].

MMP-19 and MMP-28 are two metalloproteinases that are abundantly expressed in epithelial cells (Figure 5-1) and have been shown to be involved in cell proliferation, migration, and wound healing. In detail, MMP-19 and -28 are expressed in human colon in epithelium of the mucosa [131]. MMP-19 was detected in hyperproliferating keratinocytes [250] and it is thought that its presence particular in the cryptal epithelium of stromas [131; 251] may be associated with enterocyte proliferation and regeneration.

Despite beeing constitutively expressed in normal tissues, MMP-19 -/-, MMP-28 -/-, and even double-deficient mice have no overt phenotype. This is in line with many other MMP-null mice. However, if mice are challenged in various mouse models (colitis, pneumonia, arthritis, dermatitis), a phenotype becomes obvious. MMPs exhibit redundancy in substrate specificity and cooperate in networks which are often activating but may also have destructive functions in order to limit the detrimental effects of their proteolytic activity. Therefore, this project aimed not only to investigate the single knockouts separately but also double-deficient mice to analyze their *in vivo* redundancy and substitutability. A lack of phenotype in unchallenged MMP-19- and MMP-28-deficient mice might implicate compensation by other MMPs. For example, in the MMP-19-deficient mice we found an increase in the activity of gelatinases in acute colitis, which probably tries to rescue the loss of MMP-19. In case MMP-19 and -28 have a function in innate immunity, no phenotype will be displayed until the immune system is challenged.

Nevertheless, little is known about the expression and function of MMP-19 and MMP-28 in the intestine or the innate immune system. Therefore, it was the objective of this study to elucidate the role of MMP-19 and MMP-28 in intestinal homeostasis and inflammation using a mouse model of colitis.

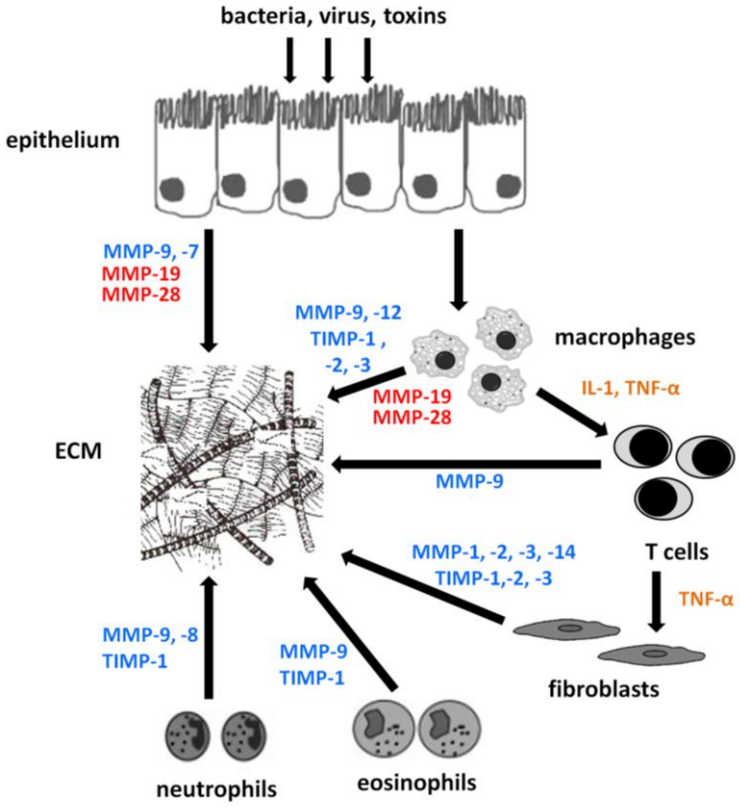

Figure 5-1: Summary of different cell types producing MMPs and TIMPs in IBD.
Luminal viruses, bacteria, or toxins can trigger immunological responses by activation of different cells such as macrophages, leucocytes and fibroblasts. These cells release several cytokines like TNF-α or IL-1. In addition activated cells can also release both MMPs and TIMPs. Inflammatory reactions can lead to an imbalance between MMPs and TIMPs followed by disturbing the ECM remodeling [130; 169; 252]. MMP-19 and -28 were included among the known proteinases and inhibitors.

5.1 MMP-19 has a more pronounced protective effect in DSS-induced colitis than MMP-28

Deficiency in the specific proteolytic activities in MMP-19 -/-, MMP-28 -/-, MMP-19/-28 double-deficient mice do not per se affect the integrity of the gut mucosa, and there were no signs of spontaneous colitis. However, challenge with moderate concentrations of DSS resulted in development of acute colitis, thus pointing to a pivotal role of MMP-19 in the pathogenesis of induced colitis. To assess the healing process, mice were allowed to recover from the acute colitis. Chronic colitis was induced by two cycles of DSS administration. Untreated mice of all groups were used as controls. Also this model of colitis disclosed the critical role of MMP-19 alone, reflected in exacerbated inflammatory and destructive processes in the colon. Moreover, in combination with MMP-28, the impact of MMP-19 on the acute as well as chronic course of the disease was even more pronounced and the double-deficient mice all died under conditions, in which the single knockout or control animals survived. The results clearly illustrated that in contrast to MMP-28-deficient mice, MMP-19-deficient animals show an increased susceptibility to acute and chronic DSS-induced colitis compared to the wildtype animals. However,

MMP-28-deficiency augments the effects of MMP-19 deficiency. Survival rates of MMP-19-deficient mice during acute and chronic colitis were significantly reduced. This correlates well with the strong colonic inflammation and tissue destruction, supported by high concentrations of chemokines (e.g. KC) and pro-inflammatory cytokines (e.g. IL-6, IL-1) in plasma and colon explant cultures. These findings point to a protective role for MMP-19 in colitis.

Interestingly, mice deficient for both metalloproteinases, the MMP-19/-28 dbKO mice, developed even more severe symptoms leading to a dramatically reduced survival and abrogated recovering capacity from acute colitis. Regarding the phenotype of MMP-28-deficient mice, a scenario may apply where an increase of MMP-19 activity overtakes most of the functions of MMP-28. This would be in line with results for gelatinase A and B, where MMP-9 is compensating for MMP-2 in the deficient mice [253].

MMP-19 and MMP-28 have probably not completely overlapping functions or substrates. Although both proteinases are expressed by epithelial cells, they exhibit distinct impacts on the development of induced colitis. Whereas the loss of MMP-19 leads to a severe disease progression, the absence of MMP-28 does not cause a phenotype in spite of the concurrent deficiency of both proteinases where the mice exhibit dramatic susceptibility to DSS-induced colitis. Functions of MMP-19 cannot be replaced by MMP-28 in the deficient mice. In contrast it seems that MMP-19, and maybe also other MMPs, can substitute for MMP-28 as mice deficient in MMP-28 exhibit no changes in comparison to wildtype mice. Moreover, MMP-28 was described as an intrinsic negative regulator of macrophage recruitment by retarding the chemotaxis of these cells. This would lead to an early increase in macrophage recruitment into the lungs in a mouse model for pneumonia in MMP-28-deficient mice [219]. The same mechanism can apply in the DSS-induced colitis model, so that there is a fast protective response of macrophages to the injury and the invading bacteria and no differences could be detected in the outcome of the disease compared to witdtype mice.

Another MMP that has a protective effect on colitis development is MMP-2 [172]. Similar to MMP-19, MMP-2 is constitutively expressed in intestinal and colon epithelia. In contrast to MMP-2, MMP-9 has a destructive effect on the course of colitis, and the extent and severity of intestinal epithelial injury was significantly attenuated in the deficient mice [248]. These opposite effects of MMPs expressed in both the epithelia and inflammatory cells suggest a complicated network, probably with a certain hierarchy, which balances the destructive and healing process in the colon. In this respect, it would be very useful to generate more such double and triple mutants to investigate the cooperative and overlapping functions of MMPs in the process of colitis development.

As MMP-19-deficient mice show exacerbated destruction of colon in epithelium, deep ulceration and progressive fibrotic changes in chronic type of colitis, we suppose it is protective for certain homeostatic barrier functions. This is in line with increased FITC-dextran translocation in these mice compared with WT counterparts. It was described in human and animal studies that epithelial dysfunction plays a central role in the

pathogenesis of intestinal inflammation [254; 255]. A similar barrier-maintenance function was described also in MMP-2 [172], MMP-7 [168], MMP-10 [256], or in ADAM-17 (TACE) whose missing proteolytic activity in ADAM-17-deficient mice results in barrier leakiness [257]. This impact on barrier function and maintenance is probably not due to processing of basement membrane components as it might be in case of MMP-19, which is known to process laminin 5□2chain, nidogen-1, tenascin C, collagen type IV and some other ECM-proteins [185; 201; 202; 229].

Evidence from human and animal studies as well as cell culture models suggest three major requirements essential for initiation and progression of IBD: First, disruption of the epithelial barrier by either a direct effect on the barrier or an impaired healing in response to injury. Second, the access of luminal contents to the lamina propria, resulting in interaction with immune cells. And third, an abnormal immune response of the organism [12; 254; 255]. Epithelial dysfunction is seen in patients much earlier than histological or clinical manifestations of IBD. It is thought that dysregulated barrier function allows contents of the intestinal lumen to enter the lamina propria, causing an immune response characterizing inflammatory diseases of the intestine. As the barrier of MMP-19-deficient mice was more severely damaged than the one of WT animals, it is likely that an enhanced contact between bacteria/luminal toxins and the host cells was the consequence. Our data show that barrier function is compromised in MMP-19 -/- mice, which possibly leads to their increased susceptibility to luminal toxins like DSS.

There are several possible mechanisms by which MMP-19 might affect barrier function. One example is that MMP-19 modules tight junctions directly by associating with tight junction proteins. A similar mechanism as described for MMP-2, which binds to claudin [258; 259; 260], can also be applied to MMP-19. Claudins are proteins extensivly involved in barrier function [261; 262]. Overexpression of MMP-2 increases the barrier function (unpublished data, S.V. Sitaraman).

MMP-19 is known to process collagen type IV, which is the major component of the basement membrane. The basement membrane is a thin sheet of fibres that underlies the epithelium and acts as a mechanical barrier. Cleavage of collagen type IV allows cells as well as chemokines to pass through the basement membrane to reach sites of tissue injury or inflammation in the up lying epithelium.

Analyzing the findings from this study, i.e. experimental colitis in MMP-19- and MMP-28-deficient mice, and results from previously published work, it appears that MMP-19 may act via several molecular and cellular mechanisms: 1/ proliferation and survival of cells as it could regulate the IGF-signaling pathway and the necessary contact to ECM, which in turn is responsible for activation or quiescence of cell state [203; 263], 2/ migration of keratinocytes and also other types of cells [200; 202; 203; 229], 3/ influx of inflammatory cells, especially macrophages that abundantly express this MMP, into inflammatory site (this study and [264]), 4/ vasculogenesis and angiogenesis [246], and 5/ bias of distribution and probably also development of immune cells [206].

5.2 MMP-19's impact on epithelial healing process due to controlling proliferation and migration

Cell proliferation is an important mechanism in maintaining tissue homeostasis and is especially needed in the healing phase following injury or inflammation. Dysregulated proliferation leads to impaired healing (reduced proliferation) and cancer development (increased proliferation). Under normal conditions no differences in proliferation of the epithelial cells was observed among the analyzed mouse strains. Upon DSS-challenge proliferation of epithelial cells in the colon mucosa was reduced in all mice, although MMP-19 -/- mice showed lower proliferation rates than counterpart wildtype mice. Even during the recovery phase, when an increase of dividing cells is expected and seen in wildtype mice, the MMP-19-deficient animals still showed decreased proliferation. This is likely one of the reasons for the impaired ability to recover from acute colitis and repair the damaged tissue in MMP-19 -/- mice. Re-epithelialization is the most crucial process [265]. Re-epithelialization during wound healing in the skin is impaired in MMP-19 -/- mice as they showed a slower kinetic at the beginning of this process (unpublished data, Dr. Radislav Sedlacek). Shedding of junctional proteins, which are required for re-epithlialization is reported for MMP-7 and can be a way how MMP-19 develops its protective effect in injured tissue [123]. MMP-19 mediates beneficial functions in response to injury as its activity seems to be required for efficient repair of damaged epithelium and is likely to also control the transepithelial influx of neutrophils and macrophages across the colonic mucosa.

Cell migration is a central process in the development and maintenance of tissues and cells often migrate in response to, and towards, specific external signals, a process called chemotaxis.

At early stages of acute DSS-induced colitis, MMP-19-deficient mice showed significantly reduced numbers of neutrophils in the colon tissue when compared to wildtype mice. Neutrophils are an essential arm of innate immunity. However, an overload or chronic influx of these cells can cause severe damage. Whereas neutrophils were dispersed throughout the mucosa/submucosa in wildtype mice during the first days of colitis, they were not accumulating in the destroyed tissue in the MMP-19-deficient mice. Following the course of the disease, numbers of neutrophils did not change in the tissue of MMP19 -/- mice, whereas in the wildtype mice a strong increase at the beginning of the colitis was seen and at later time points the numbers decreased as expected. As neutrophils do not express MMP-19, the defect in transmigration into the inflamed tissue was probably a consequence of a lack of expression of an appropriate chemoattractant in the epithelial cells or, mechanically, their removal due to excessive damage. As colon damage was progressing, the WT mice appeared to actively recruit neutrophils to the site of injury, which was not observed in the MMP-19 knockout mice in the first part of acute colitis; the response of neutrophils and their recruitment into the colon wall was strikingly

delayed. Thus, MMP-19 seems to function as a mediator for neutrophil migration to wounded mucosa.

Neutrophils migrate from the blood vessel into the interstitial tissue, following chemical signals such as IL-8 in human or KC and LIX in mouse and survive in the site of inflammation for 1–2 days. Once recruited, neutrophils kill bacteria through phagocytosis, release of soluble anti-microbial substances, and generation of neutrophil extracellular traps (NETs) [266; 267]. A massive, uncontrolled influx of neutrophils can cause indiscriminate, severe, and potentially mortal damage in experimental animal models, however, a lack of neutrophil activation can lead to unsolved inflammation caused by invading bacteria.

The reduced recruitment of inflammatory cells, especially neutrophils, to the site of tissue injury and inflammation might be an effect of impaired matrix processing and fast removal of epithelial cells that, thus, cannot send appropriate chemokine signals or due to, for instance, lacking processing of certain chemokines, which are responsible for attraction these inflammatory cells. Nevertheless, later on in the chronic process, it appears that in MMP-19-deficient mice a persistent delivery of activation and chemoattractant signals does not allow to limit and resolve this overwhelming destructive reaction of neutrophils and other inflammatory cells.

It was reported that macrophages abundantly express MMP-19 [175] as well as MMP-28 [172]. MMPs are widely reported to affect leukocyte transmigration due to processing of ECM components. Macrophages express several MMPs such as MMP-1, -3, -7, -9, -12, and MT1-MMP, which degrade interstitial collagens and basement membrane proteins [268]. As it was reported that MMP-19 is expressed in macrophages and that its expression is upregulated upon adhesion [189] it is likely that this deficiency could affect the healing process. Our current investigations have shown that MMP-19-deficient mice exhibit reduced migration (not published) in a transmigration assay (Figure 5-2A). This result was confirmed in a mouse model of acute Zymosan-induced inflammation (Figure 5-2B) [264]. In contrast, this study does not show significant differences in numbers of macrophages in the inflamed colon during acute colitis as well as during the recovery. The reason for this discrepancy might be explained by the analyzed time points. The previous studies were only focused on much shorter time points, differences were detected 40h after induction inflammation with Zymosan (Figure 5-2B), whereas the analysis in case of the colitis experiment was performed at later time points (8 days). Differences in the migratory kinetic of macrophages from WT and MMP-19 -/- mice were compensated over time. However, there is clear sign of dysregulation of macrophage migration in peripheral blood and in spleen. Using flow cytometry, an increase in the amount of F4/80 positive cells (macrophages) was detected in blood and spleen of DSS-treated wildtype mice. In contrast, the MMP-19 -/- mice did not display any changes in numbers of macrophages upon DSS treatment.

Currently, the reason for this bias is not known; however, one important stimulus could be the processing of chemokines, which are responsible for attraction of macrophages such as MCP-1 or MIP-1.

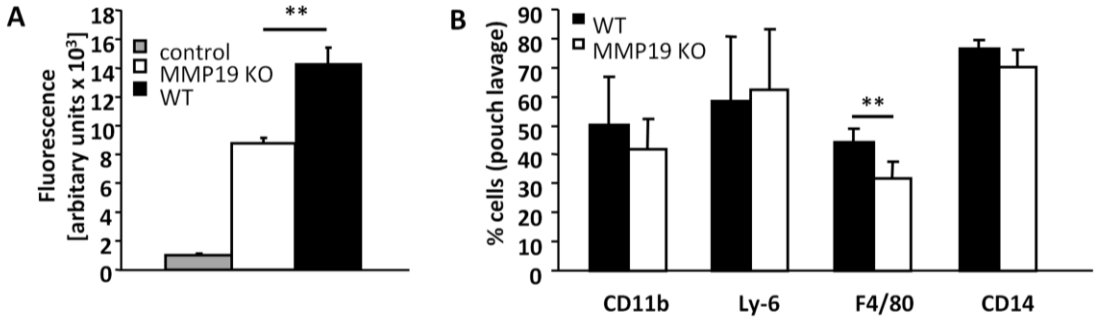

Figure 5-2: MMP-19 impacts cell migration. MMP-19 -/- macrophages showed reduced transmigration in vitro. Peritoneal monocytic cells including macrophages were isolated from WT and MMP-19 -/- mice, stained with calcein, and examined for their transmigratory capacity through a collagen type IV matrix using transwell systems. Fluorescence was measured before and 10h after seeding the cells. The pro-migratory stimulus in the lower chamber used was supernatant of 3T3 fibroblasts. Controls were done with unconditioned media (A). MMP-19 -/- macrophages showed reduced transmigration in vivo. MMP-19 -/- mice exhibit reduced migration of macrophages (F4/80+) to sites of inflammation in an air pouch model (B). **, $p < 0.01$

5.3 Splenomegaly caused by the impaired healing process in MMP-19-deficient mice in later stages of colitis

The spleen consists of two major compartments, the red pulp and the white pulp. The red pulp filters blood and its main purpose is the removal of parasites, dying red blood cells, and bacteria. It is also the site of haematopoiesis in rodents. The white pulp is the second largest lymphatic organ and initiates immune responses to blood-borne antigens [269]. Splenomegaly is the enlargement of the spleen and usually associates with anemia or congestion of the red pulp as well as severe bacterial infections.

Strikingly enlarged spleens seen in MMP-19-deficient mice recovering from acute colitis and with chronic colitis as well as MMP-19/-28 double-deficient mice in the recovery phase. However, splenomegaly is more a consequence rather than a cause of colonic inflammation but it mirrors the severity of colitis. Deficiency in MMP-19 leads to persistent inflammation in the colon and a destroyed barrier towards the intestinal lumen, which allows a constant influx of bacteria in to the tissue. These bacteria translocate into the blood and finally reach the spleen, where they are engulfed by neutrophils and macrophages. Subsequently, the white pulp will be activated and B lymphocytes start to produce antibodies. The more bacteria and/or their contents accumulate in the spleen, the more neutrophils and macrophages will be present, too. Eventually, this can lead to acute sepsis (complex systemic inflammation due to infection). A stressed spleen cannot function properly and could be another reason for the impaired wound healing [270]. The

presence of enlarged spleens is consistent with published data where evidences are provided suggesting a role for secondary lymphoid tissues, such as spleen, to contribute to the initiation and/or perpetuation of ulcerative colitis. Also for the mouse model of DSS-induced colitis, which resembles UC, enlargement of the spleen was described. Several studies suggest a correlation between spleen size and severity of DSS-induced colitis [90; 271]. Splenectomy was found to have a protective effect at early stages in the DSS model [272].

Taken together, the splenomegaly in MMP-19- and MMP-19/-28 double-deficient mice is in line with the persistent inflammation in the colon and the destroyed barrier and supports the severity of the disease as well as the impaired healing process in these animals.

5.4 Protective role of MMP-19 by mobilization of chemokines?

MMPs have recently been shown to be important regulators of inflammatory responses, mostly by processing of specific proteins, resulting in a gain-of-function activity [273], loss of activity or generation of a receptor antagonist [274]. Those proteins include cytokines, chemokines and also antimicrobial peptides. For example, IL-1β can be activated by several MMPs (MMP-2, -3, and -9) [275] and MMP-7 and -12 have been reported to activate latent TNF-α in macrophages [118; 159; 276]. However, MMP activity can also result in deactivation: MMP-8 and MMP-9, for instance, have the capacity to cleave CXCL9/MIG and CXCL10/IP-10 at their C-terminus, rendering them functionally inactive [162]. Another example is processing of CXCL12/SDF-1 by MMP-2 in the central nervous system during HIV infection: The cleaved form of CXCL12 is not only chemotactically inactive but highly neurotoxic, and induces neuronal apoptosis and inflammation in mice [161; 277].

Cleavage and activation of antimicrobial peptides is reported for MMP-7 [166; 278]. It was shown that proteolytic processing of α-defensins results in results in acquisition of defensin activity, thus, the ability to kill bacteria. MMP-7-deficient mice have an impaired ability to battle enteric pathogens due to a lack of mature defensins.

In vivo, chemokines are generally immobilized on the ECM or cell membrane through interactions with glycosaminoglycans (GAG) [279]. Several MMPs have been identified, which have the capacity to resolve these interactions and to release the active soluble form of the chemokine. This process, also termed ‘unmasking’ of chemokines [115], has been well described for the neutrophil-specific MMP-8 (collagenases 2), which cleaves the N-terminus of both CXCL8/IL-8 and LIX to enhance chemotactic potency. Indeed, MMP-8 null mice showed impaired recruitment of PMNs in an LPS-induced inflammation model, indicating the high specificity and relevance of MMP-8 in the immune response [117]. Other in vivo studies have demonstrated a role for MMP-2 and MMP-9 in mobilization of CCL11/eotaxin, CCL7/MCP-3 and CCL17/TARC [280].

Besides cytokines, MMPs can process chemokines making them more or less potent or by generating chemoattractant peptides from precursor proteins [121; 281]. A well investigated example is CXCL8 (human IL-8) [162] and LIX where the N-terminal part is cleaved by MMP9 and 8. This cleavage results in more potent chemoattractant activity than the full-length protein. MMPs can also affect chemokine gradients by shedding accessory proteins that bind or restrain chemokines, which was observed for MMP-7 shedding a transmembrane-complex of syndecan-1 and KC [124].

In the present study, MMP-19-deficient mice produced extremely high concentrations of various cytokines and chemokines, although the amount of inflammatory cells in the colon tissue was reduced in comparison to the wildtype mice. Colon explant culture supernatants of wildtype and MMP-19 -/- were used in a migration assay using mouse macrophages to investigate the chemoattractive activity of the mixture. Macrophages were migrating faster to supernatants of MMP-19 -/- colon tissue, concluding the released mixture of cytokine and chemokines to be biologically active. However, no conclusion could be drawn for a specific molecule, which was not activated by processing of MMP-19 as only the total supernatant was analyzed. We suggest that the protective effect of MMP-19 in colitis could be explained by a cleavage process leading to an activated signalling molecule as described for other MMPs. We propose, MMP-19 cleaves KC or LIX (the murine homologues for IL-8) and therefore increases the chemotactic activity, leading to an increased recruitment of neutrophils to the site of inflammation. KC and LIX are potent chemoattractants for neutrophils in mice, they especially act in early stages of inflammation to rapidly bring neutrophils to the site of inflammation. This hypothesis is in line with the decreased influx of neutrophils in MMP-19-deficient mice (Figure 5-4). Another mechanism of the protective effect of MMP-19 is the cleavage of antimicrobial peptides such as defensins, which would result in their activation and a result reduce the amount of infiltrating bacteria into the tissue, thus, inflammation.

5.4.1 MM-19 dependent processing of Fractalkine – protective role in IBD?

This study has also shown by *in vitro* cleavage assays as well as Western blot analysis of colon tissue lysates and colon explant culture (CEC) supernatants that MMP-19 can proteolytically cleave fractalkine (FKN, CX3CL1), a chemokine associated with IBD pathogenesis (Figure 5-3). FKN is expressed as a membrane-bound molecule and requires shedding from the cell surface to become chemotactically active. ADAM10 and ADAM17 (TACE) have been shown to mediate constitutive and PMA-induced cleavage of FKN to release a soluble form that attracts cells expressing the cognate receptor CX3CR1 such as macrophages and neutrophils [282]. The chemokine is up-regulated in a synergistic fashion by the pro-inflammatory cytokines TNF-α and IFN-γ, and elevated levels have been implicated in various inflammatory diseases such as atherosclerosis, rheumatoid arthritis and psoriasis. A study by Muehlhoefer et al has demonstrated that FKN is also expressed by intestinal epithelial cells and that a subpopulation of human intestinal intraepithelial lymphocytes expressed the receptor CX3CR1 [283].

In this study it was shown that colon tissue samples of wildtype mice release substantial amounts of a soluble FKN variant in the culture supernatant that was much reduced in samples of MMP-19-deficient mice. From this, one may assume an impaired capacity of the proteinase deficient mice to attract neutrophils and macrophages to the site of injury, a hypothesis that is in line with the diminished numbers of those cells seen in the inflamed colon tissue of the MMP-19 -/- animals.

We therefore propose a beneficial effect of MMP-19 through processing of colon-expressed FKN and the resulting recruitment of cells important for the wound healing process. Interestingly, it was reported that also the FKN receptor CX3CR1 is expressed on intestinal epithelial cells and that FKN can act in an autocrine fashion to induce the production of IL-8 in the colon epithelium via the ERK-1/2 signaling pathway [284]. IL-8 in turn is the master chemokine for attraction of neutrophils so the protective effect of FKN could well be an indirect one through promoting the synthesis of IL-8. This process is likely to be impaired in MMP-19-deficient mice as those cannot efficiently produce the soluble FKN variant required to induce receptor-mediated signalling (Figure 5-3 and 5-4).

We also suggest that the cleavage product generated by MMP-19 (Figure 5-3) might be more potent in signaling than the longer soluble form which is generated by ADAM17 (TACE), which cleaves fractalkine close to the membrane [285] and the long glycosylated stalk could not probably freely move as the short chemokine domain released by MMP-19. MMP-19 might be a proteinase responsible for constitutive shedding of fractalkine as it is expressed under normal conditions in many tissues. The cleavage of FKN and attraction of macrophages to the site of inflammation in the colon could be therefore faster in wildtype mice and is delayed in MMP-19-deficient animals as it has to be induced. The soluble CX3CL1 recruits bone-marrow derived monocytes/macrophages to the site of inflammation and their subsequent activation.

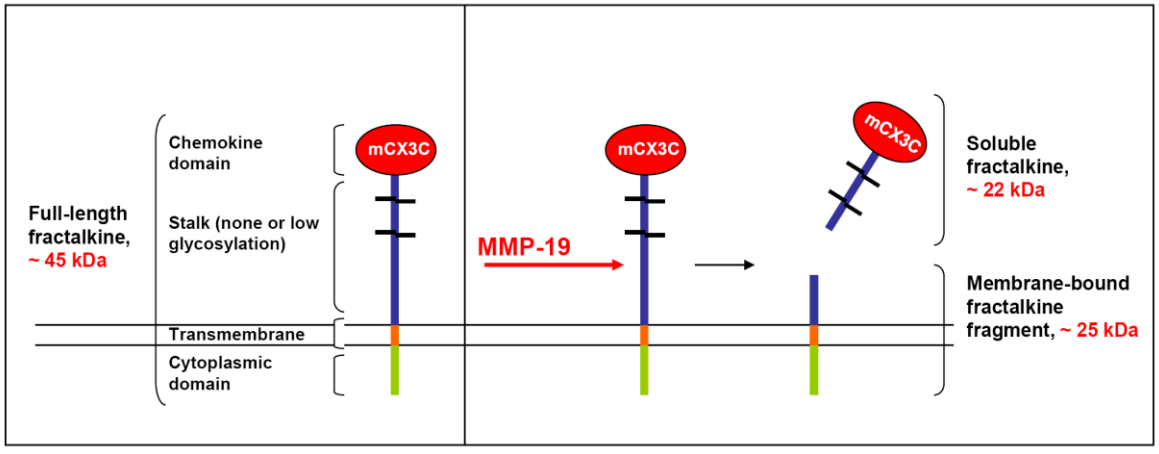

Figure 5-3: MMP-19 activity generates a soluble form of fractalkine.
Schematic representation. As Western blot and *in vitro* cleavage assays suggest (see 4.5.2 and 4.5.3), endogenous MMP-19 processes colon-expressed fractalkine to release a soluble variant of about 22 kDa, which is detectable in the supernatants of colon explant cultures. The remaining membrane-bound fractalkine fragment is detectable in colon tissue lysates and has a size of about 25 kDa. Opposed to human fractalkine expressed on endothelial cells, colon-expressed murine homolog appears to be much less glycosylated as it migrates at a lower molecular mass in SDS-PAGE (hFKN, ~90 kDa versus mFKN, ~45 kDa).

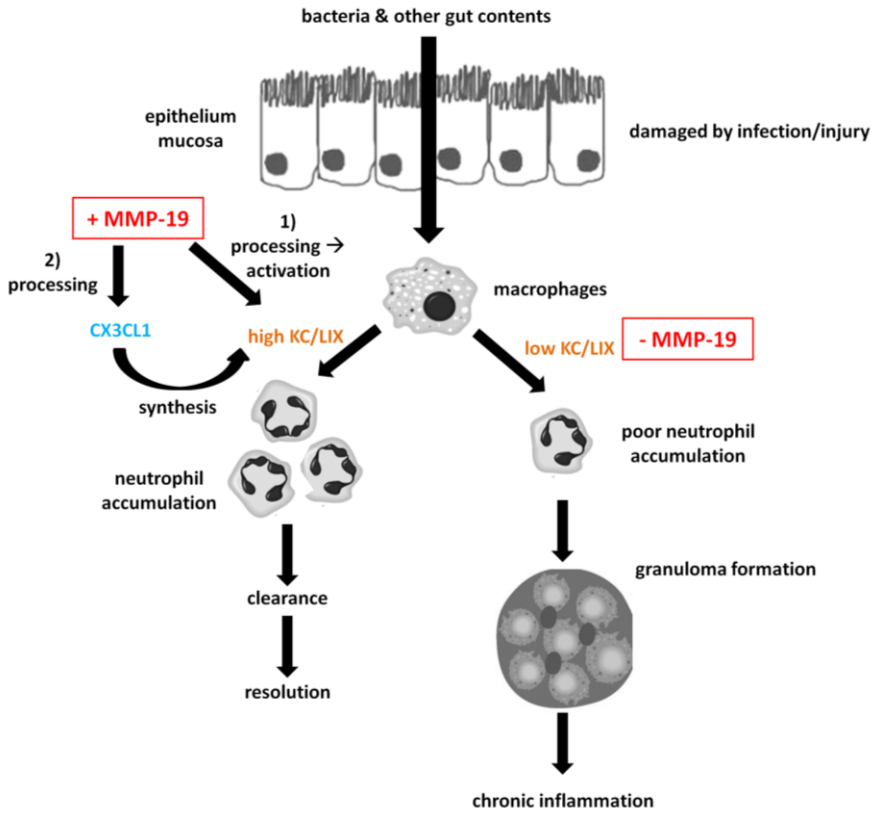

Figure 5-4: Schematic representation of suggested influence of MMP-19 on the chemoattractant KC or LIX. MMP-19 generates high concentrations of active KC or LIX by either processing the chemokine itself, leading to an increase in chemotactic activity (1) or via the processing of CX3CL1 to its soluble form, which promotes synthesis of KC/LIX (2). Modified from [286].

As MMP19-deificient mice showed profound effects on the development of colitis, and as these effects included altered influx of inflammatory cells and biased distribution and ratio of macrophages and T-cells, it is likely that MMP-19 also processes some of the cytokines and chemokines or accessory proteins. An addition to the release of the fractalkine chemotactic domain (or processing the molecule), further work should identify the substrates from these extracellular regulatory molecules. In this context, pilot experiments have shown that MMP-19 may process syndecan-4 and SDF-1 (not published) and could also release VEGF from its ECM stores.

5.5 MMP-19 deficiency leads to development of fibrosis in chronic colitis

Fibrosis is the formation of excess fibrous connective tissue in an organ or tissue in a reparative or reactive process. In case of fibrosis of the intestine, a thickening of the bowel wall can be observed due to increased amounts of collagens, mostly collagen type I. Fibrosis is one of the major symptoms in Crohn's disease [287] and can be viewed as an excessive healing response to constantly injured tissue.

We show that development of fibrosis in the MMP-19-deficient mice suffering from chronic colitis, whereas wildtype mice were healthy. Accumulation of collagen fibres was visualized by Masson Trichrome staining suggesting that MMP-19 -/- animals suffer from persistent inflammation throughout the treatment and partially also in the course of the recovery phase. The CD-like phenotype of these mice was supported by the fact that high concentrations of Th1 cytokines were detected in plasma (IL-1, IL-6) as well as in CEC supernatants (TNF-α, IFN-γ, IL-1, IL-6) of the mice. The elevated levels of acute phase cytokines like IL-6 in plasma indicate a systemic inflammatory response to chronic DSS-treatment. We conclude that by the deletion of MMP-19 we established an imbalance between MMPs and TIMPs, which is then contributing to collagen deposition and end up in fibrosis. In this regard, it is also important that MMP-19 is expressed also in healthy epithelium and, thus, its deficiency might already cause certain vulnerability of the barrier and predispose mice for exacerbated immune response.

The development of fibrosis upon multiple cycles of DSS treatment is well known and it is dependent on the mouse strain, for example C57BL/6 mice develop chronic colitis, whereas Balb/c do not [106]. Chronic DSS colitis shares some common features with CD, including activation of T and B cells, induction of T cell-derived cytokines, prominent lymphoid aggregates, and fissuring ulcerations [288]. The injury causes activation of mesenchymal cells with increased capability for ECM synthesis [289]. In fibrosis, mechanisms to degrade ECM are not working physiologically and the number of fibrogenic cells is not only maintained but also expand. Mechanisms regulating these effects are unknown but may include factors associated with CD, such as Th1 cytokines or transmural inflammation [290] or imbalance of MMPs and TIMPs [291].

Colon explants of MMP-19-deficient mice secreted enormous high concentrations of monocyte chemoattractant protein 1 (MCP-1) during the chronic phase of DSS-induced colitis. This could be part of the induction of the fibrotic process in MMP-19-deficient mice. The process starts with the accumulation of collagens in the inflamed tissue, which cannot be degraded in the knockout mice, at least the non-fibrillar collagens or degraded-fibrillar collagens, and this effect is amplified by the continuous inflammation due to impaired healing and the release of high amounts of MCP-1.

Increased levels of MCP-1 are in agreement with patient studies and revealed an increase in MCP-1 in inflammatory bowel disease (IBD), it is especially increased in the submucosa of CD patients [292; 293]. Mouse studies demonstrated that overexpression of MCP-1 induces a fibrogenic response [294] in the colon tissue. The mechanisms regulating MCP-

1-induced fibrosis include enhanced infiltration of lymphocytes and interaction between lymphocytes and fibroblasts/myofibroblasts and upregulation of TGF-b and TIMP-1.

The development of fibrosis causes problems in the re-epithelialization in the gut as the tissue hardens and cells are not able to migrate properly, leading to a decreased ability to remodel the architecture of the mucosa. The decreased ability of MMP-19-deficient macrophages to migrate and, thus, to remove or repair the provisional ECM could be also important in the fibrogenic process.

In conclusion, MMP19 -/- mice show higher susceptibility to DSS-induced colitis accompanied by strongly reduced proliferation of epithelial cells and decreased influx of inflammatory cells important for inflammatory reaction, despite increased concentrations of pro-inflammatory cytokines and chemokines. Thus, MMP-19 is involved in stimulating acute inflammation in DSS-induced colitis. However, this phenotype is even more pronounced in the MMP-19/-28 double-deficient mice.

Functional loss of MMP-19- activity shows that this MMP plays a crucial role in the severity of colitis. However, further studies are required to delineate the precise mechanism by which MMP-19 alone or in combination with MMP-28, or another MMP, are involved in intestinal inflammations and homeostasis. These future investigations have to be performed in order to elucidate the function of MMP-19 and MMP-28 in distinct cell types, tissues, and cell signaling processes. Analysis of neutrophil and macrophage chemotaxis to various recombinant chemokines may prove useful for further identification of chemokines and their receptors as novel substrates.

6 Summary

The present study investigates the role of two matrix-metalloproteinases, MMP-19 and MMP-28, in intestinal homeostasis and inflammation by means of a mouse model for inflammatory bowel disease (IBD). Based on previous experiments, the two proteinases have been implicated in cell proliferation and migration, remodelling of extracellular matrix, and wound healing. However, their *in vivo* function has remained largely elusive.

Acute or chronic colitis was induced in wildtype, MMP-19, and MMP-28 single-deficient as well as MMP-19/-28 double-deficient mice by dextran sulfate sodium (DSS). Moreover, the wound healing process was analyzed in a recovery phase following the acute colitis. Throughout the experiments, parameters of disease development and severity such as body weight loss, bleeding, stool consistency, and survival were monitored. These basic parameters were followed by histological analysis of colon and spleen tissues and pathological assessment of inflammation and symptoms of tissue destruction. Analysis of cytokine and chemokine release in plasma and in supernatants of colon explant cultures supported the investigations. Flow cytometry analysis was used to access possible bias of leukocyte subpopulations in peripheral blood and spleen. Finally, investigations into a potentially new MMP-19 substrate were carried out.

One of the major findings of this study is that in contrast to wildtype mice MMP-19-deficient mice showed an increased susceptibility to acute and chronic DSS-induced colitis accompanied by impaired healing process compared to the wildtype animals. Survival rates during acute and chronic colitis were significantly reduced, colonic inflammation and tissue destruction were markedly enhanced, and chemokine (e.g. KC) and pro-inflammatory cytokine (e.g. IL-6, IL-1) concentrations in plasma and colon explant cultures were highly elevated. Peripheral blood of MMP-19 -/- mice suffering from acute colitis contained significantly increased numbers of granulocytes whereas CD3+ T cells were dramatically reduced. During chronic colitis, the mice developed additional symptoms such as splenomegaly and colonic fibrosis. In contrast, the MMP-28-deficient mice show only moderate signs of disease and behaved similarly to the DSS-treated wildtype group in all experiments. Strikingly, the MMP-19/-28 double-deficient mice showed the most severe phenotype in acute colitis and during the recovery, which was reflected in very poor survival rates and impaired wound healing in the surviving animals.

Finally, it was demonstrated that MMP-19 processes fractalkine (CX3CL1), a membrane-bound chemokine that has been associated with IBD and which, in its soluble form, attracts monocytes and T cells. *In vitro* as well as *ex vivo* studies were performed to reveal the capacity of MMP-19 to process fractalkine to a soluble form. This missing proteolytic activity in MMP-19-deficient mice might explain the late influx of inflammatory cells in the acute phase of colitis.

In conclusion, this study provides several lines of evidence for a pivotal role of MMP-19 and MMP-28 in maintenance of intestinal tissue homeostasis. The data suggest that loss-

of-function of MMP-19 results in an increased susceptibility to colonic inflammation, mediated by an exacerbated innate immune response and inability of colonic tissue to heal. Mobilization of chemokines to facilitate migration of immune cells crucial for wound healing, e.g. macrophages, is a potential mechanism by which MMP-19 could exhibit its function. In this respect, the identification of fractalkine as a potential novel substrate of MMP-19, could pave the way for further functional studies.

7 Zusammenfassung

Die vorliegende Arbeit untersucht die Bedeutung der Metalloproteinasen MMP-19 und MMP-28 in entzündlichen Darmerkrankungen mittels eines Mausmodels. Bisherige Studien haben gezeigt, dass beide Proteinasen mit Zellproliferation, Erneuerung extrazellulärer Matrix und Wundheilung asoziiert sind. Über ihre *in vivo*-Funktionen ist jedoch nur wenig bekannt.

Akute oder chronische Kolitis wurde in Wildtyp-Mäusen, MMP-19- und MMP-28-einfach defizienten sowie MMP-19/-28 doppelt-defizienten Mäusen induziert, indem den Tieren eine 2%ige Dextran Natriumsalz (DSS)-Lösung als Trinkwasser verabreicht wurde. Der Wundheilungsprozess wurde in einer separaten Phase analysiert, in der sich die Mäuse von den Krankheitssymptomen erholen konnten. Im Verlauf der Experimente wurden Krankheitsparameter wie Körpergewichtsverlust, Blutungen, Stuhlkonsistenz und Mortalität gemessen. Zusätzlich wurden Gewebeschnitte von Darm und Milz auf Entzündungszeichen und Läsionen untersucht. Weiterhin wurden Zytokin- und Chemokinkonzentrationen im Blutplasma der Tiere sowie in Überständen von Darmgewebekulturen bestimmt. Durchflußzytometrie wurde verwendet, um mögliche Veränderungen in der Zusammensetzung der Leukozyten im Blut oder der Milz zu erfassen. Schließlich wurden Untersuchungen zu einem potentiell neuen Substrat der MMP-19 durchgeführt.

Ein Hauptergebnis der Studie ist, dass im Gegensatz zu Wildtyp-Mäusen, MMP-19-defiziente Mäuse eine höhere Anfälligkeit aufweisen, an der DSS-induizierten Kolitis zu erkranken. Dies wurde in einem verschlechterten Heilungsprozess, signifikant geringeren Überlebensraten sowie ausgedehnter Darmentzündung und -schädigung deutlich. Weiterhin wurden im Blutplasma sowie den Überständen der Darmgewebekulturen stark erhöhte Konzentrationen an Chemokinen (z.B. KC) und entzündungsfördernden Zytokinen (z.B. IL-6 und IL-1) gemessen. In dem Blut der an akuter Kolitis leidenden MMP-19 -/- Mäusen wurde zudem eine signifikant erhöhte Anzahl von Granulozyten festgestellt, wohingegen die Anzahl der T-Zellen dramatisch reduziert war. Im Verlauf der chronischen Kolitis entwickelten die Mäuse zusätzliche Krankheitssymptome wie z.B. eine Vergrößerung der Milz und Fibrose im Kolon.

Im Gegensatz zu den MMP-19-defizienten Mäusen wiesen die MMP-28-defizienten Tiere nur milde Anzeichen einer Erkrankung auf und verhielten sich während der gesamten Experimente im Wesentlichen wie die Wildtyp-Mäuse. Bemerkenswerterweise zeigten die MMP-19/-28 doppelt-defizienten Mäusen in der akuten Kolitis den gravierensten Krankheitsverlauf, was in reduzierten Überlebensraten und einer stark eingeschränkten Wundheilung zum Ausdruck kam. Schließlich konnte gezeigt werden, daß Fraktalkin (CX3CL1), ein membranständiges Chemokin, das mit der Entstehung entzündlicher Darmerkrankungen assoziiert wird und in seiner löslichen Form chemotaktisch auf Monozyten und T-Zellen wirkt, von MMP-19 prozessiert wird. Die Entstehung einer

löslichen Form wurde sowohl *in vitro* als auch *ex vivo* nachgewiesen. Dieser Mangel an proteolytischer Aktivität in den MMP-19-defizienten Mäusen kann erklären, warum hier die Entzündungszellen erst in der späten Phase der akuten Kolitis in den Darm einwandern.

Zusammengefaßt liefert diese Arbeit mehrere Hinweise, dass MMP-19 und MMP-28 eine wichtige Rolle in der Aufrechterhaltung eines gesunden Darmmilieus einnehmen. Die Daten lassen darauf schließen, dass der Verlust der MMP-19-Aktivität die Anfälligkeit für entzündliche Darmerkrankungen erhöht und dies vermutlich in einer Überreaktion des angeborenen Immunssystmes und einer eingeschränkten Wundheilung begründet ist. Die MMP-vermittelte ‚Mobiliserung' von Chemokinen, welche die Migration von heilungsfördernden Immunzellen wie z.B. Makrophagen ermöglichen, ist ein denkbarer Mechansimus für die Funktionsweise von MMP-19. In dieser Hinsicht kann die Identifikation von Fraktalkin als mögliches neues Substrat von MMP-19 den Weg für weitergehende Studien ebnen.

8 References

[1] J. Kirsch, May, C.A., Lorke, D., Winkelmann, A., Schwab, W., Herrmann, G., Funk, R., Taschenlehrbuch Anatomie, 2010.
[2] J. Bienenstock, and A.D. Befus, Mucosal immunology. Immunology 41 (1980) 249-70.
[3] J. Bienenstock, A.D. Befus, M. McDermott, S. Mirski, K. Rosenthal, and A. Tagliabue, The mucosal immunological network: compartmentalization of lymphocytes, natural killer cells, and mast cells. Ann N Y Acad Sci 409 (1983) 164-70.
[4] E.R. Lacy, H. Kuwayama, K.S. Cowart, J.S. King, A.H. Deutz, and S. Sistrunk, A rapid, accurate, immunohistochemical method to label proliferating cells in the digestive tract. A comparison with tritiated thymidine. Gastroenterology 100 (1991) 259-62.
[5] H.J. Thomson, A. Busuttil, M.A. Eastwood, A.N. Smith, and R.A. Elton, The submucosa of the human colon. J Ultrastruct Mol Struct Res 96 (1986) 22-30.
[6] E. Cario, and D.K. Podolsky, Differential alteration in intestinal epithelial cell expression of toll-like receptor 3 (TLR3) and TLR4 in inflammatory bowel disease. Infect Immun 68 (2000) 7010-7.
[7] E. Cario, I.M. Rosenberg, S.L. Brandwein, P.L. Beck, H.C. Reinecker, and D.K. Podolsky, Lipopolysaccharide activates distinct signaling pathways in intestinal epithelial cell lines expressing Toll-like receptors. J Immunol 164 (2000) 966-72.
[8] L.R. Coulthard, D.E. White, D.L. Jones, M.F. McDermott, and S.A. Burchill, p38(MAPK): stress responses from molecular mechanisms to therapeutics. Trends Mol Med 15 (2009) 369-79.
[9] J.E. Dancey, Molecular targeting: PI3 kinase pathway. Ann Oncol 15 Suppl 4 (2004) iv233-9.
[10] S. Beinke, and S.C. Ley, Functions of NF-kappaB1 and NF-kappaB2 in immune cell biology. Biochem J 382 (2004) 393-409.
[11] R. Al-Sadi, M. Boivin, and T. Ma, Mechanism of cytokine modulation of epithelial tight junction barrier. Front Biosci 14 (2009) 2765-78.
[12] A. Sturm, and A.U. Dignass, Epithelial restitution and wound healing in inflammatory bowel disease. World J Gastroenterol 14 (2008) 348-53.
[13] M.M. Lotz, I. Rabinovitz, and A.M. Mercurio, Intestinal restitution: progression of actin cytoskeleton rearrangements and integrin function in a model of epithelial wound healing. Am J Pathol 156 (2000) 985-96.
[14] B.C. McKaig, S.S. Makh, C.J. Hawkey, D.K. Podolsky, and Y.R. Mahida, Normal human colonic subepithelial myofibroblasts enhance epithelial migration (restitution) via TGF-beta3. Am J Physiol 276 (1999) G1087-93.
[15] W. Hoffmann, Trefoil factors TFF (trefoil factor family) peptide-triggered signals promoting mucosal restitution. Cell Mol Life Sci 62 (2005) 2932-8.
[16] W. Hoffmann, Trefoil factor family (TFF) peptides and chemokine receptors: a promising relationship. J Med Chem 52 (2009) 6505-10.
[17] H. Nagase, R. Visse, and G. Murphy, Structure and function of matrix metalloproteinases and TIMPs. Cardiovasc Res 69 (2006) 562-73.
[18] H. Mashimo, D.C. Wu, D.K. Podolsky, and M.C. Fishman, Impaired defense of intestinal mucosa in mice lacking intestinal trefoil factor. Science 274 (1996) 262-5.
[19] D.K. Podolsky, Inflammatory bowel disease. N Engl J Med 347 (2002) 417-29.
[20] M. Orholm, P. Munkholm, E. Langholz, O.H. Nielsen, T.I. Sorensen, and V. Binder, Familial occurrence of inflammatory bowel disease. N Engl J Med 324 (1991) 84-8.
[21] D.C. Baumgart, and S.R. Carding, Inflammatory bowel disease: cause and immunobiology. Lancet 369 (2007) 1627-40.
[22] D.C. Baumgart, and W.J. Sandborn, Inflammatory bowel disease: clinical aspects and established and evolving therapies. Lancet 369 (2007) 1641-57.
[23] R.J. Xavier, and D.K. Podolsky, Unravelling the pathogenesis of inflammatory bowel disease. Nature 448 (2007) 427-34.

[24] C.N. Bernstein, A. Wajda, L.W. Svenson, A. MacKenzie, M. Koehoorn, M. Jackson, R. Fedorak, D. Israel, and J.F. Blanchard, The epidemiology of inflammatory bowel disease in Canada: a population-based study. Am J Gastroenterol 101 (2006) 1559-68.

[25] S. Danese, S. Semeraro, A. Papa, I. Roberto, F. Scaldaferri, G. Fedeli, G. Gasbarrini, and A. Gasbarrini, Extraintestinal manifestations in inflammatory bowel disease. World J Gastroenterol 11 (2005) 7227-36.

[26] C.N. Bernstein, J.F. Blanchard, E. Kliewer, and A. Wajda, Cancer risk in patients with inflammatory bowel disease: a population-based study. Cancer 91 (2001) 854-62.

[27] I.J. Fuss, Is the Th1/Th2 paradigm of immune regulation applicable to IBD? Inflamm Bowel Dis 14 Suppl 2 (2008) S110-2.

[28] I.J. Fuss, Cytokine network in inflammatory bowel disease. Curr Drug Targets Inflamm Allergy 2 (2003) 101-12.

[29] I.J. Fuss, M. Neurath, M. Boirivant, J.S. Klein, C. de la Motte, S.A. Strong, C. Fiocchi, and W. Strober, Disparate CD4+ lamina propria (LP) lymphokine secretion profiles in inflammatory bowel disease. Crohn's disease LP cells manifest increased secretion of IFN-gamma, whereas ulcerative colitis LP cells manifest increased secretion of IL-5. J Immunol 157 (1996) 1261-70.

[30] I.J. Fuss, and W. Strober, The role of IL-13 and NK T cells in experimental and human ulcerative colitis. Mucosal Immunol 1 Suppl 1 (2008) S31-3.

[31] P.J. Mannon, I.J. Fuss, L. Mayer, C.O. Elson, W.J. Sandborn, D. Present, B. Dolin, N. Goodman, C. Groden, R.L. Hornung, M. Quezado, Z. Yang, M.F. Neurath, J. Salfeld, G.M. Veldman, U. Schwertschlag, and W. Strober, Anti-interleukin-12 antibody for active Crohn's disease. N Engl J Med 351 (2004) 2069-79.

[32] W. Strober, and I.J. Fuss, Proinflammatory cytokines in the pathogenesis of inflammatory bowel diseases. Gastroenterology 140 1756-1767 e1.

[33] B. Singh, F. Powrie, and N.J. Mortensen, Immune therapy in inflammatory bowel disease and models of colitis. Br J Surg 88 (2001) 1558-69.

[34] T.T. Macdonald, and G. Monteleone, Immunity, inflammation, and allergy in the gut. Science 307 (2005) 1920-5.

[35] S.L. Pender, and T.T. MacDonald, Matrix metalloproteinases and the gut - new roles for old enzymes. Curr Opin Pharmacol 4 (2004) 546-50.

[36] R.B. Sartor, Mechanisms of disease: pathogenesis of Crohn's disease and ulcerative colitis. Nat Clin Pract Gastroenterol Hepatol 3 (2006) 390-407.

[37] E.V. Loftus, Jr., Clinical epidemiology of inflammatory bowel disease: Incidence, prevalence, and environmental influences. Gastroenterology 126 (2004) 1504-17.

[38] F. Carbonnel, P. Jantchou, E. Monnet, and J. Cosnes, Environmental risk factors in Crohn's disease and ulcerative colitis: an update. Gastroenterol Clin Biol 33 Suppl 3 (2009) S145-57.

[39] J.H. Kurata, S. Kantor-Fish, H. Frankl, P. Godby, and C.M. Vadheim, Crohn's disease among ethnic groups in a large health maintenance organization. Gastroenterology 102 (1992) 1940-8.

[40] C.S. Probert, B.F. Warren, T. Perry, E.H. Mackay, J.F. Mayberry, and A.P. Corfield, South Asian and European colitics show characteristic differences in colonic mucus glycoprotein type and turnover. Gut 36 (1995) 696-702.

[41] H.G. Desai, and P.A. Gupte, Increasing incidence of Crohn's disease in India: is it related to improved sanitation? Indian J Gastroenterol 24 (2005) 23-4.

[42] J. Hampe, K. Heymann, M. Krawczak, and S. Schreiber, Association of inflammatory bowel disease with indicators for childhood antigen and infection exposure. Int J Colorectal Dis 18 (2003) 413-7.

[43] J. Cosnes, Smoking, physical activity, nutrition and lifestyle: environmental factors and their impact on IBD. Dig Dis 28 411-7.

[44] J. Cosnes, What is the link between the use of tobacco and IBD? Inflamm Bowel Dis 14 Suppl 2 (2008) S14-5.

[45] P. Seksik, I. Nion-Larmurier, H. Sokol, L. Beaugerie, and J. Cosnes, Effects of light smoking consumption on the clinical course of Crohn's disease. Inflamm Bowel Dis 15 (2009) 734-41.

[46] J.R. Ingram, G.A. Thomas, J. Rhodes, J.T. Green, N.D. Hawkes, J.L. Swift, E.D. Srivastava, B.K. Evans, G.T. Williams, R.G. Newcombe, E. Courtney, and S. Pillai, A randomized trial of nicotine enemas for active ulcerative colitis. Clin Gastroenterol Hepatol 3 (2005) 1107-14.

[47] G.A. Thomas, J. Rhodes, and J.R. Ingram, Mechanisms of disease: nicotine--a review of its actions in the context of gastrointestinal disease. Nat Clin Pract Gastroenterol Hepatol 2 (2005) 536-44.

[48] J.E. Mawdsley, M.G. Macey, R.M. Feakins, L. Langmead, and D.S. Rampton, The effect of acute psychologic stress on systemic and rectal mucosal measures of inflammation in ulcerative colitis. Gastroenterology 131 (2006) 410-9.

[49] J.E. Mawdsley, and D.S. Rampton, The role of psychological stress in inflammatory bowel disease. Neuroimmunomodulation 13 (2006) 327-36.

[50] J.E. Mawdsley, and D.S. Rampton, Psychological stress in IBD: new insights into pathogenic and therapeutic implications. Gut 54 (2005) 1481-91.

[51] C. Abraham, and J.H. Cho, Inflammatory bowel disease. N Engl J Med 361 (2009) 2066-78.

[52] D.K. Bonen, and J.H. Cho, The genetics of inflammatory bowel disease. Gastroenterology 124 (2003) 521-36.

[53] J.C. Barrett, S. Hansoul, D.L. Nicolae, J.H. Cho, R.H. Duerr, J.D. Rioux, S.R. Brant, M.S. Silverberg, K.D. Taylor, M.M. Barmada, A. Bitton, T. Dassopoulos, L.W. Datta, T. Green, A.M. Griffiths, E.O. Kistner, M.T. Murtha, M.D. Regueiro, J.I. Rotter, L.P. Schumm, A.H. Steinhart, S.R. Targan, R.J. Xavier, C. Libioulle, C. Sandor, M. Lathrop, J. Belaiche, O. Dewit, I. Gut, S. Heath, D. Laukens, M. Mni, P. Rutgeerts, A. Van Gossum, D. Zelenika, D. Franchimont, J.P. Hugot, M. de Vos, S. Vermeire, E. Louis, L.R. Cardon, C.A. Anderson, H. Drummond, E. Nimmo, T. Ahmad, N.J. Prescott, C.M. Onnie, S.A. Fisher, J. Marchini, J. Ghori, S. Bumpstead, R. Gwilliam, M. Tremelling, P. Deloukas, J. Mansfield, D. Jewell, J. Satsangi, C.G. Mathew, M. Parkes, M. Georges, and M.J. Daly, Genome-wide association defines more than 30 distinct susceptibility loci for Crohn's disease. Nat Genet 40 (2008) 955-62.

[54] Y. Ogura, D.K. Bonen, N. Inohara, D.L. Nicolae, F.F. Chen, R. Ramos, H. Britton, T. Moran, R. Karaliuskas, R.H. Duerr, J.P. Achkar, S.R. Brant, T.M. Bayless, B.S. Kirschner, S.B. Hanauer, G. Nunez, and J.H. Cho, A frameshift mutation in NOD2 associated with susceptibility to Crohn's disease. Nature 411 (2001) 603-6.

[55] J. Hampe, H. Frenzel, M.M. Mirza, P.J. Croucher, A. Cuthbert, S. Mascheretti, K. Huse, M. Platzer, S. Bridger, B. Meyer, P. Nurnberg, P. Stokkers, M. Krawczak, C.G. Mathew, M. Curran, and S. Schreiber, Evidence for a NOD2-independent susceptibility locus for inflammatory bowel disease on chromosome 16p. Proc Natl Acad Sci U S A 99 (2002) 321-6.

[56] J.P. Hugot, M. Chamaillard, H. Zouali, S. Lesage, J.P. Cezard, J. Belaiche, S. Almer, C. Tysk, C.A. O'Morain, M. Gassull, V. Binder, Y. Finkel, A. Cortot, R. Modigliani, P. Laurent-Puig, C. Gower-Rousseau, J. Macry, J.F. Colombel, M. Sahbatou, and G. Thomas, Association of NOD2 leucine-rich repeat variants with susceptibility to Crohn's disease. Nature 411 (2001) 599-603.

[57] D.J. Philpott, and S.E. Girardin, The role of Toll-like receptors and Nod proteins in bacterial infection. Mol Immunol 41 (2004) 1099-108.

[58] J.M. Otte, E. Cario, and D.K. Podolsky, Mechanisms of cross hyporesponsiveness to Toll-like receptor bacterial ligands in intestinal epithelial cells. Gastroenterology 126 (2004) 1054-70.

[59] J. Li, T. Moran, E. Swanson, C. Julian, J. Harris, D.K. Bonen, M. Hedl, D.L. Nicolae, C. Abraham, and J.H. Cho, Regulation of IL-8 and IL-1beta expression in Crohn's disease associated NOD2/CARD15 mutations. Hum Mol Genet 13 (2004) 1715-25.

[60] T. Hisamatsu, M. Suzuki, H.C. Reinecker, W.J. Nadeau, B.A. McCormick, and D.K. Podolsky, CARD15/NOD2 functions as an antibacterial factor in human intestinal epithelial cells. Gastroenterology 124 (2003) 993-1000.

[61] K. Hoshino, O. Takeuchi, T. Kawai, H. Sanjo, T. Ogawa, Y. Takeda, K. Takeda, and S. Akira, Cutting edge: Toll-like receptor 4 (TLR4)-deficient mice are hyporesponsive to lipopolysaccharide: evidence for TLR4 as the Lps gene product. J Immunol 162 (1999) 3749-52.

[62] A. Poltorak, X. He, I. Smirnova, M.Y. Liu, C. Van Huffel, X. Du, D. Birdwell, E. Alejos, M. Silva, C. Galanos, M. Freudenberg, P. Ricciardi-Castagnoli, B. Layton, and B. Beutler, Defective LPS signaling in C3H/HeJ and C57BL/10ScCr mice: mutations in Tlr4 gene. Science 282 (1998) 2085-8.

[63] H. Braat, M.P. Peppelenbosch, and D.W. Hommes, Immunology of Crohn's disease. Ann N Y Acad Sci 1072 (2006) 135-54.

[64] N. Inoue, K. Tamura, Y. Kinouchi, Y. Fukuda, S. Takahashi, Y. Ogura, N. Inohara, G. Nunez, Y. Kishi, Y. Koike, T. Shimosegawa, T. Shimoyama, and T. Hibi, Lack of common NOD2 variants in Japanese patients with Crohn's disease. Gastroenterology 123 (2002) 86-91.

[65] A. Mizoguchi, and E. Mizoguchi, Animal models of IBD: linkage to human disease. Curr Opin Pharmacol 10 578-87.

[66] J.M. Klapproth, and M. Sasaki, Bacterial induction of proinflammatory cytokines in inflammatory bowel disease. Inflamm Bowel Dis 16 2173-9.

[67] H.C. Rath, M. Schultz, R. Freitag, L.A. Dieleman, F. Li, H.J. Linde, J. Scholmerich, and R.B. Sartor, Different subsets of enteric bacteria induce and perpetuate experimental colitis in rats and mice. Infect Immun 69 (2001) 2277-85.

[68] R.B. Sartor, The influence of normal microbial flora on the development of chronic mucosal inflammation. Res Immunol 148 (1997) 567-76.

[69] M.R. Karlsson, H. Kahu, L.A. Hanson, E. Telemo, and U.I. Dahlgren, Neonatal colonization of rats induces immunological tolerance to bacterial antigens. Eur J Immunol 29 (1999) 109-18.

[70] R.B. Sartor, Genetics and environmental interactions shape the intestinal microbiome to promote inflammatory bowel disease versus mucosal homeostasis. Gastroenterology 139 1816-9.

[71] A.R. Jurjus, N.N. Khoury, and J.M. Reimund, Animal models of inflammatory bowel disease. J Pharmacol Toxicol Methods 50 (2004) 81-92.

[72] B. Sadlack, H. Merz, H. Schorle, A. Schimpl, A.C. Feller, and I. Horak, Ulcerative colitis-like disease in mice with a disrupted interleukin-2 gene. Cell 75 (1993) 253-61.

[73] R. Kuhn, J. Lohler, D. Rennick, K. Rajewsky, and W. Muller, Interleukin-10-deficient mice develop chronic enterocolitis. Cell 75 (1993) 263-74.

[74] S. Kitajima, S. Takuma, and M. Morimoto, Tissue distribution of dextran sulfate sodium (DSS) in the acute phase of murine DSS-induced colitis. J Vet Med Sci 61 (1999) 67-70.

[75] S. Kitajima, S. Takuma, and M. Morimoto, Histological analysis of murine colitis induced by dextran sulfate sodium of different molecular weights. Exp Anim 49 (2000) 9-15.

[76] S. Kitajima, M. Morimoto, and E. Sagara, A model for dextran sodium sulfate (DSS)-induced mouse colitis: bacterial degradation of DSS does not occur after incubation with mouse cecal contents. Exp Anim 51 (2002) 203-6.

[77] S. Wirtz, and M.F. Neurath, Mouse models of inflammatory bowel disease. Adv Drug Deliv Rev 59 (2007) 1073-83.

[78] S. Wirtz, C. Neufert, B. Weigmann, and M.F. Neurath, Chemically induced mouse models of intestinal inflammation. Nat Protoc 2 (2007) 541-6.

[79] M.F. Neurath, I. Fuss, B.L. Kelsall, E. Stuber, and W. Strober, Antibodies to interleukin 12 abrogate established experimental colitis in mice. J Exp Med 182 (1995) 1281-90.

[80] I. Okayasu, S. Hatakeyama, M. Yamada, T. Ohkusa, Y. Inagaki, and R. Nakaya, A novel method in the induction of reliable experimental acute and chronic ulcerative colitis in mice. Gastroenterology 98 (1990) 694-702.

[81] S. Kitajima, S. Takuma, and M. Morimoto, Changes in colonic mucosal permeability in mouse colitis induced with dextran sulfate sodium. Exp Anim 48 (1999) 137-43.

[82] T. Hibi, H. Ogata, and A. Sakuraba, Animal models of inflammatory bowel disease. J Gastroenterol 37 (2002) 409-17.

[83] P.J. Morrissey, K. Charrier, S. Braddy, D. Liggitt, and J.D. Watson, CD4+ T cells that express high levels of CD45RB induce wasting disease when transferred into congenic severe combined immunodeficient mice. Disease development is prevented by cotransfer of purified CD4+ T cells. J Exp Med 178 (1993) 237-44.

[84] S. Wirtz, S. Finotto, S. Kanzler, A.W. Lohse, M. Blessing, H.A. Lehr, P.R. Galle, and M.F. Neurath, Cutting edge: chronic intestinal inflammation in STAT-4 transgenic mice: characterization of disease and adoptive transfer by TNF- plus IFN-gamma-producing CD4+ T cells that respond to bacterial antigens. J Immunol 162 (1999) 1884-8.

[85] M. Mahler, I.J. Bristol, J.P. Sundberg, G.A. Churchill, E.H. Birkenmeier, C.O. Elson, and E.H. Leiter, Genetic analysis of susceptibility to dextran sulfate sodium-induced colitis in mice. Genomics 55 (1999) 147-56.

[86] M. Mahler, I.J. Bristol, E.H. Leiter, A.E. Workman, E.H. Birkenmeier, C.O. Elson, and J.P. Sundberg, Differential susceptibility of inbred mouse strains to dextran sulfate sodium-induced colitis. Am J Physiol 274 (1998) G544-51.

[87] M. Mahler, and E.H. Leiter, Genetic and environmental context determines the course of colitis developing in IL-10-deficient mice. Inflamm Bowel Dis 8 (2002) 347-55.

[88] W. Strober, I. Fuss, and P. Mannon, The fundamental basis of inflammatory bowel disease. J Clin Invest 117 (2007) 514-21.

[89] F.R. Byrne, and J.L. Viney, Mouse models of inflammatory bowel disease. Curr Opin Drug Discov Devel 9 (2006) 207-17.

[90] L.G. Axelsson, E. Landstrom, and A.C. Bylund-Fellenius, Experimental colitis induced by dextran sulphate sodium in mice: beneficial effects of sulphasalazine and olsalazine. Aliment Pharmacol Ther 12 (1998) 925-34.

[91] F.J. Zijlstra, I.M. Garrelds, A.P. van Dijk, and J.H. Wilson, Experimental colitis in mice: effects of olsalazine on eicosanoid production in colonic tissue. Agents Actions Spec No (1992) C76-8.

[92] H.S. Cooper, S.N. Murthy, R.S. Shah, and D.J. Sedergran, Clinicopathologic study of dextran sulfate sodium experimental murine colitis. Lab Invest 69 (1993) 238-49.

[93] B. Egger, M. Bajaj-Elliott, T.T. MacDonald, R. Inglin, V.E. Eysselein, and M.W. Buchler, Characterisation of acute murine dextran sodium sulphate colitis: cytokine profile and dose dependency. Digestion 62 (2000) 240-8.

[94] J. Ni, S.F. Chen, and D. Hollander, Effects of dextran sulphate sodium on intestinal epithelial cells and intestinal lymphocytes. Gut 39 (1996) 234-41.

[95] L.A. Dieleman, B.U. Ridwan, G.S. Tennyson, K.W. Beagley, R.P. Bucy, and C.O. Elson, Dextran sulfate sodium-induced colitis occurs in severe combined immunodeficient mice. Gastroenterology 107 (1994) 1643-52.

[96] L.G. Axelsson, E. Landstrom, T.J. Goldschmidt, A. Gronberg, and A.C. Bylund-Fellenius, Dextran sulfate sodium (DSS) induced experimental colitis in immunodeficient mice: effects in CD4(+) -cell depleted, athymic and NK-cell depleted SCID mice. Inflamm Res 45 (1996) 181-91.

[97] T.W. Kim, J.N. Seo, Y.H. Suh, H.J. Park, J.H. Kim, J.Y. Kim, and K.I. Oh, Involvement of lymphocytes in dextran sulfate sodium-induced experimental colitis. World J Gastroenterol 12 (2006) 302-5.

[98] L.A. Dieleman, M.J. Palmen, H. Akol, E. Bloemena, A.S. Pena, S.G. Meuwissen, and E.P. Van Rees, Chronic experimental colitis induced by dextran sulphate sodium (DSS) is characterized by Th1 and Th2 cytokines. Clin Exp Immunol 114 (1998) 385-91.

[99] S. Kitajima, M. Morimoto, E. Sagara, C. Shimizu, and Y. Ikeda, Dextran sodium sulfate-induced colitis in germ-free IQI/Jic mice. Exp Anim 50 (2001) 387-95.

[100] W. Hans, J. Scholmerich, V. Gross, and W. Falk, The role of the resident intestinal flora in acute and chronic dextran sulfate sodium-induced colitis in mice. Eur J Gastroenterol Hepatol 12 (2000) 267-73.

[101] A. Araki, T. Kanai, T. Ishikura, S. Makita, K. Uraushihara, R. Iiyama, T. Totsuka, K. Takeda, S. Akira, and M. Watanabe, MyD88-deficient mice develop severe intestinal inflammation in dextran sodium sulfate colitis. J Gastroenterol 40 (2005) 16-23.

[102] F. Obermeier, N. Dunger, U.G. Strauch, C. Hofmann, A. Bleich, N. Grunwald, H.J. Hedrich, E. Aschenbrenner, B. Schlegelberger, G. Rogler, J. Scholmerich, and W. Falk, CpG motifs of bacterial DNA essentially contribute to the perpetuation of chronic intestinal inflammation. Gastroenterology 129 (2005) 913-27.

[103] Y. Okada, Y. Tsuzuki, J. Miyazaki, K. Matsuzaki, R. Hokari, S. Komoto, S. Kato, A. Kawaguchi, S. Nagao, K. Itoh, T. Watanabe, and S. Miura, Propionibacterium freudenreichii component 1.4-dihydroxy-2-naphthoic acid (DHNA) attenuates dextran sodium sulphate induced colitis by modulation of bacterial flora and lymphocyte homing. Gut 55 (2006) 681-8.

[104] N. Osman, D. Adawi, G. Molin, S. Ahrne, A. Berggren, and B. Jeppsson, Bifidobacterium infantis strains with and without a combination of oligofructose and inulin (OFI) attenuate inflammation in DSS-induced colitis in rats. BMC Gastroenterol 6 (2006) 31.

[105] J.S. Frick, K. Fink, F. Kahl, M.J. Niemiec, M. Quitadamo, K. Schenk, and I.B. Autenrieth, Identification of commensal bacterial strains that modulate Yersinia enterocolitica and dextran sodium sulfate-induced inflammatory responses: implications for the development of probiotics. Infect Immun 75 (2007) 3490-7.

[106] S. Melgar, A. Karlsson, and E. Michaelsson, Acute colitis induced by dextran sulfate sodium progresses to chronicity in C57BL/6 but not in BALB/c mice: correlation between symptoms and inflammation. Am J Physiol Gastrointest Liver Physiol 288 (2005) G1328-38.

[107] M. Fanjul-Fernandez, A.R. Folgueras, S. Cabrera, and C. Lopez-Otin, Matrix metalloproteinases: evolution, gene regulation and functional analysis in mouse models. Biochim Biophys Acta 1803 (2010) 3-19.

[108] N. Liu, L. Nguyen, R.F. Chun, V. Lagishetty, S. Ren, S. Wu, B. Hollis, H.F. DeLuca, J.S. Adams, and M. Hewison, Altered endocrine and autocrine metabolism of vitamin D in a mouse model of gastrointestinal inflammation. Endocrinology 149 (2008) 4799-808.

[109] S. Rivera, M. Khrestchatisky, L. Kaczmarek, G.A. Rosenberg, and D.M. Jaworski, Metzincin proteases and their inhibitors: foes or friends in nervous system physiology? J Neurosci 30 (2010) 15337-57.

[110] C.B. Jones, D.C. Sane, and D.M. Herrington, Matrix metalloproteinases: a review of their structure and role in acute coronary syndrome. Cardiovasc Res 59 (2003) 812-23.

[111] C.L. Librach, Z. Werb, M.L. Fitzgerald, K. Chiu, N.M. Corwin, R.A. Esteves, D. Grobelny, R. Galardy, C.H. Damsky, and S.J. Fisher, 92-kD type IV collagenase mediates invasion of human cytotrophoblasts. J Cell Biol 113 (1991) 437-49.

[112] S.E. Gill, and W.C. Parks, Metalloproteinases and their inhibitors: regulators of wound healing. Int J Biochem Cell Biol 40 (2008) 1334-47.

[113] C.M. Overall, and C. Lopez-Otin, Strategies for MMP inhibition in cancer: innovations for the post-trial era. Nat Rev Cancer 2 (2002) 657-72.

[114] D.H. Manicourt, N. Fujimoto, K. Obata, and E.J. Thonar, Levels of circulating collagenase, stromelysin-1, and tissue inhibitor of matrix metalloproteinases 1 in patients with rheumatoid arthritis. Relationship to serum levels of antigenic keratan sulfate and systemic parameters of inflammation. Arthritis Rheum 38 (1995) 1031-9.

[115] D. Rodriguez, C.J. Morrison, and C.M. Overall, Matrix metalloproteinases: what do they not do? New substrates and biological roles identified by murine models and proteomics. Biochim Biophys Acta 1803 (2010) 39-54.

[116] T. Shiomi, V. Lemaitre, J. D'Armiento, and Y. Okada, Matrix metalloproteinases, a disintegrin and metalloproteinases, and a disintegrin and metalloproteinases with thrombospondin motifs in non-neoplastic diseases. Pathol Int 60 (2010) 477-96.

[117] A.M. Tester, J.H. Cox, A.R. Connor, A.E. Starr, R.A. Dean, X.S. Puente, C. Lopez-Otin, and C.M. Overall, LPS responsiveness and neutrophil chemotaxis in vivo require PMN MMP-8 activity. PLoS One 2 (2007) e312.

[118] A.J. Gearing, P. Beckett, M. Christodoulou, M. Churchill, J. Clements, A.H. Davidson, A.H. Drummond, W.A. Galloway, R. Gilbert, J.L. Gordon, and et al., Processing of tumour necrosis factor-alpha precursor by metalloproteinases. Nature 370 (1994) 555-7.

[119] C.M. Overall, Molecular determinants of metalloproteinase substrate specificity: matrix metalloproteinase substrate binding domains, modules, and exosites. Mol Biotechnol 22 (2002) 51-86.

[120] Q. Yu, and I. Stamenkovic, Cell surface-localized matrix metalloproteinase-9 proteolytically activates TGF-beta and promotes tumor invasion and angiogenesis. Genes Dev 14 (2000) 163-76.

[121] G.A. McQuibban, J.H. Gong, J.P. Wong, J.L. Wallace, I. Clark-Lewis, and C.M. Overall, Matrix metalloproteinase processing of monocyte chemoattractant proteins generates CC chemokine receptor antagonists with anti-inflammatory properties in vivo. Blood 100 (2002) 1160-7.

[122] W.S. Wang, P.M. Chen, H.S. Wang, W.Y. Liang, and Y. Su, Matrix metalloproteinase-7 increases resistance to Fas-mediated apoptosis and is a poor prognostic factor of patients with colorectal carcinoma. Carcinogenesis 27 (2006) 1113-20.

[123] J.K. McGuire, Q. Li, and W.C. Parks, Matrilysin (matrix metalloproteinase-7) mediates E-cadherin ectodomain shedding in injured lung epithelium. Am J Pathol 162 (2003) 1831-43.

[124] Q. Li, P.W. Park, C.L. Wilson, and W.C. Parks, Matrilysin shedding of syndecan-1 regulates chemokine mobilization and transepithelial efflux of neutrophils in acute lung injury. Cell 111 (2002) 635-46.

[125] C. Yan, and D.D. Boyd, Regulation of matrix metalloproteinase gene expression. J Cell Physiol 211 (2007) 19-26.

[126] D. Bourboulia, and W.G. Stetler-Stevenson, Matrix metalloproteinases (MMPs) and tissue inhibitors of metalloproteinases (TIMPs): Positive and negative regulators in tumor cell adhesion. Semin Cancer Biol 20 (2010) 161-8.

[127] M. Egeblad, and Z. Werb, New functions for the matrix metalloproteinases in cancer progression. Nat Rev Cancer 2 (2002) 161-74.

[128] J. Oh, R. Takahashi, S. Kondo, A. Mizoguchi, E. Adachi, R.M. Sasahara, S. Nishimura, Y. Imamura, H. Kitayama, D.B. Alexander, C. Ide, T.P. Horan, T. Arakawa, H. Yoshida, S. Nishikawa, Y. Itoh, M. Seiki, S. Itohara, C. Takahashi, and M. Noda, The membrane-anchored MMP inhibitor RECK is a key regulator of extracellular matrix integrity and angiogenesis. Cell 107 (2001) 789-800.

[129] C. Lopez-Otin, L.H. Palavalli, and Y. Samuels, Protective roles of matrix metalloproteinases: from mouse models to human cancer. Cell Cycle 8 (2009) 3657-62.

[130] T. Kirkegaard, A. Hansen, E. Bruun, and J. Brynskov, Expression and localisation of matrix metalloproteinases and their natural inhibitors in fistulae of patients with Crohn's disease. Gut 53 (2004) 701-9.

[131] V.O. Bister, M.T. Salmela, M.L. Karjalainen-Lindsberg, J. Uria, J. Lohi, P. Puolakkainen, C. Lopez-Otin, and U. Saarialho-Kere, Differential expression of three matrix metalloproteinases, MMP-19, MMP-26, and MMP-28, in normal and inflamed intestine and colon cancer. Dig Dis Sci 49 (2004) 653-61.

[132] G. Pedersen, T. Saermark, T. Kirkegaard, and J. Brynskov, Spontaneous and cytokine induced expression and activity of matrix metalloproteinases in human colonic epithelium. Clin Exp Immunol 155 (2009) 257-65.

[133] M. Vaalamo, M.L. Karjalainen-Lindsberg, P. Puolakkainen, J. Kere, and U. Saarialho-Kere, Distinct expression profiles of stromelysin-2 (MMP-10), collagenase-3 (MMP-13), macrophage metalloelastase (MMP-12), and tissue inhibitor of metalloproteinases-3 (TIMP-3) in intestinal ulcerations. Am J Pathol 152 (1998) 1005-14.

[134] W.C. Parks, Y.S. Lopez-Boado, and C.L. Wilson, Matrilysin in epithelial repair and defense. Chest 120 (2001) 36S-41S.

[135] D. Schuppan, and T. Freitag, Fistulising Crohn's disease: MMPs gone awry. Gut 53 (2004) 622-4.

[136] A. Stallmach, C.C. Chan, K.W. Ecker, G. Feifel, H. Herbst, D. Schuppan, and M. Zeitz, Comparable expression of matrix metalloproteinases 1 and 2 in pouchitis and ulcerative colitis. Gut 47 (2000) 415-22.

[137] M.D. Baugh, G.S. Evans, A.P. Hollander, D.R. Davies, M.J. Perry, A.J. Lobo, and C.J. Taylor, Expression of matrix metalloproteases in inflammatory bowel disease. Ann N Y Acad Sci 859 (1998) 249-53.

[138] M.D. Baugh, M.J. Perry, A.P. Hollander, D.R. Davies, S.S. Cross, A.J. Lobo, C.J. Taylor, and G.S. Evans, Matrix metalloproteinase levels are elevated in inflammatory bowel disease. Gastroenterology 117 (1999) 814-22.

[139] E. Louis, C. Ribbens, A. Godon, D. Franchimont, D. De Groote, N. Hardy, J. Boniver, J. Belaiche, and M. Malaise, Increased production of matrix metalloproteinase-3 and tissue inhibitor of metalloproteinase-1 by inflamed mucosa in inflammatory bowel disease. Clin Exp Immunol 120 (2000) 241-6.

[140] U. Gunther, H. Matthes, H. Herbst, A. Stallmach, E.O. Riecken, and D. Schuppan, Phenotype of cells expressing matrix metalloproteinase-3 in ulcerative colitis. Ann N Y Acad Sci 859 (1998) 237-40.

[141] S.L. Pender, C. Braegger, U. Gunther, G. Monteleone, M. Meuli, D. Schuppan, and T.T. Macdonald, Matrix metalloproteinases in necrotising enterocolitis. Pediatr Res 54 (2003) 160-4.

[142] T. Aigner, D. Neureiter, S. Muller, G. Kuspert, J. Belke, and T. Kirchner, Extracellular matrix composition and gene expression in collagenous colitis. Gastroenterology 113 (1997) 136-43.

[143] U. Gunther, D. Schuppan, M. Bauer, H. Matthes, A. Stallmach, A. Schmitt-Graff, E.O. Riecken, and H. Herbst, Fibrogenesis and fibrolysis in collagenous colitis. Patterns of procollagen types I and IV, matrix-metalloproteinase-1 and -13, and TIMP-1 gene expression. Am J Pathol 155 (1999) 493-503.

[144] S. Zucker, and J. Vacirca, Role of matrix metalloproteinases (MMPs) in colorectal cancer. Cancer Metastasis Rev 23 (2004) 101-17.

[145] D. Leppert, E. Waubant, R. Galardy, N.W. Bunnett, and S.L. Hauser, T cell gelatinases mediate basement membrane transmigration in vitro. J Immunol 154 (1995) 4379-89.

[146] G. Ratzinger, P. Stoitzner, S. Ebner, M.B. Lutz, G.T. Layton, C. Rainer, R.M. Senior, J.M. Shipley, P. Fritsch, G. Schuler, and N. Romani, Matrix metalloproteinases 9 and 2 are necessary for the migration of Langerhans cells and dermal dendritic cells from human and murine skin. J Immunol 168 (2002) 4361-71.

[147] C. Faveeuw, G. Preece, and A. Ager, Transendothelial migration of lymphocytes across high endothelial venules into lymph nodes is affected by metalloproteinases. Blood 98 (2001) 688-95.

[148] T.L. Deem, and J.M. Cook-Mills, Vascular cell adhesion molecule 1 (VCAM-1) activation of endothelial cell matrix metalloproteinases: role of reactive oxygen species. Blood 104 (2004) 2385-93.

[149] Y. Naito, T. Takagi, M. Kuroda, K. Katada, H. Ichikawa, S. Kokura, N. Yoshida, T. Okanoue, and T. Yoshikawa, An orally active matrix metalloproteinase inhibitor, ONO-4817, reduces dextran sulfate sodium-induced colitis in mice. Inflamm Res 53 (2004) 462-8.

[150] C. Medina, S. Videla, A. Radomski, M. Radomski, M. Antolin, F. Guarner, J. Vilaseca, A. Salas, and J.R. Malagelada, Therapeutic effect of phenantroline in two rat models of inflammatory bowel disease. Scand J Gastroenterol 36 (2001) 1314-9.

[151] R.L. Warner, L. Beltran, E.M. Younkin, C.S. Lewis, S.J. Weiss, J. Varani, and K.J. Johnson, Role of stromelysin 1 and gelatinase B in experimental acute lung injury. Am J Respir Cell Mol Biol 24 (2001) 537-44.

[152] R.L. Warner, C.S. Lewis, L. Beltran, E.M. Younkin, J. Varani, and K.J. Johnson, The role of metalloelastase in immune complex-induced acute lung injury. Am J Pathol 158 (2001) 2139-44.

[153] C.K. Li, S.L. Pender, K.M. Pickard, V. Chance, J.A. Holloway, A. Huett, N.S. Goncalves, J.S. Mudgett, G. Dougan, G. Frankel, and T.T. MacDonald, Impaired immunity to intestinal bacterial infection in stromelysin-1 (matrix metalloproteinase-3)-deficient mice. J Immunol 173 (2004) 5171-9.

[154] S. Maeda, D.D. Dean, R. Gomez, Z. Schwartz, and B.D. Boyan, The first stage of transforming growth factor beta1 activation is release of the large latent complex from the extracellular matrix of growth plate chondrocytes by matrix vesicle stromelysin-1 (MMP-3). Calcif Tissue Int 70 (2002) 54-65.

[155] M.A. Karsdal, L. Larsen, M.T. Engsig, H. Lou, M. Ferreras, A. Lochter, J.M. Delaisse, and N.T. Foged, Matrix metalloproteinase-dependent activation of latent transforming growth factor-beta controls the conversion of osteoblasts into osteocytes by blocking osteoblast apoptosis. J Biol Chem 277 (2002) 44061-7.

[156] A. Ito, A. Mukaiyama, Y. Itoh, H. Nagase, I.B. Thogersen, J.J. Enghild, Y. Sasaguri, and Y. Mori, Degradation of interleukin 1beta by matrix metalloproteinases. J Biol Chem 271 (1996) 14657-60.

[157] R.A. Black, C.T. Rauch, C.J. Kozlosky, J.J. Peschon, J.L. Slack, M.F. Wolfson, B.J. Castner, K.L. Stocking, P. Reddy, S. Srinivasan, N. Nelson, N. Boiani, K.A. Schooley, M. Gerhart, R. Davis, J.N. Fitzner, R.S. Johnson, R.J. Paxton, C.J. March, and D.P. Cerretti, A metalloproteinase disintegrin that releases tumour-necrosis factor-alpha from cells. Nature 385 (1997) 729-33.

[158] M.J. Mohan, T. Seaton, J. Mitchell, A. Howe, K. Blackburn, W. Burkhart, M. Moyer, I. Patel, G.M. Waitt, J.D. Becherer, M.L. Moss, and M.E. Milla, The tumor necrosis factor-alpha converting enzyme (TACE): a unique metalloproteinase with highly defined substrate selectivity. Biochemistry 41 (2002) 9462-9.

[159] A.J. Gearing, P. Beckett, M. Christodoulou, M. Churchill, J.M. Clements, M. Crimmin, A.H. Davidson, A.H. Drummond, W.A. Galloway, R. Gilbert, and et al., Matrix metalloproteinases and processing of pro-TNF-alpha. J Leukoc Biol 57 (1995) 774-7.

[160] W.R. English, X.S. Puente, J.M. Freije, V. Knauper, A. Amour, A. Merryweather, C. Lopez-Otin, and G. Murphy, Membrane type 4 matrix metalloproteinase (MMP17) has tumor necrosis factor-alpha convertase activity but does not activate pro-MMP2. J Biol Chem 275 (2000) 14046-55.

[161] G.A. McQuibban, G.S. Butler, J.H. Gong, L. Bendall, C. Power, I. Clark-Lewis, and C.M. Overall, Matrix metalloproteinase activity inactivates the CXC chemokine stromal cell-derived factor-1. J Biol Chem 276 (2001) 43503-8.

[162] P.E. Van den Steen, P. Proost, A. Wuyts, J. Van Damme, and G. Opdenakker, Neutrophil gelatinase B potentiates interleukin-8 tenfold by aminoterminal processing, whereas it degrades CTAP-III, PF-4, and GRO-alpha and leaves RANTES and MCP-2 intact. Blood 96 (2000) 2673-81.

[163] P.E. Van Den Steen, A. Wuyts, S.J. Husson, P. Proost, J. Van Damme, and G. Opdenakker, Gelatinase B/MMP-9 and neutrophil collagenase/MMP-8 process the chemokines human GCP-2/CXCL6, ENA-78/CXCL5 and mouse GCP-2/LIX and modulate their physiological activities. Eur J Biochem 270 (2003) 3739-49.

[164] T. Ayabe, D.P. Satchell, C.L. Wilson, W.C. Parks, M.E. Selsted, and A.J. Ouellette, Secretion of microbicidal alpha-defensins by intestinal Paneth cells in response to bacteria. Nat Immunol 1 (2000) 113-8.

[165] Y.S. Lopez-Boado, C.L. Wilson, L.V. Hooper, J.I. Gordon, S.J. Hultgren, and W.C. Parks, Bacterial exposure induces and activates matrilysin in mucosal epithelial cells. J Cell Biol 148 (2000) 1305-15.

[166] C.L. Wilson, A.J. Ouellette, D.P. Satchell, T. Ayabe, Y.S. Lopez-Boado, J.L. Stratman, S.J. Hultgren, L.M. Matrisian, and W.C. Parks, Regulation of intestinal alpha-defensin

activation by the metalloproteinase matrilysin in innate host defense. Science 286 (1999) 113-7.

[167] S.L. Pender, C.K. Li, A. Di Sabatino, T.T. MacDonald, and M.G. Buckley, Role of macrophage metalloelastase in gut inflammation. Ann N Y Acad Sci 1072 (2006) 386-8.

[168] M. Swee, C.L. Wilson, Y. Wang, J.K. McGuire, and W.C. Parks, Matrix metalloproteinase-7 (matrilysin) controls neutrophil egress by generating chemokine gradients. J Leukoc Biol 83 (2008) 1404-12.

[169] C. Medina, and M.W. Radomski, Role of matrix metalloproteinases in intestinal inflammation. J Pharmacol Exp Ther 318 (2006) 933-8.

[170] C. Medina, S. Videla, A. Radomski, M.W. Radomski, M. Antolin, F. Guarner, J. Vilaseca, A. Salas, and J.R. Malagelada, Increased activity and expression of matrix metalloproteinase-9 in a rat model of distal colitis. Am J Physiol Gastrointest Liver Physiol 284 (2003) G116-22.

[171] F.E. Castaneda, B. Walia, M. Vijay-Kumar, N.R. Patel, S. Roser, V.L. Kolachala, M. Rojas, L. Wang, G. Oprea, P. Garg, A.T. Gewirtz, J. Roman, D. Merlin, and S.V. Sitaraman, Targeted deletion of metalloproteinase 9 attenuates experimental colitis in mice: central role of epithelial-derived MMP. Gastroenterology 129 (2005) 1991-2008.

[172] P. Garg, M. Rojas, A. Ravi, K. Bockbrader, S. Epstein, M. Vijay-Kumar, A.T. Gewirtz, D. Merlin, and S.V. Sitaraman, Selective ablation of matrix metalloproteinase-2 exacerbates experimental colitis: contrasting role of gelatinases in the pathogenesis of colitis. J Immunol 177 (2006) 4103-12.

[173] P. Garg, M. Vijay-Kumar, L. Wang, A.T. Gewirtz, D. Merlin, and S.V. Sitaraman, Matrix metalloproteinase-9-mediated tissue injury overrides the protective effect of matrix metalloproteinase-2 during colitis. Am J Physiol Gastrointest Liver Physiol 296 (2009) G175-84.

[174] Y. Naito, and T. Yoshikawa, Role of matrix metalloproteinases in inflammatory bowel disease. Mol Aspects Med 26 (2005) 379-90.

[175] R. Sedlacek, S. Mauch, B. Kolb, C. Schatzlein, H. Eibel, H.H. Peter, J. Schmitt, and U. Krawinkel, Matrix metalloproteinase MMP-19 (RASI-1) is expressed on the surface of activated peripheral blood mononuclear cells and is detected as an autoantigen in rheumatoid arthritis. Immunobiology 198 (1998) 408-23.

[176] R. Sedlacek, RASI-1, MMP-19, Academic Press Inc., 2004.

[177] A.M. Pendas, A.R. Folgueras, E. Llano, J. Caterina, F. Frerard, F. Rodriguez, A. Astudillo, A. Noel, H. Birkedal-Hansen, and C. Lopez-Otin, Diet-induced obesity and reduced skin cancer susceptibility in matrix metalloproteinase 19-deficient mice. Mol Cell Biol 24 (2004) 5304-13.

[178] J. Cossins, T.J. Dudgeon, G. Catlin, A.J. Gearing, and J.M. Clements, Identification of MMP-18, a putative novel human matrix metalloproteinase. Biochem Biophys Res Commun 228 (1996) 494-8.

[179] A.M. Pendas, M. Balbin, E. Llano, M.G. Jimenez, and C. Lopez-Otin, Structural analysis and promoter characterization of the human collagenase-3 gene (MMP13). Genomics 40 (1997) 222-33.

[180] M.S. Mueller, M. Harnasch, C. Kolb, J. Kusch, T. Sadowski, and R. Sedlacek, The murine ortholog of matrix metalloproteinase 19: its cloning, gene organization, and expression. Gene 256 (2000) 101-11.

[181] M.S. Mueller, S. Mauch, and R. Sedlacek, Structure of the human MMP-19 gene. Gene 252 (2000) 27-37.

[182] I. Massova, L.P. Kotra, R. Fridman, and S. Mobashery, Matrix metalloproteinases: structures, evolution, and diversification. FASEB J 12 (1998) 1075-95.

[183] J. Lohi, C.L. Wilson, J.D. Roby, and W.C. Parks, Epilysin, a novel human matrix metalloproteinase (MMP-28) expressed in testis and keratinocytes and in response to injury. J Biol Chem 276 (2001) 10134-44.

[184] G.N. Marchenko, and A.Y. Strongin, MMP-28, a new human matrix metalloproteinase with an unusual cysteine-switch sequence is widely expressed in tumors. Gene 265 (2001) 87-93.

[185] J.O. Stracke, M. Hutton, M. Stewart, A.M. Pendas, B. Smith, C. Lopez-Otin, G. Murphy, and V. Knauper, Biochemical characterization of the catalytic domain of human matrix metalloproteinase 19. Evidence for a role as a potent basement membrane degrading enzyme. J Biol Chem 275 (2000) 14809-16.

[186] R. Sanchez-Lopez, R. Nicholson, M.C. Gesnel, L.M. Matrisian, and R. Breathnach, Structure-function relationships in the collagenase family member transin. J Biol Chem 263 (1988) 11892-9.

[187] A.J. Park, L.M. Matrisian, A.F. Kells, R. Pearson, Z.Y. Yuan, and M. Navre, Mutational analysis of the transin (rat stromelysin) autoinhibitor region demonstrates a role for residues surrounding the "cysteine switch". J Biol Chem 266 (1991) 1584-90.

[188] M. Yang, and M. Kurkinen, Cloning and characterization of a novel matrix metalloproteinase (MMP), CMMP, from chicken embryo fibroblasts. CMMP, Xenopus XMMP, and human MMP19 have a conserved unique cysteine in the catalytic domain. J Biol Chem 273 (1998) 17893-900.

[189] S. Mauch, C. Kolb, B. Kolb, T. Sadowski, and R. Sedlacek, Matrix metalloproteinase-19 is expressed in myeloid cells in an adhesion-dependent manner and associates with the cell surface. J Immunol 168 (2002) 1244-51.

[190] A. Rabot, F. Sinowatz, B. Berisha, H.H. Meyer, and D. Schams, Expression and localization of extracellular matrix-degrading proteinases and their inhibitors in the bovine mammary gland during development, function, and involution. J Dairy Sci 90 (2007) 740-8.

[191] A.M. Pendas, V. Knauper, X.S. Puente, E. Llano, M.G. Mattei, S. Apte, G. Murphy, and C. Lopez-Otin, Identification and characterization of a novel human matrix metalloproteinase with unique structural characteristics, chromosomal location, and tissue distribution. J Biol Chem 272 (1997) 4281-6.

[192] S. Suomela, A.L. Kariniemi, U. Impola, S.L. Karvonen, E. Snellman, T. Uurasmaa, J. Peltonen, and U. Saarialho-Kere, Matrix metalloproteinase-19 is expressed by keratinocytes in psoriasis. Acta Derm Venereol 83 (2003) 108-14.

[193] N. Hieta, U. Impola, C. Lopez-Otin, U. Saarialho-Kere, and V.M. Kahari, Matrix metalloproteinase-19 expression in dermal wounds and by fibroblasts in culture. J Invest Dermatol 121 (2003) 997-1004.

[194] C. Mauch, Matrix metalloproteinase-19: what role does this enzyme play in wound healing? J Invest Dermatol 121 (2003) xix-xx.

[195] M. Jost, A.R. Folgueras, F. Frerart, A.M. Pendas, S. Blacher, X. Houard, S. Berndt, C. Munaut, D. Cataldo, J. Alvarez, L. Melen-Lamalle, J.M. Foidart, C. Lopez-Otin, and A. Noel, Earlier onset of tumoral angiogenesis in matrix metalloproteinase-19-deficient mice. Cancer Res 66 (2006) 5234-41.

[196] M. Muller, I.M. Beck, J. Gadesmann, N. Karschuk, A. Paschen, E. Proksch, V. Djonov, K. Reiss, and R. Sedlacek, MMP19 is upregulated during melanoma progression and increases invasion of melanoma cells. Mod Pathol 23 (2010) 511-21.

[197] I. Lettau, K. Hattermann, J. Held-Feindt, R. Brauer, R. Sedlacek, and R. Mentlein, Matrix metalloproteinase-19 is highly expressed in astroglial tumors and promotes invasion of glioma cells. J Neuropathol Exp Neurol 69 (2010) 215-23.

[198] U. Impola, L. Jeskanen, L. Ravanti, S. Syrjanen, B. Baldursson, V.M. Kahari, and U. Saarialho-Kere, Expression of matrix metalloproteinase (MMP)-7 and MMP-13 and loss of MMP-19 and p16 are associated with malignant progression in chronic wounds. Br J Dermatol 152 (2005) 720-6.

[199] K.C. Chan, J.M. Ko, H.L. Lung, R. Sedlacek, Z.F. Zhang, D.Z. Luo, Z.B. Feng, S. Chen, H. Chen, K.W. Chan, S.W. Tsao, D.T. Chua, E.R. Zabarovsky, E.J. Stanbridge, and M.L. Lung, Catalytic activity of matrix metalloproteinase-19 is essential for tumor suppressor and anti-angiogenic activities in nasopharyngeal carcinoma. Int J Cancer.

[200] T. Sadowski, S. Dietrich, M. Muller, B. Havlickova, M. Schunck, E. Proksch, M.S. Muller, and R. Sedlacek, Matrix metalloproteinase-19 expression in normal and diseased skin: dysregulation by epidermal proliferation. J Invest Dermatol 121 (2003) 989-96.

[201] J.O. Stracke, A.J. Fosang, K. Last, F.A. Mercuri, A.M. Pendas, E. Llano, R. Perris, P.E. Di Cesare, G. Murphy, and V. Knauper, Matrix metalloproteinases 19 and 20 cleave aggrecan and cartilage oligomeric matrix protein (COMP). FEBS Lett 478 (2000) 52-6.

[202] B. Titz, S. Dietrich, T. Sadowski, C. Beck, A. Petersen, and R. Sedlacek, Activity of MMP-19 inhibits capillary-like formation due to processing of nidogen-1. Cell Mol Life Sci 61 (2004) 1826-33.

[203] T. Sadowski, S. Dietrich, F. Koschinsky, and R. Sedlacek, Matrix metalloproteinase 19 regulates insulin-like growth factor-mediated proliferation, migration, and adhesion in human keratinocytes through proteolysis of insulin-like growth factor binding protein-3. Mol Biol Cell 14 (2003) 4569-80.

[204] S. Lee, S.M. Jilani, G.V. Nikolova, D. Carpizo, and M.L. Iruela-Arispe, Processing of VEGF-A by matrix metalloproteinases regulates bioavailability and vascular patterning in tumors. J Cell Biol 169 (2005) 681-91.

[205] J.J. Caterina, J. Shi, C.A. Kozak, J.A. Engler, and H. Birkedal-Hansen, Characterization, expression analysis and chromosomal mapping of mouse matrix metalloproteinase-19 (MMP-19). Mol Biol Rep 27 (2000) 73-9.

[206] I.M. Beck, R. Ruckert, K. Brandt, M.S. Mueller, T. Sadowski, R. Brauer, P. Schirmacher, R. Mentlein, and R. Sedlacek, MMP19 is essential for T cell development and T cell-mediated cutaneous immune responses. PLoS One 3 (2008) e2343.

[207] M. Hooper, K. Hardy, A. Handyside, S. Hunter, and M. Monk, HPRT-deficient (Lesch-Nyhan) mouse embryos derived from germline colonization by cultured cells. Nature 326 (1987) 292-5.

[208] B. Hogan, R. Beddington, F. Constantini, and E. Lacy, Manipulating the mouse embryo, Oxford University Press, Oxford, England, 1994.

[209] S.A. Illman, J. Lohi, and J. Keski-Oja, Epilysin (MMP-28)--structure, expression and potential functions. Exp Dermatol 17 (2008) 897-907.

[210] S.A. Illman, J. Keski-Oja, and J. Lohi, Promoter characterization of the human and mouse epilysin (MMP-28) genes. Gene 275 (2001) 185-94.

[211] S.A. Illman, J. Keski-Oja, W.C. Parks, and J. Lohi, The mouse matrix metalloproteinase, epilysin (MMP-28), is alternatively spliced and processed by a furin-like proprotein convertase. Biochem J 375 (2003) 191-7.

[212] S.R. Werner, J.E. Dotzlaf, and R.C. Smith, MMP-28 as a regulator of myelination. BMC Neurosci 9 (2008) 83.

[213] H.J. Ra, and W.C. Parks, Control of matrix metalloproteinase catalytic activity. Matrix Biol 26 (2007) 587-96.

[214] U. Saarialho-Kere, E. Kerkela, T. Jahkola, S. Suomela, J. Keski-Oja, and J. Lohi, Epilysin (MMP-28) expression is associated with cell proliferation during epithelial repair. J Invest Dermatol 119 (2002) 14-21.

[215] C.M. Overall, E.M. Tam, R. Kappelhoff, A. Connor, T. Ewart, C.J. Morrison, X. Puente, C. Lopez-Otin, and A. Seth, Protease degradomics: mass spectrometry discovery of protease substrates and the CLIP-CHIP, a dedicated DNA microarray of all human proteases and inhibitors. Biol Chem 385 (2004) 493-504.

[216] D.A. Young, R.L. Lakey, C.J. Pennington, D. Jones, L. Kevorkian, D.R. Edwards, T.E. Cawston, and I.M. Clark, Histone deacetylase inhibitors modulate metalloproteinase gene expression in chondrocytes and block cartilage resorption. Arthritis Res Ther 7 (2005) R503-12.

[217] L. Li, S. He, J.M. Sun, and J.R. Davie, Gene regulation by Sp1 and Sp3. Biochem Cell Biol 82 (2004) 460-71.

[218] S.A. Illman, K. Lehti, J. Keski-Oja, and J. Lohi, Epilysin (MMP-28) induces TGF-beta mediated epithelial to mesenchymal transition in lung carcinoma cells. J Cell Sci 119 (2006) 3856-65.

[219] A.M. Manicone, T.P. Birkland, M. Lin, T. Betsuyaku, N. van Rooijen, J. Lohi, J. Keski-Oja, Y. Wang, S.J. Skerrett, and W.C. Parks, Epilysin (MMP-28) restrains early macrophage recruitment in Pseudomonas aeruginosa pneumonia. J Immunol 182 (2009) 3866-76.

[220] Hogan B, Beddington R, Constantini F, and a.L. E, Manipulating the mouse embryo. Oxford University Press, Oxford, England 2nd edition.

[221] K.B. Mullis, and F.A. Faloona, Specific synthesis of DNA in vitro via a polymerase-catalyzed chain reaction. Methods Enzymol 155 (1987) 335-50.

[222] C.A. Pinkert, Transgenic animal technology: alternatives in genotyping and phenotyping. Comp Med 53 (2003) 126-39.

[223] H. Matsunaga, R. Hokari, C. Kurihara, Y. Okada, K. Takebayashi, K. Okudaira, C. Watanabe, S. Komoto, M. Nakamura, Y. Tsuzuki, A. Kawaguchi, S. Nagao, K. Itoh, and S. Miura, Omega-3 fatty acids exacerbate DSS-induced colitis through decreased adiponectin in colonic subepithelial myofibroblasts. Inflamm Bowel Dis 14 (2008) 1348-57.

[224] B. Siegmund, F. Rieder, S. Albrich, K. Wolf, C. Bidlingmaier, G.S. Firestein, D. Boyle, H.A. Lehr, F. Loher, G. Hartmann, S. Endres, and A. Eigler, Adenosine kinase inhibitor GP515 improves experimental colitis in mice. J Pharmacol Exp Ther 296 (2001) 99-105.

[225] S. Grivennikov, E. Karin, J. Terzic, D. Mucida, G.Y. Yu, S. Vallabhapurapu, J. Scheller, S. Rose-John, H. Cheroutre, L. Eckmann, and M. Karin, IL-6 and Stat3 are required for survival of intestinal epithelial cells and development of colitis-associated cancer. Cancer Cell 15 (2009) 103-13.

[226] B. Siegmund, H.A. Lehr, G. Fantuzzi, and C.A. Dinarello, IL-1 beta -converting enzyme (caspase-1) in intestinal inflammation. Proc Natl Acad Sci U S A 98 (2001) 13249-54.

[227] A. Kobata, T. Kotani, Y. Komatsu, K. Amagase, S. Kato, and K. Takeuchi, Dual action of nitric oxide in the pathogenesis of ischemia/reperfusion-induced mucosal injury in mouse stomach. Digestion 75 (2007) 188-97.

[228] S. Melgar, K. Engstrom, A. Jagervall, and V. Martinez, Psychological stress reactivates dextran sulfate sodium-induced chronic colitis in mice. Stress 11 (2008) 348-62.

[229] T. Sadowski, S. Dietrich, F. Koschinsky, A. Ludwig, E. Proksch, B. Titz, and R. Sedlacek, Matrix metalloproteinase 19 processes the laminin 5 gamma 2 chain and induces epithelial cell migration. Cell Mol Life Sci 62 (2005) 870-80.

[230] M. Rohman, and K.J. Harrison-Lavoie, Separation of copurifying GroEL from glutathione-S-transferase fusion proteins. Protein Expr Purif 20 (2000) 45-7.

[231] F.K. Swirski, M. Nahrendorf, M. Etzrodt, M. Wildgruber, V. Cortez-Retamozo, P. Panizzi, J.L. Figueiredo, R.H. Kohler, A. Chudnovskiy, P. Waterman, E. Aikawa, T.R. Mempel, P. Libby, R. Weissleder, and M.J. Pittet, Identification of splenic reservoir monocytes and their deployment to inflammatory sites. Science 325 (2009) 612-6.

[232] Y. Yan, V. Kolachala, G. Dalmasso, H. Nguyen, H. Laroui, S.V. Sitaraman, and D. Merlin, Temporal and spatial analysis of clinical and molecular parameters in dextran sodium sulfate induced colitis. PLoS One 4 (2009) e6073.

[233] M.O. Breckwoldt, J.W. Chen, L. Stangenberg, E. Aikawa, E. Rodriguez, S. Qiu, M.A. Moskowitz, and R. Weissleder, Tracking the inflammatory response in stroke in vivo by sensing the enzyme myeloperoxidase. Proc Natl Acad Sci U S A 105 (2008) 18584-9.

[234] J.W. Chen, M.O. Breckwoldt, E. Aikawa, G. Chiang, and R. Weissleder, Myeloperoxidase-targeted imaging of active inflammatory lesions in murine experimental autoimmune encephalomyelitis. Brain 131 (2008) 1123-33.

[235] H. Yoshikawa, K. Takada, and S. Muranishi, Molecular weight dependence of permselectivity to rat small intestinal blood-lymph barrier for exogenous macromolecules absorbed from lumen. J Pharmacobiodyn 7 (1984) 1-6.

[236] E. Giannini, F. Botta, A. Fasoli, P. Ceppa, D. Risso, P.B. Lantieri, G. Celle, and R. Testa, Progressive liver functional impairment is associated with an increase in AST/ALT ratio. Dig Dis Sci 44 (1999) 1249-53.

[237] M. Tameda, K. Shiraki, K. Ooi, K. Takase, Y. Kosaka, T. Nobori, and Y. Tameda, Aspartate aminotransferase-immunoglobulin complexes in patients with chronic liver disease. World J Gastroenterol 11 (2005) 1529-31.

[238] C.N. Gamble, The pathogenesis of hyaline arteriolosclerosis. Am J Pathol 122 (1986) 410-20.
[239] J. Gerdes, H. Lemke, H. Baisch, H.H. Wacker, U. Schwab, and H. Stein, Cell cycle analysis of a cell proliferation-associated human nuclear antigen defined by the monoclonal antibody Ki-67. J Immunol 133 (1984) 1710-5.
[240] T. Scholzen, and J. Gerdes, The Ki-67 protein: from the known and the unknown. J Cell Physiol 182 (2000) 311-22.
[241] G. Murphy, N. Caplice, and M. Molloy, Fractalkine in rheumatoid arthritis: a review to date. Rheumatology (Oxford) 47 (2008) 1446-51.
[242] H. Liu, and D. Jiang, Fractalkine/CX3CR1 and atherosclerosis. Clin Chim Acta 412 1180-6.
[243] T. Kobayashi, S. Okamoto, Y. Iwakami, A. Nakazawa, T. Hisamatsu, H. Chinen, N. Kamada, T. Imai, H. Goto, and T. Hibi, Exclusive increase of CX3CR1+CD28-CD4+ T cells in inflammatory bowel disease and their recruitment as intraepithelial lymphocytes. Inflamm Bowel Dis 13 (2007) 837-46.
[244] M. Sans, S. Danese, C. de la Motte, H.S. de Souza, B.M. Rivera-Reyes, G.A. West, M. Phillips, J.A. Katz, and C. Fiocchi, Enhanced recruitment of CX3CR1+ T cells by mucosal endothelial cell-derived fractalkine in inflammatory bowel disease. Gastroenterology 132 (2007) 139-53.
[245] F.I. Kostadinova, T. Baba, Y. Ishida, T. Kondo, B.K. Popivanova, and N. Mukaida, Crucial involvement of the CX3CR1-CX3CL1 axis in dextran sulfate sodium-mediated acute colitis in mice. J Leukoc Biol 88 133-43.
[246] R. Brauer, I.M. Beck, M. Roderfeldt, E. Roeb, R. Sedlacek, Matrix metalloproteinase-19 inhibits growth of endothelial cells by generating angiostatin-like fragments from plasminogen. BMC Biochemistry (2011).
[247] A. Ravi, P. Garg, and S.V. Sitaraman, Matrix metalloproteinases in inflammatory bowel disease: boon or a bane? Inflamm Bowel Dis 13 (2007) 97-107.
[248] A. Santana, C. Medina, M.C. Paz-Cabrera, F. Diaz-Gonzalez, E. Farre, A. Salas, M.W. Radomski, and E. Quintero, Attenuation of dextran sodium sulphate induced colitis in matrix metalloproteinase-9 deficient mice. World J Gastroenterol 12 (2006) 6464-72.
[249] A.M. Manicone, and J.K. McGuire, Matrix metalloproteinases as modulators of inflammation. Semin Cell Dev Biol 19 (2008) 34-41.
[250] U. Impola, M. Toriseva, S. Suomela, L. Jeskanen, N. Hieta, T. Jahkola, R. Grenman, V.M. Kahari, and U. Saarialho-Kere, Matrix metalloproteinase-19 is expressed by proliferating epithelium but disappears with neoplastic dedifferentiation. Int J Cancer 103 (2003) 709-16.
[251] V. Bister, M.T. Salmela, P. Heikkila, A. Anttila, R. Rintala, K. Isaka, S. Andersson, and U. Saarialho-Kere, Matrilysins-1 and -2 (MMP-7 and -26) and metalloelastase (MMP-12), unlike MMP-19, are up-regulated in necrotizing enterocolitis. J Pediatr Gastroenterol Nutr 40 (2005) 60-6.
[252] B. von Lampe, B. Barthel, S.E. Coupland, E.O. Riecken, and S. Rosewicz, Differential expression of matrix metalloproteinases and their tissue inhibitors in colon mucosa of patients with inflammatory bowel disease. Gut 47 (2000) 63-73.
[253] J. Esparza, M. Kruse, J. Lee, M. Michaud, and J.A. Madri, MMP-2 null mice exhibit an early onset and severe experimental autoimmune encephalomyelitis due to an increase in MMP-9 expression and activity. FASEB J 18 (2004) 1682-91.
[254] A.U. Dignass, D.C. Baumgart, and A. Sturm, Review article: the aetiopathogenesis of inflammatory bowel disease--immunology and repair mechanisms. Aliment Pharmacol Ther 20 Suppl 4 (2004) 9-17.
[255] D.R. Clayburgh, L. Shen, and J.R. Turner, A porous defense: the leaky epithelial barrier in intestinal disease. Lab Invest 84 (2004) 282-91.
[256] M.T. Salmela, S.L. Pender, M.L. Karjalainen-Lindsberg, P. Puolakkainen, T.T. Macdonald, and U. Saarialho-Kere, Collagenase-1 (MMP-1), matrilysin-1 (MMP-7), and stromelysin-2 (MMP-10) are expressed by migrating enterocytes during intestinal wound healing. Scand J Gastroenterol 39 (2004) 1095-104.

[257] A. Chalaris, N. Adam, C. Sina, P. Rosenstiel, J. Lehmann-Koch, P. Schirmacher, D. Hartmann, J. Cichy, O. Gavrilova, S. Schreiber, T. Jostock, V. Matthews, R. Hasler, C. Becker, M.F. Neurath, K. Reiss, P. Saftig, J. Scheller, and S. Rose-John, Critical role of the disintegrin metalloprotease ADAM17 for intestinal inflammation and regeneration in mice. J Exp Med 207 (2010) 1617-24.

[258] H. Miyamori, T. Takino, Y. Kobayashi, H. Tokai, Y. Itoh, M. Seiki, and H. Sato, Claudin promotes activation of pro-matrix metalloproteinase-2 mediated by membrane-type matrix metalloproteinases. J Biol Chem 276 (2001) 28204-11.

[259] R. Agarwal, T. D'Souza, and P.J. Morin, Claudin-3 and claudin-4 expression in ovarian epithelial cells enhances invasion and is associated with increased matrix metalloproteinase-2 activity. Cancer Res 65 (2005) 7378-85.

[260] M.K. Siu, and C.Y. Cheng, Interactions of proteases, protease inhibitors, and the beta1 integrin/laminin gamma3 protein complex in the regulation of ectoplasmic specialization dynamics in the rat testis. Biol Reprod 70 (2004) 945-64.

[261] S. Tsukita, and M. Furuse, The structure and function of claudins, cell adhesion molecules at tight junctions. Ann N Y Acad Sci 915 (2000) 129-35.

[262] S. Tsukita, and M. Furuse, Pores in the wall: claudins constitute tight junction strands containing aqueous pores. J Cell Biol 149 (2000) 13-6.

[263] I.M. Beck, M. Muller, R. Mentlein, T. Sadowski, M.S. Mueller, R. Paus, and R. Sedlacek, Matrix metalloproteinase-19 expression in keratinocytes is repressed by transcription factors Tst-1 and Skn-1a: implications for keratinocyte differentiation. J Invest Dermatol 127 (2007) 1107-14.

[264] I.M. Beck, Function of Matrix Metalloproteinase 19 in Cutaneous Immunity, 2007, pp. 124.

[265] A.J. Ridley, M.A. Schwartz, K. Burridge, R.A. Firtel, M.H. Ginsberg, G. Borisy, J.T. Parsons, and A.R. Horwitz, Cell migration: integrating signals from front to back. Science 302 (2003) 1704-9.

[266] M.J. Hickey, and P. Kubes, Intravascular immunity: the host-pathogen encounter in blood vessels. Nat Rev Immunol 9 (2009) 364-75.

[267] A.W. Segal, How neutrophils kill microbes. Annu Rev Immunol 23 (2005) 197-223.

[268] S.D. Shapiro, and R.M. Senior, Matrix metalloproteinases. Matrix degradation and more. Am J Respir Cell Mol Biol 20 (1999) 1100-2.

[269] R.E. Mebius, and G. Kraal, Structure and function of the spleen. Nat Rev Immunol 5 (2005) 606-16.

[270] R. Zhang, S. Ito, N. Nishio, Z. Cheng, H. Suzuki, and K. Isobe, Up-regulation of Gr1+CD11b+ population in spleen of dextran sulfate sodium administered mice works to repair colitis. Inflamm Allergy Drug Targets 10 (2011) 39-46.

[271] O. Morteau, S.G. Morham, R. Sellon, L.A. Dieleman, R. Langenbach, O. Smithies, and R.B. Sartor, Impaired mucosal defense to acute colonic injury in mice lacking cyclooxygenase-1 or cyclooxygenase-2. J Clin Invest 105 (2000) 469-78.

[272] C.F. Krieglstein, W.H. Cerwinka, F.S. Laroux, M.B. Grisham, G. Schurmann, M. Bruwer, and D.N. Granger, Role of appendix and spleen in experimental colitis. J Surg Res 101 (2001) 166-75.

[273] W.C. Parks, C.L. Wilson, and Y.S. Lopez-Boado, Matrix metalloproteinases as modulators of inflammation and innate immunity. Nat Rev Immunol 4 (2004) 617-29.

[274] P. Van Lint, and C. Libert, Chemokine and cytokine processing by matrix metalloproteinases and its effect on leukocyte migration and inflammation. J Leukoc Biol 82 (2007) 1375-81.

[275] U. Schonbeck, F. Mach, and P. Libby, Generation of biologically active IL-1 beta by matrix metalloproteinases: a novel caspase-1-independent pathway of IL-1 beta processing. J Immunol 161 (1998) 3340-6.

[276] A. Churg, R.D. Wang, H. Tai, X. Wang, C. Xie, J. Dai, S.D. Shapiro, and J.L. Wright, Macrophage metalloelastase mediates acute cigarette smoke-induced inflammation via tumor necrosis factor-alpha release. Am J Respir Crit Care Med 167 (2003) 1083-9.

[277] K. Zhang, G.A. McQuibban, C. Silva, G.S. Butler, J.B. Johnston, J. Holden, I. Clark-Lewis, C.M. Overall, and C. Power, HIV-induced metalloproteinase processing of the chemokine stromal cell derived factor-1 causes neurodegeneration. Nat Neurosci 6 (2003) 1064-71.

[278] C.L. Wilson, A.P. Schmidt, E. Pirila, E.V. Valore, N. Ferri, T. Sorsa, T. Ganz, and W.C. Parks, Differential Processing of {alpha}- and {beta}-Defensin Precursors by Matrix Metalloproteinase-7 (MMP-7). J Biol Chem 284 (2009) 8301-11.

[279] A. Amara, O. Lorthioir, A. Valenzuela, A. Magerus, M. Thelen, M. Montes, J.L. Virelizier, M. Delepierre, F. Baleux, H. Lortat-Jacob, and F. Arenzana-Seisdedos, Stromal cell-derived factor-1alpha associates with heparan sulfates through the first beta-strand of the chemokine. J Biol Chem 274 (1999) 23916-25.

[280] D.B. Corry, A. Kiss, L.Z. Song, L. Song, J. Xu, S.H. Lee, Z. Werb, and F. Kheradmand, Overlapping and independent contributions of MMP2 and MMP9 to lung allergic inflammatory cell egression through decreased CC chemokines. FASEB J 18 (2004) 995-7.

[281] G.A. McQuibban, J.H. Gong, E.M. Tam, C.A. McCulloch, I. Clark-Lewis, and C.M. Overall, Inflammation dampened by gelatinase A cleavage of monocyte chemoattractant protein-3. Science 289 (2000) 1202-6.

[282] C. Hundhausen, D. Misztela, T.A. Berkhout, N. Broadway, P. Saftig, K. Reiss, D. Hartmann, F. Fahrenholz, R. Postina, V. Matthews, K.J. Kallen, S. Rose-John, and A. Ludwig, The disintegrin-like metalloproteinase ADAM10 is involved in constitutive cleavage of CX3CL1 (fractalkine) and regulates CX3CL1-mediated cell-cell adhesion. Blood 102 (2003) 1186-95.

[283] A. Muehlhoefer, L.J. Saubermann, X. Gu, K. Luedtke-Heckenkamp, R. Xavier, R.S. Blumberg, D.K. Podolsky, R.P. MacDermott, and H.C. Reinecker, Fractalkine is an epithelial and endothelial cell-derived chemoattractant for intraepithelial lymphocytes in the small intestinal mucosa. J Immunol 164 (2000) 3368-76.

[284] S. Brand, T. Sakaguchi, X. Gu, S.P. Colgan, and H.C. Reinecker, Fractalkine-mediated signals regulate cell-survival and immune-modulatory responses in intestinal epithelial cells. Gastroenterology 122 (2002) 166-77.

[285] K.J. Garton, P.J. Gough, C.P. Blobel, G. Murphy, D.R. Greaves, P.J. Dempsey, and E.W. Raines, Tumor necrosis factor-alpha-converting enzyme (ADAM17) mediates the cleavage and shedding of fractalkine (CX3CL1). J Biol Chem 276 (2001) 37993-8001.

[286] D.J. Marks, and A.W. Segal, Innate immunity in inflammatory bowel disease: a disease hypothesis. J Pathol 214 (2008) 260-6.

[287] J.M. Becker, Surgical therapy for ulcerative colitis and Crohn's disease. Gastroenterol Clin North Am 28 (1999) 371-90, viii-ix.

[288] C.O. Elson, Y. Cong, S. Brandwein, C.T. Weaver, R.P. McCabe, M. Mahler, J.P. Sundberg, and E.H. Leiter, Experimental models to study molecular mechanisms underlying intestinal inflammation. Ann N Y Acad Sci 859 (1998) 85-95.

[289] J.B. Pucilowska, K.L. Williams, and P.K. Lund, Fibrogenesis. IV. Fibrosis and inflammatory bowel disease: cellular mediators and animal models. Am J Physiol Gastrointest Liver Physiol 279 (2000) G653-9.

[290] C. Fiocchi, Inflammatory bowel disease: etiology and pathogenesis. Gastroenterology 115 (1998) 182-205.

[291] S. Chakraborti, M. Mandal, S. Das, A. Mandal, and T. Chakraborti, Regulation of matrix metalloproteinases: an overview. Mol Cell Biochem 253 (2003) 269-85.

[292] M.C. Grimm, S.K. Elsbury, P. Pavli, and W.F. Doe, Enhanced expression and production of monocyte chemoattractant protein-1 in inflammatory bowel disease mucosa. J Leukoc Biol 59 (1996) 804-12.

[293] L. Mazzucchelli, C. Hauser, K. Zgraggen, H.E. Wagner, M.W. Hess, J.A. Laissue, and C. Mueller, Differential in situ expression of the genes encoding the chemokines MCP-1 and RANTES in human inflammatory bowel disease. J Pathol 178 (1996) 201-6.

[294] Y. Motomura, W.I. Khan, R.T. El-Sharkawy, M. Verma-Gandhu, E.F. Verdu, J. Gauldie, and S.M. Collins, Induction of a fibrogenic response in mouse colon by overexpression of monocyte chemoattractant protein 1. Gut 55 (2006) 662-70.

9 Appendix

Table 9-1: Genetic association with Crohn's disease and ulcerative colitis.
Adapted from [51].

Gene	Genomic region	No. Of Genes in Region	Associated with CD	Associated with UC	Function
Innate immune response					
NOD2 (nucleotide-binding oligomerization domain 2)	16q12	1	yes	no	senses bacterial peptidoglycan to activate cell signaling
ATG16L1 (autophagy-related, 16-like)	2q37	1	yes	no	component of autophagy complex
IRGM (immunity-related GTPase M)	5q33	3	yes	equivocal	role in autophagy; required for IFN-γ-mediated clearance of intracellular pathogens
Interleukin-23-Th17 pathway					
IL23R (interleukin-23 receptor)	1p31	1	yes	yes	unique component of heterodimeric IL-23 receptor
IL12B (interleukin-12B, p40 subunit)	5q33	1	yes	yes	component of IL-23 cytokine; common to IL-12
STAT3 (sinal transducer and activator of transcription 3)	17q21	4	yes	yes	major STAT downstream of various cytokines, including IL-6, -10, -17, -21, -22, and -23
CCR6 (chemokine (C_C motif) receptor 6)	6q27	3	yes	no	cell-membrane protein mediating migration and recruitment of inflammatory cells
Other genes in association with regions					
PTGER4 (prostglandin E receptor 4)	5p13	0	yes	no	one of the receptors for the inflammatory mediator PGE2
ZNF365 (zinc finger protein 365)	10q21	1	yes	no	reported role in mitosis
SLC22A4 (solute-carrier faminly 22, organic cation transporter)	5q31	7	yes	equivocal	plasma membrane polyspecific organic cation transporter
PTPN2 (T-cell protein tyrosine phosphatase)	18p11	1	yes	no	multiple interactions with STAT proteins; also associated with type 1 diabetes
MHC (Major histocompatibility complex)	6p21	-	yes	yes	distinct MHC class II associations between UC and CD
NKX2-3 (NK2-transcription-factor-related, locus 3)	10q24	1	yes	yes	homeodomain-containing transcription factor affecting lymphoid and spleen development
MST1 (macrophage stimulating 1)	3p21	35	yes	yes	involved in macrophage chemotaxis and activation following proinflammatory signals
PLA2G2E (secretory phospholipase A2)	1p36	0	no	yes	releases arachinoidic acid from membrane phospholipids
IL10 (interleukin-10)	1q32	1	equivocal	yes	immunosuppressive cytikine with a central role in regulating intestinal inflammation
IFNG (interferon-γ)	12q15	2	no	yes	critical cytokine in innate and adaptive immunity against intracellular pathogens

Table 9-2: List of MMPs and their substrates.
Matrix metalloproteinases, systematically listed with their trivial description and substrates. Families of MMPs are listed by their proteolytic activity: collagenases, gelatinases, stromelysins, matrilysins, MT-MMPs, and other MMPs. Adapted from C. Overall's web page (www.clip.uba.ca/archive/mmp_timp_folder/).

Systematic name	Trivial description	Matrix substrates	Non-matrix substrates
Collagenases			
MMP-1	Collagenase-1	collagen type I-III, VII, X, gelatin, aggrecan, nidogen, tenascin, perlecan	MCP-1, -3, -4, SDF-1, proIL-1β, proTNF-α, proMMP-2, IGFBP-2, -3, α2-macroglobulin, α1-proteinase inhibitor
MMP-8	Collagenase-2 neutrophil collagenase	collagen type I-III, VII, X, gelatin, aggrecan, nidogen, tenascin,	MCP-1, L-selectin, proTNF-α, proMMP-8, α2-macroglobulin, α1-proteinase inhibitor
MMP-13	Collagenase-3	collagen type I-III, VII, X, gelatin, aggrecan, nidogen, tenascin,	MCP-3, SDF1, proTNF-α, proMMP-9, α1-antichymotrypsin
MMP-18	Collagenase-4 xCol4 (only in *Xenopus*)	collagen type I-III, gelatin	
Gelatinases			
MMP-2	Gelatinase A 72 kDa-gelatinase	collagen type I, IV, V, VII, X, XI, gelatin, elastin, laminin5, fibronectin, brevican, decorin, vitronectin, aggrecan	MCP-3, SDF-1, proIL-1β, proTNF-α, IGFBP-3, FGFR-1, proTGF-α1, endothelin-1, galectin-3, proMMP-1 and -13, α2-macroglobulin, α1-proteinase inhibitor

MMP-9	Gelatinase B 92 kDa-gelatinase	collagen type I, IV, V, VII, X, XI, elastin, fibronectin, laminin, aggrecan, vitronectin	SDF-1, Gro-α, proTNF-α, proTGF-β, IL-2Rα, plasminogen, galectin-3, proMMP-9 and -13, α2-macroglobulin, α1-proteinase inhibitor
Stromelysins			
MMP-3	Stroelysin-1 Proteoglycanase	collagen II-V, IX, X, gelatin, aggrecan, laminin, fibronectin, nidogen, tenascin, perlecan, elastin, vitronectin, fibrin/fibrinogen	proMMP-1, -7, -8, -9, -13 α2-macroglobulin, α1-proteinase inhibitor α1-antichymotrypsin
MMP-10	Stromelysin-2	gelatin type I, III, IV, V, fibronectin, proteoglycan	proMMP-1, proMMP-8
MMP-1	Stromelysin-3	fibronectin, laminin, aggrecan	IGFBP-1, α2-macroglobulin, α1-proteinase inhibitor
Matrilysin			
MMP-7	Matrilysin PUMP-1	non-helical collagen IV, V, IX-XI, laminin, gelatin, fibronectin, aggrecan, nidogen, tenascin, vitronectin, fibrin/fibrinogen	α-defensin, proTNF-α, plasminogen, FasL, E-cadherin, β4 integrin, proMMP-1, -2, -9, α1-proteinase inhibitor, α2-macroglobulin,
MMP-26	Matrilysin-2 Endometase	collagen type IV, fibronectin, gelatin, fibrin/fibrinogen	IGFBP-1, proMMP-9, α1-proteinase inhibitor

MT-MMPs			
MMP-14	MT1-MMP	collagen I-III, gelatin, aggrecan, fibronectin, vitronectin	MCP-3, SDF-1, CD44, proTNF-α, proMMP-2, α2-macroglobulin, α1-proteinase inhibitor, tissue transglutaminase
MMP-15	MT2-MMP	proteoglycans	proTNF-α, proMMP-2 tissue transglutaminase
MMP-16	MT3-MMP	collagen type III, fibronectin	proTNF-α, proMMP-2 tissue transglutaminase
MMP-17	MT4-MMP	gelatin, fibrin/fibrinogen	proTNF-α, proMMP-2
MMP-24	MT5-MMP	gelatin, fibronectin, proteoglycans	proMMP-2
MMP-25	MT6-MMP	collagen type IV, gelatin, laminin, fibronectin, fibrinogen, proteoglycans (chondroitinsulfate)	proMMP-2, proMMP-9 α1-proteinase inhibitor
other MMPs			
MMP-12	Metalloelastase Macrophage elasrase	elastin, fibronectin, laminin, proteoglycans, fibrin/fibrinogen	proTNF-α, plasminogen α1-proteinase inhibitor
MMP-19	RASI Stromelysin-4	collagen type IV, gelatin, fibronectin, nidogen tenascin, aggrecan, COMP, laminin, fibrin/fibrinogen	IGFBP-3, VEGF, plasminogen
MMP-20	Enamelysin	amelogenin, aggrecan, COMP	not determined

MMP-21	XMMP (*Xenopus*)	not determined	not determined
MMP-22	CMMP (chicken)	not determined	not determined
MMP-27	human homologue	not determined	not determined
MMP-23	CA-MMP (cystein-array-MMP)	gelatin	not determined
MMP-28	Epilysin	casein, NCAM	not determined

Table 9-3: Chemokines systematically listed including their trivial description.
Families of chemokines classified by arrangement of cysteins (C) in their sequence are grouped (CXC, CX3C, and CC chemokines). Only chemokines mentioned in this work are mentioned.

Systematic name	Trivial description (human)	Trivial description (mouse)
CXCL1	Gro-α	KC
CXCL2	Gro-β	MIP-2α
CXCL3	Gro-γ	MIP-2β
CXCL5	ENA-78	LIX
CXCL8	IL-8	Unknown
CXCL9	MIG	MIG
CXCL10	IP-10	IP-10
CXCL11	I-TAC/IP-9	I-TAC
CXCL12	SDF1α	SDF1α
CXCL13	BLC	BLC
CXCL16	SRPSOX	SRPSOX
XCL1	Lymphotactin-α/ATAC	Lymphotactin-α
XCL2	Lymphotactin-β	Lymphotactin-β
CX3CL1	Fractalkine	Fractalkine/neurotactin
CCL1	I-309	TAC-3
CCL2	MCP-1	MCP-1
CCL3	MIP-1α	MIP-1α
CCL4	MIP-1β	MIP-1β
CCL5	RANTES	RANTES
CCL7	MCP-3	MCP-3
CCL8	MCP-2	MCP-2
CCL9	unknown	MIP-1γ
CCL11	Eotaxin	Eotaxin
CCL12	MCP-5	MCP-5
CCL13	MCP-4	MCP-4
CCL17	TARC	TARC
CCL19	MIP-3β	MIP-3β
CCL20	MIP-3α	MIP-3α
CCL24	Eotaxin-2	Eotaxin-2
CCL25	TECK	TECK
CCL27	CTACK	CTACK

List of primers

Genotyping

MMP-19

WT forward: m1-U10, 5'-CCGCATCTTCAATGTGCCC-3'

WT reverse: mD1-21, 5'-GATCGCCAGGTTCACTCC-3'

KO forward: m1-U3, 5'-AGATGGATGACGCCACAAG-3'

KO reverse: neofwd, 5'- CTTCTATCGCCTTCTTGACG-3'

MMP-28

WT forward: Epi WT, 5'-GTGAAGATGTCCCATGCCCACAGT-3'

KO forward: MMP28 KO For, 5'-GCTGACCGCTTCCTCGTGCTTTAC-3'

WT and KO reverse: MMP28 rev common, 5'-AGGGCCCTCTTTCATCTTCCTGATG-3'

RT-PCR

mGAPDH

mGAPDH_RT_F: 5'-AACTTTGGCATTGTGGAAGG-3'

mGAPDH_RT_R: 5'-GTCTTCTGGGTGGCAGTGAT-3'

mMMP19

mMMP19_RT_F3: 5'-ATCTTCAATGTGCCCTCCAC-3'

mMMP19_RT_R3: 5'-CCACGCTGCTCCAGTACTTA-3'

mMMP28

mMMP28_RT_F3: 5'-CCTGTACGGAAAGCCTCTGG-3'

mMMP28_RT_R3: 5'-GTCTGCTCTGGGAGTTGTGG -3'

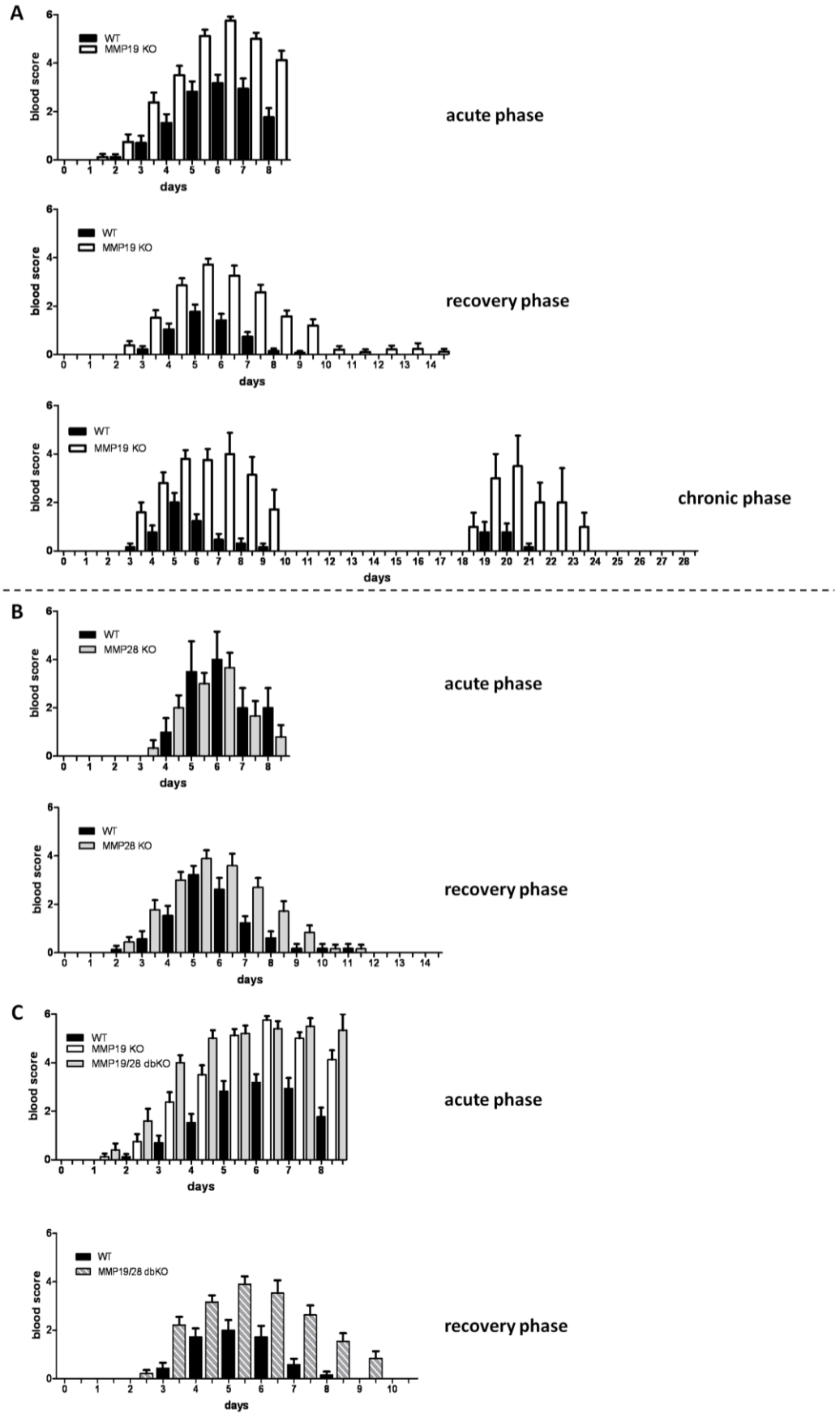

Figure 9-1: Blood scores of all colitis experiments.

10 Publications

- MMP19 is essential for T cell development and T cell-mediated cutaneous immune responses. Beck IM, Rückert R, Brandt K, Mueller MS, Sadowski T, **Brauer R**, Schirmacher P, Mentlein R, Sedlacek R., PLoS One. 2008 Jun 4;3(6):e2343.

- Matrix metalloproteinase-19 is highly expressed in astroglial tumors and promotes invasion of glioma cells. Lettau I, Hattermann K, Held-Feindt J, **Brauer R**, Sedlacek R, Mentlein R, J. Neuropathol Exp Neurol. 2010 Mar;69(3):215-23.

- Matrix metalloproteinase-19 inhibits growth of endothelial cells by generating angiostatin-like fragments from plasminogen. **Brauer R**, Beck IM, Roderfeld M, Roeb E, Sedlacek R, BMC Biochemistry (manuscript accepted)

- Expression and regulation of murine LEKTI2. Reiss K, Meyer-Hoffert U, Fischer J, Sperrhacke M, Wu Z, Dimitrieva O, Krenek P, Suchanova S, Buryova H, **Brauer R**, and Sedlacek R, Experimental Dermatology (manuscript submitted)

- MMP-19-deficient mice develop severe intestinal inflammation in dextran sulfate sodium-induced colitis. **Brauer R**, Dziechciarkova M, Skarda J, Hajduch M, Sedlacek R (manuscript in preparation)

11 Acknowledgments

I would like to thank my supervisor and Coreferent, Prof. Dr. Radek Sedlacek, for his great support throughout my Ph.D. studies. I would like to thank him for entrusting me with the project, for his advice, many useful discussions and his willingness to help whenever necessary. I am also very grateful to him for creating a pleasant working atmosphere and, not least, for his efforts to make me feel at home in Prague.

I would also like to thank Prof. Dr. Dr. Thomas Bosch for taking over the supervision of my Ph.D. project as Referent and the interest he showed in my work.

I am further grateful to Prof. Dr. Stefan Rose-John for giving me the opportunity to start my studies at the Insitute of Biochemistry in Kiel, for his advice and continuous support.

In particular, I would like to thank Dr. Marián Hajdúch (Ph.D.) from the Medical Faculty of the Palacký University in Olomouc, Czech Republic, for the opportunity to join his lab to learn immunohistochemistry and also for the helpful discussions we had about my work. My special thanks go to Dr. Marta Dziechciarková (Ph.D.) who introduced me to the techniques and who became a good friend.
Dr. Joseph Škarda (M.D., D.V.M.) from the Department of Pathology at the Palacký University in Olomouc did a fantastic job with helping me analyze all my samples – thanks a lot!
I would also like to thank Prof. Dr. Karl-Heinz Herzig (M.D., Ph.D.) from the Institute of Biomedicine, Division of Physiology and Biocenter of Oulu, Finland and his group for the help with the cytokine analysis.

Finally, I want to express my thanks to my friends and colleagues in the lab, Olga Žbodáková, Markéta Jiroušková, Martin Gregor, Pavel Křenek, Petr Kašpárek, Halka Buryová, Dana Průková, Inken Beck, and Karel Chalupský. Many thanks also to our technicians from the TGU Irena Placerová, Veronika Libová, and Sandra Potysová who helped a lot with the genotyping of the mice. I also wish to thank two former members of the lab, Šárka Suchanová and Lenka Hašlerová for their help and support at the beginning of my stay in Prague.

Special thanks go to my family back in Germany and close friends for their support and encouragement during my Ph.D. but especially during my stay abroad.

12 Erklärung

Hiermit erkläre ich, dass ich die vorliegende Dissertation unter Einhaltung der Regeln guter wissenschaftlicher Praxis eigenständig verfasst und keine anderen als die angegeben Hilfsmittel und Quellen benutzt habe. Dabei habe ich keine Hilfe, außer der wissenschaftlichen Beratung durch meinen Doktorvater Dr. Radislav Sedlacek in Anspruch genommen. Des Weiteren erkläre ich, dass ich noch keinen Promotionsversuch unternommen habe.

Kiel, den

_____

Rena Brauer